IDENTIFICATION OF SYSTEM PARAMETERS OF MULTI-STOREY BUILDINGS WITH LIMITED SENSORS

Thesis submitted in partial fulfillment of the requirements

for the Degree of

DOCTOR OF PHILOSOPHY

By

ARUN CHANDRA BORSAIKIA

DEPARTMENT OF CIVIL ENGINEERING

INDIAN INSTITUTE OF TECHNOLOGY GUWAHATI

GUWAHATI-781039 (INDIA)

MAY 2011

CANDIDATE'S DECLARATION

I hereby declare that the work presented in the thesis entitled **"Identification of System Parameters of Multi-Storey Buildings with Limited Sensors"** in fulfillment of the requirement for the award of the Degree of *Doctor of Philosophy* is an authentic record of my own work carried out in Department of Civil Engineering of the Institute. The work has been carried out under active guidance of Dr. S. K. Deb and Dr. A. Dutta.

The content presented in this thesis has not been submitted by me for the award of any other degree of this or any other Institute.

Arun Chandra Borsaikia

This is to certify that the above statement made by the candidate is correct to the best of our knowledge.

Dr. Anjan Dutta
Professor
Dept of Civil Engineering
Indian Institute of Technology
Guwahati-781039 (INDIA)

Dr. Sajal Kanti Deb
Professor
Dept of Civil Engineering
Indian Institute of Technology
Guwahati-781039 (INDIA)

ACKNOWLEDGEMENT

This thesis is the outcome of experimental investigations carried out in the department of Civil Engineering at Indian Institute of Technology, Guwahati (India). At the outset, I would like to express my sincere gratitude to my supervisors, Prof Anjan Dutta and Prof Sajal Kanti Deb for initiating an interesting and innovative research topic and for their personal commitment, unconditional support, valuable advices and continuous guidance. I appreciate the opportunities I got to develop myself in a new area of Structural Engineering.

The study in this thesis is based on laboratory as well as field experimentations. This would not have been possible without the support of technical staff of Structural Engineering of IIT Guwahati. I express my gratitude to Mr. Biswajit Debnath, Junior Technical Superintendent for his earnest effort during data collection, post processing and experimentation. I want to thank Mr. Nripen Kalita, technical staff of the laboratory for his continuous help during preparation and experimentation of test models. Further, I extend my heartful thanks Mr. Suresh Boro, Mr. Tarun Bhuyan and others who helped me directly or indirectly in carrying out experiments.

I gratefully acknowledge the help of Mr. Rupam Nath for his overall assistance in numerical phase of the work. I am thankful to Mrs. Jurijyoti Hazarika for her devotion in preparing AutoCAD drawings related to my work.

I would like to thank the members of my doctoral committee, Prof Sudip Talukdar (Chairman), Prof Uday Shanker Dixt and Dr. Hemant B. Kaushik for their remarks and valuable suggestions about the work.

I would like to acknowledge the suggestions and comments I received via E-mail from Prof Satish Nagarajaiah (USA) and Dr. Juan M Caicedo (USA) at various occasions whenever I sought clarification of any doubts.

I would like to thank Prof Gautam Barua, Director, Indian Institute of Technology Guwahati, India for allowing me to pursue the PhD degree.

Last but not the least, I would like to thank my loving wife Karabi for her sacrifice and moral support.

Arun Chandra Borsaikia

To the loving memory

of my parents

TABLE OF CONTENTS

ABSTRACT

Evaluations of system parameters of civil engineering structures using system identification techniques are attracting considerable attention in recent years. Recorded dynamic responses induced in the structures due to ambient or earthquake excitations are utilized for identifications of system parameters of the structures. The potential of system identification procedures have been explored by number of researchers for identification of system properties of buildings.

In this thesis, system identifications strategies have been adopted for identification of system parameters of two existing multi-storey shear buildings. The system identification strategies have been initially verified by identifying system parameters of laboratory test models. N4SID subspace identification technique has been employed for identification of modal parameters of a symmetric-plan nine storey shear building using on recorded acceleration histories. Similarly, identification of modal parameters of a four storey torsionally coupled shear building has been carried out using ITD method based on recorded acceleration histories. An iterative approach has been used for the determination of complete modal matrix incase of availability of only limited sensor data. Both the modal parameters as well as structural parameters identification techniques have been elaborated in the thesis. Further, detailed instrumentations adopted for acquiring acceleration histories from laboratory test models and existing buildings have also been described in this thesis.

The verification through scaled laboratory models is done by exciting them on a uni-axial shake table. The acceleration responses are recorded from different floor levels and identification techniques are applied. The N4SID technique applied to symmetric plan shear building has been initially verified through tests on three numbers of two storey bare frame reinforced concrete 1/5th scale models. Variations of column dimensions in ground

storey of the test models have been deliberately introduced to verify the effectiveness of the identification scheme. Additional loads have been attached to each floor of the test models for gravity load simulation. Studies on laboratory test models with and without infill walls have been carried out separately. Identification of modal parameters of all the three test models have been carried out using N4SID algorithm based on acquired acceleration histories during shake table test.

Three dimensional finite element models of all the scaled laboratory buildings have been developed using SAP 2000 Nonlinear (version 12). Modal analyses of all the numerical models have been carried out for the evaluation of natural frequencies. Computed modal frequencies of all the numerical models have been compared with the corresponding identified frequencies of the laboratory test models. The numerical models have been updated by applying appropriate adjustment in material properties so that the computed frequencies match with those of the identified natural frequencies of the test models. Thereafter, time history analyses have also been carried out using updated numerical model subjected to table acceleration histories. Floor acceleration histories from the numerical models have been compared with the corresponding recorded floor acceleration histories from the test models. The studies on all the three test models have been repeated after adding masonry infill walls in the direction of excitation. Recorded acceleration histories have been utilized for the identification of modal system parameters of these test models. Changes in modal and structural parameters of these test models have been observed due to the presence of infill walls. Considering the infill wall as an equivalent diagonal strut, an empirical relationship has been developed for the assessment of stiffness of the strut utilizing the data derived from the experiment.

Further, all the three test models with different sizes openings in the central region of the infill walls have again been tested in the shake table. Changes in modal and structural

parameters have been observed due to the presence openings in infill walls. The contribution of infill walls to the overall stiffness of the building frame becomes insignificant corresponding to 45% opening in infill wall. The difference in storey stiffness of test models with and without openings in infill walls have been utilized to arrive at a stiffness reduction factor showing the influence of sizes of opening in infill walls. The infill walls in first storey of all the three numerical models have been modeled using proposed correlation. Modal analysis of all the numerical models of the test specimens with different percentage of opening in infill walls have been carried out and natural frequencies along the plane of infill wall (direction of shake table excitation) have been compared with those obtained from identification. Thereafter, time history analyses have been carried out on these models using table accelerations as input and computed time histories have been compared with corresponding recorded acceleration histories of these test models. Very good agreements have been observed among the results from numerically simulated model and corresponding experimental observations. The modal characteristics of all the above-mentioned numerical models with full infill have been also compared with numerical models, whose infill walls are modeled as diagonal strut based on a few existing recommendations. Then, the applicability of the proposed correlation for prototype building has been verified through studies on numerical models. Numerically simulated prototype models of one of the test models with different percentage of opening in infill walls have been considered. The natural frequencies of these numerically developed prototype models with infill walls have been compared with those of numerically simulated scaled models with infill walls and have been found to be perfectly related through their scale factors.

The understanding developed from this study under control environment has been subsequently utilized for the identification of system parameters of an existing multi-

storey building. Floor as well as ground acceleration histories acquired during two earthquakes in two horizontal directions of an existing symmetric-plan multistory shear building have been used for identification of system parameters. Ground acceleration response history and floor acceleration histories have been used to assemble the input and output response matrices respectively. However, acceleration histories at all the floor levels of the building are not available due to limited numbers of sensors used. Thus, as the identified modal matrix remains incomplete, an iterative scheme has been introduced to evaluate the complete modal matrix and hence the structural parameters are also obtained at the end of convergence. A three dimensional finite element model of the same building has also been developed using SAP 2000 Nonlinear from the available drawings. The walls in the frames of the building in both the directions have been modeled following the developed empirical relationship proposed in this study and considering 20% wall opening. Modal analysis has been carried out and the computed natural frequencies are compared with those obtained from the identification studies. Updating of the model has been carried out by adjusting compressive strength of masonry infill alone as minor variations have been observed between the computed natural frequencies with those of identified frequencies. Time history analyses have been carried out in two horizontal directions using actual earthquake records as input. The validated numerical model has been used to evaluate the optimal requirement of sensors and it is observed that a minimum of two sensors at two suitable floor levels are sufficient for accurate identification of modal parameters. This indicates the potential of identification strategy for the evaluation of system parameters of existing multi storey buildings with limited numbers of sensors.

In order to address a more general type of building having asymmetricity, an existing four storey asymmetric building is considered. However for better understanding, a two storey

scaled steel frame model has been initially considered and tested in a shake table. Non-uniform distributions of loads on each floor panels have been made in order to impose asymmetricity in the model. The model is excited on a shake table and the recorded responses at different floor levels have been used for the identification process. The torsional components of acceleration histories at a particular floor level have been computed from the acceleration histories recorded by two sensors installed in two parallel lines in the same direction. Extended random decrement (RANDOMDEC) method has been utilized to obtain free decay responses required to form response matrices. Different time shift have been considered to assemble the original as well as delayed response matrices. Eigenvalue equation formulated using response matrices has been solved by least square technique for identification of system matrix. Structural parameters are finally evaluated using identified modal parameters and estimated mass matrix. A three dimensional finite element model of the test model with similar material properties and load asymmetricity has been numerically simulated for verification of the adopted system identification technique. Modal analysis of the test model has been carried out and modal frequencies have been compared with those of identified frequencies of the test model. The acceleration responses have been extracted from the same locations as those of the test model after conducting time history analysis of the modal considering 2% proportional damping. The peak acceleration at floor level and RMS values of floor acceleration histories are compared with those obtained from laboratory test and a very good agreement has been observed. The ITD technique is then used to identify the modal parameters of an existing asymmetric building. Different floor acceleration responses have been acquired during two earthquakes and identification of system parameters has been carried out. The records have been studied to determine the time shifts required to formulate two response matrices.

LIST OF TABLES

LIST OF FIGURES

LIST OF SYMBOLS AND ABBREVIATIONS

Symbols	Meaning
$\boldsymbol{A}$	System matrix for state space identification and ITD technique
A	Sectional area of diagonal strut
Ar	Wall opening ratio
$\mathbf{A}^T$	Transpose of $\mathbf{A}$
$\mathbf{a}$	Displacement vector
a	Width of the diagonal strut
$\dot{\mathbf{a}}$	Velocity vector
$\ddot{\mathbf{a}}$	Acceleration vector
$a_k + ib_k$	k^{th} complex eigenvalue of $\mathbf{A}$
$\boldsymbol{B}$	System matrix for state space identification
$\boldsymbol{C}$	Output influence matrix for state space identification
$\mathbf{C_a}$	Output influence matrix for acceleration
$\mathbf{C_v}$	Output influence matrix for displacement
$\mathbf{C_d}$	Output influence matrix for velocity
c	Damping coefficient
$(\frac{c}{c_c})_k$	k^{th} Damping factor
$\boldsymbol{D}$	System matrix for state space identification
D	Length of the diagonal strut
$\mathbf{\Lambda_i}$	Global mode shape matrix of structural system
$(\Delta t)_1$	Time increment between the two response matrices
$(\Delta t)_2$	Time increment in forming "transformed stations"
$(\Delta t)_3$	Time increment between the data in upper and lower halves of the response matrices
$\delta(\tau)$	Random decrement signature
E	Young's modulus of concrete/steel
E_c	Young's modulus of concrete
E_{fe}	Young's modulus of frame material
E_m, E_{me}	Young's modulus of masonry infill

$e_{x_{i,i}}$	Static eccentricity in x-axis at floor *i* with respect to storey *i*
$e_{x_{i,i+1}}$	Static eccentricity in x-axis at floor *i* with respect to storey *i+1*
$e_{y_{i,i}}$	Static eccentricity in y-axis at floor *i* with respect to storey *i*
$e_{y_{i,i+1}}$	Static eccentricity in y-axis at floor *i* with respect to storey *i+1*
F_i^a	i^{th} identified frequency for any particular sensor allocation case
F_i^b	i^{th} identified frequency for full sensor allocation case
$\mathbf{f}(a,t)$	Forcing function at time t for a particular location
f_m	Compressive strength of masonry
f_k	Frequency corresponding to k^{th} eigenvalue of system matrix $\boldsymbol{A}$ obtained using ITD
$\boldsymbol{\phi}_i$	i^{th} eigenvectors of system matrix $\boldsymbol{A}$
$\varphi_{l,i}^a$	Modal amplitude at the location *l* of the i^{th} mode of model *a*
$\varphi_{l,i}^b$	Modal amplitude at the location *l* of the i^{th} mode model *b*
$\varphi_i^{(n)}$	Mode shape values for i^{th} mode at n^{th} location
$\boldsymbol{\Phi}$	Modal Matrix
$[\Phi]$	Response matrix whose rows contain the free-response functions
$[\hat{\Phi}]$	Response matrix $[\Phi]$ delayed by $(\Delta t)_1$
g	Acceleration due to gravity
H	Storey height
$\mathbf{H}(z)$	Transfer function
h, h_{inf}	Net height of infill wall
h_{col}	Height of column
I	Moment of inertia of section
I_b	Index for full sensor allocation case
I_{col}	Moment of inertia of column
I_i	Mass moment of inertia at floor *i*
I_s	Index for a particular sensor allocation case
$\mathbf{K}$	Global stiffness matrix for symmetric-plan shear building
$\mathbf{K}_T$	Global stiffness matrix for torsionally coupled shear building
$K_{i,i-1}$, $K_{i,i}$, $K_{i,i+1}$	Stiffness submatrices
k	Stiffness of individual section

$\mathbf{k}$	Stiffness vector
k_d	Stiffness of diagonal strut
k_{do}	Stiffness of diagonal strut with opening
k_l	Lateral stiffness of infill wall
k_n	Stiffness at nth location
l	Length of infill wall
λ	Eigenvalues
λ_i	i^{th} eigenvalues of system matrix $\mathbf{A}$
$\mathbf{M}$	Global mass matrix for symmetric-plan shear building
$\mathbf{M_T}$	Global mass matrix for torsionally coupled shear building
M_i	Mass submatrix at floor i
m	Mass of a single degree-of-freedom system
N_s	Number of segments
$\mathbf{\Lambda_i}$	i^{th} modal matrix
$(\omega_d)_k$	Damped natural frequency of k^{th} mode
$(\omega_n)_k$	Undamped natural frequency of k^{th} mode
ω_j	Natural frequency of j^{th} mode
p	Number of assumed modes
PI	Performance index
R_k	Stiffness reduction
r_{inf}	Diagonal length of infill wall
r_j	Magnitude of j^{th} pole
ρ_w	Stiffness reduction factor
S	Scale factor
s	Number of time samples in each free-response function
σ_k	Damping value of k^{th} mode
ψ	Mode shape vales
ψ_{ik}	kth mode shape values at location i
$\mathbf{\Psi}$	Matrix whose columns are system eigenvectors
$\hat{\mathbf{\Psi}}$	Matrix $\mathbf{\Psi}$ with response delayed by $(\Delta t)_1$

t_d	Length of the response segments
t_{ff} , t_{inf}	Thickness of the diagonal strut
t_j	Crossing time
t_o	Initial time
τ	Time interval for free decay response
θ	Inclination of diagonal strut with horizontal floor
θ_j	Phase angle of j^{th} pole
u(z)	z - transform of input
v(t)	Noise at time t
w(t)	Noise at time t
W_{ds}	Width of diagonal strut
W_{do}	Width of diagonal strut with opening
x	Displacement
x_d	Response due to initial displacement
x_f	Response due to forcing function
x_i	Displacement response at i^{th} location
x_{ij}	Free-response of station i at time instant j
x_s	Root mean square value of response
x_v	Response due to initial velocity
$\dot{x}$	Velocity
$\dot{x}_i$	Velocity response at i^{th} location
$\ddot{x}$	Acceleration
y_k	Output vector at k^{th} location
y(z)	z - transform of output
z_j	j^{th} pole
ξ_j	Damping ratio of j^{th} mode
$\mathbf{\Gamma}$	Modal displacement vector

Abbreviations	Meaning
3-D	Three Dimensional
AR	Auto Regressive
ARX	Auto Regressive eXogenous
ARMAX	Auto Regressive Moving Average eXogenous
ASCE	American Society of Civil Engineers
BSNL	Bharat Sanchar Nigam Limited
COMAC	Coordinate Modal Assurance Criteria
Comp	Component
CVA	Canonical Variate Algorithm
DAS	Data Acquisition System
DLV	Damage Locating Vector
EMD	Empirical Mode Decomposition
ERA	Eigen Value Realization Algorithm
FEM	Finite Element Model
FFT	Fast Fourier Transform
FRF	Frequency Response Function
IASC	International Association for Structural Control
ITD	Ibrahim Time Domain
LDEF	Long Duration Exposure Facility
MAC	Modal Assurance Criteria
MOESP	Multivariable Output-Error State sPace
MSCC	Mode Shapes Correlation Constant
N4SID	Numerical Algorithms for Subspace State Space System Identification
NDE	Nondestructive Evaluation
NDT	Nondestructive Testing
NExT	Natural Excitation Technique
PC	Principal Component
PEM	Prediction Error Method
RANDOMDEC	Random Decrement
RDT	Random Decrement Technique
SID	System Identification

SHM	Structural Health Monitoring
UPC	Unweighted Principal Component
UPV	Ultrasonic Pulse Velocity
UTC	Coordinated Universal Time

CHAPTER 1

INTRODUCTION AND LITERATURE REVIEW

1.1 INTRODUCTION

The concern about the deteriorating condition of world's infrastructures mostly started from last four-five decades. A large number of causalities have been reported from various parts of the world, which are primarily due to ill-attention on the health of the structures. The loss of lives and infrastructures during various devastating natural hazards are due to collapse of civil engineering structures such as building and bridges. Several factors such as faulty design, poor quality construction material, faulty construction practice etc. have been established as causes of failure of structures. Some disastrous incidents like the accident of Aloha Airlines (USA) or the collapse of the Mianus River bridge (USA) and the Mandovi River bridge (India) are due to unsatisfactory maintenance. Collapse of Injaka bridge (South Africa) or viaduct at Hyderabad (India) due to ill-controlled construction process are examples of structural failure. Besides the above mentioned causes, aging of structures has also been observed as one of the causes of failures. The studies carried out by Balageas *et al*. [2006] based on the inspection in late 1980 showed that out of 576,000 US highway bridges, 236,000 were found to be deficient to meet the requirements of present day codes. Thus, inspection of health of structures is becoming important area for engineers to define usability of the old structures.

Numbers of experimental schemes came into existence for assessing health of structures since the beginning of 20^{th} century. In 1930s, the effort for assessment of various old structures led to the development of number of methods to evaluate likelihood of any failure in future. In many of the post accidents and post devastations instances, it was realized that monitoring of structures in the field of civil engineering, aerospace

engineering, mechanical engineering etc. were mandatory to observe the health of a structure for facilitating immediate access of emergency teams. The condition assessment of structures is gradually becoming a regular practice at present. The adopted experimental schemes are based on either periodic or continuous monitoring of the health of the structures and is termed as structural health monitoring (SHM). SHM helps in identifying damage of structures by identifying the changes in properties of the structures. SHM methodologies have been classified depending on various factors such as level of identification, type of experimental data used, type of representative models used etc. Rytter [1993] in his Ph.D. dissertation classified SHM techniques into four levels of identification. According to him, SHM techniques may be assigned one of the 4 different levels as shown in Table 1.1. He further classified SHM techniques according to the type of data used, type of excitations and model used in the identification.

Table 1.1 Classification of structural health monitoring techniques [Rytter 1993]

Parameter	**Classification**
Level of identification	Level I: Existence of damage
	Level II: Existence of damage and location
	Level III: Existence of damage, location and quantification of damage
	Level IV: Existence of damage, location and quantification of damage and life expectation of the structure
Data used	Time domain
	Frequency domain
Excitation	Known excitation
	Unknown excitation
Identification model	Structural model needed for identification
	No structural model needed for identification

Further, in order to enhance the effectiveness and reliability of SHM, the advancement in information technology and wireless communications were integrated. Many methods were developed or improved including Wireless and Information Technologies (IT) based strategies with the goal that could lead to the development of commercial, cost-effective, yet reliable SHM systems. SHM methods are primarily based on test data acquired from the structures under consideration.

In the Design Manual No.2 [2001] prepared by Intelligent Sensing for Innovative Structures (ISIS), Canada, SHM has been broadly categorized based on testing procedures, namely static field testing and dynamic field testing. Static field testing and dynamic field testing philosophies are adopted in periodic as well as continuous monitoring. Static field testing facilitates in-situ assessment of damage in structures, while dynamic field testing facilities are used to acquire vibration characteristics to estimate modal properties of structure. The basic scheme of testing based structural monitoring of civil engineering structures may be represented in the form of a tree as shown in Fig. 1.1.

As the structures degrade or experience damage during natural disasters, they no longer behave according to the original design. Damages are accompanied by the changes in stiffness and hence dynamic responses also undergo changes. Many researchers assumed that the building degradation is directly linked to the degradation of columns, joints, beams and breakage of braces etc. in the last two decades, advancement in technologies and evaluation methodologies, the developments of new, reliable, scientific and efficient SHM techniques have taken place. Study on SHM may be categorized under the following subsections based on the adopted methodologies.

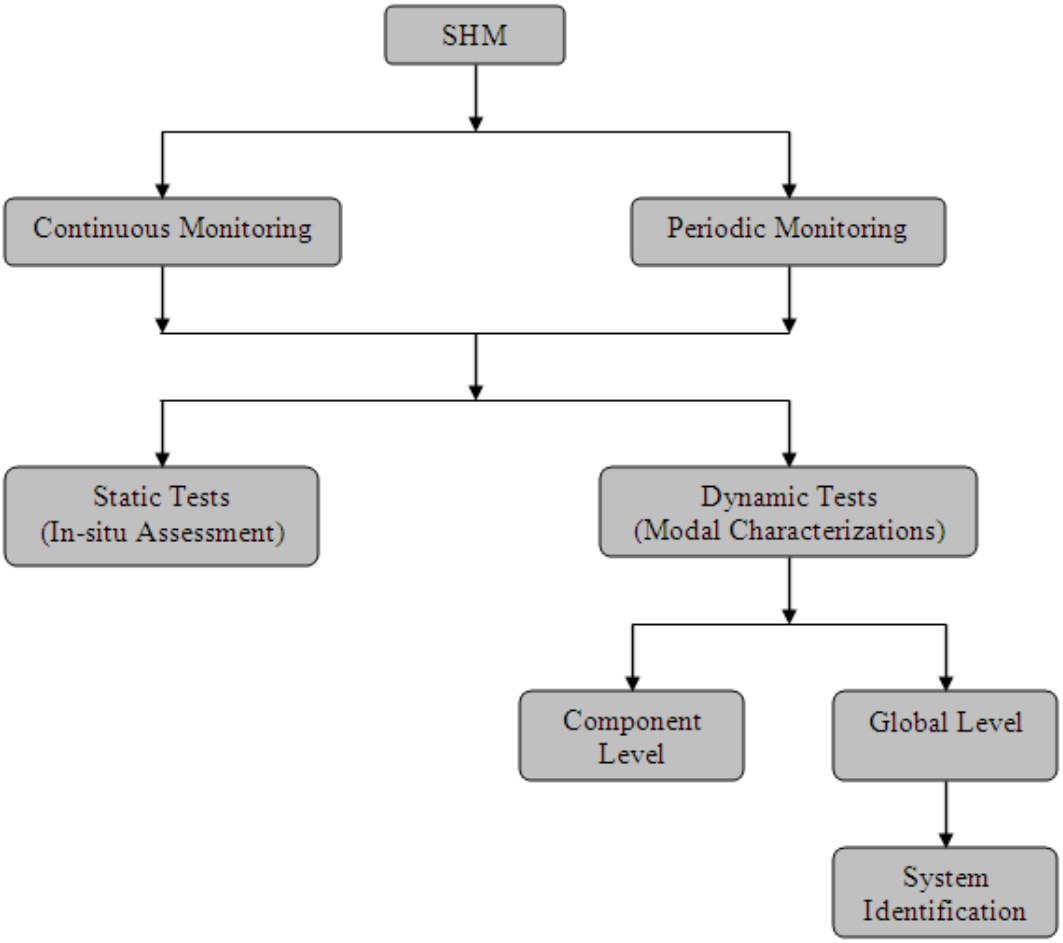

Fig. 1.1 Structural health monitoring tree

1.1.1 Conventional Nondestructive Testing (NDT) Technique

Several Nondestructive Evaluation (NDE) techniques which are known in medical diagnostics, aerospace, geophysical applications and in inspection of metals have been adopted in the condition assessment of structural systems. Nondestructive Testing (NDT) of concrete structures is becoming increasingly important due to the aging and deterioration of infrastructures like bridge, buildings, ports, harbors etc. Scarcity of funds available for repair or replacement of structurally deficient or functionally obsolete structures led to the development of more advanced NDT techniques which could enable rapid, cost efficient and reliable condition assessment of existing infrastructure.

Incorporation of quantitative results of standardized NDT techniques in infrastructure management systems have provided feedback needed for the detection and identification of deficiencies and setting up priorities for repair, retrofitting or replacement actions. Traditionally used damage detection methods are based on either visual inspection or localized experimental methods such as surface hardness method, ultrasonic methods, eddy current methods, radiograph methods etc. Hoke from United States applied for the first patent on magnetic inspection method in 1919. During World War II, accelerated research regarding NDT resulted in development of ultrasonic pulse velocity (UPV) method. In 1938, Powers from United States established the fundamentals of resonant frequency testing method by matching the musical tone created by concrete specimen. In 1948, a Swiss Engineer, Ernst Schmidt, developed a test hammer for measuring the hardness of concrete based on rebound principle. Half cell potential method became very popular for determination of the electrical potential of reinforcement in concrete. Likewise many more NDT methods were developed as needs towards fulfillment of practical requirements increased for assessment of health of structures. However, it may be noted that all of these methods are suitable for conditions assessment of structure at component level and should be accessible for testing.

1.1.2 Vibration Characterization Based Technique

The changes in modal properties of structures play important role in identification of damage in structures. As the natural frequencies are directly related to degradation of stiffness of a structure, changes in natural frequencies can be used to detect existence of damage. Similarly, changes in mode shapes helps in identifying location of damage in a structure. Indices like modal assurance criteria (MAC) and coordinate modal assurance criteria (COMAC) are used by various researchers for identification of locations of damage. The changes in natural frequencies and mode shapes can be evaluated by

studying the vibration characteristics of the structures. However, as the structures become larger and more complex, more reliable and efficient methods are needed to monitor the health of the structures. Hence, newer methods have evolved, which utilizes vibration data from a structure for the development of a mathematical model representing the physical system. This enables engineers to extract modal and structural parameters of a structure. Based on modal parameters, it is possible to locate damage or deterioration in a structure. These methods have been named as *System Identification* (SID). The models are developed following Time-Domain and Frequency-Domain approaches. In time domain approach, dynamic systems are typically modeled by continuous-time or discrete-time equations. In continuous-time models, the input-output relations are described by differential equations, but the same are represented by algebraic equations in the frequency-domain. In discrete-time models, the relationships are described by linear difference equations. Among the available SHM methodologies, system identification based techniques have emerged as a powerful and accurate technique. System identification involves number of steps like obtaining input, output and noise signals from structures under investigation. The data are re-sampled, if required and filtered through digital filters. The mathematical model is thereafter built with processed input and output data. According to Juang [1994], techniques to identify a mathematical model from measured data typically contain two steps. First, a family of candidate models is chosen and then the particular member of the family is determined which satisfactorily maps the observed data and there after the selected model is transformed to the desired form for further use. Unlike NDT techniques, SHM through vibration based studies are suitable for monitoring properties of structures in component as well as global level. The properties of simple structures are generally evaluated by studying acquired vibration characteristics. The global properties of large and complex structures are better identified through system identification technique using vibration signatures from the structure. Number of

parametric and non-parametric system identification techniques have been so far been developed for identification system parameters of structures. Non-parametric system identification techniques such as Natural Excitation Technique (NExT), eigen value realization algorithm (ERA), Hilbert–Huang transformation, Damage index method, Flexibility based damage characterization technique, Bayesian system identification, Statistical model updating methodology etc. have been used by researchers for identification damages in structures. Similarly, parametric identification techniques such as Auto Regressive (AR), Auto Regressive eXogenous (ARX) model, Auto Regressive Moving Average eXogenous model (ARMAX), Box-Jenkins model, State Space Models etc. have also been utilized by the researchers for identification of modal parameters of damaged and undamaged structures. All of these methods are based on acquired acceleration histories from structures. However, this requires good supporting sensors as well as data acquisition system to acquire vibration responses. Thus, additional research is needed towards the development of cost effective and accurate sensor technology. A detailed survey on available literatures on SHM methodologies is presented in the following subsections.

1.2. LITERATURE REVIEW

Numerous literatures are available on SHM methodologies for detection of existence, location and severity of damage. Design manual [2001] gives wide idea about health monitoring of civil engineering structures where descriptions of damage assessment using both static and dynamic field tests are elaborated. Monitoring of health of structures is generally carried out broadly on the basis of background mentioned in Table 1.1. Depending on the type of structure to be studied, appropriate monitoring techniques may be decided. Literature review presented in this section has been grouped into following categories:

i) Traditional damage detection techniques

ii) Conventional techniques based on vibration characteristics

iii) System identification based techniques

1.2.1 Traditional Damage Detection Techniques

The field of damage detection is very broad and encompasses both local and global methods. The traditional damage detection methods are generally limited to local methods which are based on static field tests. Evolution of non destructive testing (NDT) techniques based on advancement in instrumentation has made it easier to detect any local damage in civil and mechanical structures. Some of the recent literatures which use NDT to assess health of a structure or structural component are discussed.

Shah *et al.* [2000] described that ultrasonic longitudinal wave (also called L-wave or P-wave) signal transmission (attenuation) measurements were sensitive to the presence of damage in concrete. They carried out measurements of ultrasonic pulse on concrete specimen to study sensitivity of distributed cracks in the specimen.

Hemalatha and Mary [2000] proposed an empirical expression to determine depth of inclined crack in concrete with results obtained from UPV testing. However, the derived expression could assess the depth of crack with a tolerance of ±5 mm for crack depth and $\pm 3^0$ for inclination.

Brandes *et al.* [2000] tried to study the present condition of old structures for further use. They adopted radiographic inspection strategy to inspect old steel bridges to determine fatigue life and fatigue resistances. They observed the riveted portions of number of bridges in normal as well as loaded condition through radiographic inspection and found that cracks were more prominent under loaded condition.

Malhotra and Carino [2004] in their book, compiled all the possible methods to determine concrete quality. They termed concrete as highly non-homogeneous composite material and unsuitable to verify with traditional nondestructive testing techniques as easily as steel. They mentioned the procedures of measuring surface hardness, ultrasonic pulse velocity, resonant frequency, acoustic emission etc. along with pullout and pull-off tests to measure concrete quality. They also described X-radiography and radiometry method to determine anomalies in concrete. Methods to evaluate corrosion and penetration resistance to non-destructively measure compressive strength of concrete nondestructively were described. The text book described various NDT methods to qualitatively assess concrete and detect damage in concrete specimen.

Talukdar and Borsaikia [2005] showed the experimental findings of ultrasonic pulse velocity test on concrete cubes during progressive compressive loading. Concrete cubes were tested under progressively increasing compression loading till failure, during which the pulse velocity was recorded at each increment of the load. The pulse velocity measurements during the progressive loading revealed that the pulse velocity increases slightly during the initial stage of compression. Thereafter, the pulse velocity decreases due to the development of micro-cracks. They concluded that the UPV can be used as indicator to determine the growth of crack in concrete.

Basheer [2005] mentioned various techniques useful for health assessment of RC structures. He described the classifications of health assessment techniques and tried to explain about the systematic way to carry out assessment of RC structures. Based on mechanism of action, he classified the deterioration of concrete as abrasion/erosion, alkali-aggregate reaction, chemical attacks and corrosion of reinforcement, cracking, freezing and frost damage.

In all of the above mentioned studies it has been observed that the tentative location of the damage is known a priori and the portion of the structure being inspected is readily accessible. Hence, visual inspection generally precedes such NDT evaluation. Visual inspection is the most common technique for damage identification and is always required prior to any nondestructive evaluation. The consistency of visual inspection however remains questionable, time consuming and prone to human error.

1.2.2. Conventional Techniques Based on Vibration Characteristics

Natural frequencies are global property of any structure and hence the shift in natural frequencies indicates existence of damage. Similarly, dynamic responses of any structure have also been utilized for visualizing any degradation. Lifshitz and Rotem [1969] proposed use of vibration measurements for detecting damage, which is considered as the first research paper in the concerned area. They tried to determine the dynamic moduli and relate the same to the frequency shift for particle-filled elastomers.

Begg, *et al.* [1976] observed that locating damage from changes in frequencies alone was impractical. They used scaled offshore structure model for determining the resonant frequencies and could observe around 10% increase in frequency for addition of one extra bracing member in the structure. However, severance of a connected member showed about 5-30% reduction in resonant frequencies. They concluded that bending modes were more indicative about the presence of cracks.

Vandiver [1977] used the concept of changes in natural frequencies to identify damage of an offshore light station tower. He considered frequencies associated with first two bending modes and one torsional mode of the numerically simulated model of the tower. He studied the behavior of the numerical model by systematically removing members. He found greater than 1% reduction in frequencies on removal of members individually. The

changes in resonant frequencies that are likely to take place due to formation of rust in the members were also studied with the help of the numerical model.

Adams, *et al.* [1978] studied axial vibration modes for identification of damage of structure which can be represented as one-dimensional. They concluded that changes in resonant frequencies associated with two modes are sufficient for detection of damage. They could properly correlate the damage with receptance functions on either side of damage.

Kenley and Dodds [1980] carried out damage detection studies on an old offshore platform. Complete damage of diagonal member could changes in resonant frequencies. They also stated that changes in resonant frequencies occurred when the changes in overall stiffness were more than 5%.

Gudmundson [1982] presented a first order perturbation method that predicts the changes in resonant frequencies of a structure resulting from cracks, notches or other geometrical changes. The eigenfrequency changes due to a crack are shown to be dependent on the strain energy of a static solution which is easily obtainable for small cracks and other small cut-outs. The method has been tested for three different cases, and the predicted results correlate very closely to experimental and numerical results.

Nataraja [1983] programmed to monitor an offshore platform for a two-year period. He could identify only lowest frequencies accurately throughout the monitoring period. He studied vibration signatures from the structure and concluded that measured acceleration can only be used to detect global changes in the structures.

Qian *et al.* [1990] studied a beam containing edge crack. They tried to determine eigen frequencies for different crack depths and locations. They proposed a relationship for determining crack position based on crack size and eigencouple. They observed effects of opening and closing pattern of the crack during the shaft rotation and found difference in

mechanical behaviour while closing and opening. They found reduction in the difference between the displacement response of the beam without crack and with crack while closing effect was considered. The proposed method is suitable for complex structures only if the stress intensity factors are known *a priori.*

Rizos *et al.* [1990] tried to measure flexural vibration characteristics of cracked beam for the evaluation of location and depth of transverse crack. They validated experimentally observed characteristics through an analytical model. They attempted to find out location and estimate depth of crack from measured amplitudes at two points of structure vibrating at one of the natural modes. Further, crack depths were observed to be related to the change in natural frequencies of the first three harmonics of the structure. This method could not be used for accurate results for very small crack $a/H<0.10$, where a is the crack depth and H is the depth of the structural element.

Pandey *et al.* [1991] introduced curvature mode shape for detection of location of damage in a beam under simply supported and cantilever conditions. They suggested that the change in the curvature mode shapes increase with increase in size of damage. They used finite element analysis to obtain displacement mode shapes of damaged and undamaged models and then by using central difference approximation they found curvature mode shapes. They found that the absolute changes in the curvature mode shapes were localized in the region of damage.

Richardson and Mannan [1992] assumed that the changes in stiffness were one of the factors for damage quantification. They tried to determine the pre-damage mode shapes, pre-damage frequencies and post-damage frequencies to identify the damage through a sensitivity equation. They used stiffness sensitivity method to locate induced cracks in a plate based on measured mode shapes and resonant frequencies. They found the largest stiffness changes in the nearby region of a fault.

Armon *et al.* [1994] studied about reduction in natural frequencies due to presence of slots and cracks in a beam using rank-ordering of the modes through non destructive testing. They used aluminium and perspex beam damaged at different location and with varying magnitudes for experimental investigation. They found good agreement of theoretical and experimental results. However, presence of small cracks was insensitive to the rank-ordering of modes and hence possibility of evaluation of such damage magnitude is ignored in this method.

Narkis [1994] studied dynamics of cracked simply supported beam for either bending or axial vibration. He represented crack between two segments of a beam through an equivalent spring. He came up with algebraic expressions relating the natural frequencies and crack characteristics. Finally he used these expressions to determine crack characteristics from observed first two natural frequencies of the beam. This was verified through FEM models. The method is simple and accurate as demonstrated.

Salawu and Williams [1994] evaluated damage by comparing mode shapes and modal curvatures. They could observe that the relative difference in mode shape measure was not a good indicator of damage. They pointed out that the most important factor in this approach was proper selection of modes to be analysed.

Salawu [1995] applied integrity index method for nondestructive assessment of a concrete highway bridge. They presented a review of various methods proposed for detecting damage using natural frequencies. The global damage integrity index was evaluated from weighted ratio of damaged natural frequency to the undamaged natural frequency. The weights were used to reflect the relative sensitivity of each mode to the damage event. They further calculated local integrity index to locate defective areas.

Doebling *et al.* [1996] provided an overview of the methods to detect, locate, and characterize damage in structural and mechanical systems by examining changes in

measured vibration response. They mentioned the forward problem which usually falls into the category of Level 1 damage identification, consists of calculating frequency shifts from known type of damage. They also defined the inverse problem as level 2 or level 3 damage identification, consisting of calculating the damage parameters, e.g. crack length and/or location, from the frequency shifts. Nandwara and Maiti [1997] presented a study for detection of location and size of a crack in stepped cantilever beam. They modeled crack by a rotational spring and evaluated first three natural frequencies and corresponding modes. They established the location of damage as the point of intersection of any three natural modes associated with natural frequencies of the structure.

Ratcliffe [1997] developed a procedure for damaged detection using a 1-D finite element model of a beam. He applied a finite difference approximation of Laplace differential operator to the mode shapes to localize the damage. For a less severe damage he used further processing of the Laplacian output to localize the damage. He also concluded that lower modes were more sensitive than higher modes in damage detection. This procedure is however not well suited for complex structures as it is developed and examined on one dimensional finite element model.

Wahab and Roeck [1999] applied the concept of change in modal curvatures to detect damage in prestressed concrete bridge. They used simply supported and continuous beams containing damaged parts at different locations for experimental investigation. They could draw some important conclusions concerning the computation of modal curvatures. They introduced “curvature damaged factor” as a damage indicator and found that the modal curvatures for the lower modes were more accurate than those of the higher modes.

Maeck and Roeck [1999] presented a technique to determine dynamic stiffness of a reinforced concrete beam in the undamaged and damaged state. In the experimental programme, they used a concrete beam of 6 m length and applied gradually increasing

load for producing crack. Then, dynamic test were carried out to obtain modal parameters. They elaborated the technique to derive direct stiffness from measured displacement derivatives, dynamic bending stiffness from modal curvatures and torsion stiffness from modal torsion rates. They concluded that the technique is advantageous as no numerical model was included to obtain results.

Shah *et al.* [2000] presented an approach for monitoring fatigue-induced crack in concrete specimens. They carried out fatigue test on concrete prisms and could correlate changes in the vibration frequency to remaining fatigue life of the specimen.

Vestroni and Capecchi [2000] illustrated both forward and inverse problem through finite element models of simply supported beams. They represented damage by a more or less concentrated decrease in stiffness. They adopted two different procedures for detection of damage and its location based on modal equation error and response equation error. These two approaches were demonstrated through studies on experimental and analytical response quantities of damaged and undamaged simply supported beams. They studied first five modes of a simply supported beam and defined location of damage as the point of intersection of all the five modes. They concluded that the modification of frequencies is the main criteria for detection of damage.

Farrar and Hoon [2000] mentioned that vibration-based damage detection is one of the important statistical pattern recognition paradigms for monitoring of health of structures. They tried to differentiate between damaged and undamaged structure by observing the pattern of modal properties of the structures.

Saavedra and Cuitino [2001] presented theoretical and experimental dynamic behavior of different multi-beams systems containing transverse crack. They used strain energy density function to evaluate the additional flexibility that a crack generates in its vicinity. They carried out FEM analysis of a crack system using a cracked finite element stiffness

matrix based on this evaluated flexibility. They noticed significant changes in the frequency spectrum of the steady state vibration with peaks at crack position. However, the principal inconvenience of this method is that the crack has small effects for moderate crack size and it is very difficult to determine the mode shape of an engineering structure.

Yang *et al.* [2001] investigated influence of cracks on structural dynamic characteristics vibration of a beam with open crack using numerical model. They used Galerkin's method to solve for the frequencies and vibration modes of a cracked beam. They plotted the frequency contours and the intersection of contours from different modes was used to identify the crack location and depth.

Khiem and Lien [2001] worked on transfer matrix method and rotational spring model of crack. The transfer matrix helps in analyzing the natural frequency of beam with an arbitrary number of cracks. Numerical computation was carried out to investigate the effect of crack, the number of cracks and boundary conditions on natural frequencies of a beam.

Sinha *et al*. [2002] presented a crack modeling approach in beams undergoing transverse vibration. They used Euler-Bernouli beam elements with small modification to the local flexibility in the vicinity of the cracks. They illustrated the approach with experimental data obtained from a beam having multiple cracks.

Dutta and Talukdar [2004] carried out eigen value analysis using Lanczos algorithm for accurate evaluation of modal parameters. They observed the changes of natural frequencies between damaged and intact model of bridge deck. Numerical studies were carried out to demonstrate the necessity of adaptive eigen frequency analysis and also tried to localize the damage using curvature of the mode shapes.

Borsaikia *et al.* [2006] carried out vibration tests on intact and notched concrete prisms to evaluate the changes in frequencies due presence of crack. They used resonant frequency

tester to evaluate changes in resonant frequencies for different concrete prisms with different crack depth. They studied the FRF (Frequency Response Function) obtained from a FFT analyzer for evaluation of curvature differential values to see the effect of depth of notch in the prism specimen.

Detailed reviews of these literatures have revealed that shift in frequencies can be utilized for distinguishing between damaged and undamaged specimens. However, these literatures are mainly confined to the methods which deal with detection of damage in simple structures and structural elements. Behavior of complex structures depends on the characteristics of all the individual structural elements associated with the structure. The methods described in the reviewed literatures are basically based on direct estimation of modal properties of structures without using any mathematical model based on experimental data. Therefore, global and computationally efficient methodologies which deal with methods based on mathematical model using experimental or simulated data are needed to facilitate detection, quantification and location of damage in complex structures like building and bridges.

1.2.3 System Identification Based Techniques

Monitoring health of structures or online (near real-time) data collection mode helps in eliminating the uncertainties in the integrity of the structure and also provide valuable information to decision makers after a major event. SHM of civil structures through System Identification techniques has received significant attention by researchers in recent days. Among all technique of SHM, system identification techniques are found to be scientifically efficient and reliable. Ho and Kalman [1965] and Åström and Bohlin [1965] initiated works on identification system parameters of structures. Thereafter system identification is dominating the research of SHM. The first paper described solutions to state-space realization, stochastic realization and subspace identification theories.

Similarly, the second paper laid the foundations for Maximum Likelihood methods based on parametric input-output models.

Pappa and Ibrahim [1981] tried to check the accuracy of Ibrahim Time Domain (ITD) algorithm in extracting the modal parameters from free-response functions. An isotropic uniform-thickness plate was simulated and free response time histories were collected from 65 different positions simultaneously. Only 15 plate modes were arbitrarily assigned to form the free response functions and the results were checked by mode shapes correlation constant (MSCC).

Ibrahim and Pappa [1982] studied the ability of ITD technique for identification of complete modal parameters from free-response time histories of a computer simulated rectangular plate and an actual long duration exposure facility (LDEF) space shuttle payload. They used 225 measurement stations for simulated plate and 142 measurement stations for experimental responses from LDEF space shuttle payload. They could identify first few frequencies and damping ratios of the plate and LDEF The use of significantly oversized model helps in increasing the identification accuracy. The suitability of mode shapes correlation constant (MSCC) was explained with the different sets of measurements of the same structure and the accuracy of the identification process was verified.

Ibrahim [1983] presented a technique to compute normal mode shapes from identified complex modes. Normal modes are defined as modal vectors whose phase angles are either 0.0 or 180.0 deg. Such modes exist for extremely simple structures that do not need any modification anyway. They also exist for structures with no damping or structures tailored with proportional damping, none of which represents today's complex structures. Unlike normal modes, complex modes may possess any phase angle distribution. They described the methodology to compute normal modes from complex modes through

numerical example of a simply supported beam with 10 degree of freedom. Two different approaches were demonstrated for determining normal modes from identified complex modes, where in the first one they used oversized mathematical model and in the second they assumed modes that satisfy the equation of motion.

Yang and Everstine [1983] investigated the basic of the Random Decrement analysis technique and could determine the natural frequencies and damping ratios of different structural systems with recorded responses. The observed results were validated through analytical studies of the different structural systems.

Chen [1984] described about the analytical study of a physical system that roughly consists of four parts: modeling, development of mathematical-equation description, analysis and design. He explained about mathematical expressions of a system with linear space and operator used for identification of modal parameters. He also described about stability of linear system.

Ljung [1987] did significant contribution in the form of a text book by defining system identification as a method of building mathematical models for dynamical systems based on observed data from the systems. He described about wide application of system identifications techniques. He presented the whole book in three parts, where in part I, he mentioned about systems and related models. In part II, he explained about nonparametric time and frequency domain methods and parameter estimation methods. Lastly in part III, he included objective and experiment design for applying system identification techniques for studying scaled laboratory models.

Juang [1994] contributed immensely on system identification in the form of a text book. He described about various identification methods. The book covers different mathematical models based on both time-domain and frequency-domain methods along with system realization theory.

Ghanem and Shinozuka [1995] reviewed a number of structural-identification algorithms and applied them to identify structural systems subjected to earthquake excitations. The performance of various identification algorithms was critically assessed by applying to experimental data obtained in controlled laboratory conditions. They have expressed a generic mathematical model suitable for most physical system and thereafter evaluation of parameters used in identification in conjunction to that. They described about the Extended Kalman Filter algorithm that derived from the state-space form of the differential equation of motion. They also used maximum likelihood, recursive least squares, recursive instrumental variable for comparing the best one for identification. They used acceleration records from two building models subjected to various loading conditions in various identification algorithms to obtain the best among them.

Overschee and Moor [1996] proposed subspace identification approach of linear system and implemented the same in practical applications. They explained about various geometric tools used in system identification. They described about deterministic, stochastic identification and combination of deterministic-stochastic identification process. The evaluation of system matrices was described properly along with number of subspace identification algorithms. They presented principal component (PC) algorithm, unweighted principal component (UPC) algorithm, canonical variate algorithm (CVA) and their usefulness in stochastic identification. Some combined deterministic-stochastic algorithm like Numerical Algorithms for Subspace State Space System Identification (N4SID), Multivariable Output-Error State sPace (MOESP) were also explained in conjunction with simulation examples.

Nagarajaiah [1999] adopted frequency domain system identification technique to identify frequencies and damping ratios of 8-storey base isolated USC hospital building with recorded responses. He used cross spectrum and power spectrum of recorded response to

estimate transfer functions. Frequencies and damping ratios were evaluated for first few modes in EW and NS directions from extracted complex poles.

Chaudhary [2000] tried to find out system parameters from seismic accelerations recorded on a base-isolated bridge. They used two steps system identification method, one of which entails identification of complex modal parameters of a non-classically damped base-isolated bridge-pier-pile-foundation system along with development of theoretical background. In the second step a global search scheme was introduced to identify the structural parameters of the system corresponding to the identified modal parameters. They applied the proposed identification method to two base–isolated bridges in Matsunohama Viaduct, Japan using recorded acceleration histories during 1995 Kobe earthquake. They could demonstrate the affect of friction in metal bearing from the identified bearing stiffness.

Nagarajaiah and Xiaohong [2000] studied structural responses of base-isolated USC hospital building acquired during Northridge earthquake. The objective of this study was to evaluate the seismic performance of the base-isolated USC hospital building based on the 1994 Northridge earthquake. They developed a nonlinear analytical model of the USC hospital building for verification of identified system parameters. Parametric identification methods were used to obtain natural periods and damping ratios from the transfer functions determined using nonparametric methods.

Ueng *et al.*[2000] used ITD technique to calculate the modal frequencies and damping ratios for a seven storey torsionally coupled using extracted numerical responses under ambient random excitation. They applied extended random decrement (RANDOMDEC) method to obtain the free decay signatures from the extracted response measurements. They demonstrated the interpolation method to estimate the modal displacement at

different locations without measured responses at those locations. The method also demonstrated its suitability for identification of system without any input excitation.

Caicedo [2001] described two structural health-monitoring methodologies. The first methodology comprises of Natural Excitation Technique (NExT) and Eigensystem Realization Algorithm (ERA) for identification of modal parameters of a structure. Least square solution of eigen value problem was carried out to evaluate structural parameters. He tried to identify the damage by comparing the stiffness of the undamaged structure with the damaged structure. In the second methodology he tried determine the inter storey transfer functions using acceleration data of each storey. The damage in the structure was detected by identifying changes in these transfer functions. The extent of damage was obtained by comparing stiffness values of the damaged and undamaged structure. Verification of the technique was done by carrying out experiments in Washington University Structural Control and Earthquake Engineering Lab.

Sohn and Farrar [2001] demonstrated the applicability of parametric system identification through eight degrees of freedom spring-mass system using a two-stage prediction model. The prediction error method (PEM) was considered as combination of AR and ARX techniques. First they tried to normalize the acceleration time histories recorded from the structure and thereafter determined the reference signal which is closest to a newly obtained signal from an ensemble of signals recorded from the undamaged state of the structure. The residual error, which is the difference between the actual acceleration measurement for the new signal and the prediction obtained from the AR-ARX model developed from the reference signal. The damage sensitive feature i.e. residual error is more prominent with the data obtained from the sensor instrumented near the actual damage location.

Lei *et al.* [2003] proposed a damage diagnosis approach using time series analysis of vibration signals. The benchmark problem designed by the ASCE task group on health monitoring was used to explore and verify the damage detection scheme. The damage detection approach was modified to consider the influence of excitation variability and the orders of the ARX prediction model on the originally extracted damage-detection feature. Residual error of a new signal from an unknown structural condition associated with the prediction model was compared with those of signals from the undamaged structure in the damage decision. The applicability of the modified approach was investigated using various acceleration responses generated with different combinations of structural finite element models, excitation conditions and damage patterns in the benchmark study.

Caicedo [2003] proposed a methodology for identification of system parameters of cable-stayed bridges and high rise buildings. This work includes detail description of the technique and its implementation on IASC-ASCE SHM benchmark building and Bill Emersion Memorial Bridge. NExT and ERA were used to identify the natural frequencies and mode shapes of the structures. Then, the least squares solution of the eigenvalue problem was carried out to determine structural parameters. Damage has been identified by finding changes in the identified structural parameters over time. The study also includes implementation of the technique to laboratory test model of a cable-stayed bridge.

Caicedo *et al.* [2003] described the methodology of system identification for different types of structural systems. They put thrust on studies related to identification of system parameters of flexible structures such as cable-stayed bridges. They tried to propose and experimentally verify a structural health monitoring methodology for large structures. They also validated identification algorithms like NExT in conjunction with ERA through study on a scaled laboratory test model.

Swartz [2004] mentioned about active sensing system in system identification. He defined various active sensing parameters for structural health monitoring. He reviewed about Piezoelectric Ceramic Transducers, Piezoceramic Composite actuators, and Fibre Optics.

Lynch [2004] introduced the concept of linear classifications of poles obtained from the parametric identification of a structure. Their basic emphasis was on active sensing system and application of active sensing in cantilevered aluminium plate to determine damage by hack saw cuts. Piezoelectric pads were used as a tool for active sensing device and data were used in damage detection algorithms. Discrete-time transfer function poles of the system identification were plotted upon the discrete- time complex planes (z plane) which were treated as powerful graphical tool since location of poles tied to the frequencies and damping ratios.

Johnson *et al.* [2004] studied Phase I IASC-ASCE Structural Health Monitoring Benchmark Problem using simulated data. They used $1/3^{rd}$ scale laboratory test model of steel building having different damage patterns. Two analytical models of shear buildings one having 12 DOF and other having 120 DOF were considered as examples for SHM.

Yuen *et al.* [2004] presented a two stage structural health monitoring methodology and applied it to the Phase-I benchmark study sponsored by the IASC-ASCE Task group on structural health monitoring. They considered 4 DOF linear shear building in case 1-3 damage identification and 12 DOF linear shear building in case 4-6 while doing system identification study. Using MODE-ID modal identification procedure, modal properties like modal frequencies and damping ratios were identified for both damage and undamaged cases in stage 1. In the 2^{nd} stage, model updating was emphasized using the results obtained in stage 1.

Lam *et al.* [2004] applied a Statistical Model Updating Approach on Phase-I of the IASC-ASCE Structural Health Monitoring Benchmark Study utilizing the measured vibration

responses of the structure without any knowledge of the input excitation. Their basic focus was to observe the stiffness reduction due to damage through a statistical model updating methodology. They explicitly emphasized on the important issues like measurement of noise, modeling noise, lack of input measurements, and limited number of sensors. Bayesian identification approach was utilized for statistical model updating methodology and different damage cases were treated with different class of models. It is understood that appropriate class of model needs to be used for different class of damage pattern for identifying proper parameters.

Hilmi *et al.* [2004] proposed an approach which includes two well–defined phases such as identification of a state space model using Observer/Kalman (OKID) filter identification algorithm and identification of modal parameters based on realized state space model. In the first phase, they considered ERA and a nonlinear optimization approach based on sequential quadratic programming techniques to obtain a state space model. In the second phase, identification of the second order dynamic modal parameters from the realized state space model has been carried out. Investigation on the changes of second order parameters (mass, damping, and stiffness matrices) was observed by studying both reference and damaged model. An extensive numerical analysis, along with the underlying theory, was presented in order to assess the advantages and disadvantages of the proposed identification methodology. They concluded that only one sensor-actuator collocated pair and knowledge of sensor and actuator locations are essential to determine location and extent of damage in a structure and the same was validated by numerical examples.

Natural excitation technique in conjunction with eigen value realization algorithm (ERA) was used for identification of system parameters of four story scaled steel building with simulated data by Caicedo *et al.* [2004]. The focus of the problem was on simulated acceleration response data from an analytical model of an existing physical structure. They mentioned three step techniques such as obtaining cross-correlation functions from forced

vibration data, treating cross-correlation functions as free vibration data and thereafter identifying modal parameters as well as structural parameters. They tried to determine the location and severity of damage by comparing the results of modal parameters and stiffness parameters for both damaged and undamaged models. For limited sensor case, they tried to determine mode shape values using an iterative approach by relocating the available sensors and keeping the reference sensor in the same position.

Yang *et al.* [2004] used an approach that includes empirical mode decomposition (EMD), the random decrement technique (RDT) and the Hilbert-Huang transform for identification of natural frequencies and damping of in-situ tall building based on ambient wind vibration data. The only noisy acceleration data was processed through EMD method to determine the response of each mode. Then, RDT was used to obtain the free vibration response and finally Hilbert-Huang transformation was applied to each free vibration modal response to identify natural frequencies and damping ratios of in-situ tall building. They applied this methodology using simulated response data corrupted with noise in a 76-storey benchmark building. They used both along wind and across wind vibration data for identifying parameters and found the approach very effective in parametric identification scheme.

Yang *et al.* [2004] in another instant used to gather information of damage such damage spikes and damage time instants from measured data. They tried to detect damage spike and thereby damage time instants and damage locations with help of EMD. Later on, they used EMD and Hilbert transform to detect damage time instants and evaluated modal parameters such as natural frequencies and damping ratios before and after damage. They applied these two methods to benchmark problem established by the ASCE Task Group on Structural Health Monitoring with computer simulation.

Barroso and Rodriguez [2004] applied damage index method to detect the location and severity of damage of a structure. They used first generation benchmark problem established by the ASCE Task Group on Structural Health Monitoring and modal parameters were identified using frequency domain decomposition (FDD). The method was suitable to determine the state of only highly damage patterns.

Xu and Chen [2004] applied EMD method for identifying structural damage caused by sudden change in structural stiffness through experimentally acquired acceleration histories from shake table test of three storey laboratory test model.

Hera and Huo [2004] used wavelet approach to identify and study modal parameters that could indicate any structural damage. They also tried to define the damage regions using ASCE structural health monitoring benchmark data. They considered a four story prototype building structure provided ASCE Task Group to generate simulated response data using a FEM program under simulated stochastic wind loading. Wavelets analysis was used to identify induced damage and time when the damage occurred. For on-line application they could determine the damage region by the spatial distribution pattern of the observed spikes. However, the wavelet damage spike is not suitable in general for cumulative damages over relatively long period such as those caused by fatigue and corrosion.

Chakraverty [2004] presented a procedure to identify the structural parameters, viz. mass and stiffness matrices, from the model test data for multi-storey shear building. Holzer criteria was implemented to shear building to estimate the global mass and stiffness matrices when measurement points are less than the total number of structural degrees of freedom. They divided identification process into two parts: analysis of recorded data and estimation of modal parameters. Thereafter assessment of the damage in structure has been made. They considered building with second '*n*' standard floors, i.e. floors with the same

mass and stiffness, to determine coefficient relating mass and stiffness to use in the mathematical equation to identify mode shapes.

Furukawa *et al.* [2005] used Prediction Error Method (PEM) in conjunction with non-linear state space models for system identification of a base-isolated building. They considered variety of nonlinear restoring force models including multiple shear spring (MSS) model and conducted several identification runs based on bidirectional recorded seismic responses to evaluate the accuracy of the selected models.

Flexibility based damage characterization technique in context with Phase I of the benchmark study developed by the IASC-ASCE SHM Task Group. The methodology was used by Bernal and Gunes [2006] to identify the system parameters of structures. In the study, they divided the context in three sections wherein first the extraction of flexibility matrices for both deterministic and stochastic inputs, secondly the changes in flexibilities and finally quantification of damage were exercised. Damage locating vector (DLV) approach was considered to localize the damage.

Silva *et al.*[2007] carried out parametric identification using AR-ARX model for linear prediction of damage diagnosis in IASC-ASCE benchmark problem. They tried to evaluate residual error as damage-sensitive indexes to detect damage. Various tests were made in the benchmark problem with different damage pattern. They also presented principal component analysis to investigate the possibility of data compression. The diagnosis that was obtained showed high correlation with the actual integrity state of the structure. The study was limited to stationary signal and linear systems.

Medhi *et al.* [2008] adopted Parametric State Space modeling for health monitoring of shear building. Modal parameters like eigen frequencies and eigen vectors have been extracted from the State Space model after introducing appropriate transformation. Least square technique has been utilized for the evaluation of the stiffness matrix after having

obtained the modal matrix for the entire structure. Highly accurate values of stiffness of the structure could be evaluated corresponding to both the undamaged as well as damaged state of a structure. Noise in the simulated output response, analogous to real time scenario, was considered. The damaged floor could also be located very conveniently and accurately by the adopted strategy. This method of damage detection can be applied in case of output acceleration responses recorded by sensors from the actual structure. Further, in case of even limited availability of sensors along the height of a multi-storied building, the methodology could yield very accurate information related to structural stiffness.

Bani-Hani *et al.* [2008] considered a seven and half century old minaret located in Ajloun, Jordan for evaluation of health through system identification. Output-only modal identification technique was applied to extract the modal parameters such as natural frequencies and mode shapes. A three dimensional finite element model of the minaret was developed using SAP 2000 nonlinear version and the same was updated according to modal parameters obtained experimentally by ambient vibration test-results and measured characteristic of old stone. Parametric identification using N4SID state space model was carried out to model dynamic behaviour of the minaret and a robust, immune and noise tolerant model was built.

Detail review of these few literatures has established that system identification techniques are quite efficient for identification of system parameters of structures based on acquired time histories. However, very limited works on identification of system parameters of actual building based on experimentally acquired time histories have been reported.

1.3 OBJECTIVES AND SCOPES OF STUDY

From the detailed literatures review, it has been observed that system identification is an active area of research in the field of health monitoring of structures. In few of the literatures, subspace identification scheme (N4SID) has effectively been used for identification of modal parameters of numerically simulated framed buildings. A study on adaptation of this identification technique for SHM of actual buildings can thus be a significant contribution. Therefore, this identification methodology has been used to identify the system parameters of $1/5^{th}$ scale RC test models based on recorded unidirectional responses during shake table test. Thereafter, studies on identification of system parameters of an actual multi-storey RC building using recorded responses during actual earthquakes have been undertaken. Further, number of sensors to be used for acquiring data from a large existing structure may be limited due to high cost of sensors and hence the study on system identification of existing structure with limited sensors has also been undertaken.

Contribution of infill walls in the overall stiffness of entire structural system has been modeled using system identification technique. Openings in infill walls in the form of doors/windows are common and the issues pertaining to the influence of opening in infill wall has also been included in the scope of the present study. Thus, in order to address the various issues mentioned above for identification of system parameters of existing shear buildings the following objectives are finalized.

- Identification of system parameters of three different RC frame test models of buildings with and without infill walls using parametric system identification technique. Development of expressions based on identified results for representing contribution of infill wall in the lateral stiffness of building.

- Identification of system parameters of an existing multi-storey symmetric-plan shear building with limited sensors.
- To study sensitivity of sensor allocation in an existing building using acquired time histories from numerically simulated building.

Buildings may behave asymmetrically during an earthquake. The possibilities of existence of torsional component in an existing building can be due to various causes such as geometric irregularities, mass difference at various locations, sizes of structural components etc. of the building. Very few literatures which address system identification of torsionally coupled buildings are available. Moreover, most of them are limited to identification of system parameters of numerically developed torsionally coupled building models. Hence, an available system identification technique (e.g. ITD), which uses multi-directional acceleration histories for identification of torsionally coupled building has been considered for the present study. However, the ITD identification technique needs to be verified through laboratory based experimental studies before applying to identify parameters of existing buildings. Thus, the following are also addressed in this thesis.

- Identification of system parameters of asymmetric scaled steel building model.
- Identification of system parameters of an existing multi-storey asymmetric-plan shear building through system identification**.**

1.4 OVERVIEW OF THE THESIS

In this dissertation appropriate system identification techniques are identified for determination of system parameters of existing symmetric-plan and torsionally coupled shear buildings. These have been utilized for identification of system parameters of two different classes of existing multi-storey shear buildings using recorded earthquake acceleration histories. These system identification techniques have been initially verified

through studies on scaled laboratory test models. The studies reported in this thesis for fulfilling the objectives are presented in eight chapters. Introduction, detailed review on available literatures on SHM methodologies and techniques is presented along with objectives and scopes of this study in the Chapter 1.

Chapter 2 provides detailed descriptions of a subspace identification technique (N4SID) used for identification of modal parameters of multi-storey symmetric-plan shear buildings using acquired unidirectional acceleration histories. Descriptions of ITD system identification technique which uses RANDOMDEC signatures of multi-directional acceleration histories for identification of modal parameters of multi-storey torsionally coupled building is also included in this chapter. Then, procedures for identification stiffness of symmetric-plan as well as torsionally coupled shear buildings using identified modal parameters are discussed. This chapter includes descriptions of methodologies used for assessing stability of a system and that for detection of damage in structures.

In Chapter 3, the descriptions of Shake Table facility, Data Acquisition System, different types of sensors and their arrangements are included. Methodologies adopted for processing of recorded responses are also furnished in this chapter.

In Chapter 4, results of identification of system parameters of various laboratory bare frame RC test models using acquired unidirectional acceleration histories from shake table tests are presented. Then, comparison of identified system parameters of the laboratory test models with those obtained from corresponding numerically simulated models of the laboratory test models is also made in this chapter.

Chapter 5 presents derivation of two expressions, one of which represents contribution of full masonry infill walls towards overall stiffness of structure and the other represents influence of door/window openings in masonry infill walls. Then, comparison of identified system parameters of the laboratory test models with those obtained from corresponding

numerical models with masonry infill walls simulated using proposed expressions. Modal parameters of numerical model of a laboratory test model with full masonry infill walls simulated using few available models are also presented in this chapter. Studies on suitability of the proposed expressions for prototype buildings are presented.

Chapter 6 presents the implementation of N4SID algorithm and least squares of eigenvalue problem for identification of system parameters in two lateral directions of an existing multi-storey symmetric-plan shear building using limited numbers of recorded unidirectional acceleration histories during two earthquakes. Studies on sensor sensitivity using extracted unidirectional acceleration histories from a numerical model of the sample building are presented in this chapter.

In Chapter 7, studies on adaptation of ITD system identification technique for identification of laboratory test model of torsionally coupled building using acquired multidirectional acceleration histories from shake test are included. Then, results of identification of system parameters of a torsionally coupled multi-storey shear building using multidirectional acceleration histories are presented.

Chapter 8 presents the general conclusions of works carried out in the previous chapters along with the possible scopes for future work.

CHAPTER 2

DESCRIPTION OF SELECTED SYSTEM IDENTIFICATION TECHNIQUES

2.1. INTRODUCTION

The detailed literature survey carried out in the previous chapter has highlighted various SHM techniques useful for civil engineering structures. The capabilities of various SHM schemes could also be recognized and it is found that the monitoring of health of a structure as a whole is possible only through system identification. System identification has been established as very meaningful tool to evaluate health of old structures before and after any event. System identification is the process of identifying system parameters of physical system by building new models or improving existing models using experimental data. System identification techniques can result in the mathematical model of a structure. For example, Eigenvalue Realization Algorithm (ERA) is being used for state space realization of a structure. The basic objective of system identification is the evaluation of parameters of dynamic models of system by building appropriate mathematical models. Numbers of system identification techniques have been developed to identify natural frequencies, corresponding mode shapes and damping ratios. All the system identification techniques for determination of modal parameters are based on measurement of the response of a dynamic system with or without input excitations as shown in Fig.2.1. The frequency domain approach as well as time domain approach is used to identify modal parameters of structures depending on data used for identification. The discrete time experimental data can be directly used in case of time domain approach and hence losses of information contained in the time history can be avoided.

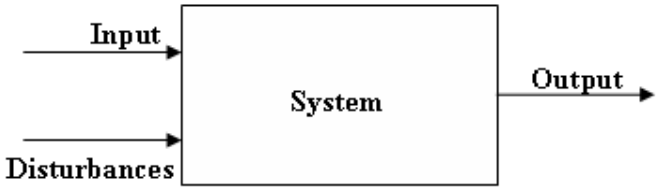

Fig. 2.1 A dynamic system with inputs, outputs and disturbances [Overschee and Moor, 1996]

In this thesis it is intended to identify system parameters of three different types of laboratory test models of buildings and two existing multi-storey buildings for achieving the objectives identified in the Chapter 1. It is planned to adopt some existing time domain system identification models to achieve the objectives of this study. Among the sub-classes of time domain system identification, the subspace identification technique has been found to be faster than classical system identification technique as this does not require convergence through iteration.

In this chapter an available system identification technique which is found to be suitable for identification of modal parameters of test models of symmetric-plan and shear building through development of input-output relationship using experimental data is described first. Another system identification technique which uses the response matrices to identify modal parameters of torsionally coupled building is also described. In case of torsionally coupled building, the response matrices are constituted with free decay responses of the recorded floor responses of the building. The methodology that is used to obtain free decay responses from recorded floor response is also presented.

Description of least square technique, which is used to determine structural parameters of any building system, is also presented in this chapter. The method uses the eigenvalue problem (undamped) to identify the stiffness values. An iterative approach is proposed to identify the missing mode shape values in the locations where the floor acceleration are

not available. The iterative approach estimates the mode shape values which are later used to identify the stiffness.

The robustness of the identified system parameters depends on the stability of the identification techniques. There are various measures to study stability of a system. One of the measures used to study stability of a system is discussed in this chapter. The shift of natural frequency as well as change the mode shapes are good indicators of presence of damage in a structure. Damage identification indexes use mode shapes of the structures to indicate presence of damage. In the last part of the chapter, a damage identification index which is used to compare the mode shapes of two similar structural systems is also presented.

Mathematical formulations of the above mentioned methods like modal parameter identification model, structural parameter identification model, checking of stability of a modal parameter identification model and damage identification index are presented in the following subsections.

2.2. MODAL PARAMETERS IDENTIFICATION OF MULTI-STOREY SYMMETRIC-PLAN SHEAR BUILDING

In case of symmetric-plan structures, the modal parameters, namely, natural frequencies, mode shapes and damping ratios are identified in two orthogonal directions separately. The subspace identification techniques identify the system matrices from relationship of input-output experimental data. The system matrices contain information of modal parameters and can be directly evaluated mathematically. Overschee and Moor [1996] observed that the subspace identification algorithms are fast as they are not iterative. The problem with convergence is eliminated in this approach, which is not the case in classical identification techniques.

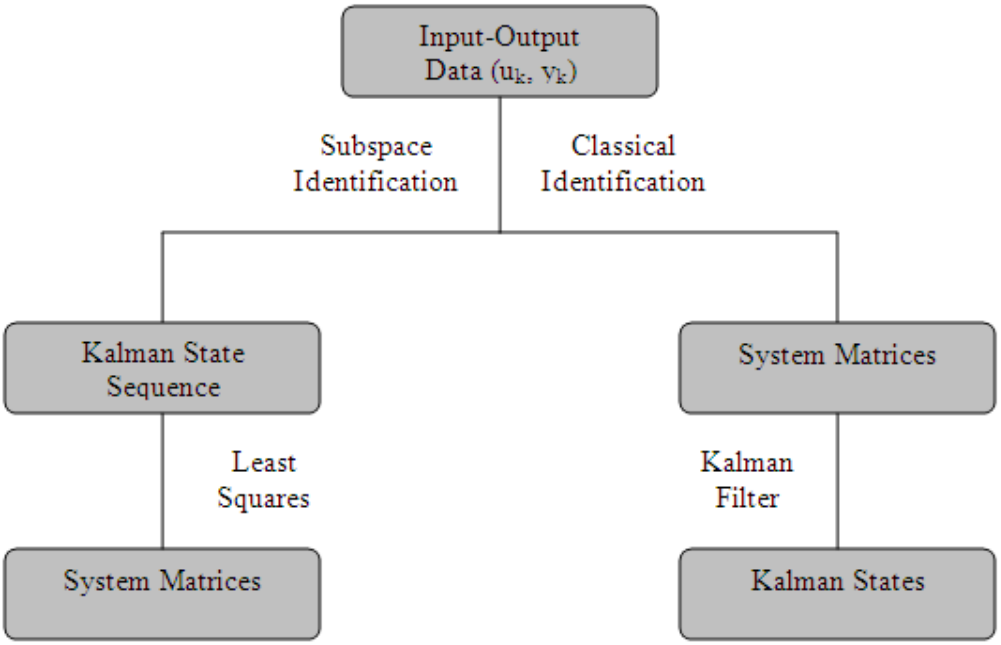

Fig. 2.2 Flowchart for subspace and classical system identification approach [Overschee and Moor, 1996]

It is evident from the Fig. 2.2 that the subspace identification using state space models first determines the Kalman state sequence and thereafter evaluates system matrices of a dynamic system where as the sequence is reverse in case of classical identification schemes. In this section, the state space basis of a model known as N4SID used for identification of modal parameters through subspace identification technique is discussed. The acronym N4SID stands for ***N****umerical algorithms for* ***S****ubspace* ***S****tate* ***S****pace* ***S****ystem* ***Id****entification*. The N4SID is recently developed subspace state space system identification model. This algorithm can be applied to systems subjected to known or unknown excitations. The algorithm is robust and noise tolerant and suitable for identification of system which posses combined deterministic-stochastic behaviour. Hence, the algorithm has been chosen for use in identification of buildings with earthquake induced structural responses. Mathematical formulation of the N4SID model for a multi degree of freedom linear dynamic system is presented in the following sub-section:

2.2.1 Fundamental Equations

The equation of motion for a finite dimensional linear dynamic system with $\mathbf{M}, \zeta$ and $\mathbf{K}$ as mass, damping and stiffness matrices respectively can be expressed by the second order differential equation as:

$$\mathbf{M}\ddot{\mathbf{a}} + \zeta\dot{\mathbf{a}} + \mathbf{K}\mathbf{a} = \mathbf{f}(a,t) \tag{2.1}$$

where, $\ddot{\mathbf{a}}, \dot{\mathbf{a}}$ and $\mathbf{a}$ are the vectors of acceleration, velocity and displacement respectively and $\mathbf{f}(a,t)$ is the forcing function over the period of interest at certain specific locations. It is desirable to change the system equation for an 'n'degree of freedom system with n second order differential equation to '$2n$' first order differential equations. The first order form of equations for the system is called as state space form.

The system defined by Eq. 2.1 can be represented in State Space form as:

$$\dot{\mathbf{x}}(t) = \mathbf{A}_c\,\mathbf{x}(t) + \mathbf{B}_c\,\mathbf{u}(t) + \mathbf{w}(t) \tag{2.2}$$

where,

$\mathbf{A}_c = \begin{bmatrix} 0 & \mathbf{I} \\ -\mathbf{M}^{-1}\mathbf{K} & -\mathbf{M}^{-1}\zeta \end{bmatrix}$ is $2n$ x $2n$ state matrix

$$\mathbf{x} = \begin{bmatrix} \mathbf{a} \\ \dot{\mathbf{a}} \end{bmatrix}$$

$$\mathbf{B}_c = \begin{bmatrix} 0 \\ \mathbf{M}^{-1}\mathbf{B}_2 \end{bmatrix}$$

$$\mathbf{f}(a,t) = \mathbf{B}_2\mathbf{u}(t)$$

$\mathbf{u}(t)$ is the input

and $\mathbf{B}_2$ is n x r input influence matrix characterizing the locations and types of inputs. The integer r is the number of inputs.

If the response of the dynamic system is measured by the n output quantities using sensors like accelerometers, velocity meter, displacement sensors etc. a matrix output equation can be written as:

$$\mathbf{y}(t) = \mathbf{C}_a\ddot{\mathbf{a}} + \mathbf{C}_v\dot{\mathbf{a}} + \mathbf{C}_d\mathbf{a} \tag{2.3}$$

where, $\mathbf{C}_a, \mathbf{C}_v$ and $\mathbf{C}_d$ are the output influence matrix for acceleration, velocity and displacement respectively. The output influence matrices basically indicate the location of appropriate sensor. A unity will be put corresponding to a particular degree of freedom, where sensor has been placed.

Substituting Eq. 2.1 and 2.2 in Eq. 2.3 and after rearranging, it can be written as:

$$\mathbf{y}(t) = \mathbf{C}\,\mathbf{x}(t) + \mathbf{D}\,u(t) + \mathbf{v}(t) \tag{2.4}$$

where,

$$\mathbf{C} = [\mathbf{C}_d - \mathbf{C}_a\mathbf{M}^{-1}\mathbf{K} \quad \mathbf{C}_v - \mathbf{C}_a\mathbf{M}^{-1}\zeta] \;\&\; \mathbf{D} = \mathbf{C}_a\mathbf{M}^{-1}\mathbf{B}_2.$$

$\mathbf{w}(t)$ and $\mathbf{v}(t)$ are noise terms and these two can be filtered by applying Butterworth filter to corrupted discrete input and outputs.

Since digital sensors are generally used for collection of output response data, Eq. 2.2 and 2.3 must be represented in discrete time. Considering initial condition $x(t_o)$ at $t = t_o$ and solving Eq. 2.2 gives

$$\mathbf{x}(t) = \mathbf{e}^{A_c(t-t_o)}\mathbf{x}(t_o) + \int_{t_o}^{t} \mathbf{e}^{A_c(t-\tau)}\mathbf{B}_c(\tau)d\tau \tag{2.5}$$

Considering equally spaced time given by $0, \Delta t,\ 2\Delta t, \ldots\ldots, (k+1)\Delta t$, where Δt is the constant sampling time interval, the solution of Eq. 2.5 can be represented in a discrete time as:

$$\mathbf{x}[(k+1)\Delta t] = \mathbf{e}^{\mathbf{A}_c \Delta t}\mathbf{x}(k\Delta t) + \int_{k\Delta t}^{(k+1)\Delta t} \mathbf{e}^{\mathbf{A}_c[(k+1)\Delta t - \tau]}\mathbf{B}_c\,\mathbf{u}(\tau)d\tau \qquad (2.6)$$

Considering that the input $\mathbf{u}(\tau)$ is constant between two successive time interval and rearranging Eq. 2.6 for one discrete time interval,

$$\mathbf{u}(\boldsymbol{\tau}) = \mathbf{u}(k\Delta t) \quad \text{for } k\,\Delta t \le \tau \le (k+1)\Delta t \; k = 1,2,3,4\ldots\ldots$$

$$\mathbf{x}[(k+1)\Delta t] = \mathbf{e}^{\mathbf{A}_c \Delta t}\mathbf{x}(k\Delta t) + [\int_{0}^{\Delta t} \mathbf{e}^{\mathbf{A}_c \tau}\, d\tau\ \ \mathbf{B}_c]\mathbf{u}(k\Delta t)$$

(2.7)

Eq. 2.6 can be rewritten in the following form,

$$\mathbf{x}(k+1) = \mathbf{A}\,\mathbf{x}(k) + \mathbf{B}\,\mathbf{u}(k) \qquad (2.8)$$

Similarly, Eq. 2.4 can also be rewritten as:

$$\mathbf{y}(k) = \mathbf{C}\,\mathbf{x}(k) + \mathbf{D}\,\mathbf{u}(k) \qquad (2.9)$$

The Eq. 2.8 is termed as state equation and Eq. 2.9 is termed as output equation. The numerical algorithms for subspace state space system identification (N4SID) introduced by Overschee and Moor [1993] has been used in this study for the evaluation of system matrices $\mathbf{A}, \mathbf{B}, \mathbf{C}$ and $\mathbf{D}$.

Z-transformation of $\mathbf{x}(k+1)$ is obtained as**:**

$$z[x(k+1)] = \sum_{k=0}^{\infty} \mathbf{x}(k+1)z^{-k} = z\sum_{k=0}^{\infty} \mathbf{x}(k+1)z^{-(k+1)}$$

$$= z\sum_{k=0}^{\infty} \mathbf{x}(k+1)z^{-(k+1)} - \mathbf{x}(0)$$

$$= z\sum_{k=0}^{\infty}\mathbf{x}(k')z^{-(k')} - \mathbf{x}(0)$$

$$= z[\mathbf{x}(z)-\mathbf{x}(0)] \tag{2.10}$$

where $z = e^{s\Delta t}$ and $k' = k+1$

Considering $\mathbf{x}(0) = 0$ and applying z-transformation to Eq. 2.8 and Eq. 2.9 and using Eq. 2.10,

$$\mathbf{x}(z) = (z\mathbf{I} - \mathbf{A})^{-1}\mathbf{B}\mathbf{u}(z) \tag{2.11}$$

$$\mathbf{y}(z) = \mathbf{C}\,\mathbf{x}(z) + \mathbf{D}\,\mathbf{u}(z) \tag{2.12}$$

Using the parameters defined in Eq. 2.11 into Eq. 2.12, we get

$$\mathbf{y}(z) = [\mathbf{C}[z\mathbf{I}-\mathbf{A}]^{-1}\mathbf{B} + \mathbf{D}]\mathbf{u}(z)$$

$$= [\mathbf{D} + \sum_{k=0}^{\infty} z^{-(k+1)}\mathbf{C}\mathbf{A}^{\mathbf{k}}\,\mathbf{B}\,]\mathbf{u}(z)$$

$$= \mathbf{H}(z)\,\mathbf{u}(z)$$

$$\mathbf{H}(z) = \frac{\mathbf{y}(z)}{\mathbf{u}(z)} \tag{2.13}$$

where, $\mathbf{H}(z)$ is the system transfer function relating the input and output. The values of z for which $\mathbf{H}(z)$ is infinity are called *poles*.

The j^{th} *pole* of the system is given by

$$z_j = e^{(-\xi_j\omega_j \pm\, i\omega_j\sqrt{1-\xi_j^2})\Delta t} \tag{2.14}$$

where, ξ_j and ω_j are damping ratio and frequency of the j^{th} mode of vibration. The frequency and damping ratio can be determined as follows:

$$\omega_j = \frac{1}{\Delta t}\sqrt{\ln^2 r_j + \theta_j^2} \tag{2.15}$$

$$\xi_j = -\frac{\ln r_j}{\sqrt{\ln^2 r_j + \theta_j^2}} \tag{2.16}$$

where, $r_j = |z_j|$, the magnitude; and $\theta_j = \tan^{-1}[\mathrm{Im}\, g(z_j)/\mathrm{Re}(z_j)]$, the phase angle of the j^{th} *pole*.

The flow chart as shown Fig. 2.3 explains different steps used to identify modal parameters of a building through parametric state space models in subspace identification scheme. Formulation of input-output matrices and implementation of N4SID has been executed in MATLAB (Ver.7) using available subroutines.

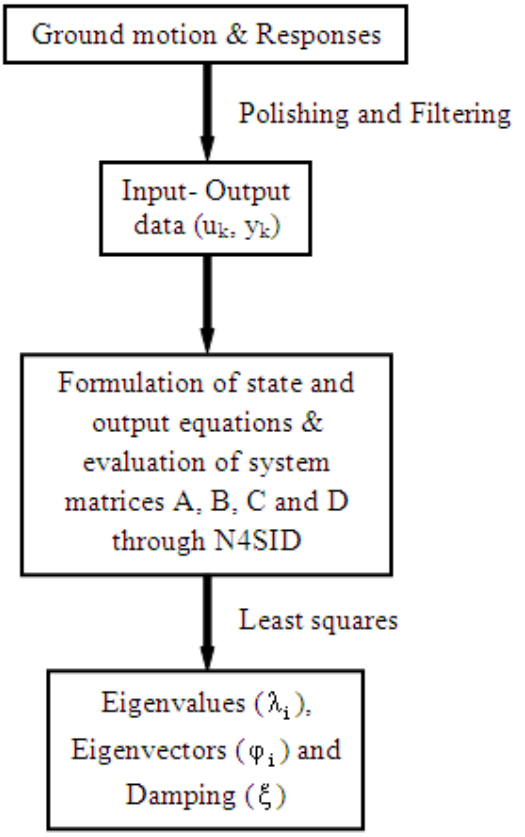

Fig. 2.3 Flow Chart for identification of eigenpairs and damping ratios using N4SID

2.2.2 Extraction of Normal Modes for Symmetric-Plan Shear Building

The system matrix **A** evaluated from the state equation is utilized for the evaluation of eigenvalues (λ_i) and their corresponding eigenvectors $\boldsymbol{\phi}_i$. It has been found that the evaluated eigenvalues (λ_i) represent the poles of the structure. Hence, eigenvector $\boldsymbol{\phi}_i$ corresponding to the eigenvalues of the matrix **A** must also represent the modal displacement vector of the structure. Eq. 2.15 and 2.16 are used for the determination of the natural frequencies and the damping ratios of the structure. Similarly, the stability of the system is observed from the value of the pole of Eq. 2.14. However, the modal matrix ($\boldsymbol{\Phi}$) corresponds to the non-physical state of the structure and hence, the output influence matrix **C** evaluated from output equation is used to transform the computed eigenvector from the non physical state to the mode shape vector at the structural floor level, where the response data have been measured. Thus, the modal displacement vector for the structure corresponding to all the modes can be calculated as:

$$\boldsymbol{\Gamma} = \mathbf{C}\boldsymbol{\Phi} \tag{2.17}$$

The modes are often found to be in complex form. These complex modes are further processed to obtain normal modes. Identified complex modes and corresponding characteristic roots λ_i (and their conjugates) are required to compute normal modes. The approach adopted by Ibrahim [1982] uses an oversized mathematical model for computation of normal modes from corresponding complex modes. The displacement, velocity and acceleration responses are formed from the given modal parameters. The free response displacement response can be expressed as:

$$\mathbf{y}_n(t) = \sum_{i=1}^{2q} \boldsymbol{\psi}_i e^{\lambda_i t} + \mathbf{o}_i(t) \tag{2.18}$$

where, q and λ_i are the nos. of available complex modes and corresponding characteristic roots respectively. $\mathbf{y}_n(t)$ is the normal mode corresponding to complex mode $\boldsymbol{\psi}.\mathbf{o}_i(t)$ is noise term which is removed using digital filter for experimental works.

State vector equations are formed as:

$$\begin{Bmatrix}\dot{\mathbf{y}}(t)\\ \ddot{\mathbf{y}}(t)\end{Bmatrix}=\begin{bmatrix}0 & \mathbf{I}\\ -\mathbf{M}^{-1}\mathbf{K} & -\mathbf{M}^{-1}\mathbf{C}\end{bmatrix}\begin{Bmatrix}\mathbf{y}(t)\\ \dot{\mathbf{y}}(t)\end{Bmatrix}$$

or

$$\dot{\mathbf{x}}=\mathbf{A}\mathbf{x} \tag{2.19}$$

By repeating Eq.2.19 for $2n$ time instants

$$\dot{\mathbf{X}}=\mathbf{A}\mathbf{X} \tag{2.20}$$

where $\mathbf{X}$ and $\dot{\mathbf{X}}$ contain responses measured at the $2n$ instants.

$$\mathbf{A}=\dot{\mathbf{X}}\mathbf{X}^{-1} \tag{2.21}$$

By computing matrix $\mathbf{A}$, the $\left[\mathbf{M}^{-1}\mathbf{K}\right]$ matrix gives normal modes according to the eigenvalue equation, $\left[\mathbf{M}^{-1}\mathbf{K}\right]\boldsymbol{\phi}=\omega^2\boldsymbol{\phi}$.

2.3. MODAL PARAMETERS IDENTIFICATION OF MULTISTOREY TORSIONALLY COUPLED SHEAR BUILDING

Hejal and Chopra [1989] mentioned that the disregard of torsional vibration may cause an underestimation of structural responses of structures. Therefore, it is essential to consider the torsional behaviour of asymmetric buildings while carrying out identification of system parameters using recorded responses. The torsional responses are treated differently from those of the translational responses as observed from literatures review. Chopra [2001] has stated that there are various chances to come across the situations like

(1) multistory building with symmetric plan and symmetric mass distribution in rigid floor diaphragm, (2) multistory building with symmetric plan and non-standard mass distribution in rigid floor diaphragms, (3) multistory building with asymmetric plan and symmetric mass distribution in rigid floor diaphragms, (4) multistory building with asymmetric plan and asymmetric mass distribution in rigid floor diaphragms. The most important thing is the characteristic of floor responses change from case to case for similar input pattern. The collection of floor response and analysis of the same is very important and difficult. The total response of a structure is the combination of all the modes participated in the dynamics of the structure due to ground motion.

Buildings do not oscillate only in pure translational modes when excited by dynamic loads. Buildings with nominally symmetric plans are actually asymmetric to some degree and will undergo lateral as well as torsional vibrations simultaneously when subjected to purely translational excitations. The torsional motion is due to two major factors: the building is usually not perfectly symmetric, and the spatial variations in ground motion may cause rotation (about the vertical axis) of the building's base, which will induce torsional motion in the building even though its plan is perfectly symmetric.

Limited studies on system identification of torsionally coupled buildings from dynamic response measurements are available in the literature. Most papers discussed identification of system parameters only for planar frame structures or identified two translational and one torsional modal parameter for building structures separately as mentioned by Ueng *et al*. [2000]. However, buildings with nominally symmetric plans are actually asymmetric to some degree and will undergo lateral as well as torsional vibrations simultaneously when subjected to purely translational excitations. A two steps system identification method is proposed to deal with the identification of system parameters of a torsionally coupled building. First the free decay responses from measured dynamic responses of the building are computed. The extended random decrement method which is modified version of

random decrement (RANDOMDEC) method is used to extract the free vibration responses of a multi-storey torsionally coupled building. The obtained free decay responses are thereafter used to identify the modal frequencies, damping ratios, and mode shapes using Ibrahim Time Domain (ITD) technique.

2.3.1 Extended Random Decrement Method for Obtaining RANDOMDEC

The successful identification of various parameters of any system depends on use of appropriate segment of collected data. The Random Decrement (RANDOMDEC) technique is one of the accurate and fast converging methods for extracting meaningful information from random data. The Randomdec technique was originally developed by Cole [1971] for the measurement of damping and for detection of structural deterioration of airplane wings subjected to wind flutter excitation. The method was developed in the year of 1971 and has been used in research in different field of engineering in the early seventies. In this technique the segments of the random vibration response of a transducer placed on an object subjected to random excitation are ensemble averaged to form a signature which is representative of the free vibration decay curve of the structure. This signature can be used to measure damping or to detect incipient failures. Cole [1971] defined random decrement signature as unique form and it does not require the knowledge input excitation measurements. The evaluation of RANDOMDEC signature may be explained in following paragraphs.

The equation of motion for SDOF linear system is given by

$$m\ddot{x} + c\dot{x} + kx = 0 \qquad (2.22)$$

The response $x(t)$ of the linear system can be decomposed into three parts; response due to initial displacement $x_d(t)$, response due to initial velocity $x_v(t)$ and response due to forcing function $x_f(t)$ or it can be said that the response of linear system is superposition

of these three terms. The random decrement analysis consists of averaging N_s segments of the length η of the system response with following steps [Yang *et al*., 1983]:

1. Determination of x_s, which is a root mean square value of $x_i(t)$, response at location i of a structure.
2. Starting time t_j of each segment are selected such that

   $x_i(t_j) = u_s = \text{RMS of } x_i(t)$ $\qquad j = 1,2,3,.....$

   $\dot{x}_i(t_j) \geq 0$ $\qquad j = 1,3,5,.....$

   $\dot{x}_i(t_j) \leq 0$ $\qquad j = 2,4,6,.....$

3. Averaging N_s segments of the length η of the system response to get a time function, $\delta(\tau)$ as:

   $$\delta(\tau) = \frac{1}{N_s}\sum_{i=1}^{N_s} x_i(t_j + \tau) \qquad (2.23)$$

   The function $\delta(\tau)$ is called the random decrement signature and is defined only in the time interval $0 \leq \tau \leq \eta$.

Extraction of RANDOMDEC signature has been executed in MATLAB. The free decay response $\delta(\tau)$ represents the response due to initial displacement. Out of three parts of the response $x_i(t)$ at location i of the structure, the part due to initial velocity cancels out because the positive and negative slopes are alternatively taken and their distributions are random. In addition, the part due to external excitation vanishes since it is assumed to be a stationary random process with zero-mean. The diagrammatic explanation of the phenomenon is shown in Fig. 2.4.

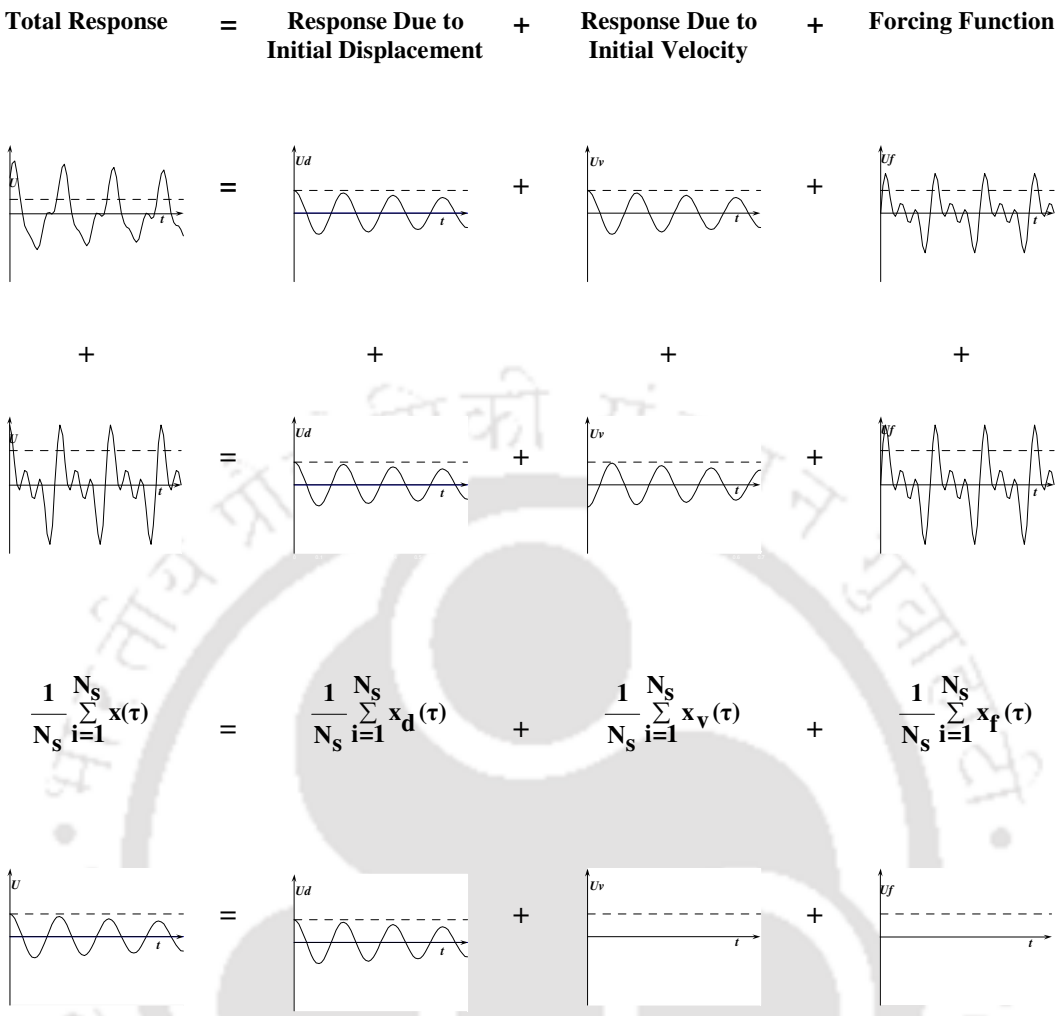

Fig. 2.4 Principle of RANDOMDEC technique [Yang *et al.,* 1983]

The principle for extraction of random decrement signature can be illustrated as shown in the Fig. 2.5. The Fig. 2.5 (b) and 2.5 (c) represent the segments with positive slope and negative slope respectively. Fig. 2.5 (d) represents addition and averaging of the response segments with time duration t_d of the same response used to obtain free decay signature. Fig. 2.5 (e) shows the obtained free decay signature.

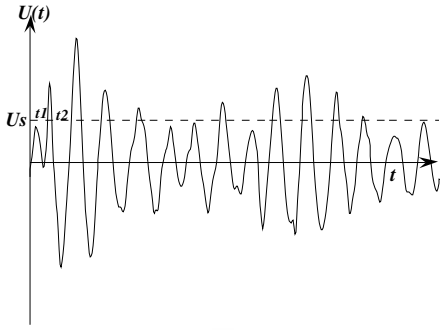

(a) Response measurement and crossing time

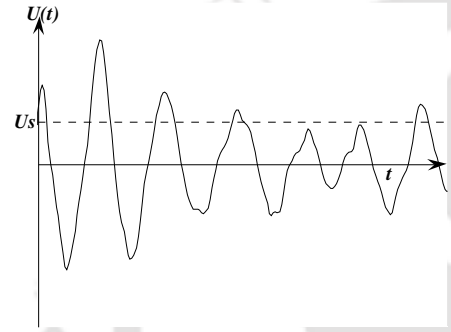

(b) Response segment starting from t1

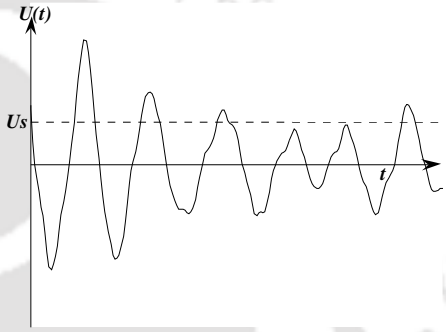

(c) Response segment starting from t2

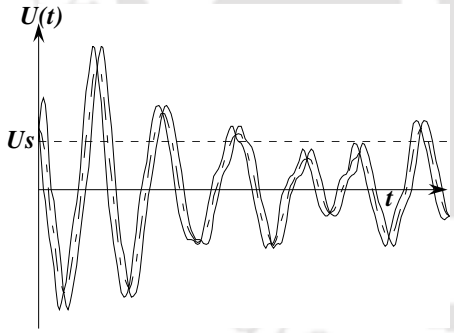

(d) Averaging of response segments

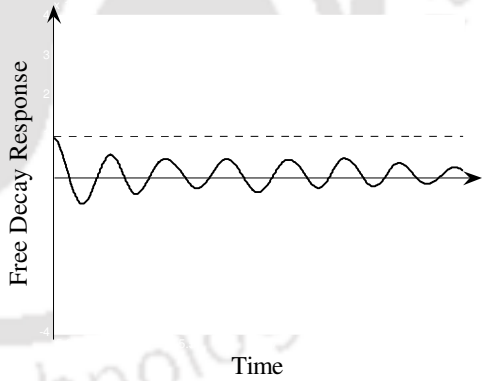

(e) Free decay signature

Fig. 2.5 Extraction of free decay response from response measurement [Yang *et al.,* 1983]

Basically, the original random decrement method was developed to process a single measurement. In case of multiple measurements from a real building, the correlations will be lost if the above averaging procedure is adopted for each measurement locations individually. This can be overcome with help of *Extended Random Decrement* where

crossing times t_j are determined from one designated measurement. Ueng *et al*. [2000] suggested for utilizing lower floor measurements for determination of crossing times as because it contains greater weight for higher modes. Then all the measurements are processed using step (3) with starting time t_j to obtain their free decay signatures.

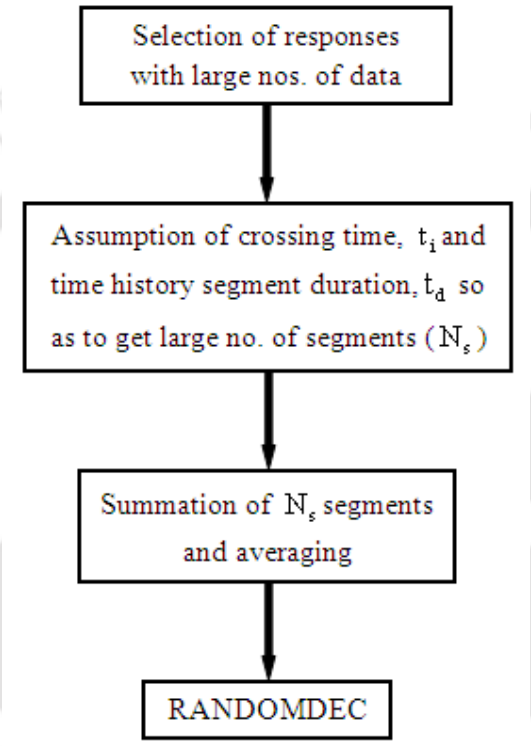

Fig. 2.6 Flow chart for extraction of RANDOMDEC signature

2.3.2 Ibrahim Time Domain Identification Technique

The *time domain modal identification technique* referred to as the Ibrahim Time Domain (ITD) technique is described here. The technique was first proposed by Ibrahim (1973). The ITD algorithm has been used to analyze test data from several structures by number of researchers. The ITD is a straightforward modal parameter identification method in which free-response functions in form of any one amongst displacement, velocity, or acceleration time histories are used in an eigenvalue solution scheme to obtain desired modal

parameters. Here, the procedure of obtaining modal parameters of a single degree of freedom system is explained first and formulation is extended for a multi degree of freedom system.

A classical damped single degree of freedom system governed by free vibration can be expressed as:

$$m\ddot{x} + c\dot{x} + kx = 0 \tag{2.24}$$

The characteristic equation is given by

$$\lambda^2 m + \lambda c + k = 0 \tag{2.25}$$

and solution of the above equation is given as:

$$u(t) = \psi e^{\lambda t} \tag{2.26}$$

for an over damped system, ψ and λ are both real-valued; for an under damped system, they are complex and occur in a conjugate pairs.

In the more common under damped case, the roots of the characteristic equation are

$$\lambda = \sigma + i\omega_d \tag{2.27}$$

where ω_d is the damped natural frequency in rad/sec and the corresponding undamped natural frequency is $\omega_n = \sqrt{\sigma^2 + \omega_d^2}$ and damping factor or fraction of critical damping is $\xi = \frac{\sigma}{\omega_n}$.

For a multi-degree-of-freedom linear-dynamic system with 'p'excited modes, the free response of the structure at any sensor location 'i' and instant of time 't_j'can be expressed by summation of the individual response of each mode as:

$$x_i(t_j) = x_{ij} = \sum_{k=1}^{2p} \psi_{ik} e^{\lambda_k t_j} \tag{2.28}$$

where, ψ_{ik} and λ_k are both complex numbers. The free response values for location i, x_i is available from extended random decrement method.

With help of Eq. 2.28 free-response values for '$2p$'locations and 's'instants of time can be represented as:

$$\begin{bmatrix} x_{11} & x_{12} & \ldots\ldots\ldots x_{1s} \\ x_{21} & x_{22} & \ldots\ldots\ldots x_{2s} \\ . & & \\ . & & \\ . & & \\ x_{2p1} & x_{2p2} & \ldots\ldots x_{2ps} \end{bmatrix} = \begin{bmatrix} \psi_{11} & \psi_{12} & \ldots\ldots\ldots \psi_{1s} \\ \psi_{21} & \psi_{22} & \ldots\ldots\ldots \psi_{2s} \\ . & & \\ . & & \\ . & & \\ \psi_{2p1} & \psi_{2p2} & \ldots\ldots \psi_{2ps} \end{bmatrix} \mathrm{X} \begin{bmatrix} e^{\lambda_1 t_1} & e^{\lambda_1 t_2} & \ldots\ldots\ldots e^{\lambda_1 t_s} \\ e^{\lambda_2 t_1} & e^{\lambda_2 t_2} & \ldots\ldots\ldots e^{\lambda_2 t_s} \\ . & & \\ . & & \\ . & & \\ e^{\lambda_{2p} t_1} & e^{\lambda_{2p} t_2} & \ldots\ldots\ldots e^{\lambda_{2p1} t_s} \end{bmatrix} \tag{2.29}$$

or simply in matrix form

$$\boldsymbol{\Phi}_{2pxs} = \boldsymbol{\Psi}_{2px2p} \mathrm{x} \boldsymbol{\Lambda}_{2pxs} \tag{2.30}$$

Similarly, free response value after a time interval of $(\Delta t)_1$ than those in Eq. 2.28 at the same stations

$$\begin{aligned} x_i\left[t_j + (\Delta t)_1\right] &= \sum_{k=1}^{2p} \psi_{ik} e^{\lambda_k \left[t_j + (\Delta t)_1\right]} \\ &= \sum_{k=1}^{2p} \left[\psi_{ik} e^{\lambda_k (\Delta t)_1}\right] e^{\lambda_k t_j} \\ &= \sum_{k=1}^{2p} \left[\hat{\psi}_{ik}\right] e^{\lambda_k t_j} \end{aligned} \tag{2.31}$$

or in matrix form

$$\hat{\boldsymbol{\Phi}}_{2pxs} = \hat{\boldsymbol{\Psi}}_{2px2p} \mathrm{x} \boldsymbol{\Lambda}_{2pxs} \tag{2.32}$$

Eq. 2.30 and 2.32 can be related by eliminating $\boldsymbol{\Lambda}$.

$$\mathbf{A}_{2px2p} \mathrm{x} \boldsymbol{\Psi}_{2px2p} = \hat{\boldsymbol{\Psi}}_{2px2p} \tag{2.33}$$

where, $\boldsymbol{\Phi}^{T}{}_{sx2p} \mathrm{x} \mathbf{A}^{T}{}_{2px2p} = \hat{\boldsymbol{\Phi}}^{T}{}_{sx2p}$ (2.34)

From Eq. 2.31 we have

$$\hat{\boldsymbol{\psi}}_k = e^{\lambda_k (\Delta t)_1} \boldsymbol{\psi}_k$$

The system can be defined with single eigenvalue problem

$$\mathbf{A}\boldsymbol{\psi}_k = e^{\lambda_k (\Delta t)_1} \boldsymbol{\psi}_k \tag{2.35}$$

The matrix $\mathbf{A}$ is referred to as system matrix and contains information of modal parameters of the system. The desired damped natural frequencies and damping factors are determined from the eigenvalues of $\mathbf{A}$, $e^{\lambda_k (\Delta t)_1} = a_k + ib_k$ as follows:

The damped natural frequency is

$$(\omega_d)_k = 2\pi f_k = \frac{1}{(\Delta t)_1} \tan^{-1}\left(\frac{b_k}{a_k}\right) \tag{2.36}$$

and damping factor or fraction of critical damping is

$$\left(\frac{c}{c_c}\right)_k = \frac{\sigma_k}{\sqrt{\sigma_k{}^2 + (\omega_d)_k{}^2}} \tag{2.37}$$

where, $\sigma_k = \frac{1}{2(\Delta t)_1} \ln(a_k{}^2 + b_k{}^2)$.

The eigenvectors of $\mathbf{A}$ are desired structural mode shapes (complex), $\boldsymbol{\psi}_k$.

$\mathbf{A}^T$ can be obtained from Eq. 2.34 and 2.35. First the free response functions are placed into the rows of $\boldsymbol{\Phi}$ and the free response functions from the same locations after time shift $(\Delta t)_1$ are placed into the rows of $\hat{\boldsymbol{\Phi}}$. Matrices $\boldsymbol{\Phi}$ and $\hat{\boldsymbol{\Phi}}$ are termed as response matrices whose time shift is $(\Delta t)_1$. The least square solution of Eq. 2.35 gives the complex

eigenvalues and eigenvectors of $\mathbf{A}$. It may be clearly seen that the size of the matrix $\mathbf{\Phi}$ is $2p$ x s. Thus, pseudo-inverse of this matrix is computed in MATLAB using the command "pinv" and the solution corresponds to a least squares estimate of eigen parameters. The system modal parameters can be evaluated directly from the complex eigenvalues of $\mathbf{A}$ using Eq. 2.36 and 2.37. The various steps mentioned in the flow chart [Fig. 2.7] have been executed in MATLAB to obtain modal parameters. The modes identified through ITD are in complex form. Procedures adopted through Eq. 2.18 to 2.21 are used to process complex modes for computing the corresponding normal modes.

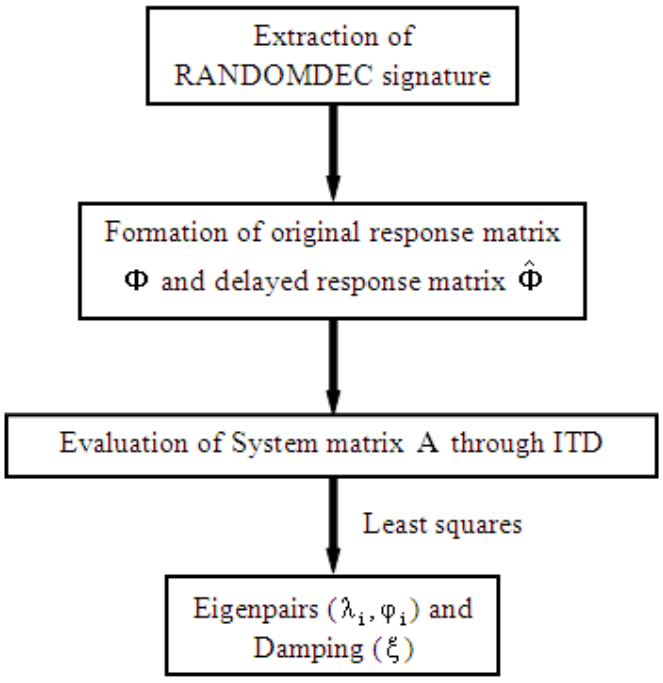

Fig. 2.7 Flow chart for identification of eigenpairs and damping using ITD

Construction of response matrices Φ and $\hat{\Phi}$ of free decay responses of measured responses:

Ibrahim [1981] explained the method of construction of response matrices Φ and $\hat{\Phi}$. The fundamental time increment between all data placed into Φ and $\hat{\Phi}$ is $(\Delta t)_1$. Two other user-selectable time shifts are used in positioning overlapping segments of the measured free decay responses into the rows of the response matrices. The selection of time shifts denoted by $(\Delta t)_1$, $(\Delta t)_2$ and $(\Delta t)_3$ is very critical. The eigenvalues of the system matrix **A** depends on the fundamental time shift $(\Delta t)_1$. The dimension '*p*' is referred as the "number of allowed (computational) degrees-of-freedom" or NDOF. The number of rows in the response matrices is kept twice the degree of freedom desired in the identification process. When the number of free decay responses (i.e. number of response measurements) p_0 is less than the number of desired degrees-of-freedom, fewer than half the rows of Φ are filled up by the original unshifted free decay responses. Under these circumstances, 'assumed' or 'transformed' stations are created for the additional rows of both response matrices by shifting the original free decay responses placed in the first p_0 by multiples of a second user-selectable time shift, $(\Delta t)_2 : (\Delta t)_2, 2(\Delta t)_2$, $3(\Delta t)_2$ etc., until the upper half of the matrix Φ are filled. On the other hand, if the NDOF is smaller than p_0, only NDOF of the available free decay responses are used in the analysis. The bottom half of the response matrix Φ are formed by duplicating the upper rows, but delaying an additional user-selectable time shift, $(\Delta t)_3$. Pappa and Ibrahim [1981] established a relationship between $(\Delta t)_3$ and $(\Delta t)_1$ or $(\Delta t)_2$. There they refrained from using the time shift $(\Delta t)_3$ equal to either $(\Delta t)_1$ or $(\Delta t)_2$. They used to get satisfactory results in most of the cases by putting $(\Delta t)_3$ equal to one-half of the value of $(\Delta t)_2$. Again if all the data of lower half are obtained by delaying the data in the upper half by $(\Delta t)_3$, frequencies, $f_r = n/2(\Delta t)_3$, for integer values

of '*n*' will not be identified. They got acceptable results by considering $(\Delta t)_3 < (\Delta t)_1$. It essential to know the Nyquist frequency f_r of the structure before selecting $(\Delta t)_1$. The value of f_r is simply $1/2(\Delta t)_1$. Hence, pre-filtering is required to ignore identification of frequency larger than f_r. Thus, $(\Delta t)_1$ should be kept lower than $1/2 f_r$.

2.4 STRUCTURAL PARAMETER IDENTIFICATION OF MULTI-STOREY SYMMETRIC–PLAN SHEAR BUILDING

The stiffness which is directly related to moment of inertia or Young's modulus of the structure is considered to be the most important structural parameter of a structure. Presences of damage affect the moment of inertia or Young's modulus of structure and in turn reduction of stiffness is observed. The change in these parameters will allow us to identify, locate and quantify the damage of a structure. In this section a method is proposed to identify structural parameters from the modal parameters obtained from N4SID identification techniques.

2.4.1 Least Squares Solution of Eigenvalue Problem

The realization of eigenvalue problem can be used as the basis for structural parameter identification [Caicedo, 2004]. The obtained modal parameters such as undamped natural frequencies and mode shapes can be used to determine the parameters that form the elemental stiffness matrices of the structure. A generalized lumped mass model of one dimensional *n*-storey shear structures is shown in Fig. 2.8.

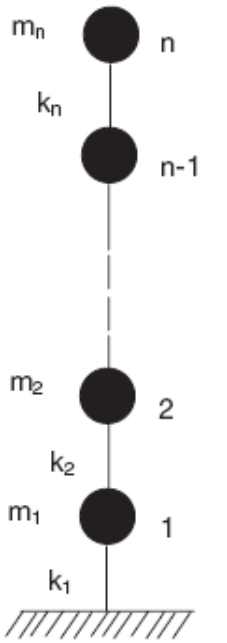

Fig. 2.8 Lumped mass model of an *n*-storey shear building

In general for a multi degree of freedom system, the undamped eigenvalue problem can be defined as [Chopra, 2001]:

$$(\mathbf{K} - \lambda_i \mathbf{M})\{\phi_i\} = \{0\} \qquad \text{or} \qquad (\mathbf{K}\{\phi_i\} = \lambda_i \mathbf{M}\{\phi_i\} \tag{2.38}$$

where,

$$\mathbf{K} = \begin{bmatrix} k_1 + k_2 & -k_2 & \cdots & 0 & 0 \\ -k_1 & k_2 + k_3 & \cdots & 0 & 0 \\ \vdots & \vdots & \ddots & \vdots & \vdots \\ 0 & 0 & \cdots & k_{n-1} + k_n & -k_n \\ 0 & 0 & \cdots & -k_n & k_n \end{bmatrix}$$

&

$$\mathbf{M} = \begin{bmatrix} m_1 & 0 & \cdots & 0 & 0 \\ 0 & m_2 & \cdots & 0 & 0 \\ \vdots & \vdots & \ddots & \vdots & \vdots \\ 0 & 0 & \cdots & m_{n-1} & 0 \\ 0 & 0 & \cdots & 0 & m_n \end{bmatrix} \tag{2.39}$$

are stiffness matrix with storey stiffness of the structure and the estimated mass matrix of 'n' degree of freedom system respectively.

λ_i and $\boldsymbol{\phi}_i$ are i^{th} undamped eigenvalue and eigenvector respectively as obtained from modal identification process. Now, the $\mathbf{K}$ can be determined easily for an undamped system and thereafter the values of storey stiffness. The solution of Eq. 2.39 may be achieved using two different approaches depending upon the availability of measurements and these two approaches are discussed as below.

Case 1: When the full mode shape matrix is available

In case of a multi-storey building if the measurements are available in all the locations where the mode shape values are required this approach can be applied to determine the structural properties. The following steps will be useful for the evaluation of structural stiffness matrix [Caicedo et al. 2004].

Step 1:

For shear building, the characteristics equation can be written as:

$$(\mathbf{K} - \lambda_i \mathbf{M}) \begin{Bmatrix} \phi_i^{(1)} \\ \phi_i^{(2)} \\ \phi_i^{(3)} \\ .... \\ .... \\ \phi_i^{n} \end{Bmatrix} = \begin{Bmatrix} 0 \\ 0 \\ 0 \\ ... \\ ... \\ 0 \end{Bmatrix} \tag{2.40}$$

where $\lambda_i = \omega_i^2$ is the i^{th} Eigenvalue and $\phi_i^{(r)}$, $r = 1, 2, 3 \ldots\ldots n$ is the i^{th} mode shape value at the r^{th} floor level.

Step 2:

The equation can be expanded and rearranged as:

$$\mathbf{\Delta_i k} = \mathbf{\Lambda_i} \tag{2.41}$$

where,

$$\mathbf{\Delta_i} = \begin{bmatrix} \phi_i^{(1)} & \phi_i^{(1)} - \phi_i^{(2)} & 0 & \ldots\ldots & 0 \\ 0 & \phi_i^{(2)} - \phi_i^{(1)} & \phi_i^{(2)} - \phi_i^{(3)} & \ldots\ldots & 0 \\ . & . & . & \ldots\ldots & \ldots \\ . & . & . & \ldots\ldots & \ldots \\ 0 & 0 & \ldots\ldots & \phi_i^{(n-1)} - \phi_i^{(n-2)} & \phi_i^{(n-1)} - \phi_i^{(n)} \\ 0 & 0 & \ldots\ldots & 0 & \phi_i^{(n)} - \phi_i^{(n-1)} \end{bmatrix} \tag{2.42}$$

$$\mathbf{k} = \begin{bmatrix} k_1 \\ k_2 \\ . \\ . \\ k_n \end{bmatrix} \tag{2.43}$$

$$\mathbf{\Lambda_i} = \begin{bmatrix} \phi_i^{(1)} \lambda_i m_1 \\ \phi_i^{(2)} \lambda_i m_2 \\ . \\ . \\ \phi_i^{(n)} \lambda_i m_n \end{bmatrix} \tag{2.44}$$

$\phi_i^{(n)} = n^{\text{th}}$ element of ϕ_i . Eq. 2.41 can be written for each of the n eigenvalues and eigenvectors identified. Assembling all of the eigenvector matrices, we get

$$\begin{bmatrix} \mathbf{\Delta}_1 \\ \mathbf{\Delta}_2 \\ . \\ . \\ \mathbf{\Delta}_n \end{bmatrix} \begin{bmatrix} k_1 \\ k_2 \\ . \\ . \\ k_n \end{bmatrix} = \mathbf{\Delta k} = \begin{bmatrix} \Lambda_1 \\ \Lambda_2 \\ . \\ . \\ \Lambda_n \end{bmatrix} \tag{2.45}$$

This equation represents a total of n^2 equations, which is used to solve the vector of stiffness

$$\mathbf{k} = \mathbf{\Delta}^{-1}\mathbf{\Lambda} \tag{2.46}$$

It may be clearly seen that the size of the matrix Δ is n^2 x n. Thus the problem is over specified and a pseudo-inverse of this matrix is computed in MATLAB using the command "pinv" and the solution corresponds to a least squares estimate of the stiffness. It may be noted that at least a single frequency and mode shape are necessary to obtain a solution. However, the results improve when the frequencies and mode shapes of multiple modes are utilized because the error from a single mode will not dominate.

Case 2: When partial mode shape matrix is available due to limited number of sensors

The first approach becomes inadequate for identification of vector of stiffnesses when modal matrix is incomplete. The incomplete eigenvector is due to non availability of measurements at all the locations where the mode shape values are required. The identifications of system stiffness for cases with limited measurements have been addressed by researchers like Caicedo *et al.* [2004] and Chakravarty [2004]. Chakravarty used a modified Holzer Criteria for evaluation of system stiffness for cases with limited measurements; the building structure considered in their study was limited to having standard floor masses only. Medhi *et al.* [2008] demonstrated the functioning of this strategy by evaluating stiffness for both undamaged and damaged numerically simulated building with standard mass instrumented with limited numbers of accelerometer. However, the iterative approach proposed by Caicedo *et al.* [2004] for the determination of stiffness of building with limited sensors does not have the limitations of standard mass across all the floors of the building and has been adapted in the present study. The approximate building floor modal displacements corresponding to the instrumented floors have been obtained with the help of N4SID and considered as known elements of eigenvectors.

The stepwise approach of the iterative method for the determination of unknown elements of full eigenvector matrix, converged eigen values and system stiffness has been presented below [Caicedo et al., 2004]:

1. As an initial value, the mode shape matrix $\mathbf{\Gamma}_i$ is set equal to the full mode shape matrix of the undamaged system. In the present study, the mode shapes of the undamaged structure of numerically simulated model of the building are used as the initial values. Similarly, the lumped mass matrix $\mathbf{M}$ in Eq. 2.39 is formed using the estimated floor masses.
2. The known values from the identified eigenvectors are inserted into the eigenvector matrix, which is optional.
3. These mode shapes are used in Eq. 2.46 in order to determine the stiffness vector of the floors of the structure.
4. The stiffness matrix, $\mathbf{K_i}$ is formed using the stiffness as identified in step 3 and the corresponding eigenvector matrix, $\mathbf{\Phi_i}$ is computed.
5. Setting $i=i+1$, step 2 will be revisited using the eigenvectors computed in step 4. However, if step 2 is not used in the iterative procedure, only the identified frequencies are required to determine the least squares estimate of the stiffness. Thus, iterative approach can be used to determine the eigenvectors, eigenvalues, and stiffness of the structure.

The flow chart shown in Fig. 2.9 well describes the iterative procedure for obtaining converged eigenvectors, eigenvalues and stiffnesses.

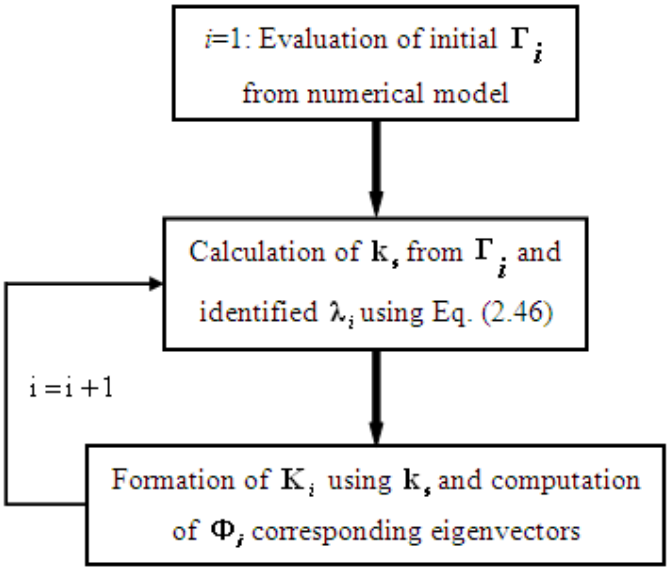

Fig. 2.9 Flow chart for evaluation of stiffness using iterative approach

The adequacy of such a limited number of sensors for accurate estimation of system parameters needs to be examined in details.

2.5 STRUCTURAL PARAMETER IDENTIFICATION OF MULTI-STOREY TORSIONALLY COUPLED SHEAR BUILDING

The dynamic responses of torsionally coupled shear buildings are different from those of symmetric-plan shear building. The building vibrates in lateral-torsional motions and behaves depending upon the value of static eccentricity (difference in centers of mass and rigidity). Therefore, besides lateral stiffness, torsional stiffness needs to be included in formulation of stiffness matrix of a three dimensional building system. Similarly, mass matrix of three dimensional building system includes mass moment of inertia. In this section, a method is proposed to identify structural parameters from identified modal parameters of torsionally coupled shear buildings with measured data from all the floor locations using ITD techniques.

2.5.1 Least Square Solution of Eigenvalue Problem

Least square solution of eigenvalue problem needs mass matrix, natural frequencies and modal matrix to obtain stiffnesses of a structural system. The eigenvalue equation (Eq. 2.38) adopted for identification of stiffnesses of the symmetric-plan shear building has been modified for identification of stiffnesses of a torsionally coupled building. A generalized lumped mass model of three dimensional *n*-storey shear structures is shown in Fig. 2.10.

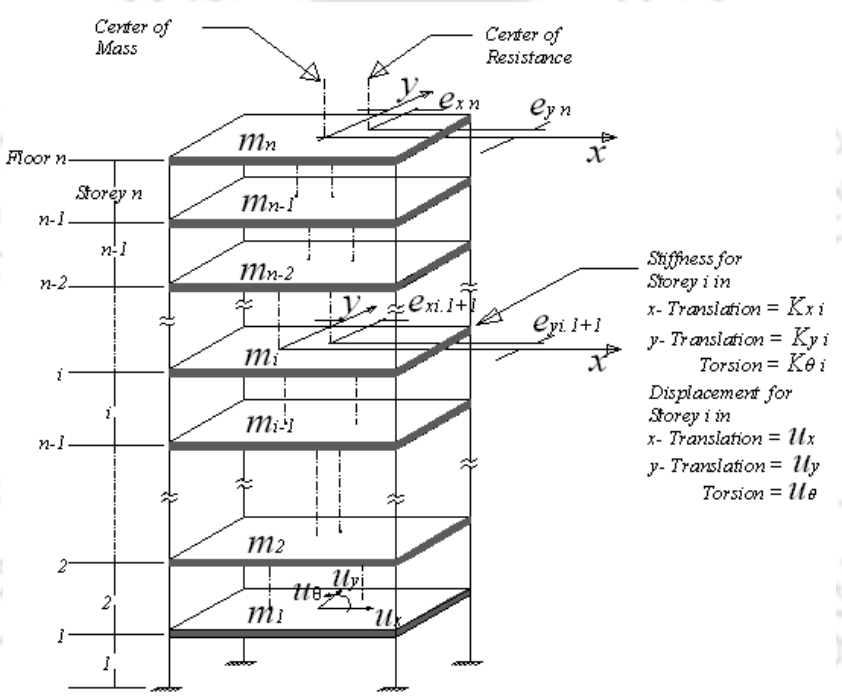

Fig. 2.10 Lumped mass model of a three dimensional multi-storey shear building

For a MDOF torsionally-coupled system, the undamped eigenvalue problem defined by Eq. 2.38 can be rewritten as:

$$(\mathbf{K}_T - \mathbf{M}_T)\boldsymbol{\varphi}_i = \{0\} \tag{2.47}$$

where $\mathbf{K}_T$ and $\mathbf{M}_T$ for three dimensional '*n*' degree of freedom system are represented as [Ueng *et al*. 2000]:

$$\mathbf{M}_{\mathrm{T}} = \begin{bmatrix} \boldsymbol{\lambda_i M_1} & & & \\ & \boldsymbol{\lambda_i M_2} & & \\ & & . & \\ & & & \boldsymbol{\lambda_i M_n} \end{bmatrix}$$

where $\boldsymbol{\lambda_i} = \begin{bmatrix} \lambda_{i,x} & 0 & 0 \\ 0 & \lambda_{i,y} & 0 \\ 0 & 0 & \lambda_{i,\theta} \end{bmatrix}$, $\lambda_{i,x}, \lambda_{i,y}, \lambda_{i,\theta}$ are i^{th} natural frequencies in X, Y and θ directions.

$\boldsymbol{M_i} = \begin{bmatrix} m_i & & \\ & m_i & \\ & & I_i \end{bmatrix}$ is the mass submatrix in which m_i and I_i are lumped mass and mass moment of inertia at floor i.

&

$$\mathbf{K}_{\mathrm{T}} = \begin{bmatrix} \boldsymbol{K}_{1,1} & \boldsymbol{K}_{1,2} & & & & & & \\ \boldsymbol{K}_{2,1} & \boldsymbol{K}_{2,2} & \boldsymbol{K}_{2,3} & & & & & \\ & \boldsymbol{K}_{3,2} & \boldsymbol{K}_{3,3} & \boldsymbol{K}_{3,4} & & & & \\ & & . & . & . & & & \\ & & & . & . & . & & \\ & & & & . & . & . & \\ & & & & & \boldsymbol{K}_{n-1,n-2} & \boldsymbol{K}_{n-1,n-1} & \boldsymbol{K}_{n-1,n} \\ & & & & & & \boldsymbol{K}_{n,n-1} & \boldsymbol{K}_{n,n} \end{bmatrix} \tag{2.48}$$

where

$$\boldsymbol{K}_{i,i-1} = \begin{bmatrix} -k_{x_i} & 0 & k_{x_i} e_{y_{i-1,i}} \\ 0 & -k_{y_i} & k_{x_i} e_{y_{i-1,i}} \\ & & -k_{\theta_i} \\ k_{x_i} e_{y_{i,j}} & -k_{y_i} e_{x_{i,i}} & -k_{x_i} e_{y_{i,i}} e_{y_{i-1,i}} \\ & & -k_{y_i} e_{x_{i,i}} e_{x_{i-1,i}} \end{bmatrix} \qquad (i = 2, \ldots, n)$$

$$\boldsymbol{K}_{i,i} = \begin{bmatrix} k_{x_i} + k_{x_{i+1}} & 0 & -k_{x_i} e_{y_{i,i}} - k_{x_{i+1}} e_{y_{i,i+1}} \\ 0 & k_{y_i} + k_{y_{i+1}} & k_{y_i} e_{x_{i,i}} + k_{y_{i+1}} e_{x_{i,i+1}} \\ & & k_{\theta_i} + k_{\theta_{i+1}} \\ -k_{x_i} e_{y_{i,i}} - k_{x_{i+1}} e_{y_{i,i+1}} & k_{y_i} e_{x_{i,i}} + k_{y_{i+1}} e_{x_{i,i+1}} & +k_{x_i} e_{y_{i,i}}^2 + k_{x_{i+1}} e_{y_{i,i+1}}^2 \\ & & +k_{y_i} e_{x_{i,i}}^2 + k_{y_{i+1}} e_{x_{i,i+1}}^2 \end{bmatrix} \quad (i = 2, \ldots, n\text{-}1)$$

$$\boldsymbol{K}_{i,i} = \begin{bmatrix} k_{x_i} & 0 & -k_{x_i}e_{y_{i,i}} \\ 0 & k_{y_i} & k_{y_i}e_{x_{i,i}} \\ -k_{x_i}e_{y_{i,i}} & k_{y_i}e_{x_{i,i}} & k_{\theta_i} + k_{x_i}e_{y_{i,i}}^2 + k_{y_i}e_{x_{i,i}}^2 \end{bmatrix} \qquad (i = n)$$

$$\boldsymbol{K}_{i,i+1} = \begin{bmatrix} -k_{x_{i+1}} & 0 & k_{x_{i+1}}e_{y_{i,i+1}} \\ 0 & -k_{y_{i+1}} & -k_{y_{i+1}}e_{x_{i,i+1}} \\ & & -k_{\theta_{i+1}} \\ k_{x_{i+1}}e_{y_{i,i+1}} & -k_{y_{i+1}}e_{x_{i,i+1}} & -k_{x_{i+1}}e_{y_{i,i+1}}e_{y_{i+1,i+1}} \\ & & -k_{y_{i+1}}e_{x_{i,i+1}}e_{x_{i+1,i+1}} \end{bmatrix} \qquad (i = 1,\ldots., n\text{-}1)$$

$\boldsymbol{\varphi}_i$ is i^{th} undamped eigenvector obtained from modal identification process. Now, the $\mathbf{K}_T$ can be determined easily for an undamped system and thereafter the storey stiffness can be identified.

In case of a multi-storey building if the measurements are available in all the locations where the mode shape values are required, following steps are used for the evaluation of structural stiffness matrix.

Step 1:

For shear building, the characteristics equation can be written as:

$$(\mathbf{K}_T - \mathbf{M}_T)\begin{Bmatrix} \boldsymbol{\varphi}_i^{(1)} \\ \boldsymbol{\varphi}_i^{(2)} \\ \boldsymbol{\varphi}_i^{(3)} \\ \ldots. \\ \ldots. \\ \boldsymbol{\varphi}_i^{(n)} \end{Bmatrix} = \begin{Bmatrix} 0 \\ 0 \\ 0 \\ \ldots \\ \ldots \\ 0 \end{Bmatrix} \qquad (2.49)$$

where $\boldsymbol{\varphi}_i^{(r)} = \begin{bmatrix} \phi_{i,x}^{(r)} & 0 & 0 \\ 0 & \phi_{i,y}^{(r)} & 0 \\ 0 & 0 & \phi_{i,\theta}^{(r)} \end{bmatrix}$, r =*1, 2, 3……n* is the i^{th} modal displacements in X, Y and θ directions at the r^{th} floor level.

Step 2:

It may be noted that single frequency and mode shape are necessary to obtain a solution. The equation can be expanded and rearranged as:

$$\mathbf{\Delta_i k = \Lambda_i}$$

The stiffness vector may be obtained as:

$$\mathbf{k = \Delta_i^{-1} \Lambda_i} \tag{2.50}$$

where,

$$\mathbf{\Delta_i} = \begin{bmatrix} \boldsymbol{\varphi}_i^{(1)} & \boldsymbol{\varphi}_i^{(1)} - \boldsymbol{\varphi}_i^{(2)} & 0 & ..... & \mathbf{0} \\ 0 & \boldsymbol{\varphi}_i^{(2)} - \boldsymbol{\varphi}_i^{(1)} & \boldsymbol{\varphi}_i^{(2)} - \boldsymbol{\varphi}_i^{(3)} & ..... & \mathbf{0} \\ . & . & . & ..... & ... \\ . & . & . & ..... & ... \\ \mathbf{0} & \mathbf{0} & ..... & \boldsymbol{\varphi}_i^{(n-1)} - \boldsymbol{\varphi}_i^{(n-2)} & \boldsymbol{\varphi}_i^{(n-1)} - \boldsymbol{\varphi}_i^{(n)} \\ \mathbf{0} & \mathbf{0} & ..... & ..... & \boldsymbol{\varphi}_i^{(n)} - \boldsymbol{\varphi}_i^{(n-1)} \end{bmatrix} \tag{2.51}$$

$$\mathbf{k} = \begin{bmatrix} \boldsymbol{k}_1 \\ \boldsymbol{k}_2 \\ . \\ . \\ \boldsymbol{k}_n \end{bmatrix} \text{ with } \boldsymbol{k}_n = \begin{bmatrix} k_x^{(n)} & 0 & 0 \\ 0 & k_y^{(n)} & 0 \\ 0 & 0 & k_\theta^{(n)} \end{bmatrix}, \; k_x^{(n)}, \; k_y^{(n)} \text{ and } k_\theta^{(n)} \text{ are } n^{\text{th}} \text{ storey stiffness in X, Y and } \theta \text{ directions} \tag{2.52}$$

&

$$\mathbf{\Lambda_i} = \begin{bmatrix} \boldsymbol{\varphi}_i^{(1)} \boldsymbol{\lambda}_i \boldsymbol{M}_1 \\ \boldsymbol{\varphi}_i^{(2)} \boldsymbol{\lambda}_i \boldsymbol{M}_2 \\ . \\ . \\ \boldsymbol{\varphi}_i^{(n)} \boldsymbol{\lambda}_i \boldsymbol{M}_n \end{bmatrix} \text{ with } \boldsymbol{\varphi}_i^{(n)} = n^{\text{th}} \text{ element of } \boldsymbol{\varphi}_i . \tag{2.53}$$

Estimated mass matrices $\boldsymbol{M_i}$ are utilized for identification of storey stiffness $\mathbf{k}$ from identified mode $\{\phi_i\}$ and corresponding model frequencies λ_i using Eq. 2.50.

2.6 STABILITY OF SYSTEMS

The accuracy of identified results depends on the stability of the system identification techniques. In state-space terminology, a system is said to be *asymptotically stable* if the homogeneous response of the state vector $x(t)$ returns to the origin of the state-space $x = 0$ from any arbitrary set of initial conditions $x(0)$ as time $t \to \alpha$. The statement can be represented in the mathematical form as:

$$\lim_{t \to \alpha} x_i = 0 \qquad \text{for all } i = 1,2,3,.....n$$

Again, all the elements of the system matrix $\mathbf{A}$ are linear combinations of the modal components $e^{\lambda_i t}$, therefore the stability of a system depends on all such components decaying to zero with time. Hence, for a stable system $\lambda_i < 0$, since any positive eigenvalue generates a modal response that increases exponentially with time.

The stability of a system can be checked by the characteristics of the measures like *poles* and *zeros* which are also roots of characteristic function of a dynamical equation. The *poles* and *zeros* can be derived from the transfer functions of input and output relationship of a system. The counterpart of *s*-transform in case of a continuous time function is *z*-transform in case of discrete time function. The transfer function $H(z)$ as shown in the Eq. 2.13 is z-transformation the state Eq. 2.8. The roots, z_i of the equation $\mathbf{y}(z) = 0$ are defined as system *zeros*. Similarly, the roots, z_i of the equation $\mathbf{u}(z) = 0$ are defined as *poles* of the system. The transfer function, $\mathbf{H}(z)$ vanishes when the $\mathbf{y}(z) = 0$, i.e. $\lim_{t \to \alpha} H(z) = 0$ and similarly when $\mathbf{u}(z) = 0$, the transfer function becomes unbounded, i.e. $\lim_{t \to \alpha} H(z) = \alpha$. All of the coefficients of polynomials $\mathbf{y}(z) = 0$ and $\mathbf{u}(z) = 0$ are real, therefore the *poles* and *zeros* must be either purely real, or appear in complex conjugate pairs. The existence of a single complex *pole* without a corresponding conjugate *pole*

would generate complex coefficients in the polynomial $\mathbf{u}(z)=0$. Similarly, the system *zeros* are either real or appear in complex conjugate pairs.

The system dynamics may be represented graphically by plotting their locations on the complex z-plane, whose axes represent the real and imaginary parts of the complex variable *z*. Such plots are known as *pole-zero plots*. It is usual to mark a zero location by a circle (O) and a pole location a cross (x). The location of the *poles* and *zeros* provide qualitative insights into the response characteristics of a system. Many computer programs are available to determine the *poles* and *zeros* of a system from either the transfer function or the system state equations. The *poles* can be projected in z-plane of any system and the stability of the system can be checked as shown in the Fig. 2.11. MATLAB command z-plane plot has been used to *poles* plot after obtaining the system matrices.

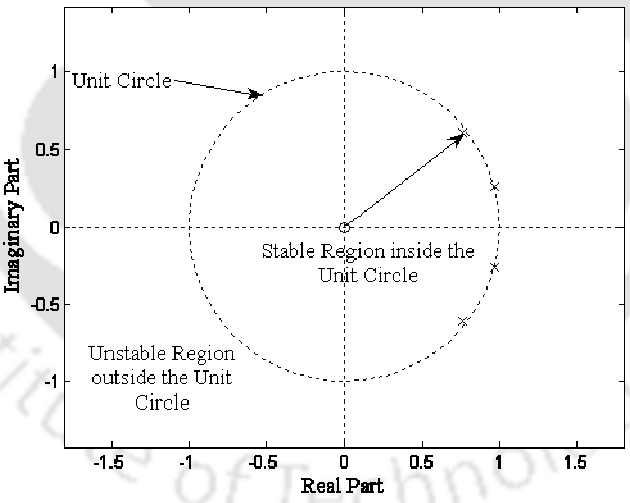

Fig. 2.11 Stable region for discrete time system [Juang,1994]

For a stable system, all poles must have a magnitude <1. From the Eq. 2.14 it can be inferred that the *pole* of system is related to its corresponding damping ratio and frequency of the mode of vibration. The amplitude is related to the damping values and the phase of

the *pole* is related to the frequency. Thus, plot of *poles* in z-plane can be used to indicate the stability of the identification system.

2.7 INDICES FOR DAMAGE IDENTIFICATION

Numbers of measures are available for detection of damage and identify the location of damage in a structure. In various literatures the indices are being used to identify damage and location of the damage from changes of physical parameters of structures. Indices like Modal Assurance Criteria (MAC), Mode Orthogonality, Mode Shape Correlation Constant (MSCC), Modal Curvature, Curvature Differential Values etc. used to determine damage and location of damage in a structure are not directly related to identification models. The indices proposed to use in this study compares the mode shape of experimental building to corresponding mode shapes of a numerical simulated building.

2.7.1 Modal Assurance Criterion

Modal Assurance Criterion (MAC) is a factor with values 0 to 1. The values depend on the correlation between two similar mode shapes. Two mode shapes of similar kind will have MAC value 1 if they are identical. Physically similarity or dissimilarity of different the mode shapes of experimental model can not be examined with the corresponding mode shapes of numerical model. The MAC is a procedure to compare different mode shapes of experimental model with corresponding modes shapes of numerical model. The MAC number is defined as matrix of normalized inner product of mode shape vectors and expressed as below,

$$MAC = \frac{\left|\sum_{l=1}^{p} \varphi_{l,i}^{a} \varphi_{l,i}^{b}\right|^{2}}{\left(\sum_{l=1}^{p} \varphi_{l,i}^{a} \varphi_{l,i}^{a}\right)\left(\sum_{l=1}^{p} \varphi_{l,i}^{b} \varphi_{l,i}^{b}\right)} \tag{2.54}$$

where, $\varphi_{l,i}^{a}$ is the modal amplitude at the location l of the i^{th} mode of model a, while $\varphi_{l,i}^{b}$ is the modal amplitude at the location l of the i^{th} mode model b.

If two mode shapes are not linearly correlated, the MAC factor will be equal to zero. Lower values of MAC for the same mode shape between measurements a and b indicates that the structure has changed, possibly due to damage. Damage in complex structures can be cause the order of the modes to change. In many literatures the MAC has been used to see the shifts in the order of mode shapes between two measurements.

2.8 CONCLUDING REMARK

System identification is very young among the available SHM techniques. Subspace identification technique can appropriately describe the state of a system based on recorded input and output data. Subspace identification deals with combined deterministic-stochastic linear system and hence is useful for identification of modal parameters in two horizontal directions of symmetric-plan shear buildings using recorded unidirectional acceleration histories. Parametric subspace identification algorithm N4SID which uses input and output data is fast and robust (noise tolerant) as demonstrated by Medhi *et al.*[2008]. Therefore, it is suitable for identification of modal parameters in two horizontal directions of symmetric-plan shear building using recorded unidirectional acceleration histories. In case of torsionally coupled buildings, the horizontal acceleration histories are always accompanied by a torsional component. It is not possible to record torsional ground motion during an earthquake with available instrumentation facilities at present. Thus, N4SID is not suitable for identification of modal parameters of a torsionally coupled building. ITD system identification scheme which uses free decay responses of recorded acceleration histories in two horizontal directions and computed rotational component at upper floors is used for identification of modal parameters of torsionally coupled building.

Free decay responses contain information of modal parameters inherited in the recorded acceleration histories. These can be used to develop an oversized mathematical model using time shifting technique and thereafter modal parameters can be identified.

Stiffness is directly related to moment of inertia or Young's modulus of structures and gives idea about the health of a structure. Stiffness of building system can be easily evaluated through least squares solution of an eigenvalue problem. The identified modal frequencies and modal displacements are used to formulate the eigenvalue problem. Least square solution needs a full mode shape and its corresponding frequency to estimate the stiffness vector. However, the results are accurate when the complete modal matrix and corresponding modal frequencies are utilized. In case of high rise building with limited number of sensors, iterative approach would be useful for determination of complete modal matrix for identification of stiffness.

In general, modal displacements are changed due to presence of any damage in a structure. The MAC compares the mode shapes of a damaged structure with corresponding mode shapes of the same structure in its undamaged state. Thus, MAC is a useful measure for detection of damage and their locations.

CHAPTER 3

DETAILS OF EXPERIMENTAL ARRANGEMENT FOR SYSTEM IDENTIFICATION STUDY

3.1 INTRODUCTION

Identification of system parameters of building uses measured structural responses to form the system matrices. Structural responses are generally recorded when the buildings are excited by ambient vibration or earthquake excitations. Adequate instrumentation is required to acquire proper structural responses. Numerous strategies on collection of experimental data for use in system identification have been reported in various literatures. Juang [1994] explained procedure adopted for identification of system parameters in six steps. The third and fourth steps are directly related to instrumentation and collection of experimental data. Nagarajaiah and Xiaohong [2000] described about detailed instrumentation used to record structural responses during earthquake from an existing base isolated building for use in system identification scheme. Caicedo [2001 and 2003] described about the instruments used for collection of experimental data from laboratory test models. Marwala [2003] instrumented a bridge for recording acceleration data for using in identification model. Maruki [2004] explained in detail about instrumentation for collection of vibration data from a five storey laboratory test model of building. Procedure adopted for selection of useful and high frequency ranges of data were also described in the study. Bani-Hani [2008] instrumented an old high rise minaret to acquire ambient as well as earthquake data. It has been observed from detailed literature surveys that arrangement for collection of experimental data for laboratory test model is different from that of an existing structure. In the present work, system identification studies have been carried out using recorded data based on laboratory test models as well as existing buildings. In case of laboratory test model, prescribed earthquake excitations are used to

excite the test model. However, structural responses of existing multi-storey buildings are recorded during earthquake ground motions. Therefore, the entire experimental programme is presented into two sections. In the first section, the arrangements for acquiring structural response of laboratory test models are described. Details of instrumentations in existing multi-storey buildings are provided in the subsequent section. Thus, in this chapter description of overall instrumentation for acquiring structural responses of laboratory test models as well as existing multi-storey building has been presented.

3.2 DETAILS OF EXPERIMENTAL ARRANGEMENT FOR LABORATORY TEST MODELS

Details of experimental arrangements for dynamic testing of a laboratory test models are shown in Fig. 3.1.

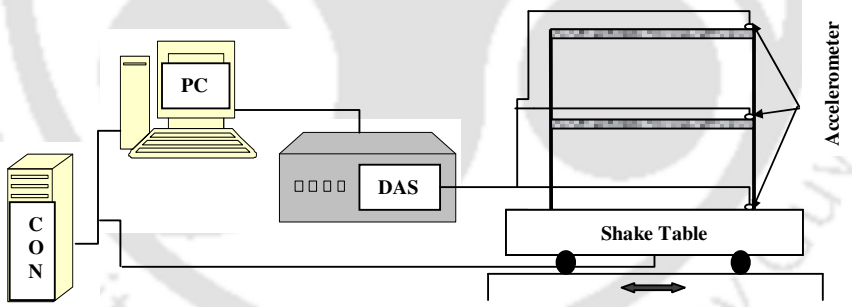

Fig. 3.1 Schematic diagram of instrumentation for laboratory test models

Laboratory test models are excited by Shake Table using time scaled prescribed earthquake motions. Digital controller reproduces prescribed earthquake acceleration histories through servo-hydraulic system. Floor responses measured by the accelerometers are recorded and stored in data acquisition system (DAS). Different aspects of testing of laboratory test models are described separately in the following subsections.

3.2.1 Laboratory Shake Table

Shake Table is utilized to excite test models by reproducing prescribed earthquake excitations or simulated ground motions. A 2500 x 2500 mm size uni-axial Shake Table installed in Civil Engineering Department laboratory of Indian Institute of Technology Guwahati (IIT Guwahati) is shown in Fig. 3.2.

Fig. 3.2 Uni-axial Shaking Table (Make: BiSS, India)

Pay load capacity of the shake table is 5000 kg. The shake table is equipped with a powerful servo-hydraulic actuator to excite test models in a displacement range up to ± 500 mm. This shake table can produce maximum acceleration up to ±2g. The shake table has an operational frequency range 0 to 100 Hz.

3.2.2 Sensors and Data Acquisition System (DAS)

Uni-axial force balance accelerometers (Model: ES-U2, Make: Kinemetrics Inc., USA) have been selected for measuring structural responses of laboratory test models during shake table excitations. This force balance accelerometer can measure acceleration amplitudes from ambient noise level to a maximum of ± 1g. The ES-U2 can detect any structural motion that may vibrate in frequency range of DC to 200 Hz. It has the facility

of amplification and conditioning measured digital data. The amplified and conditioned digital signals can directly be transferred to a compatible data acquisition system. A 48-channel DAS (Make: HBM Inc., Germany) has been used to record and store digital data measured by accelerometers. Out of forty eighth channels, sixteen channels are exclusively meant for recording accelerations time histories from sixteen accelerometers simultaneously.

3.2.3 Details of Sample Ground Motions for Shake Table Test

Four different earthquake ground motions have been considered for subjecting excitation to the test models by shake table. Earthquake records with different peak accelerations, displacements and durations have been selected for use in the laboratory experiment. These were recorded during El Centro (1940): Comp - 180, Victoria (1980): Comp - CPE045, Parkfield (1966): Comp - C02065 and Koyna (1967): Comp - Transverse earthquakes. The descriptions of relevant characteristics of the earthquake records are presented in Table 3.1.

Table 3.1 Characteristics of selected earthquake records

Earthquake Components	**Peak Ground Acceleration (g)**	**Frequency Range (rad/sec)**
El Centro (1940): Comp - 180	0.32	0-65
Victoria (1980): Comp - CPE045	0.62	0-160
Parkfield (1966): Comp - C02065	0.48	0-40
Koyna (1967): Comp - Transverse	0.50	0-12

Acceleration time histories of the selected earthquake records are shown in Fig. 3.3.

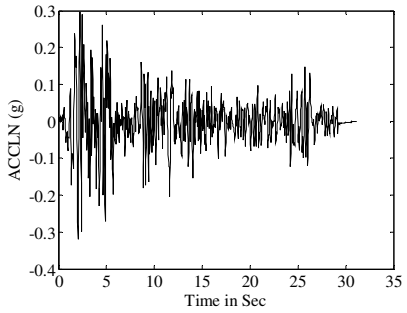

(a) El Centro (1940): Comp - 180

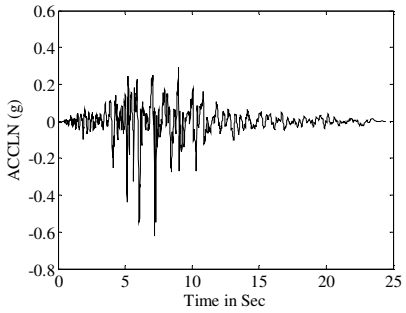

(b) Victoria (1980): Comp - CPE045

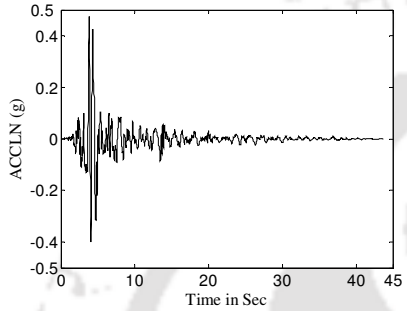

(c) Parkfield (1966): Comp - C02065

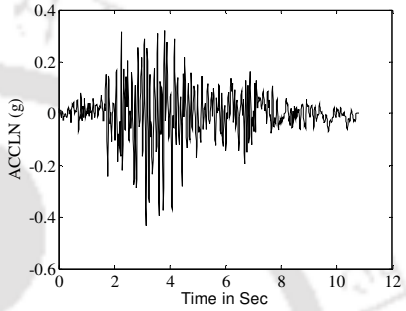

(d) Koyna (1967): Comp - Transverse

Fig. 3.3 Acceleration time histories of four different earthquakes

3.3 INSTRUMENTATIONS OF EXISTING MULTI-STOREY BUILDINGS

In this study, acceleration responses of two sample buildings have been recorded during actual ground motions. One of these is a multi-storey symmetric-plan shear building while the other is a torsionally coupled shear building. Both of the buildings have been instrumented for acquiring earthquake induced structural responses. Details of instrumentation of an existing multi-storey building are shown in Fig. 3.4.

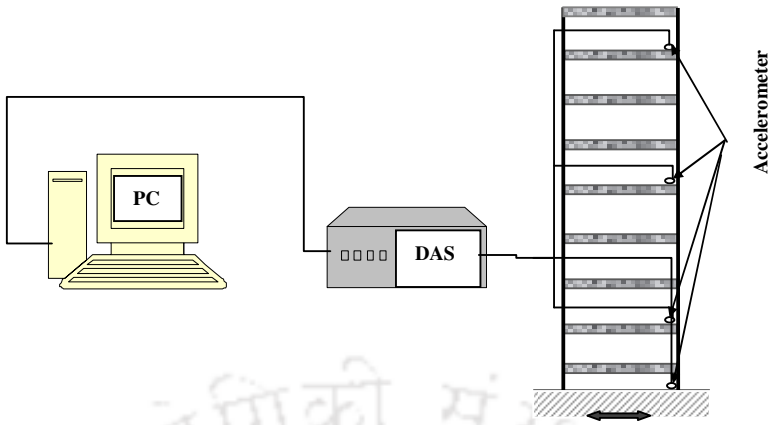

Fig. 3.4 Schematic diagram of instrumentation for existing multi-storey building

Accelerometers are installed to measure accelerations in two lateral directions of a symmetric-plan building. In case of a torsionally coupled building, the torsional component of acceleration time history at each floor level needs to be measured. In absence of rotational accelerometers, the torsional accelerations of a floor have been measured by installing two uni-axial accelerometers along two parallel lines in any direction. Difference in instantaneous acceleration values recorded by the two accelerometers is divided by the distance between the accelerometers to compute torsional response of the floor [Chopra, 2001]. The accelerometers at different floor levels are connected to a DAS to record the measured data by the accelerometers. The recorded data are stored in in-built memory of the system and transferred to computing device for further processing.

3.3.1 Sensors and Data Acquisition System (DAS)

Two different types force balanced accelerometers manufactured by Kinemetrics Inc., USA have been selected for measuring acceleration data from the selected sample buildings. One of these is a uni-axial type (Model: EpiSensor ES-U2) while the other is a tri-axial type (Model: ES-T) accelerometer. The description of ES-U2 has already been

presented in section 3.2.3. Tri-axial accelerometer (Model: ES-T) consists of three force balance accelerometer modules mounted orthogonally in one small convenient package.

DAS manufactured by Kinemetics Inc., USA (Model: Altus K2) has been selected for recording and storing acceleration data measured by the accelerometers at different floor levels of the selected sample buildings. The K2 has 4 inbuilt auxiliary ports to acquire data from twelve channels simultaneously. Three uni-axial accelerometers can be connected to a single port through a junction box. Similarly, a tri-axial accelerometer that has three channels can be connected to a port directly. Thus, measured acceleration data by twelve accelerometers can be recorded simultaneously. Data recording is possible at a rate of 200 samples per second (sps). The system is powered with 10.5-15 V power supply with a back up facility up to 36 hours. The acquisition mode is continuous and recording starts at the onset of user selectable trigger timing and stops recording just after user selectable detrigger timing. The recorded data are stored in a PMCIA card in the form of a 24 bit system data format. Stored data can be retrieved remotely via modem or telemetry, or by a hand held computer.

3.3.2 Details of Earthquake Excitations

Both the sample buildings considered for system identification studies are situated in the seismic Zone-V (i.e. zone with highest seismicity) of seismic zone map of India. Earthquakes are regularly felt in this seismic zone. Hence, structural responses as well as ground motions have been recorded during actual earthquakes. Numbers of earthquakes had occurred in the building sites since instrumentation of the buildings. Structural responses recorded during earthquakes on February 11, 2006 and other on August 12, 2006 have been considered for use in identification of both the instrumented existing multi-storey buildings. The February 11, 2006 (5:4:16.4 UTC) earthquake occurred at depth of 33.00 km in latitude 27.6^0N and longitude 92.3^0E near Arunchal Pradesh (India)-

Tibet border. The August 12, 2006 (20:46:12.1 UTC) earthquake took place at depth of 66.00 km in latitude 24.4^0N and longitude 92.8^0E near India-Bangladesh border. The magnitude of the earthquakes was 5.0 in Richter scale.

3.4 PROCESSING OF RECODED DATA

Processing of recorded data basically includes polishing and filtering of original data. Fig. 3.5 shows plot of resampled and polished data of high amplitude portion of acceleration history which will be used to build the identification model.

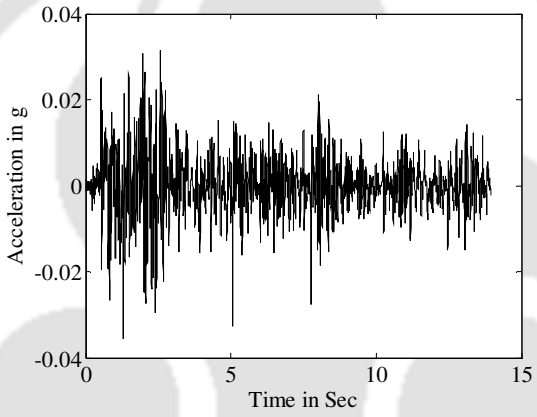

Fig. 3.5 Plot of processed high amplitude part of acceleration history

The acceleration data acquired from a structural system may contain noise and unimportant parts. Only high amplitude portion of recorded acceleration histories is used in the identification process. In addition, data points may be reduced by changing sampling frequency. Use of only useful portion of data helps in increasing efficiency of the identification process. Therefore, raw acceleration data need to be polished and filtered before using in the mathematical model for identification of system parameters.

Further, information inherited in recorded data of a dynamic system can be well described through Fourier amplitude spectrum (FFT) plot. The FFT plot of a recorded data gives information about predominant frequencies of the system. Fig. 3.6 represents FFT plot of the high amplitude part of the acceleration time history shown in Fig. 3.5.

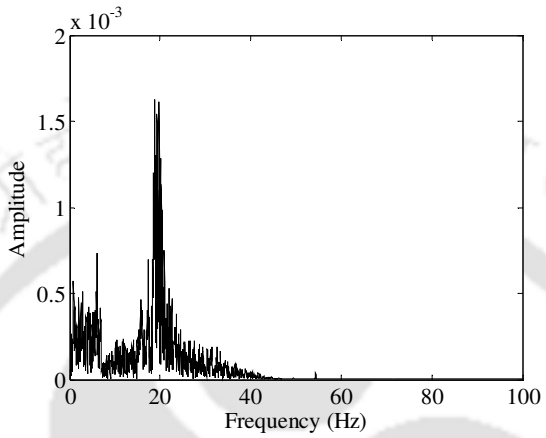

Fig. 3.6 Fourier amplitude spectrum of high amplitude part of recorded acceleration history

The FFT as shown in Fig. 3.6 gives an idea about the cutoff frequency to be considered, which is generally double of the highest prominent frequency (i.e. Nyquist frequency) available in the plot. The sampling frequency for recording experimental data is generally kept higher so as to collect maximum possible information of the system. The high amplitude portion of the acceleration time history as shown in Fig. 3.5 is considered for re-sampling. The re-sampling frequency is selected based on the observed frequency content in the FFT plot to avoid any loss of important information during processing of data. The sampling frequency of original data shown in the plot 3.5 is 200 Hz and resample frequency is considered to be 100 Hz, which reduces number of data points from 2800 to 1400. The Nyquist frequency observed in the FFT plot is approximately 20 Hz. Hence, a cutoff frequency of 40 Hz is considered for adopting a low pass digital filter.

3.5 CONCLUDING REMARK

The accuracy of any identification scheme depends on the use of accurate experimental data, which depends on the adequacy of instrumentations. Different types of sensors and data acquisition system have been selected for conducting tests on laboratory test models and existing multi-storey buildings. The available accelerometers are rugged and suitable to sense ambient vibration as well as forced vibration. Both types of available data acquisition system are capable of acquiring the data that will be sensed by the accelerometers. However, the test models can be excited in only one direction with help of the available uni-axial Shake Table test facility in the laboratory.

High amplitude parts of the recorded excitation responses are used in the proposed identification models. The sampling frequency of data set in the DAS sometimes found to be much higher that of the frequency of the system. Therefore, to increase the efficiency of the identification scheme, the numbers of data points are reduced by considering a low re-sampling frequency. Further, noise in the data in the form of high frequency content can be eliminated through screening the original data using a low pass filter. Studying the FFT plots of all of the high amplitude parts of original acceleration data, low pass filters and re-sampling frequencies have been easily selected.

CHAPTER 4

IDENTIFICATION OF SYSTEM PARAMETERS OF SCALED LABORATORY TEST MODELS

4.1 INTRODUCTION

System identification techniques are used to build models of dynamic system for the evaluation of a system matrix. However, the model needs to be verified before implementing on existing structure. The verification can be realistically carried out through laboratory based experimental studies. The laboratory based experiments facilitate consistent acquisition of data for verification of the mathematical model. This chapter uses parametric state space model to identify modal parameters of scale laboratory test models subjected to various known earthquake excitations. Three scaled laboratory models of different configuration have been considered for the experimental study.

The dynamic behavior of a building is influenced by the stiffness of the supporting elements like columns and beams. Thus, three test models with different column sizes have been considered for studies on identification of system parameters. This will help to verify the adequacy of the adopted identification technique. The structural responses at different floor levels due to the shake table excitations in form of prescribed earthquake motions are used in the modal parameters identification of these test models. The identified modal parameters are used for the solution of characteristics equation through least square technique for the determination structural parameters. Further, studies have been conducted on numerically simulated models of all the three test models developed in SAP 2000 Nonlinear (version 12).

4.2 STUDIES ON LABORATORY TEST MODELS

Laboratory test on models of structures started since World War II as mentioned by Harris and Sabnis [1999]. Since then, number of researchers carried out investigation on laboratory test models. In the present study, test models of two storey reinforced concrete building with floor size 2.0 m (2 bays of 1.0 m each) x 1.0 m and having 0.66 m storey height have been considered. Scale factor (S) of these models is 1:5 (model: prototype). In the following subsections, details of test models with geometric scale factor, testing requirements and identified parameters are discussed.

4.2.1 Similitude and Scaling

The *laws of similitude* are followed to arrive at appropriate input motion, dimensions of test models as well as for finalization of additional mass requirement for gravity load simulation. The similitude requirements are derived from dimensional analysis which depends on physical characteristics like length, force, time, temperature etc. The Table 4.1 shows derived scaling relationship of the parameters relevant to the present study.

Table 4.1 Similitude requirements [Harris and Sabnis, 1999]

Parameters	**Scale**	**Prototype**
		1/5th-scale model
Length	S	5
Mass	S^2	25
Displacement	S	5
Time	$\sqrt{S}$	2.236
Acceleration	S	5

4.2.2 Modeling Process

Careful planning is required for successful preparation of test models. Following steps describe the procedure adopted for the preparation of scaled laboratory test models and dynamic testing on a shake table.

1) Selection of scale of test models has been done based on available size of test facility. The available shake table size has the table dimension of 2.5 m x 2.5 m. Scale of 1:5 has been considered for test models with base size 1.0 m x 2.0 m. Further, the total weight of the models has also been finalized keeping in mind the payload capacity of the shake table.
2) Selection of materials to geometrically represent those of the prototype structure.
3) Fabrication of test models with precision and estimation of required compensatory mass to be distributed over various floors.
4) Selection of earthquake excitations as input motion to the shake table and acquisition of acceleration data from different floor levels.

4.2.3 Bare Frame Scaled Laboratory Test Models

The reliability of results from a laboratory model testing depends on the precision in fabrication of the structural model satisfying similitude requirements. In this chapter, studies on scaled test models of reinforced concrete buildings under different prescribed earthquake excitations have been presented. Three different $1/5^{th}$ scale laboratory models have been constructed with different column sizes at ground floor to study changes in modal and structural parameters. Fig. 4.1 shows a view of one such model during construction. Similar material properties have been kept for the construction of all the models. As may be seen from Fig. 4.1, tie beams have been provided to integrate the

columns of the models at base level and steel angle sections have been provided along the outer periphery of the base to fix the models to the shake table.

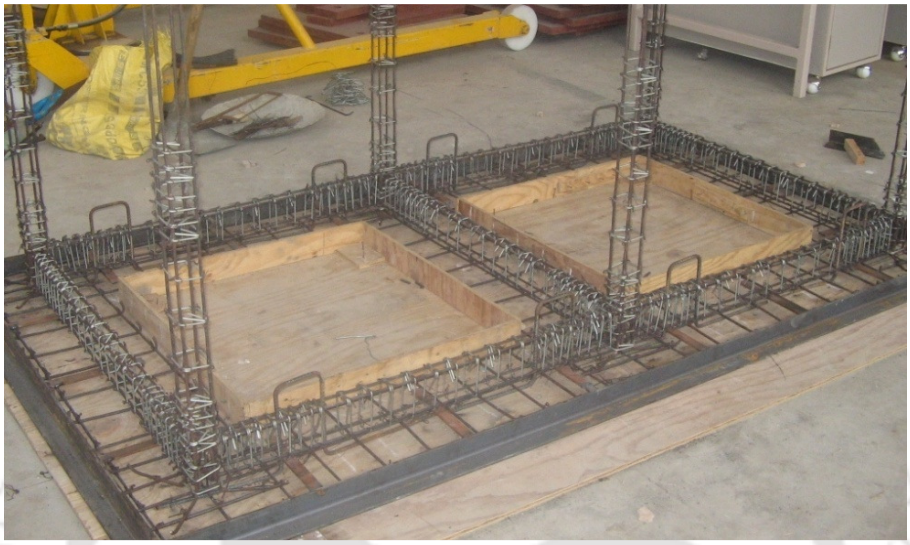

Fig. 4.1 Construction of laboratory test model

The test models have been designated as Model I, Model II and Model III. The descriptions of various geometrical properties of all test models are furnished in Table 4.2. The overall depth of the beam for all the floors have been kept 90 mm measured from top of the slab. The clear heights of columns in both the storey of Model I have been kept as 660 mm. The geometrical properties of first storey elements of all the three test models are similar. However, the geometrical properties of ground storey of Model II and III are different from those of Model I. The height of column at the ground storey of Model II has been reduced to 490 mm from 660 mm as provided in Model I. The sizes of ground storey columns of Model III have been increased to 100 x 100 mm from 75 x 75 mm as provided in the Model I. Pictorial views of all the test models are shown in the Fig. 4.2. The column positions of the laboratory test models are shown in Appendix – A [Fig. A – 1].

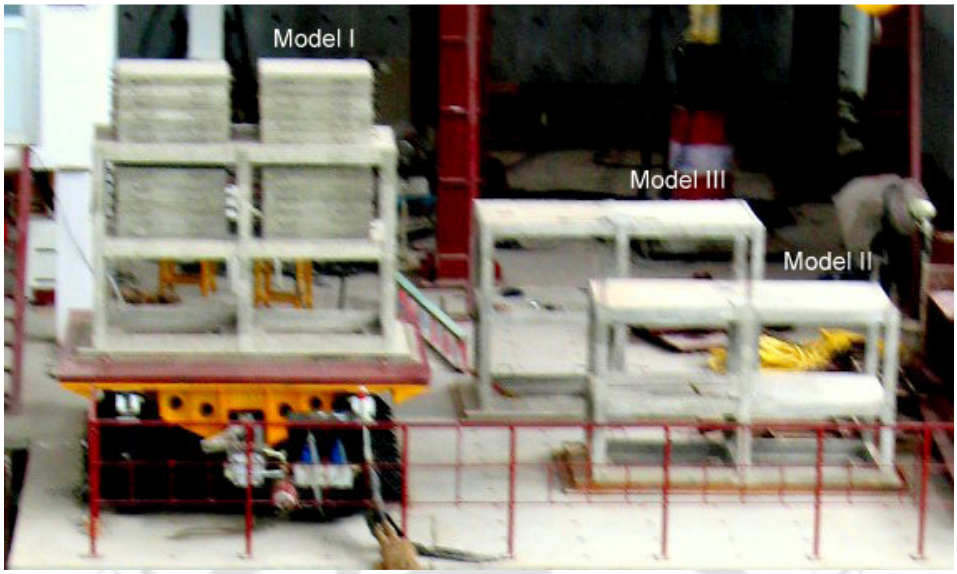

Fig. 4.2 Photograph of bare frame test models

Table 4.2 Elemental properties of laboratory test models

Particulars	**Model I**	**Model II**	**Model III**
Floor Panel Size (mm)	1000 x 1000	1000 x 1000	1000 x 1000
Slab Thickness (mm)	40	40	40
Column Height (mm) at GS	660	490	660
Column Height (mm) at FS	660	660	660
Column size (mm) at GS	75 x 75	75 x 75	100 x 100
Column size (mm)at FS	75 x 75	75 x 75	75 x 75
Beam size (mm)	60 x 90	60 x 90	60 x 90

GS: Ground Storey; FS: First Storey

4.2.4 Material Properties of Test Models

The models have been cast with locally available construction materials. Some of the physical and mechanical properties of the materials used are presented in the Table 4.3. Material homogeneity has been maintained by providing similar materials for the construction of all the models.

Table 4.3 Material properties for scaled laboratory test models

Particulars	Model I	Model II	Model III
Concrete			
Water Cement Ratio	0.55	0.55	0.55
Maximum size of aggregate (mm)	6	6	6
Density (kg/m^3)	2435	2435	2435
Average Compressive Strength (N/mm^2)	15	15	15
Reinforcing Steel			
Type of Steel	M S Fe 250	M S Fe 250	M S Fe 250
Size of the Steel bar, mm	6	6	6
Young's Modulus of Steel (x 10^5 N/mm^2)	2	2	2

4.2.5 Scaled Time Histories

As mentioned in the section 3.3.3, the sampling rate of earthquake records used for shake table excitation need to be scaled through a factor $1/\sqrt{S}$, where S denotes scale factor. The Table 4.4 represents original and scaled sampling rate of earthquake records used for the study.

Table 4.4 Time interval of earthquake records selected for shake table excitations

Earthquake Motions	Original Time Interval (sec)	Scaled Time Interval (sec)
El Centro (1940): Comp - 180	0.02	0.008944
Victoria (1980): Comp - CPE045	0.01	0.004472
Parkfield (1966): Comp - C02065	0.01	0.004472
Koyna (1967): Comp - Transverse	0.01	0.004472

Fig. 4.3 shows time scaled representation of four selected earthquake records. The time duration of the acceleration histories have been observed to be reduced through the factor of $1/\sqrt{S}$.

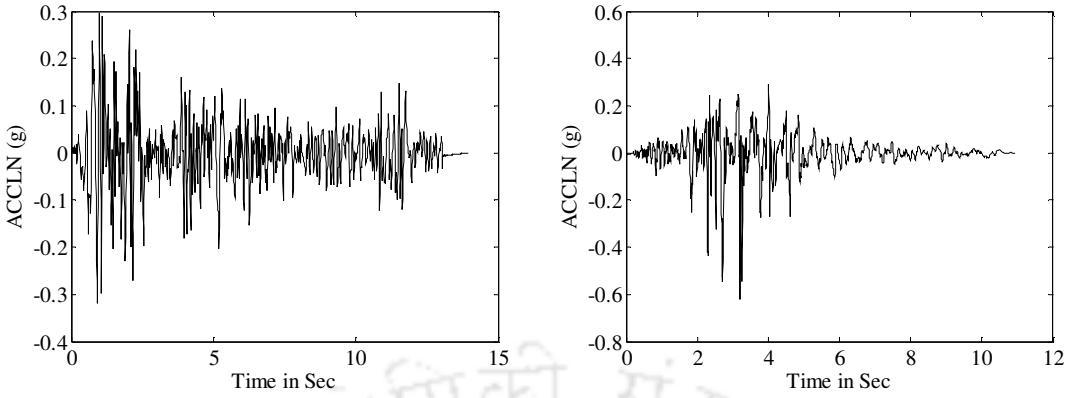

(a) El Centro (1940): Comp - 180 (b) Victoria (1980): Comp - CPE045

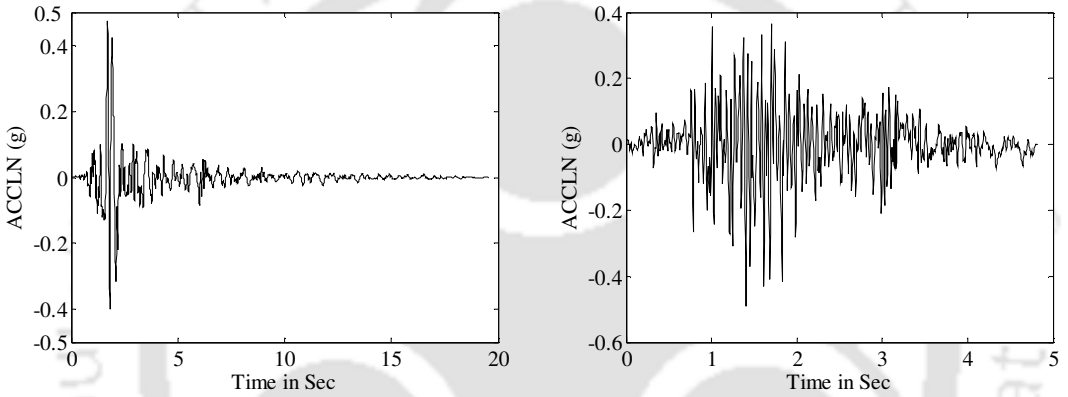

(c) Parkfield (1966): Comp - C02065 (d) Koyna (1967): Comp - Transverse

Fig. 4.3 Time scaled accelerations histories of four selected earthquake components

4.2.6 Compensating Mass for Scaled Test Models

In case of scaled test model, the geometry of the structure is decided in accordance to the scale factor. However, the mass of the prototype structure does not get proportionately reduced as per similitude requirement. Hence, additional masses need to be added to maintain requirement of scaling relationship for gravity load similitude as mentioned in Table 4.1. The mass of the prototype building have been determined as 75088 kg considering unit weight of concrete as 2435 kg/m^3. The detailed calculation of mass (floor wise) for the prototype building is shown in Appendix – A [Table A – 4]. The total mass of the test model is 600 kg. The mass required for fulfilling similitude requirement is

about 3000 kg. Hence, an additional mass of 2400 (=3000-600) kg is required to be uniformly distributed over two floors of the model.

4.2.7 Shake Table Test

Shake Table as described in section 3.2.1 has been used to carry out experimental studies. The test models have been placed centrally on the table with appropriate clamping. Concrete blocks as shown in Fig. 4.4 have been placed on each floor to account for the compensating mass. Uni-axial force balanced accelerometers have been fixed to each floor of the test model as shown in Fig. 4.4. While table acceleration data from sensor 1 is used as input to the identification model, responses from first floor (sensor 2) and roof (sensor 3) levels are used as output. These accelerometers are connected to DAS (Model: MGCplus, Make: HBM, Germany) for recording structural responses from different floor levels. Displacement histories of time scaled acceleration histories as depicted in Fig. 4.3 have been applied to the shake table through digital control system. The amplitude of displacement time history has been scaled down to 10% for the model testing to avoid any damage in the specimen. Fig. 4.5 shows digital controller and the DAS used for laboratory tests.

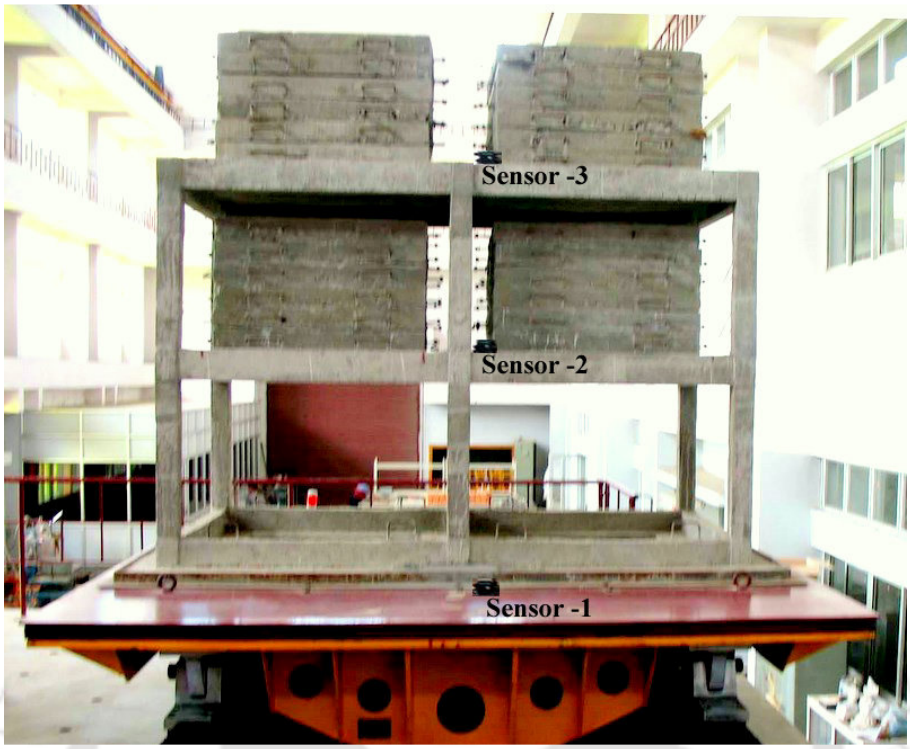

Fig. 4.4 Model I on shake table

Further, models have also been tested with displacement amplitude reduced to 20% of that of the original earthquake record. This has been carried out in order to verify the effect of amplitude of the displacement in the experimental investigation. The sampling rate for data recording has been considered as 200 Hz.

Fig. 4.5 Control system for the shake table testing

Shake Table is an electro-mechanical system which is excited by linear servo hydraulic actuator using displacement time histories. Therefore, proper tuning is needed so as to obtain feedback which is identical to applied input used to excite the shake table. Tuning has been carried out for every set of test specimen using electronic gain control. Thereafter, shake table tests have been carried out for all the test models with four selected earthquake excitations as input.

4.2.8 Characteristics of Recorded Responses

The table accelerations acquired through the DAS have been processed to retain only the high amplitude part of the response. The high amplitude part of the recorded data at the base level (sensor 1) of test Model I for all the four selected earthquakes are shown in Fig. 4.6.

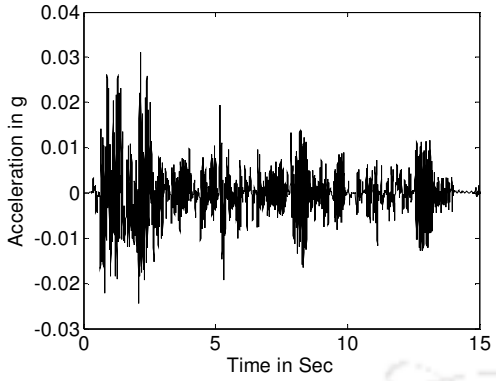

(a) For El Centro (1940): Comp - 180

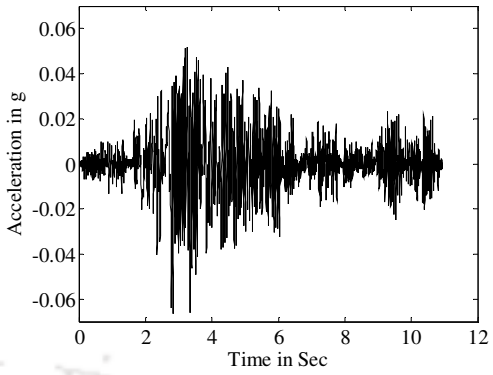

(b) For Victoria (1980): Comp - CPE045

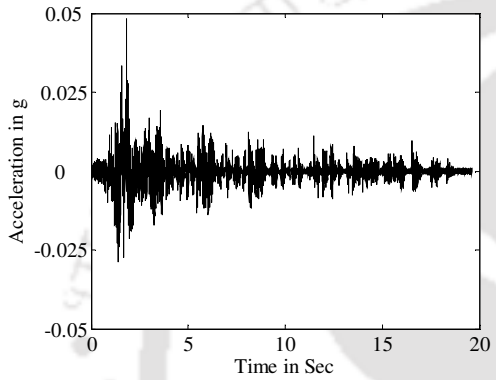

(c) For Parkfield (1966): Comp - C02065

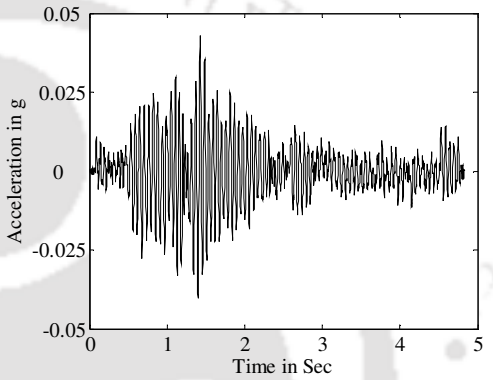

(c) For Koyna (1967): Comp - Transverse

Fig. 4.6 Table accelerations recorded for four selected earthquakes with Model I

The values of amplitude of acceleration at the base level of the model for all the earthquake excitations are 10% of the amplitude of respective original earthquake records. The structural responses at first floor and roof level of all the models corresponding to prescribed excitation (as recorded by sensor 1) have been acquired and a few typical plots are shown in Fig. 4.7.

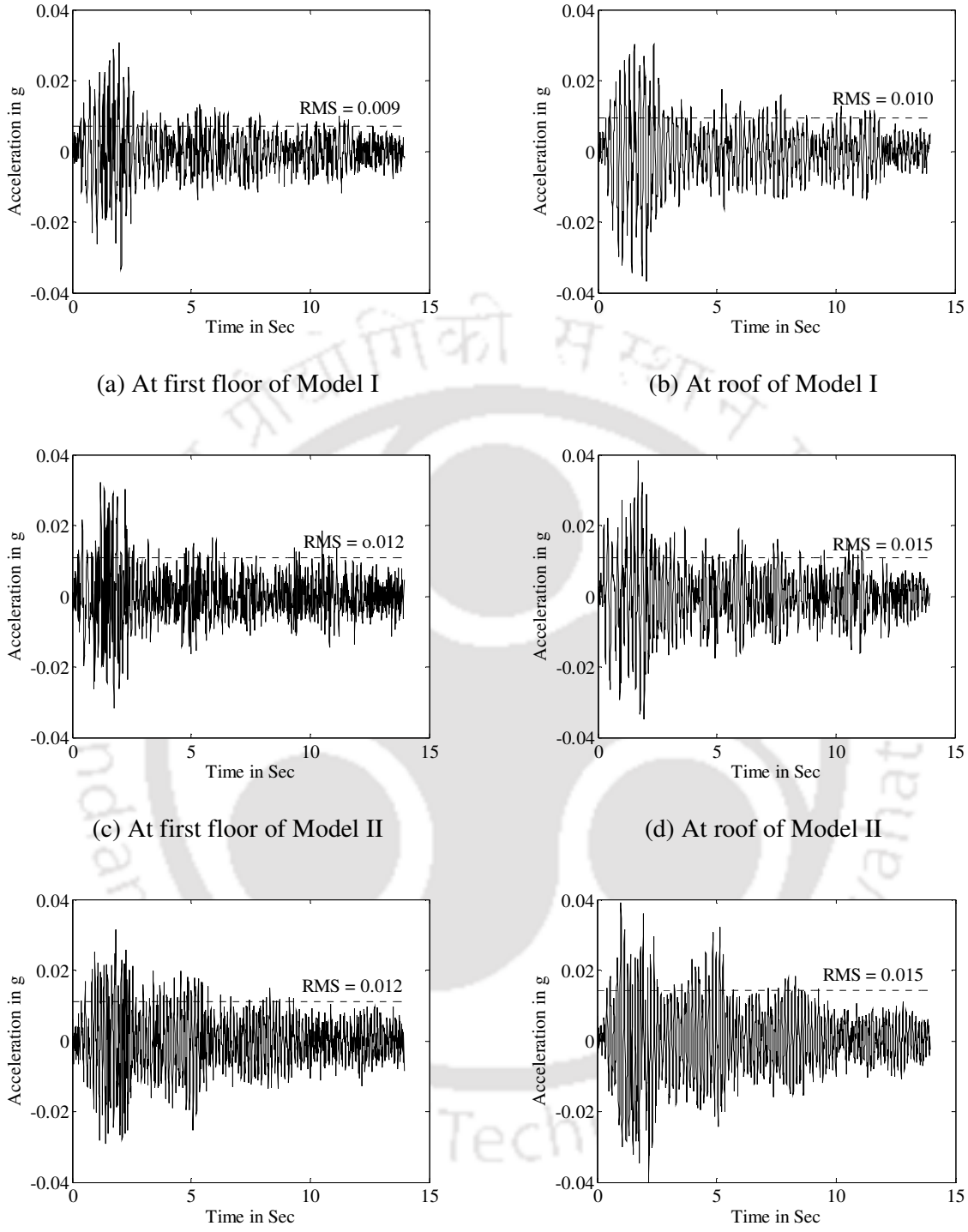

(a) At first floor of Model I

(b) At roof of Model I

(c) At first floor of Model II

(d) At roof of Model II

(e) At first floor of Model III

(f) At roof of Model III

Fig. 4.7 Responses at first floor and roof level for El Centro (1940): Comp - 180 earthquake

The peak values of accelerations have been found to be increasing from base to roof level of each of the test models. As shown in Table 4.5, this trend may be observed for all the three test models corresponding to all the excitation considered.

Table 4.5 Peak acceleration of base motion and floor responses for El Centro (1940): Comp - 180 earthquake

Models	**Peak Accelerations (g)**		
	At Base	**At First Floor**	**At Roof Floor**
Model I	0.032	0.034	0.037
Model II	0.031	0.033	0.039
Model III	0.032	0.035	0.039

Further, the FFTs of high amplitude part of floor responses of the test models for all the input earthquake excitations have been studied to examine the frequency contents in the recoded data. Frequency contents of floor responses of the same test models have been found to be almost similar. A few typical Fourier amplitude spectrum of first floor response for all the models under El Centro (1940): Comp - 180 earthquake excitation are shown in Fig. 4.8.

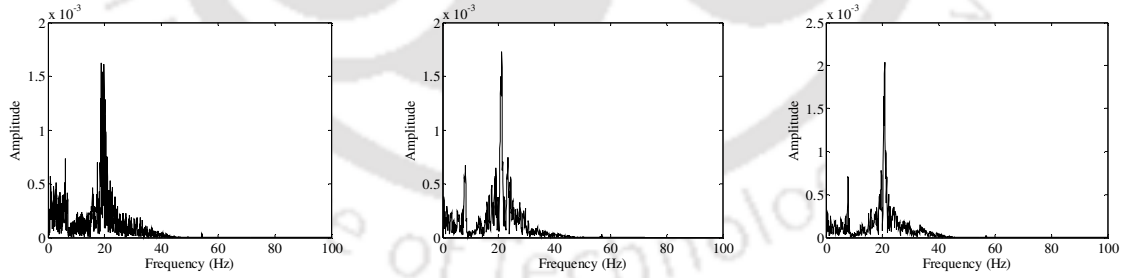

Model I Model II Model III

Fig. 4.8 Fourier amplitude spectra of first floor responses of test models for El Centro (1940): Comp - 180

The FFTs shown in the Fig. 4.8 indicate the prominent frequency contents of the responses and expected frequencies in system identification. The FFT of Model I contains second peak in Fourier amplitude spectrum at around 20 Hz and thereafter no significant peak has

been observed in the plots and hence cut-off frequency has been considered to be 40 Hz (twice the Nyquist frequency). The re-sampling frequency has been considered as 100 Hz to reduce data. Thereafter, filtering of the recorded data has been carried out using 5^{th} order Butterworth low pass digital filter to remove frequency components above 20 Hz. Similarly, FFTs of recorded data of Model II and III have been examined to observe frequencies of the models. 5^{th} order Butterworth low pass digital filters have been adopted to remove frequency components above 22 and 24 Hz of recorded data obtained from Model II and III respectively. The FFT plots of responses from all the test models corresponding to all the four earthquake excitations with 20% amplitude of original earthquake records have also been examined. The frequency contents in the FFT plots have been observed to be similar as that of FFT plots corresponding to responses acquired from the test models excited with 10% of amplitude of earthquake records. Thus, all the subsequent studies have been conducted for time scaled displacement histories with 10% of original earthquake records.

4.2.9 Modal Parameter Identification of Laboratory Test Models

N4SID subspace identification model described in Chapter 2 under section 2.2 has been used for the identification of modal parameters like frequencies, damping ratios and mode shapes. The processed structural responses at first floor and roof levels have been utilized as outputs and corresponding table acceleration as input for identification algorithm. The order of identification algorithm has been considered as four to identify two modal parameters of two storey shear building. Digital filter as presented in section 4.2.8 have been used to remove noises in the response data. Identifications of modal parameters of the test Model I have been carried out with responses obtained for all the four different earthquake excitations separately. Identified modal parameters for all the prescribed earthquake excitations are presented in Table 4.6.

Table 4.6 Identified modal parameters of test Model I with different input excitations

Excitations	First Mode		Second Mode	
	Frequency (rad/sec)	Damping (%)	Frequency (rad/sec)	Damping (%)
El Centro (1940): Comp - 180	38.09	5.57	121.19	4.73
Victoria (1980): Comp - CPE045	37.93	5.50	121.31	5.10
Parkfield (1966): Comp - C02065	38.22	7.06	120.87	4.22
Koyna (1967): Comp - Transverse	38.29	6.89	121.65	4.67

It may be observed from Table 4.6 that the identified natural frequencies of the test Model I corresponding to four different excitations are in close agreement. Similarly, N4SID identification algorithm has been utilized for the identification of modal parameters of Model II and III based on the floor responses from respective models which have been excited with four prescribed earthquake motions. The identified results are shown in Table 4.7 and 4.8.

Table 4.7 Identified modal parameters of test Model II with different input excitations

Excitations	First Mode		Second Mode	
	Frequency (rad/sec)	Damping (%)	Frequency (rad/sec)	Damping (%)
El Centro (1940): Comp - 180	46.10	4.27	133.80	7.65
Victoria (1980): Comp - CPE045	45.50	6.64	136.40	9.20
Parkfield (1966): Comp - C02065	45.90	4.77	134.50	5.98
Koyna (1967): Comp - Transverse	45.87	4.85	134.21	5.25

Table 4.8 Identified modal parameters of test Model III with different input excitations

Excitations	First Mode		Second Mode	
	Frequency (rad/sec)	Damping (%)	Frequency (rad/sec)	Damping (%)
El Centro (1940): Comp - 180	47.50	2.00	144.50	6.14
Victoria (1980): Comp - CPE045	47.20	2.60	145.50	7.18
Parkfield (1966): Comp - C02065	47.83	2.53	145.15	6.67
Koyna (1967): Comp - Transverse	47.77	2.78	145.69	6.10

From Table 4.7 and 4.8, it may again be observed that identified natural frequencies of both Model II and III are very consistent irrespective of earthquake data used for the excitation of the Models II and III. This witnesses the efficacy of the modal identification technique. However, some variation in identified damping may be observed.

4.2.10 Stability of Identified System

Poles of transfer functions evaluated using Eq. 2.14 have been plotted in z-plane to examine the stability of the system. In cases of all the test models, the poles have been found to be within unit circle on z-plane confirming the stability of system. Plotted poles for all the three test models corresponding to El Centro (1940): Comp - 180 earthquake excitations are shown in Fig. 4.9**.**

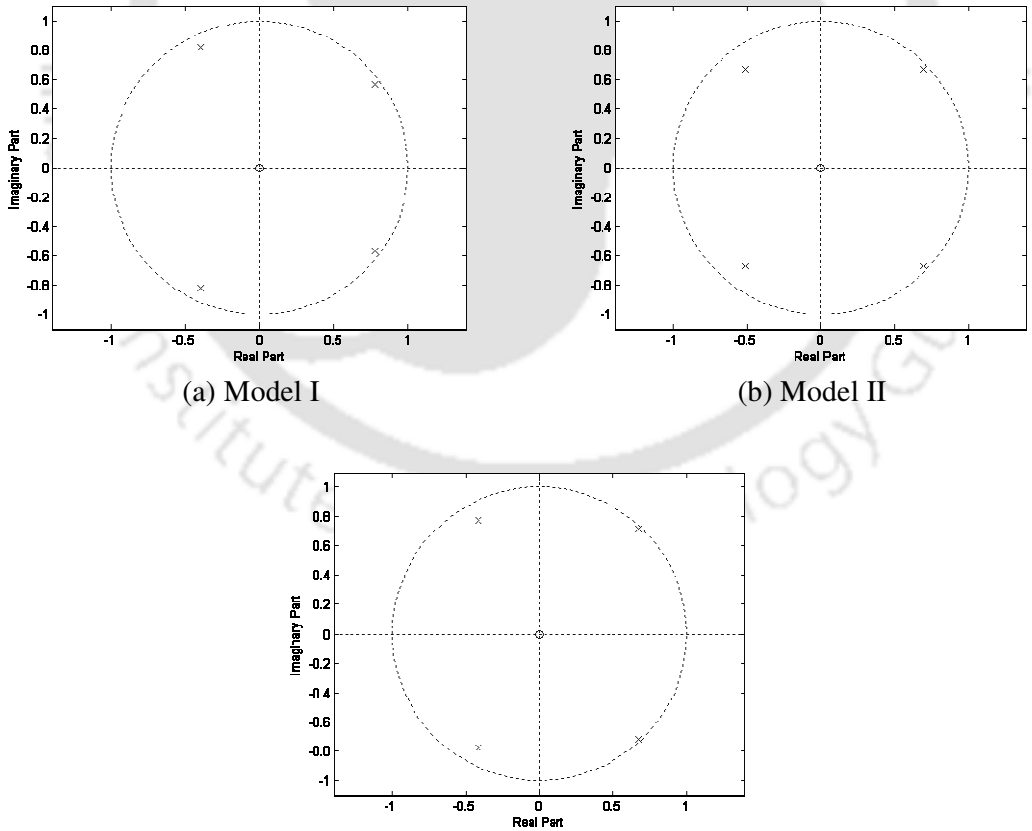

(a) Model I

(b) Model II

(c) Model III

Fig. 4.9 Poles for laboratory test models

4.2.1 Mode Shapes

The eigenvectors are evaluated based on the identified system matrix **A**, which actually correspond to a non-physical state. Hence, mode shape vectors of the actual structure are evaluated using Eq. 2.17. Modal displacement values are available at all the floor levels of the laboratory test models as acceleration response data have been measured at all the floor levels and have been used in the identification scheme. The identified modal displacements have been processed through Eq. 2.18 to 2.21 for obtaining normal modes. Typical mode shapes from identification study for Model I are shown in Fig. 4.10.

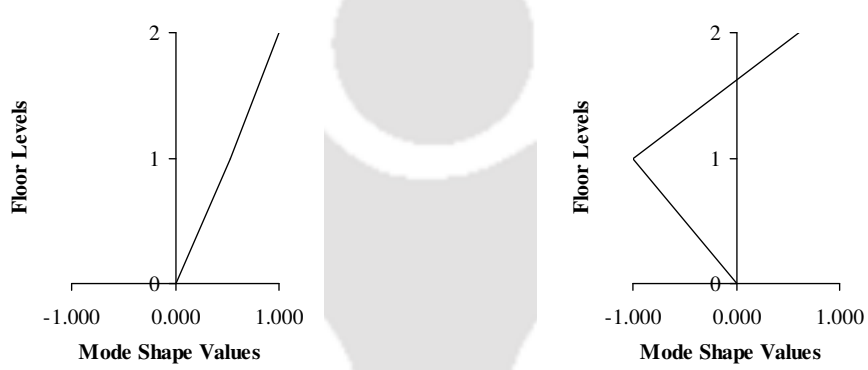

(a) Mode 1 (b) Mode 2

Fig. 4.10 Normalized mode shapes of Model I

4.2.12 Structural Parameter Identification

Characteristic equation has been solved by least square technique for the evaluation of stiffness of a structure as mentioned in section 2.4 under Chapter 2. The evaluation of stiffness can be accomplished for a known mass matrix as represented by Eq. 2.38 and modal matrix. Matrices of masses in kg for each of the models have been estimated by considering all the components of the respective models along with compensating mass on each floor. Thus, the mass matrices for different models are obtained as:

$$\mathbf{M}_{\mathrm{I}} = \begin{bmatrix} 1575 & 0 \\ 0 & 1555 \end{bmatrix} \qquad \mathbf{M}_{\mathrm{II}} = \begin{bmatrix} 1560 & 0 \\ 0 & 1555 \end{bmatrix} \qquad \mathbf{M}_{\mathrm{III}} = \begin{bmatrix} 1590 & 0 \\ 0 & 1555 \end{bmatrix} \tag{4.1}$$

Complete modal matrix has been formed with the available recorded data for all the floor levels. Therefore, the approach explained in section 2.4.1 under Case 1 has been used for the evaluation of storey stiffness. Identified storey stiffness are presented in Table 4.9.

Table 4.9 Identified storey stiffness in (10^6) N/m of the test Models

Excitations	**Storey**	**Model I**	**Model II**	**Model III**
El Centro (1940): Comp - 180	Ground	9.04	21.59	27.80
	First	9.04	8.87	8.86
Victoria (1980): Comp - CPE045	Ground	9.00	21.76	28.03
	First	9.00	8.90	8.93
Parkfield (1966): Comp - C02065	Ground	8.80	21.39	28.14
	First	8.80	8.83	9.03
Koyna (1967): Comp - Transverse	Ground	9.01	21.80	28.11
	First	9.01	8.91	9.02

The identified stiffness values of all the test models have been observed to be quite consistent for all cases of earthquake excitations considered. Further, the evaluated first storey stiffness values for all cases are in close agreement since the first storey of all the three test models are identical. It may also be mentioned that Model II has shorter ground storey column height, while Model III has larger ground storey column dimensions as compared to those of Model I. Hence, the stiffness of ground storey of Model II and III have been observed to be higher than that of Model I. Thus, it may be mentioned that the effect of deliberately introduced changes in Model II and III as compared to Model I has been very precisely captured through the adopted system identification technique in the form of modal and structural properties.

A simple theoretical estimation storey stiffness of the three test models have been carried out by the method of static analysis for determination of deflection per unit force. Thus, for a single column, the equivalent stiffness for a shear building can be considered as

$$k = \frac{12EI}{l^3} \tag{4.2}$$

where, E = is the modulus of elasticity of concrete, I is the moment of inertia of only the concrete section and l is centre to centre distance between floors. The geometrical and material properties of the columns have been considered as per Table 4.2 and 4.3 respectively. Since the columns act in parallel, the total stiffness per storey has been evaluated by adding contribution of all the six columns. The computed storey stiffness of three test models are presented in Table 4.10.

Table 4.10 Theoretical storey stiffness ($x10^6$) N/m of the test models

Storey	Model I	Model II	Model III
Ground	10.68	24.72	33.90
First	10.68	10.68	10.68

Thus, comparing Table 4.9 and 4.10, it may be inferred that the identified storey stiffness values are very good estimation of the actual storey stiffness of the laboratory test models.

4.3 STUDY OF NUMERICALLY SIMULATED MODELS OF TEST MODELS

The laboratory testing of structural models are quite involved and hence any repetition of tests with slight modification in structural or material properties is not easily achievable. These difficulties can however be avoided easily through tests on numerical simulated models. However, the model performance needs to be validated with experimental observation and updating the model in terms of size and/or material properties are carried out, if any discrepancies are observed. Thus, numerical models of all the three test models

have been simulated using SAP 2000 Nonlinear (version 12). Modal and time history analyses of the numerical models have been carried to obtained modal frequencies. Further, the evaluated modal parameters have been compared to the identified results of the corresponding test models.

4.3.1 Description of Bare Frame Numerical Models

Three dimensional finite element models have been simulated in SAP 2000 Nonlinear (version 12) for all the three test models using detailed geometrical and material properties presented in Table 4.2 and 4.3. In the modeling, beams and columns have been modeled as frame elements. Dead and superimposed loads from slab have been transferred to beams in the form of a triangular distribution. Floors have been assumed rigid in-plane and diaphragm constraints have been imposed at individual floor level. All the columns are assumed fixed at the base and hence does not allow translational and rotational motions.

4.3.2 Modal Analysis of Numerical Models and Updating of the Models

Modal analyses of numerical models of all the three test specimen described in subsection 4.3.1 have been carried out and frequencies along the shorter direction (i.e. direction of excitation in the shake table) have been compared with the identified results as shown in Table 4.6 to 4.8. The obtained modal frequencies of all the models have been observed to be slightly higher than the identified frequencies of the corresponding test models. Therefore, the models have been updated by changing compressive strength of concrete and the modulus of elasticity. The frequencies as obtained from modal analysis of the updated numerical model are shown in Table 4.11.

Table 4.11 Comparison of natural frequencies of numerically simulated building

Scaled Models	Frequency (rad/sec)		
	Identified	Initial SAP Model	Updated SAP Model
Model I	38.09	41.48	39.14
	121.19	125.26	117.85
Model II	46.10	52.20	47.17
	133.80	157.02	135.96
Model III	47.50	51.53	46.55
	144.50	160.19	138.91

The modal analyses based frequencies from all the three updated numerical models have been found to agree well with the identified frequencies of the corresponding test models. Hence, these updated models have been considered for further studies.

4.3.3 Responses of Numerically Developed Models of the Test Models

Recorded acceleration time histories at the base level of the laboratory test models presented in 4.2.8 have been considered for time history analysis of all the numerical models. Proportional damping of 5% has been considered for time history analysis of the numerical models. A few typical accelerations time histories from different floor levels of the initial and updated numerical models are shown in Fig. 4.11 (A) and Fig. 4.11(B) respectively. These responses of numerical models have been compared with those from laboratory test models and peak accelerations at different floor levels have been observed to be agreeing very well. Comparison of observed RMS values from Fig. 4.11 with those from Fig. 4.7, a very good agreement may be observed between laboratory test models and their corresponding updated numerical models. Further, the peak floor accelerations are also presented in the Table 4.12 for comparison.

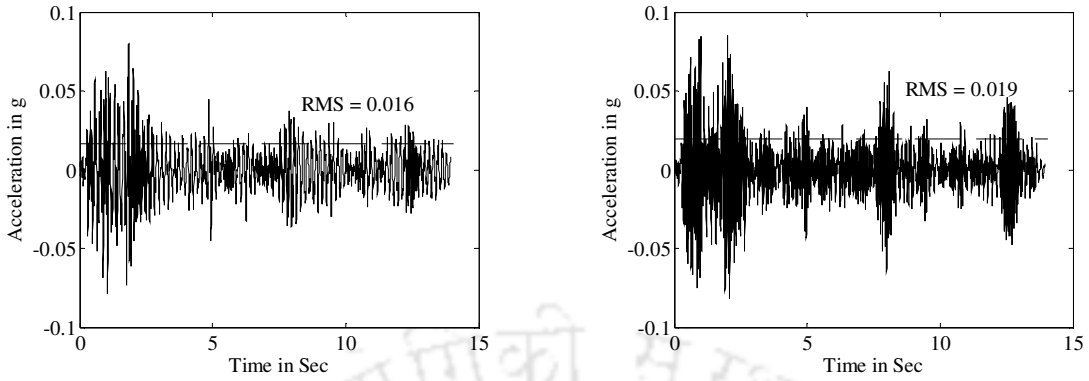

(a) At first floor of Model I

(b) At roof of Model I

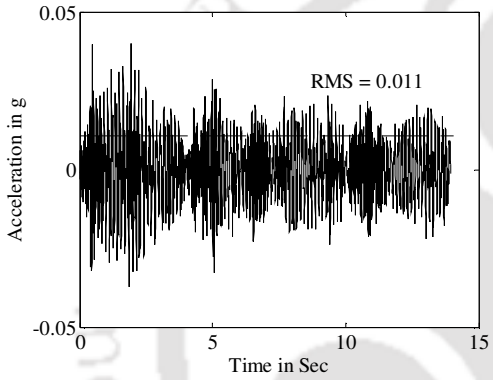

(c) At first floor of Model II

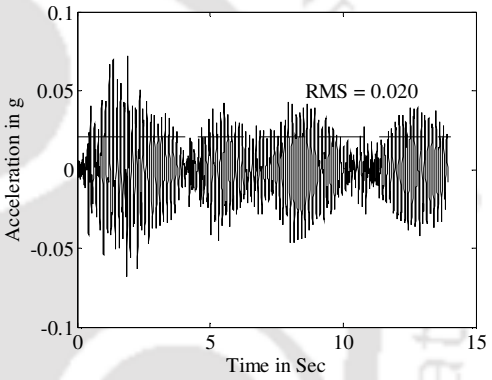

(d) At roof of Model II

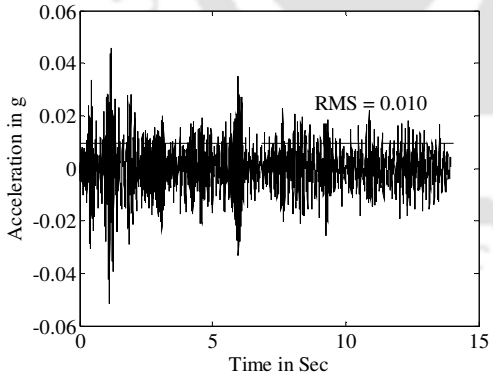

(e) At first floor of Model III

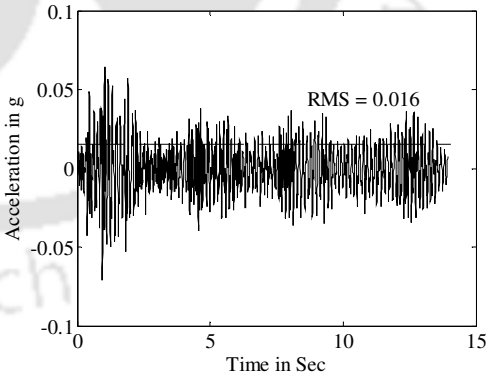

(f) At roof of Model III

Fig. 4.11(A) Responses at first floor and roof levels of initial numerical models due to El Centro (1940): Comp – 180 earthquake input

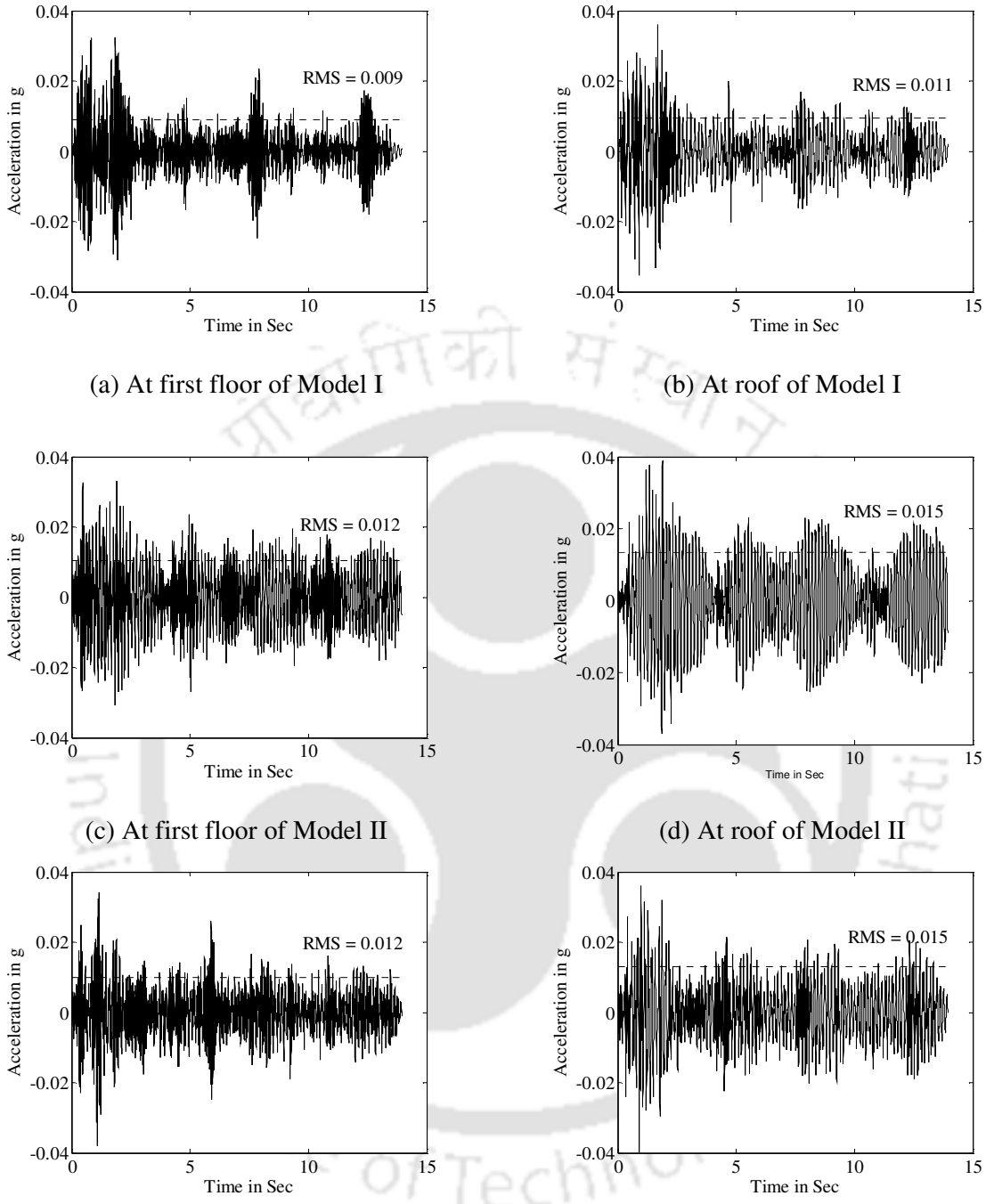

(a) At first floor of Model I

(b) At roof of Model I

(c) At first floor of Model II

(d) At roof of Model II

(e) At first floor of Model III

(f) At roof of Model III

Fig. 4.11(B) Responses at first floor and roof levels of updated numerical models due to El Centro (1940): Comp – 180 earthquake input

Table 4.12 Peak floor accelerations of different models for El Centro (1940): Comp – 180 earthquake

Models	Peak floor accelerations (g)					
	First floor			Roof floor		
	Measured	Initial SAP	Updated SAP	Measured	Initial SAP	Updated SAP
Model W-I	0.034	0.080	0.033	0.037	0.085	0.036
Model W-II	0.033	0.040	0.033	0.039	0.072	0.039
Model W-III	0.035	0.051	0.034	0.039	0.069	0.039

Thus, the updated numerical models are considered as well representation of the actual models as both modal and time history analyses have shown very well conformity in their analysed results with those from experimental studies.

4.4 CONCLUDING REMARK

The identification of modal parameters of three different test models have been carried out using parametric state space identification technique. The modal parameters have been identified for four selected earthquake excitations and are found to be very consistent. The identified modal frequencies of these test models have also been verified by modal analysis of corresponding numerically simulated models. The changes in storey stiffness due to changes in column dimension in ground storey have been observed to reflect very well in both theoretical and experimental identification. Thus, it may be concluded that the N4SID subspace identification algorithm is suitable and effective for the evaluation of parameters of laboratory models of buildings. The identified results have been quite consistent under different earthquake excitations and hence the methodology can be considered for system identification of existing structures. Thus, these laboratory model based studies have helped to draw concrete conclusion regarding adequacy of the adopted modal parameters identification model for more practical application.

CHAPTER 5

EVALUATION OF INFILL WALL CONTRIBUTION THROUGH SYSTEM IDENTIFICATION

5.1 INTRODUCTION

Existing buildings always contain infill walls in the frames. Further, it has been observed that multi-storey buildings with only ground storey having no infill wall are commonly used building type. A building with infill walls behaves differently than that of a bare frame building during an earthquake. Detailed review of literatures on system identification of building indicates that the studies have been carried out mainly on simulated frame buildings without any infill walls in the frames. Identification of system parameters of existing building based on experimental studies has been rarely addressed. However, few experimental studies have been found available those accounts for lateral stiffness due to presence of infill wall in building frames. Experimental studies conducted by Chaker and Cherifati [1991], Mehrabi *et al.* [1996], Ghassan *et al.* [2002] and Colangelo F. [2005] clearly concluded that the presence of infill wall led to the increase of lateral stiffness as compared to a bare frame building and hence the building exhibited better seismic performance. They further observed increase in initial lateral stiffness as well as overall strength of the building with infill walls. Thus, it is understood that the role of infill wall in building frame systems is quite significant and hence contribution of infill walls in building frames has been evaluated through system identification. The difference in dynamic response of a building with and without infill walls when subjected to seismic excitation is utilized for assessing the contribution of infill wall. Further, openings in the form of doors and windows in infill walls lead to unequal distribution of forces in building and the effect of such opening on system parameters of test models has also been studied.

5.2 STUDIES BASED ON LABORATORY TEST MODELS

The evaluation of modal parameters through system identification can be efficiently carried out based on acceleration histories from laboratory test models. Hence, scaled laboratory test models with infill walls have been considered for Shake Table testing to obtain dynamic responses to be used as input in identification scheme. The test models with scale factor of 1:5 have been subjected to different time scaled prescribed earthquake excitations for acquiring structural responses.

5.2.1 Description of Test Models with Infill Walls

Three bare frame test models introduced in Chapter 4 have been utilized again after providing infill walls within the frames. Three full masonry walls have been constructed at the first storey along the shorter directions of each of the test models. The thicknesses of all the brick walls have been kept as 60 mm for all the three models. The laboratory building models with infill walls are shown in the Fig.5.1 and are renamed as Model W-I for Model I with infill. Similarly, Model II and Model III are renamed as Model W-II and Model W-III respectively.

(a) Model W-I

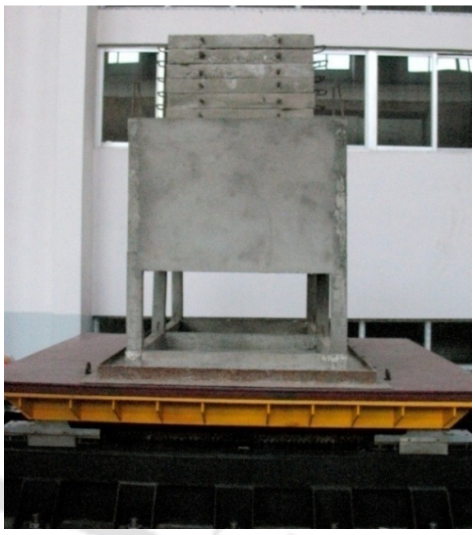

(b) Model W-II

(c) Model W-III

Fig. 5.1 Three test models with infill wall at first storey

5.2.2 Properties of Brick Masonry used for Test Models

Traditional clay bricks have been used for the construction of infill walls in the scaled test models. The thickness of the bricks has been reduced to 60 mm using rock cutter and 1: 4 (cement: sand) mortar has been used to prepare the masonry walls. Compressive strengths

of brick masonry prisms have been evaluated in the laboratory and average results are presented in Table 5.1.

Table 5.1 Properties of brick masonry for scale models

Particulars	Model W-I	Model W-II	Model W-III
Thickness of bricks (mm)	60	60	60
Compressive Strength of Prism (N/mm^2)	2.00	2.00	2.00
Density (kg/m^3)	1550	1550	1550

5.2.3 Sizes of Openings in Walls

Different sizes of opening in infill wall have been considered to study its influence on the stiffness of the model. The openings have been made by cutting the infill walls of the test models from the central region. Altogether eight cases of wall openings have been considered for studying the behavior of each of these models under dynamic excitations. These cases of sizes of wall opening are presented in Table 5.2. The sizes of opening in percentage have been calculated as:

$$\frac{\text{Area of Opening in Infill Wall}}{\text{Area of Fullsize Wall}} \times 100\%$$

Fig. 5.2 shows some typical cases of wall opening in different test models.

Table 5.2 Percentage of opening in infill walls

Cases	Size of openings (%)
Case-1	Nil
Case-2	5
Case-3	10
Case-4	20
Case-5	30
Case-6	35
Case-7	40
Case-8	45

(a) Five percent wall opening in Model W-I (b) Forty five percent wall opening in Model W-III

Fig. 5.2 Different sizes of wall opening in laboratory test models

5.2.4 Shake Table Test

Shake Table tests have been carried out for recording dynamic responses of the test models subjected to time scaled prescribed earthquake motions. Each one of the test models with different opening sizes in walls have been mounted on the shake table along with required amount of compensating masses as described in the sub section 4.2.6. Three numbers of force balance accelerometers have been fixed at three different floor levels of the models as shown in Fig. 5.3. Sensor 1 records the table acceleration histories while sensors 2 and 3 record the first and roof floor acceleration histories respectively. For each case of wall opening, four different earthquake excitations as mentioned in the sub section 3.2.3 have been considered for exciting the test models. The structural responses have been collected through MGCplus DAS.

Fig. 5.3 Sensor locations in Model W-II during test

5.2.5 Characteristics of Recorded Responses

In this section, characteristics of recorded acceleration responses have been examined. Structural responses at different floor levels of the test models with full infill wall subjected to El Centro (1940): Comp - 180 earthquake excitation are shown in Fig. 5.4.

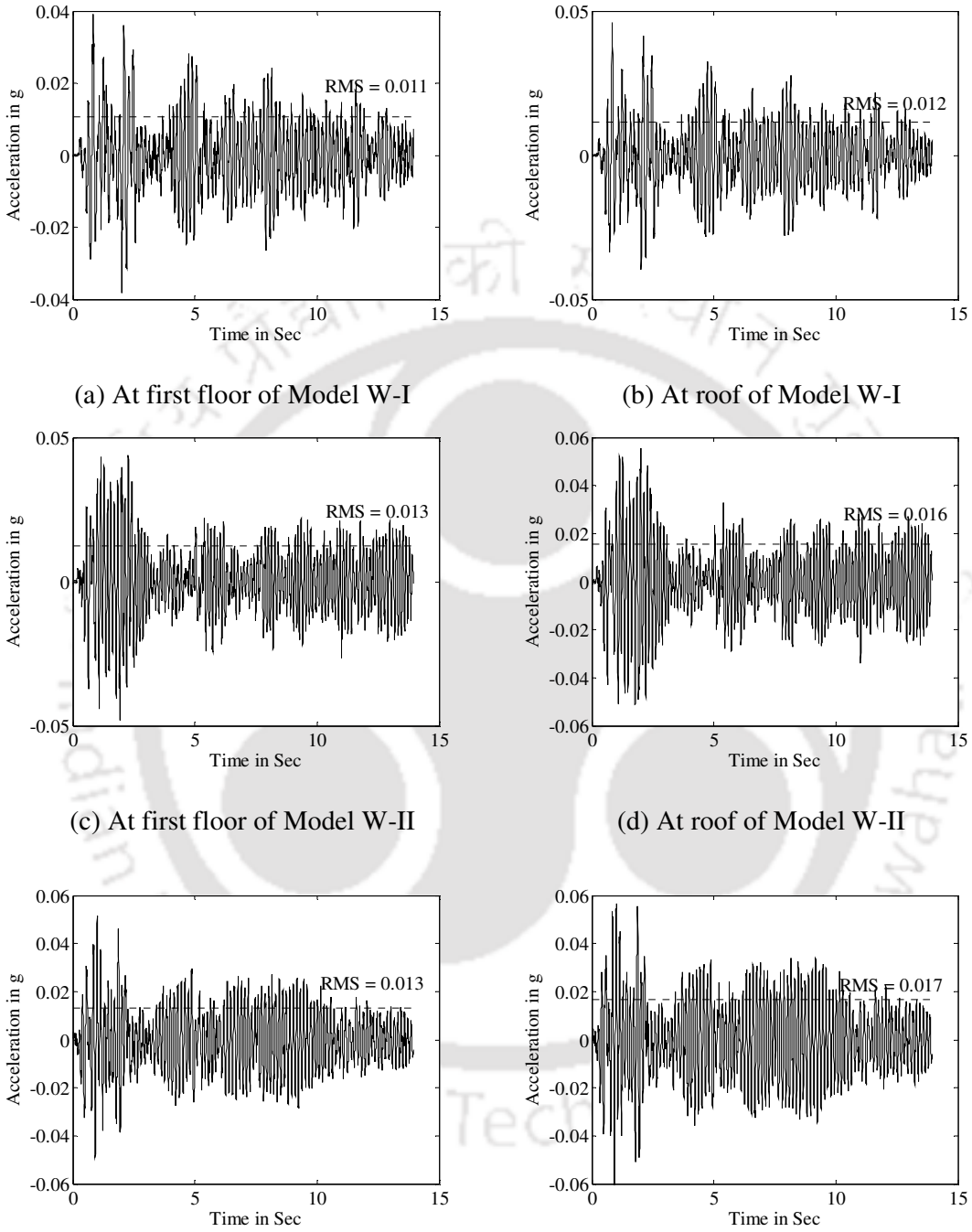

(a) At first floor of Model W-I

(b) At roof of Model W-I

(c) At first floor of Model W-II

(d) At roof of Model W-II

(e) At first floor of Model W-III

(f) At roof of Model W-III

Fig. 5.4 Floor acceleration histories of test models with full infill wall subjected to El Centro (1940): Comp - 180 earthquake

It may be seen that the peak values of accelerations time histories consistently increasing with increase in floor levels of all the test models. Fast Fourier transform (FFT) of high amplitude portions of acceleration time histories have been performed to obtain corresponding Fourier amplitude spectrum. The FFT plots of floor acceleration time histories for all the cases of wall opening of all the three test models have been studied for finalizing cut-off as well as re-sampling frequencies.

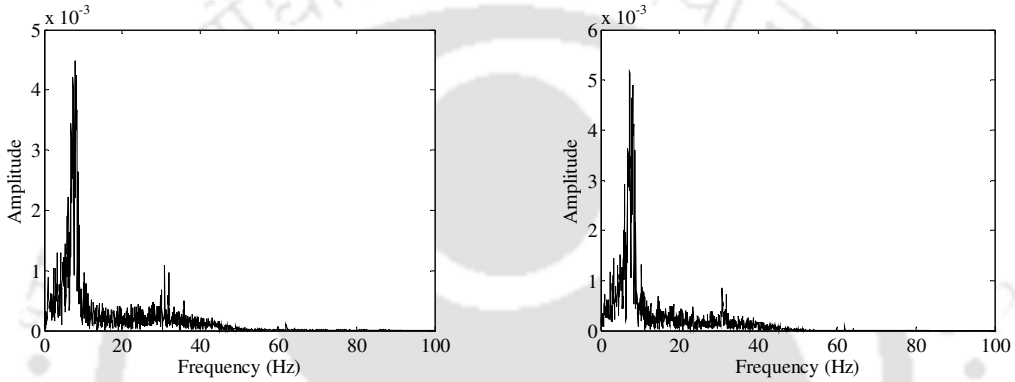

(a) First floor (b) Roof

Fig. 5.5 Fourier amplitude spectra of floor acceleration time histories of Model W-I subjected to El Centro(1940): Comp - 180 earthquake excitation

The FFT plots shown in the Fig. 5.5 indicate predominant frequencies of the test model with full infill wall (case-1) and hence provide information about the range of expected frequency to be obtained from system identification. The FFT plots of model W-I corresponding to case-1 of wall opening indicates second peak at around 35 Hz and hence cut-off frequency has been considered to be 70 Hz (twice the Nyquist frequency). The sampling interval for recording floor accelerations has been kept as 0.005 sec (200 Hz) so as to acquire maximum possible frequency. However, in order to reduce number of data points, a re-sampling frequency of 100 Hz has been considered.

Thus, a 5th order Butterworth low pass filter has been adopted to filter out frequency contents more than 35 Hz. Similarly, different digital filters have been configured for different cases of openings in walls of three different test models.

5.2.6 Modal Parameters Identification of Test Models with Different Sizes of Opening in Infill Walls

Parametric state space identification scheme has been used to identify the modal parameters of test models using recorded floor acceleration time histories. The N4SID algorithm, which has been used for identification of modal parameters of bare frame test models, has been adopted for identification of modal parameters of the test models with infill walls. Table acceleration history has been considered to form the input matrix while the floor acceleration histories have been considered to form the output matrix of the identification scheme. The order of the state space model has been considered as four for identification of two modal parameters of two storey shear building as poles exist as pair of complex conjugate corresponding to each frequency. The identified modal parameters of all the three test models with all the cases of wall openings are presented in Tables 5.3 to 5.5. Substantial increase in identified frequencies as expected have been observed for Case-1 of wall opening when compared to those from corresponding bare frame models evaluated in Chapter 4 under subsection 4.2.11. Thus, it demonstrates the enhancement of lateral stiffness due to the presence of infill wall. Further, consistency in the evaluated frequencies can be observed corresponding to all four seismic excitations considered.

Table 5.3 Identified modal parameters of test Model W-I with different sizes of wall openings

Cases	First Mode		Second Mode	
	Frequency (rad/sec)	Damping (%)	Frequency (rad/sec)	Damping (%)
Input Excitation-El Centro (1940): Comp - 180				
Case-1	45.95	5.21	204.60	4.67
Case-2	45.27	4.69	186.80	4.23
Case-3	44.76	9.09	172.54	4.32
Case-4	44.05	2.66	153.86	9.74
Case-5	43.62	3.52	144.23	2.29
Case-6	42.72	2.65	136.75	2.88
Case-7	41.97	2.61	129.25	4.06
Case-8	39.25	2.71	122.60	3.67
Input Excitation- Victoria (1980): Comp - CPE045				
Case-1	45.87	4.11	204.85	4.82
Case-2	45.24	5.34	186.67	4.89
Case-3	44.63	8.11	171.97	4.94
Case-4	43.98	3.34	153.45	9.61
Case-5	43.79	3.48	143.75	2.63
Case-6	42.78	2.29	135.85	3.19
Case-7	41.95	2.81	129.81	5.03
Case-8	39.24	2.93	122.56	3.89
Input Excitation-Parkfield (1966): Comp - C02065				
Case-1	45.85	6.73	205.24	8.35
Case-2	45.25	6.14	186.34	7.36
Case-3	44.72	8.29	170.93	5.32
Case-4	43.85	2.77	153.23	7.42
Case-5	43.50	4.12	143.75	2.78
Case-6	42.73	2.44	134.96	3.60
Case-7	41.91	2.80	129.76	3.98
Case-8	39.30	2.92	122.30	3.90
Input Excitation-Koyna (1967) : Comp - Transverse				
Case-1	45.94	4.56	204.96	4.67
Case-2	45.32	5.78	188.65	5.32
Case-3	44.65	1.41	170.95	3.31
Case-4	43.86	2.81	154.22	4.77
Case-5	43.51	3.75	143.35	1.88
Case-6	42.74	2.14	134.68	2.77
Case-7	41.95	2.12	129.16	4.32
Case-8	39.31	2.75	121.90	4.21

Table 5.4 Identified modal parameters of test Model W-II with different sizes of wall openings

Cases	First Mode		Second Mode	
	Frequency (rad/sec)	Damping (%)	Frequency (rad/sec)	Damping (%)
Input Excitation-El Centro (1940): Comp - 180				
Case-1	69.85	5.78	209.85	7.64
Case-2	65.75	5.56	194.65	6.94
Case-3	63.40	2.89	184.50	6.05
Case-4	60.15	3.31	168.95	8.58
Case-5	57.20	2.97	156.30	4.65
Case-6	55.93	5.17	152.04	3.74
Case-7	52.21	1.09	144.21	3.06
Case-8	46.35	2.40	137.60	3.89
Input Excitation- Victoria (1980): Comp - CPE045				
Case-1	69.96	5.54	209.74	3.98
Case-2	65.64	5.51	184.97	3.95
Case-3	63.36	3.28	173.95	6.28
Case-4	60.16	5.40	166.10	7.60
Case-5	57.55	3.74	156.76	3.67
Case-6	55.29	5.36	151.37	5.08
Case-7	52.15	1.30	144.96	3.01
Case-8	46.27	2.67	137.20	4.22
Input Excitation-Parkfield (1966): Comp - C02065				
Case-1	69.90	7.18	209.65	2.45
Case-2	65.92	6.97	184.10	4.65
Case-3	63.40	2.96	174.75	4.61
Case-4	60.00	4.69	164.12	6.21
Case-5	57.35	2.63	156.50	6.58
Case-6	55.83	5.39	151.37	4.61
Case-7	52.83	0.98	144.05	3.29
Case-8	46.18	1.75	136.94	2.67
Input Excitation-Koyna (1967): Comp - Transverse				
Case-1	69.89	5.23	209.63	4.78
Case-2	65.52	5.12	184.00	4.75
Case-3	62.95	2.68	173.82	6.00
Case-4	60.26	5.00	165.38	5.89
Case-5	56.92	4.11	157.05	7.30
Case-6	55.74	4.30	151.68	3.74
Case-7	52.35	0.82	144.22	4.20
Case-8	46.20	2.32	136.80	4.78

Table 5.5 Identified modal parameters of test Model W-III with different sizes of wall openings

Cases	First Mode		Second Mode	
	Frequency (rad/sec)	Damping (%)	Frequency (rad/sec)	Damping (%)
Input Excitation-El Centro (1940): Comp - 180				
Case-1	68.53	5.68	215.70	5.78
Case-2	66.12	5.12	198.60	5.06
Case-3	62.73	5.76	186.58	9.73
Case-4	59.36	2.90	171.40	8.10
Case-5	57.32	1.41	163.20	2.75
Case-6	55.43	3.55	157.36	4.43
Case-7	52.44	1.46	150.44	1.94
Case-8	47.69	2.53	145.94	2.67
Input Excitation- Victoria (1980): Comp - CPE045				
Case-1	68.67	5.68	215.78	5.78
Case-2	66.19	5.43	198.65	5.10
Case-3	62.68	6.39	186.65	9.37
Case-4	59.41	4.46	172.02	6.45
Case-5	57.33	2.29	164.95	3.12
Case-6	55.53	3.74	158.08	5.15
Case-7	52.23	1.43	150.99	1.63
Case-8	47.82	2.67	145.90	2.80
Input Excitation-Parkfield (1966): Comp - C02065				
Case-1	68.47	5.68	216.45	5.78
Case-2	66.26	5.23	198.93	4.97
Case-3	62.62	6.50	187.06	7.04
Case-4	59.30	4.46	172.15	6.85
Case-5	57.30	1.46	164.62	1.97
Case-6	55.48	3.99	158.47	5.12
Case-7	52.12	1.70	150.48	1.81
Case-8	47.78	2.76	145.87	2.12
Input Excitation-Koyna (1967): Comp - Transverse				
Case-1	68.71	5.68	216.93	5.78
Case-2	66.23	4.67	198.41	5.56
Case-3	62.79	7.62	187.40	9.31
Case-4	59.21	3.97	172.98	5.39
Case-5	57.27	2.27	165.78	2.93
Case-6	55.39	3.35	158.65	5.06
Case-7	52.10	1.08	150.86	1.48
Case-8	47.65	2.90	145.90	2.75

Reduction in values of identified frequencies has been observed with increase in sizes of wall openings for all the three test models. The identified frequencies corresponding to wall opening Case-8 have been found to be very close to those corresponding to bare frame test models as reported in Chapter 4 under subsection 4.2.10. Thus, it shows clearly that corresponding to around 45% opening in infill wall, the contribution from infill wall to overall lateral stiffness of building frame becomes insignificant.

5.2.7 Stability of Identified System

The poles of the transfer functions have been plotted on the complex plane using the polar coordinates according to Eq. 2.12. Poles within the unit circle in the complex plane refer to the stable dynamic system, while poles outside the unit circle refer to the unstable dynamic system. Plots of poles based on responses corresponding to Input Excitation-El Centro (1940): Comp - 180 earthquake excitation for all the cases of openings in infill walls of Model W-I are as shown in Fig. 5.6. As observed from the Fig. 5.6, two numbers of complex conjugate poles marked as 'x' have been found to be lying within the unit circle signifying a stable system. Similarly, all the cases of remaining two test models, the poles have been found to be lying within unit circle on z-plane confirming the stability criteria of the adopted system identifications technique.

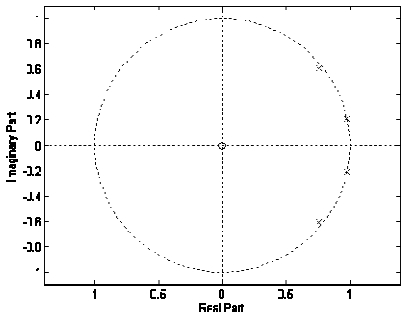

(a) Full wall

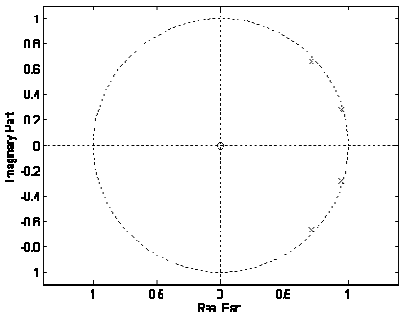

(b) Five percent wall opening

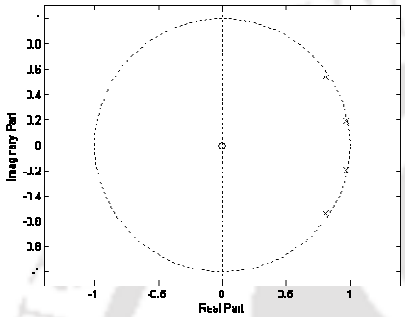

(c) Ten percent wall opening

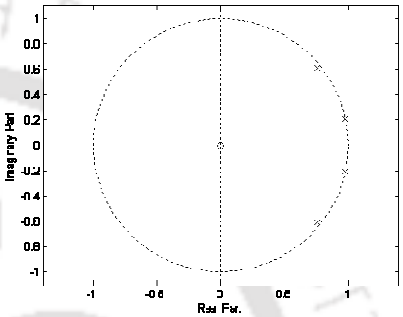

(d) Twenty percent wall opening

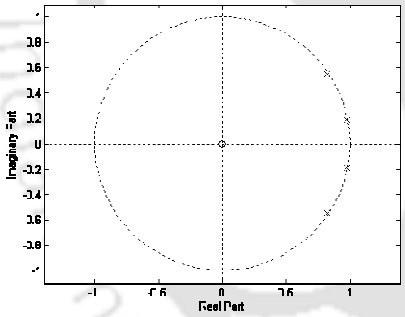

(e) Thirty percent wall opening

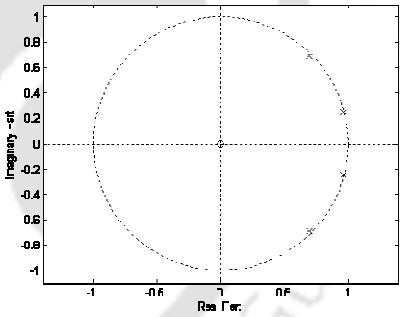

(f) Thirty five percent wall opening

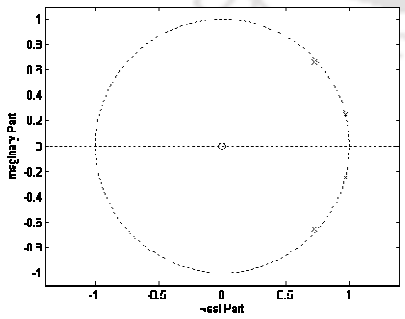

(g) Forty percent wall opening

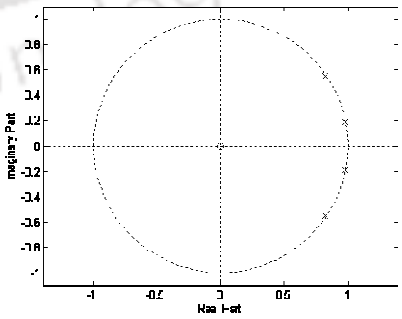

(h) Forty five percent wall opening

Fig. 5.6 Poles obtained from test Model W-I subjected to El Centro (1940): Comp - 180 earthquake excitation

5.2.8 Mode Shapes

The modal matrix (Φ) identified from the system matrix **A**, corresponds to the non-physical state of the structure and hence, the output influence matrix **C** is used to transform the extracted eigenvector from the non physical state to the mode shape vector at the structural floor level, where the acceleration response data have been measured. Typical mode shapes along the directions of excitation for Case-1 of Model W-I have been plotted as shown in Fig. 5.7.

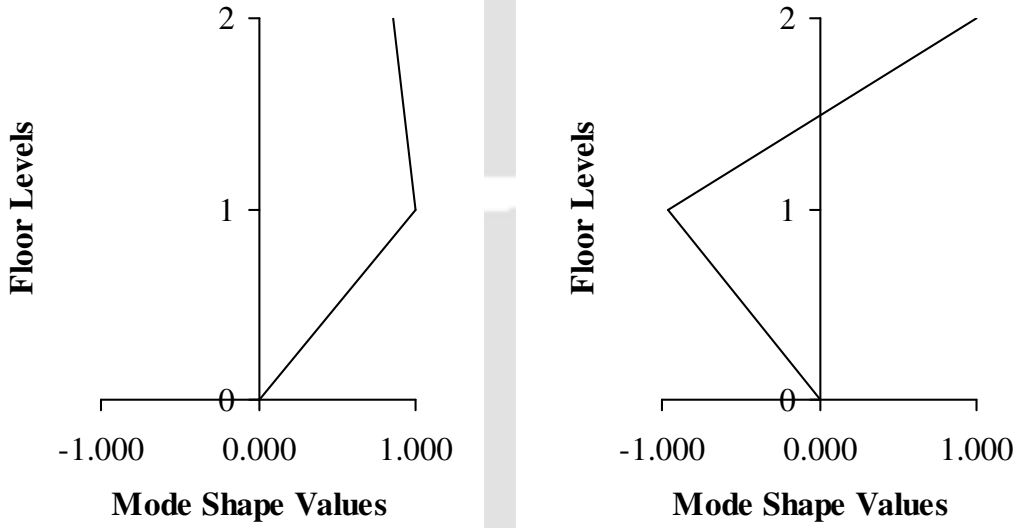

(a) Mode 1 (b) Mode 2

Fig. 5.7 Normalized mode shapes of Model W-I under El Centro (1940): Comp – 180 earthquake excitation

5.2.9 Structural Parameter Identification

Modal displacement values are available at all the floor levels of the laboratory test models as acceleration response data have been measured at all the floor levels. The identified mode shapes and modal frequencies have been used to estimate the stiffness of the building through least square solution of the Eigenvalue problem. Lumped floor mass

matrices for all the test models with all the cases of wall opening have been estimated. Approximate lumped floor mass matrices in kg for Case-1 for all the three test models are

$$\mathbf{M}_{\text{W-I}} = \begin{bmatrix} 1655 & 0 \\ 0 & 1630 \end{bmatrix} \qquad \mathbf{M}_{\text{W-II}} = \begin{bmatrix} 1645 & 0 \\ 0 & 1630 \end{bmatrix} \qquad \mathbf{M}_{\text{W-III}} = \begin{bmatrix} 1670 & 0 \\ 0 & 1630 \end{bmatrix}.$$

The identified stiffness of all the test models with different sizes of openings in wall have been presented in Table 5.6 - 5.8. The tabulated values of stiffness for Case - 1 show significant increase in first storey stiffness for all the three test models as expected over their respective bare frame Models. The stiffness at the storey with full infill wall have been observed to be about three times the stiffness of storey without infill wall for all the building models. Thus, the additional stiffness can be attributed to contribution from infill walls. The contributions of infill walls have been observed to be similar for all the prescribed earthquake excitations.

Similar reduction in first storey stiffness has been observed in all the three test models with increase in sizes of wall openings. The storey stiffness of all the test models corresponding to Case – 8 have been observed to be equal to those corresponding to bare frame test models. Thus, it may be concluded that infill wall contribution towards lateral stiffness may be disregarded, if percentage opening becomes 45% or more.

Table 5.6 Identified stiffness in (10^6) N/m for test Model W-I with different cases of wall openings subjected to different time scaled acceleration histories

Excitations	Storey	Stiffness								
		Bare Frame	Cases of Wall Opening Sizes							
			Case-1	Case-2	Case-3	Case-4	Case-5	Case-6	Case-7	Case-8
El Centro (1940) Comp - 180	Ground	9.04	11.88	10.98	9.45	9.34	9.28	9.22	9.15	9.05
	First	9.04	27.11	22.54	18.84	15.88	13.41	12.87	10.35	9.05
Victoria (1980) Comp - CPE045	Ground	9.00	11.83	10.94	9.46	9.37	9.27	9.19	9.13	9.02
	First	9.00	26.99	22.42	18.75	15.68	13.40	12.85	10.37	9.02
Parkfield (1966) Comp - C02065	Ground	8.80	11.82	10.80	9.40	9.35	9.22	9.14	9.10	8.82
	First	8.80	26.98	22.48	18.90	15.73	13.30	12.70	10.31	8.82
Koyna (1967) Comp - Transverse	Ground	9.01	11.83	10.94	9.43	9.33	9.27	9.23	9.13	9.02
	First	9.01	27.00	22.56	18.74	15.70	13.37	12.85	10.32	9.02

Table 5.7 Identified stiffness in (10^6) N/m for test Model W-II with different cases of wall openings subjected to different time scaled acceleration histories

Excitations	Storey	Stiffness								
		Bare Frame	Cases of Wall Opening Sizes							
			Case-1	Case-2	Case-3	Case-4	Case-5	Case-6	Case-7	Case-8
El Centro (1940) Comp - 180	Ground	21.59	25.25	24.20	22.25	22.19	22.12	21.98	21.67	21.60
	First	8.87	26.62	22.01	18.45	15.30	12.94	12.21	10.12	8.89
Victoria (1980) Comp - CPE045	Ground	21.76	25.32	24.48	22.38	22.21	22.15	22.01	21.95	21.78
	First	8.90	26.69	22.09	18.66	15.58	12.97	12.17	10.16	8.92
Parkfield (1966) Comp - C02065	Ground	21.39	25.30	24.21	22.53	22.41	22.14	21.99	21.61	21.44
	First	8.83	26.67	22.17	18.67	15.69	13.01	12.22	10.14	8.86
Koyna (1967) Comp - Transverse	Ground	21.80	25.29	24.29	22.57	22.36	22.18	22.11	21.88	21.82
	First	8.92	26.66	21.93	18.65	15.39	12.98	12.42	10.20	8.93

Table 5.8 Identified stiffness in (10^6) N/m for test Model W-III with different cases of wall openings subjected to different time scaled acceleration histories

Excitations	Storey	Stiffness								
		Bare Frame	Cases of Wall Opening Sizes							
			Case-1	Case-2	Case-3	Case-4	Case-5	Case-6	Case-7	Case-8
El Centro (1940) Comp - 180	Ground	27.80	32.81	30.96	29.01	28.86	28.67	28.43	28.22	27.83
	First	8.86	26.67	21.86	18.42	15.47	13.48	12.37	10.44	8.89
Victoria (1980) Comp - CPE045	Ground	28.03	32.84	30.99	29.12	28.78	28.66	28.45	28.28	28.05
	First	8.93	26.69	21.90	18.65	15.41	13.39	12.43	10.47	8.95
Parkfield (1966) Comp - C02065	Ground	32.80	31.12	29.33	28.93	28.71	28.57	28.41	28.17	28.14
	First	26.66	21.93	18.64	15.40	13.36	12.34	10.48	9.05	9.03
Koyna (1967) Comp - Transverse	Ground	28.11	32.88	30.97	29.17	28.92	28.73	28.56	28.41	28.14
	First	9.02	26.63	22.43	18.58	15.39	13.27	12.61	10.38	9.04

5.2.10 Evaluation of Contribution of Infill Walls

Researchers proposed few strategies to represent infill walls in building frames. Polyakov [1960] observed the behaviour of infilled frame during testing and proposed a simple strategy for replacing the masonry infill with an ***equivalent compressive masonry strut*** as shown in Fig. 5.8. The stiffness of the assumed equivalent diagonal strut depends on thickness and width of the strut (*a*) and material properties of the infill wall. In this study, system parameters of three scaled test models have been identified using system identification. These identified system parameters have been utilized to arrive at the dimension of an equivalent strut.

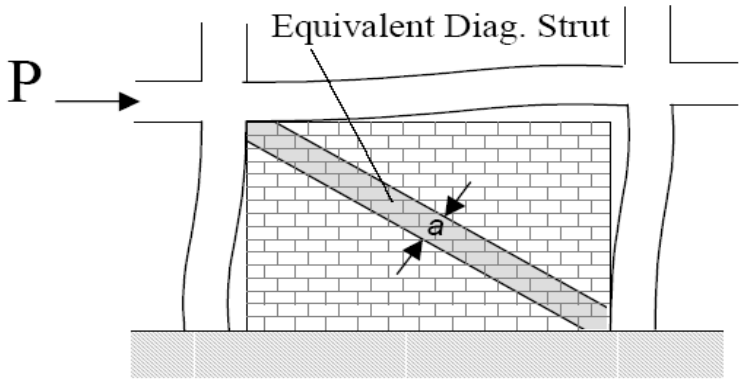

Fig. 5.8 Equivalent diagonal strut

Comparison of the identified storey stiffness of test Model W-I with full infill wall and those of bare frame model are shown in Fig. 5.9. Identified storey stiffness corresponding to all the four earthquake excitations are shown on the same plot. The plot shows the extent of enhancement in first storey stiffness of test model W-I compared to that of bare frame test model due to the presence of three full infill walls along the direction of excitation at first storey level.

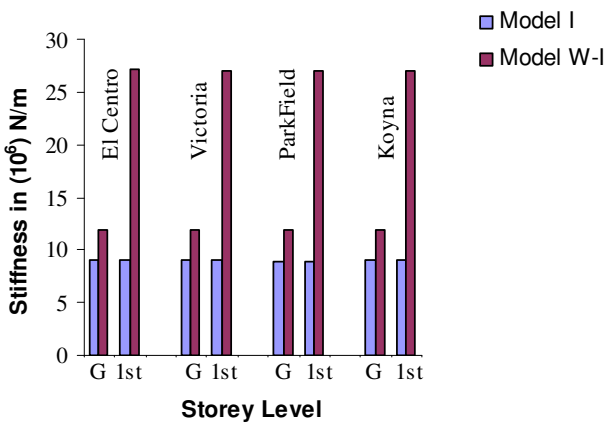

Fig. 5.9 Stiffness of model W-I with full wall and corresponding bare frame model

Thus, the increase in stiffness for the presence of one infill wall can be taken as one third of the total increase in stiffness as shown in Table 5.6. Similar trends of increase in first storey stiffness have been observed for test models W-II and W-III. The mean value of increase in lateral stiffness due to the presence of one infill wall considering all the three models is found as 5.95 x 10^6 N/m with a standard deviation of 0.06 x 10^6 N/m. Identified stiffness corresponding to all the four earthquake excitations have been considered for the evaluation of mean and standard deviation. The increase in lateral stiffness due to the infill wall can be resolved along the diagonal direction for assessing the stiffness of the idealized diagonal strut. Fig. 5.10 shows a view of a typical diagonal strut on first storey with dimensions as indicated in the diagram.

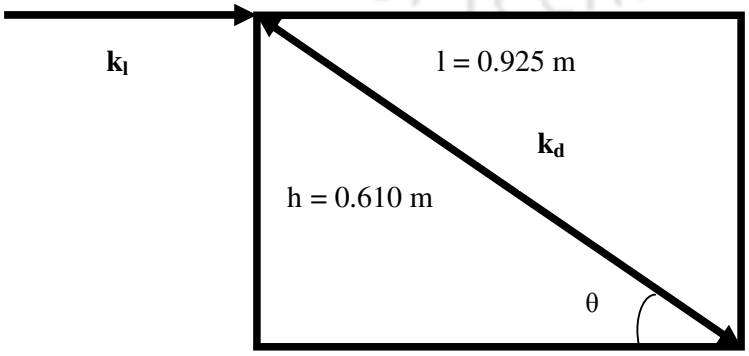

Fig. 5.10 Stiffness of diagonal strut

From this figure, the resolved component along diagonal direction can be written as:

$(k_d) = k_l/\text{Cos}\,\theta$, where $\cos\theta = \dfrac{0.925}{1.108}$.

Thus, the stiffness of the diagonal strut can be considered as $7.13\text{x}10^6$ N/m. Further, a diagonal strut is a skeletal member, whose stiffness is taken as:

$$\frac{A\,E}{D} = \frac{a\,t\,E}{D} = \frac{(D/C)\,t_{ff}\;E}{D} \tag{5.1}$$

where A is the sectional area of the equivalent strut [i.e. width (a) x thickness (equal to the thickness of infill wall, t_{ff} = 0.060 m)], D is the length of the diagonal strut and E is Young's modulus of Elasticity of the masonry and has been taken as equal to 550 f_m [Kaushik *et al.,*2007]. Width of the diagonal strut a is again considered as a fraction of diagonal length L and hence a factor C as introduced above needs to be evaluated. Thus, from Table 5.1, corresponding to compressive strength of masonry prism f_m = 2 N/mm^2, E_m = 1100 N/mm^2 and hence, C is obtained as 9.25.

Thus, the stiffness of a diagonal strut may be written as:

$$k_d = \frac{(D/9.25)\,t_{ff}\;E_m}{D} \tag{5.2}$$

5.2.11 Correlation between Sizes of Wall Opening and Stiffness

Mathematical representation of effects of openings in infill walls has been found to be one of the difficult tasks due to the absence of any standard empirical relationship. Hence, there is a need for determining a correlation between stiffness and sizes of openings in walls. This correlation will help to properly account for the contribution of infill walls during modeling. Fig. 5.11 indicates the changes in stiffness of storey with infill wall due to changes in sizes of wall opening for test model W-I.

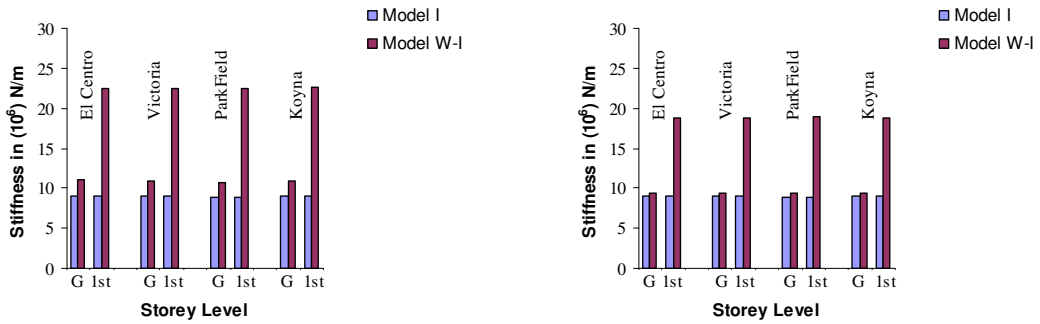

(a) 5% wall opening

(b) 10% wall opening

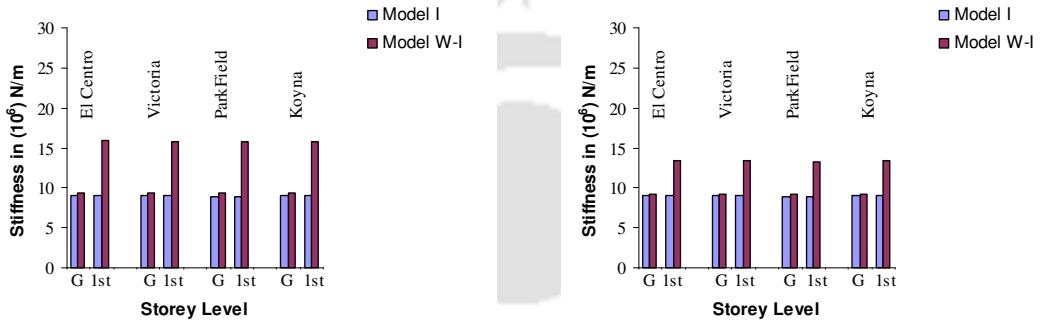

(c) 20% wall opening

(d) 30% wall opening

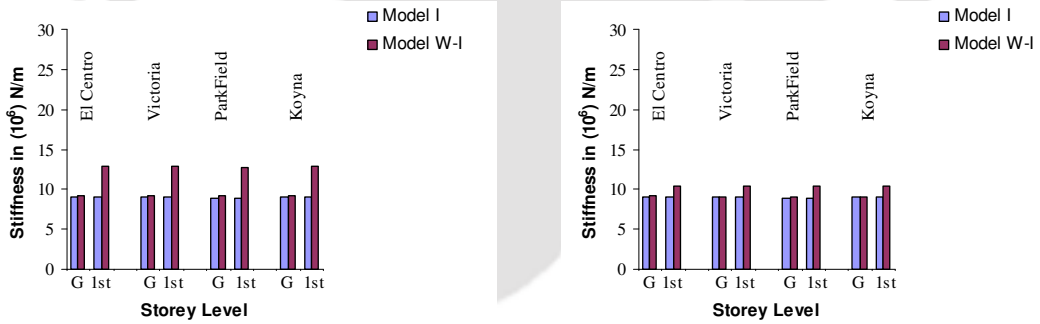

(e) 35% wall opening

(f) 40% wall opening

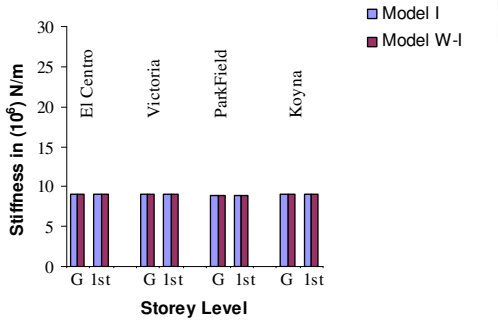

(g) 45% wall opening

Fig. 5.11 Storey stiffness of model W-I with different percentage of wall openings and corresponding bare frame model

Stiffness of first storey for all the cases of wall openings have been compared with stiffness of the corresponding bare frame models. It can be seen from Fig. 5.11 (g) that the floor stiffness of model W-1 with 45 % opening in infill wall are almost same as that of bare frame model.

Thus, the identified stiffness for all the models have very clearly shown that the presence of infill wall in a storey leads to a substantial increase in stiffness of that storey. However, the influence becomes insignificant as the opening percentage increases up to 45% and need not be accounted for in the modeling of a building. Percentage reductions in stiffness of a storey with opening in infill wall have been calculated for all the models and are plotted as shown in Fig. 5.12 - 5.15. It may be seen that the trend in reduction in storey stiffness are identical for all the models irrespective of table acceleration histories considered. In the previous section, contribution of a full infill wall in the lateral stiffness of a storey with infill wall has been evaluated.

A correlation has been developed for modeling an infill wall in the form of an equivalent diagonal strut.

However, the contribution to storey stiffness reduces with opening in infill wall as observed in Fig. 5.12-5.15. Thus, relative stiffness factor, R_k is evaluated by considering the relative storey stiffness for each case of wall openings with respect to the storey stiffness of full wall model i.e. the storey stiffness corresponding to Case-1. Data corresponding to all the three models and all the four considered earthquake excitations have been considered altogether as the first storey with infill wall is identical for all the three test models. A regression analysis has been carried out using these relative stiffness data to correlate with the ratio of wall openings. The ratio of wall opening is considered as independent variable and relative storey stiffness as the dependent variable for the regression analysis.

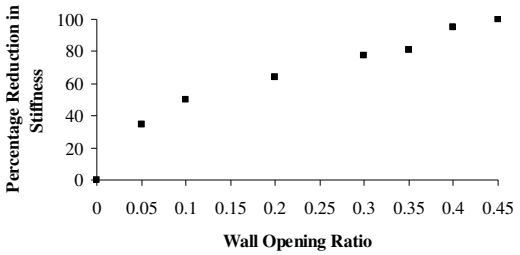

(a) Model W-I

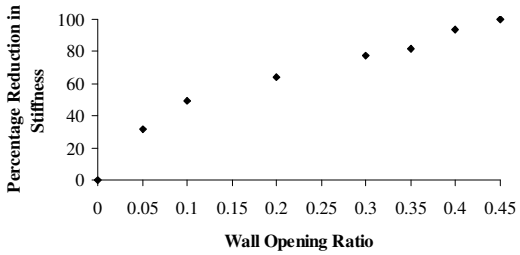

(b) Model W-II

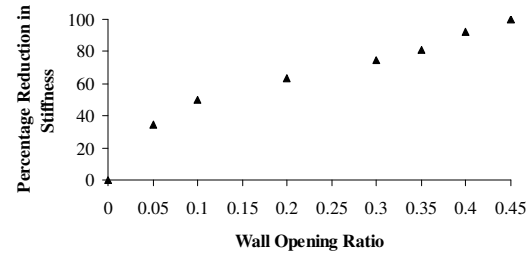

(c) Model W-III

Fig. 5.12 Changes in storey stiffness with sizes of wall openings for El Centro (1940): Comp - 180 earthquake excitation

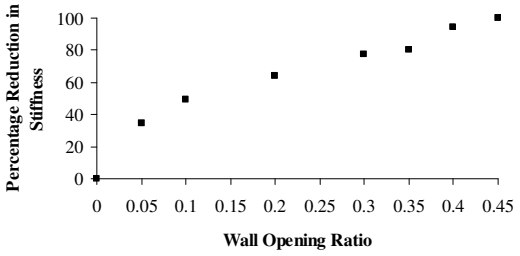

(a) Model W-I

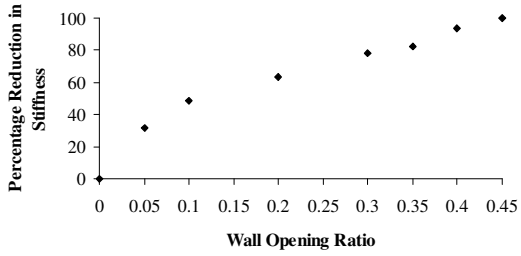

(b) Model W-II

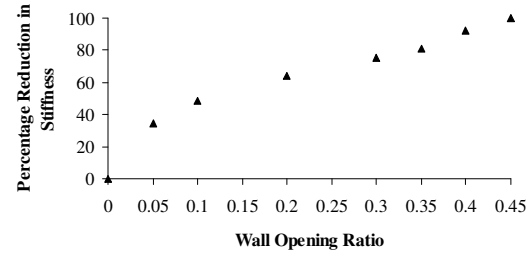

(c) Model W-III

Fig. 5.13 Changes in storey stiffness with sizes of wall openings for Victoria (1980): Comp - CPE045 earthquake excitation

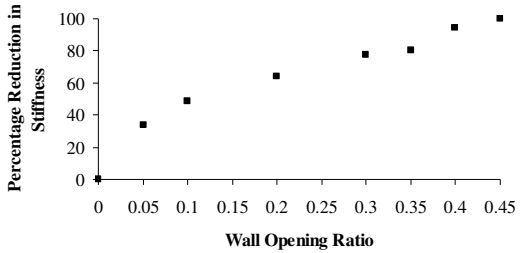

(a) Model W-I

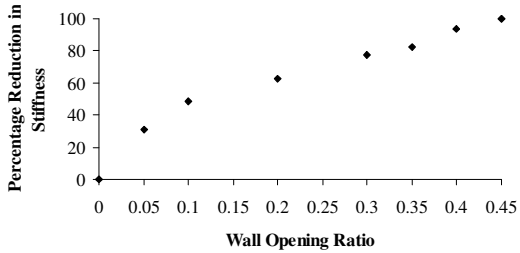

(b) Model W-II

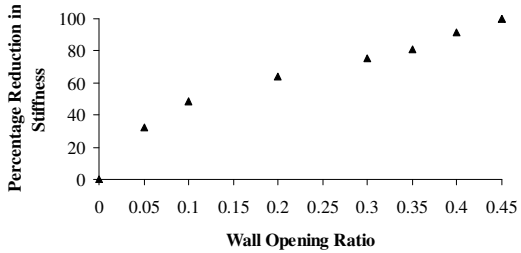

(c) Model W-III

Fig. 5.14 Changes in storey stiffness with sizes of wall openings for Parkfield (1966): Comp - C02065 earthquake excitation

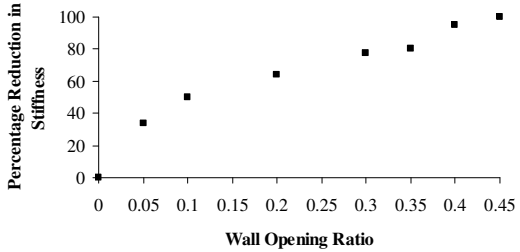

(a) Model W-I

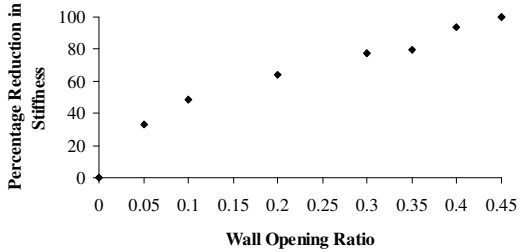

(b) Model W-II

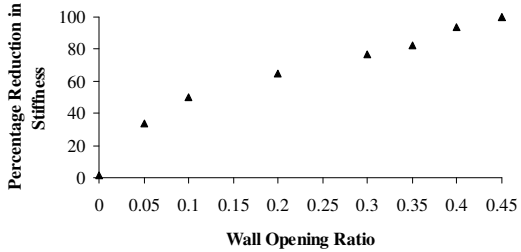

(c) Model W-III

Fig. 5.15 Changes in storey stiffness with sizes of wall openings for Koyna (1967): Comp - Transverse earthquake excitation

A correlation representing the best fit curve of the scattered data have been derived. Best fit curve correlating ratio of wall openings and relative stiffness is shown in Fig. 5.16 shows the. A very simple relationship as shown in Eq. 5.3 is obtained for the evaluation of reduction in the value of stiffness of a diagonal strut with different ratios of wall opening. It may also be seen that the best fit curve has been obtained with a coefficient of determination very close to unity.

$$R_k = 1 - 5.88\,Ar + 17.73\,Ar^2 - 21.30\,Ar^3 \qquad (5.3)$$

Eq. 5.2 representing stiffness of a full wall can thus be appropriately modified by multiplying with R_k as obtained from Eq. 5.3 to account of opening in the infill wall. The stiffness of wall with opening can thus be written as

$$k_{do} = k_d \text{ x } R_k \qquad (5.4)$$

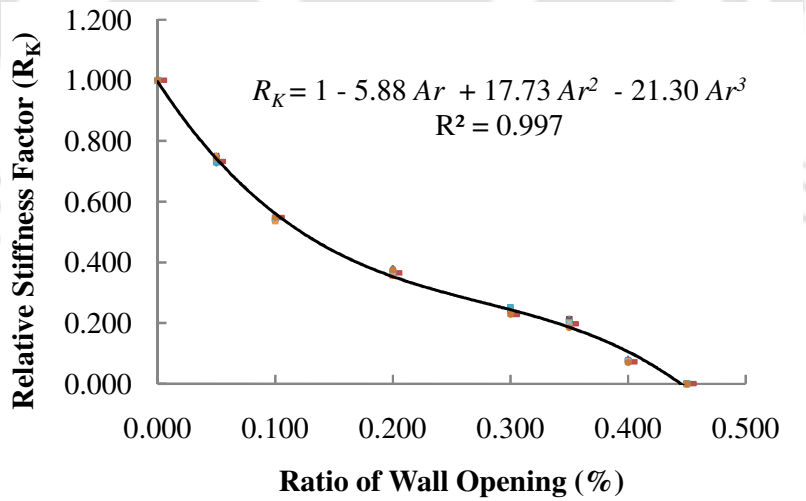

Fig. 5.16 Variation in relative stiffness factor with ratio of wall opening

5.3 STUDIES ON NUMERICAL MODELS FOR VERIFICATION OF EXPERIMENTAL RESULTS

In the previous section, empirical relationships have been developed for the evaluation of contribution of infill wall, considering infill wall as a compression strut. Numerical models of test models developed in the Chapter 4 do not have infill walls. A number of researchers and agencies proposed empirical relationships for assessing the contribution of masonry infill to the lateral stiffness of a building. However, variations have been observed in the evaluated stiffness based on different recommendations, which may be attributed to the influence of country specific design and construction practice. Some of these relationships are discussed in the following subsection.

5.3.1 Existing Recommended Methods for Infill Wall Contribution

All the existing methods for the evaluation of infill wall contributions use the concept of an equivalent diagonal strut for masonry infill, where an equivalent strut width is specified. Some of the available methods have been summarized as below:

(a) The most simplistic approach presented by Paulay and Priestly [1992] assumed constant values for the strut width, a, between 12.5 to 25 percent of the diagonal dimension of the infill, with no regard for any infill or frame properties.

(b) Stafford-Smith et al. [1962] derived complex expressions to estimate the equivalent strut width, a, that considered parameter like length of contact between the column/beam and the infill, as well as the relative stiffness of the infill to the frame. The masonry infill panel was represented by an equivalent diagonal strut of width, a, and net thickness t_{ff} as shown in Fig. 5.17.

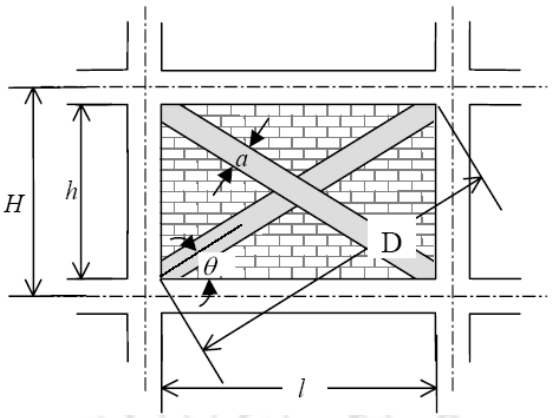

Fig. 5.17 Strut geometry

The equivalent strut width, *a*, was observed as dependent on relative flexural stiffness of the infill to that of the columns of the confining frame, written as:

$$\lambda_1 H = H\left[\frac{E_m t \sin 2\theta}{4E_c I_{col} h}\right]^{\frac{1}{4}} \tag{5.5}$$

Using this expression, Mainstone [1971] considered the relative infill to frame flexibility in the evaluation of the equivalent strut width of the panel as:

$$a = 0.175\mathrm{D}\ \ (\lambda_1 H)^{0.4} \tag{5.6}$$

where E_m and E_c are the moduli of elasticity of the masonry and the concrete (i.e. the frame material), respectively, $\theta = \arctan\left(\frac{H}{D}\right)$ is the inclination of the diagonal, t is the thickness of the of the infill wall, and I_{col} is the moment of inertia of the column of the frame, whereas *h, H* and *l* are the net height of the infill wall, storey height and the length of the infill panel with $\mathrm{D} = \sqrt{l^2 + h^2}$.

(c) Original Stafford-Smith and Carter [1969] equations accounted for varying aspect ratios. They did so by representing their findings with four curves for aspect ratios (*l*/*h*) equal to 1.0, 1.5, 2.0, and 2.5. These curves translated into Eq. 5.7 through 5.10 respectively, with linear interpolation for aspect ratios that fall between these values.

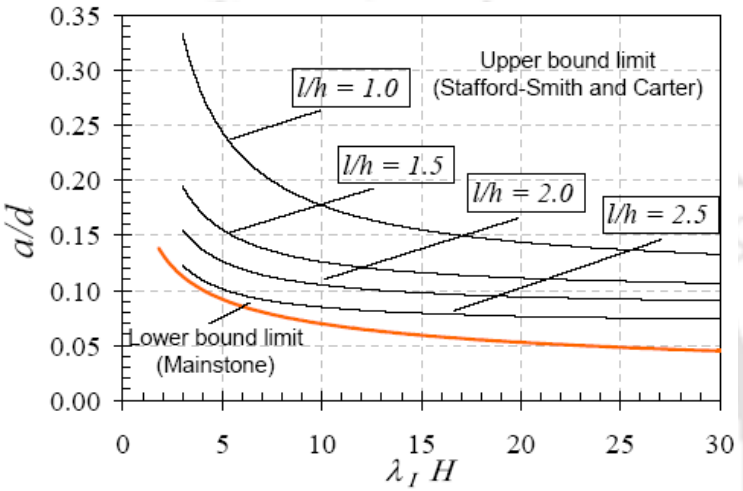

Fig. 5.18 Upper/ Lower limit of strut width

$$a = 0.110d\left(1+\frac{6.027}{\lambda_1 H}\right) \quad for \;\; l/h=1.0 \tag{5.7}$$

$$a = 0.0966d\left(1+\frac{3.035}{\lambda_1 H}\right) \quad for \; l/h=1.5 \tag{5.8}$$

$$a = 0.0835d\left(1+\frac{2.574}{\lambda_1 H}\right) \quad for \; l/h=2.0 \tag{5.9}$$

$$a = 0.0683d\left(1+\frac{2.410}{\lambda_1 H}\right) \quad for \; l/h=2.5 \tag{5.10}$$

(d) IITK-GSDMA Report [2005] modeled the masonry infill within RC frame using an equivalent diagonal strut as follows:

- The modulus of elasticity (in MPa) of masonry, E_m was taken as

$$E_m = 550 f_m \tag{5.11}$$

where f_m is the compressive strength of masonry prism in MPa.

- The ends of diagonal struts should be pin jointed to the RC frame [Fig. 5.19] such that the moment transfer would not take place from RC frame to struts.

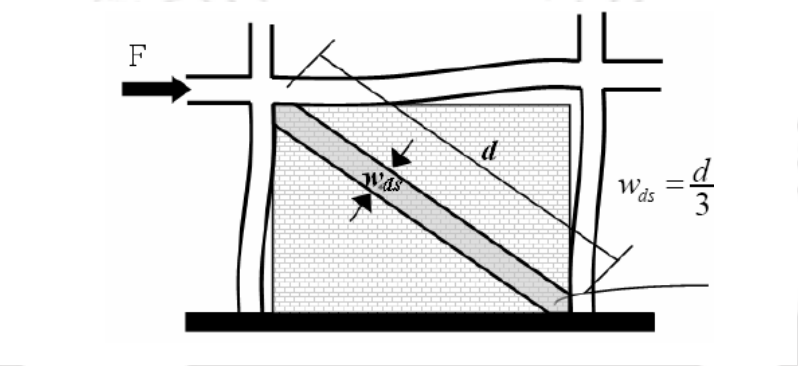

Fig. 5.19 Equivalent diagonal strut

- For *solid walls* (without any openings) width of equivalent diagonal strut (W_{ds}) would be taken as one third of the diagonal length of the infill wall (d) as shown in Fig. 5.19.

- *Infilled frames with openings* should be modeled with reduced width of strut as,

$$W_{do} = \rho_w W_{ds} \tag{5.12}$$

where W_{do} is the width of diagonal strut for infill walls with openings and ρ_w is the reduction factor, which accounts for openings in infill, which is given by

$$\rho_w = 1\text{-}2.5A_r \tag{5.13}$$

A_r is the opening ratio, which is the ratio of face area of opening to the face area of infill. No reduction in the width of diagonal strut would be needed for an opening

ratio less than 0.05, while infill contribution would be ignored in that panel for an opening area ratio more than 0.4.

- Thickness of the strut would be taken as the actual thickness of the wall.

(e) **FEMA 306 [1999]** recommended the following equation to calculate the effective width of diagonal compression strut

$$a = 0.175(\lambda_1 h_{col})^{-0.4} r_{\inf} \tag{5.14}$$

where h_{col} and r_{inf} are the column height and diagonal length of the masonry infill panel in inches. And λ_1 (inch^{-1}) is given by,

$$\lambda_1 = \left[\frac{E_{me} t_{\inf} \sin 2\theta}{4 E_{fe} I_{col} h_{\inf}} \right]^{0.25} \tag{5.15}$$

where E_{me} and E_{fe} are expected modulus of elasticity of masonry and frame material in psi respectively. In the above equation, t_{inf} (inch) is the actual thickness in inch of masonry infill in contact with frame, θ (rad) is the inclination of diagonal strut with horizontal, I_{col} (inch^4) is the moment of inertia of column, and h_{inf} (inch) is the height of masonry infill panel. Thickness of equivalent strut was recommended as equal to the actual thickness of the wall.

From Table 5.9 it may be observed that the evaluated width and stiffness of an equivalent diagonal strut corresponding three infill walls of the test models varies from method to method. This will also lead to different modal properties and variation in dynamic characteristics of a building with infill wall. The observed variations among these recommended values have motivated the present study for the evaluation of influence of infill wall based on system identification technique using scaled laboratory building models.

Table 5.9 First storey stiffness in (10^6) N/m of test model with equivalent diagonal strut using various recommendations

Analogies	Width (m)	*Total Stiffness
Paulay and Priestly (P&P)	0.217	39.53
Stafford-Smith (S-S)	0.355	64.66
Original Stafford-Smith & Carter (OSSC)	0.162	29.51
IITK-GSDMA	0.272	49.73
FEMA 306	0.098	17.85

*** Total Stiffness:** Sum of Stiffness of three identical walls

5.3.2 Numerical Models with Equivalent Diagonal Strut

The infill walls have been modeled as a diagonal strut with expression as per proposed Eq. 5.2. GAP element has been used to model the diagonal strut in the first storey of all the numerically simulated bare frame scaled building model in SAP 2000 Nonlinear (version 12). GAP elements are basically link elements which are active in compression and therefore used to represent compression strut for modeling infill walls. Sizes of infill walls in all the three test models are identical with the dimension as 0.925 x 0.610 m. The modulus of elasticity of masonry has been derived using expression given by Kaushik *et al.* [2007] based on evaluated prism compressive strengths of masonry. 3-D finite element models of all the three scaled buildings with infill walls have been simulated in SAP 2000. Further, for all the cases of wall opening as mentioned in Table 5.2, the partial contribution of infill walls have been evaluated as per the proposed Eq. 5.4. The stiffness of the GAP elements have been accordingly defined for different opening ratio and analyses have been carried out.

5.3.3 Modal Analysis of Numerical Models

Modal analyses of all the SAP models with different case of wall openings described in subsection 5.3.3 have been carried out and the frequencies along the direction of excitation have been presented in Table 5.10. It may be mentioned that the computed modal

frequencies for all the cases of wall openings of all the three test models are in good agreement with identified frequencies of their respective test models.

Table 5.10 Natural frequencies corresponding to mode shapes of different numerical models with different cases of wall openings

Test Models	Cases of Wall Opening	Frequency (rad/sec)		Error in Frequency (in %) for	
		First Mode	Second Mode	First Mode	Second Mode
Model W-I	Case-1	49.15	209.69	6.96	2.49
	Case-2	48.55	191.97	7.25	2.77
	Case-3	47.83	177.57	6.86	2.92
	Case-4	46.64	158.94	5.88	3.30
	Case-5	45.69	148.14	4.75	2.71
	Case-6	45.00	142.08	5.34	3.90
	Case-7	43.74	133.00	4.22	2.90
	Case-8	40.14	117.85	2.27	3.87
Model W-II	Case-1	67.55	218.26	3.29	4.01
	Case-2	65.82	200.11	0.11	2.81
	Case-3	64.05	186.38	1.03	1.02
	Case-4	60.87	169.19	1.20	0.14
	Case-5	58.38	159.69	2.06	2.17
	Case-6	56.67	154.41	1.32	1.56
	Case-7	53.49	146.63	2.45	1.68
	Case-8	47.17	135.96	1.77	1.19
Model W-III	Case-1	67.16	221.13	2.00	2.52
	Case-2	65.31	202.69	1.23	2.06
	Case-3	63.48	188.87	1.20	1.23
	Case-4	60.21	171.73	1.43	0.19
	Case-5	57.68	162.31	0.63	0.55
	Case-6	55.95	157.10	0.94	0.17
	Case-7	52.77	149.42	0.63	0.68
	Case-8	46.55	138.91	2.39	4.82

The computed modal frequencies for all the cases of wall openings of Model W-I as shown in Table 5.10 are comparable with the corresponding identified frequencies of Model W-I as furnished in Table 5.3. Similar observations have also been drawn for test Models W-II and W-III.

5.3.4 Comparison of Dynamic Responses of Numerical Models with Laboratory Model based results

Time history analyses of the numerical models with infill walls have been carried out with recorded table acceleration histories acquired during shake table test as input. Floor acceleration responses have been acquired from each test models and are as shown in Fig. 5.20.

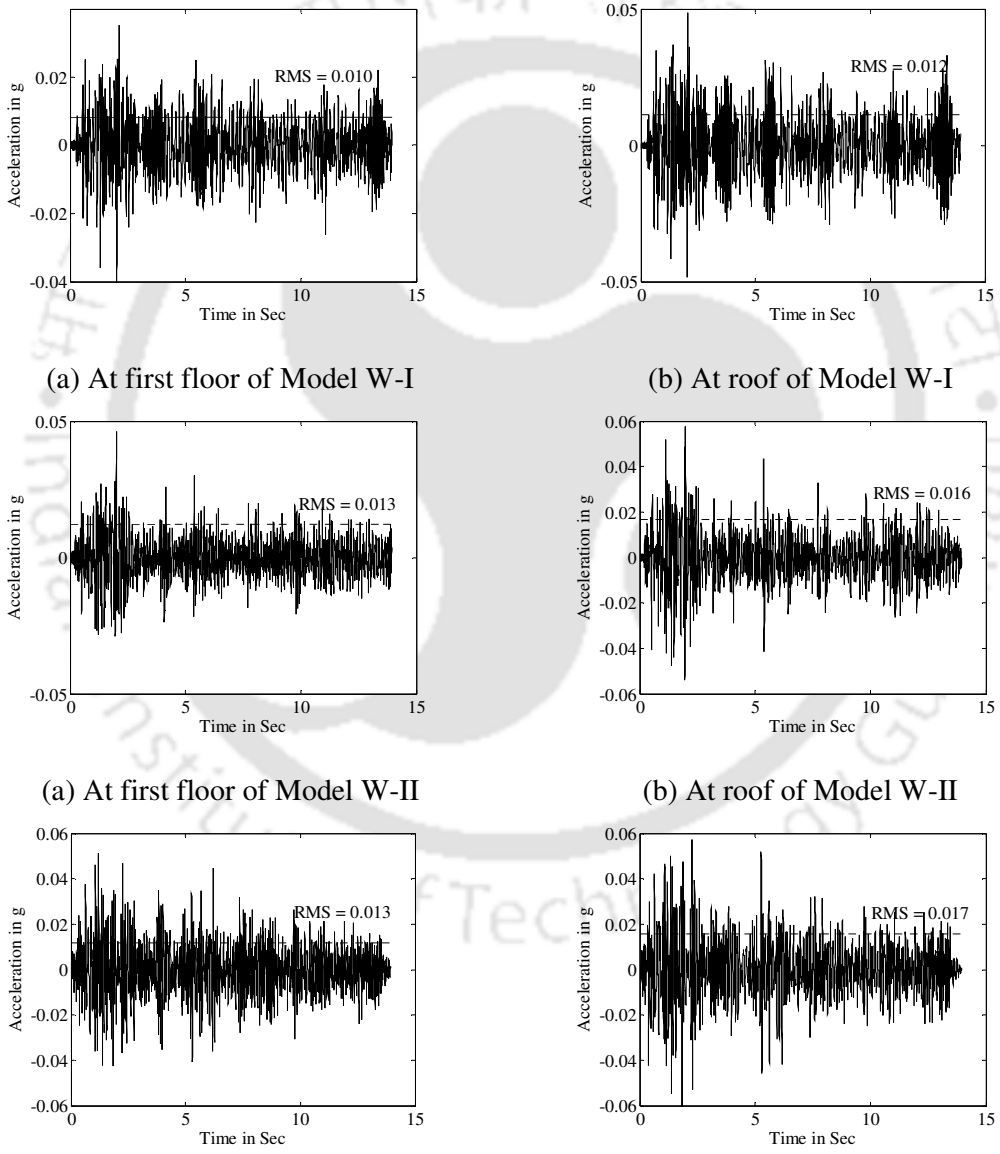

(a) At first floor of Model W-I (b) At roof of Model W-I

(a) At first floor of Model W-II (b) At roof of Model W-II

(a) At first floor of Model W-III (b) At roof of Model W-III

Fig. 5.20 Computed floor acceleration time histories under El Centro (1940): Comp - 180 earthquake component

The root-mean-square (RMS) values of acceleration amplitudes of dynamic responses at first and roof floor levels of the numerical models subjected table acceleration due to scaled El Centro (1940): Comp - 180 earthquake motion as input excitation have also been estimated and are shown in Fig.5.21.

Comparison of Fig. 5.21 and 5.5, established a good agreement in the RMS values of acceleration histories obtained from scaled test models and the numerical models. Further, the peak values of floor accelerations are also presented in the Table 5.11 for comparison of the same with peak floor accelerations of the corresponding numerical models.

Table 5.11 Peak values of floor accelerations of different models

Models	**Peak floor accelerations (g)**			
	First floor		**Roof floor**	
	Experimental	**Numerical**	**Experimental**	**Numerical**
Model W-I	0.040	0.040	0.048	0.049
Model W-II	0.048	0.048	0.059	0.059
Model W-III	0.051	0.051	0.061	0.061

Peak values acceleration histories established a good agreement between scale test models and corresponding numerical models. Thus, the numerically simulated models are appropriate representations of their respective laboratory models.

5.3.5 Comparison of Modal Parameters from Numerical Models with Equivalent Diagonal Strut Based on Different Recommendations

The stiffness of the infill wall have been observed to be different for different analogies of diagonal strut recommended by different investigators as observed from the Table 5.9. The infill walls in the first storey of the test Model W-I have been modeled separately by GAP element using recommendations mentioned in Table 5.9 and proposed expression. The numerical models with GAP element representing different diagonal strut have been

analyzed for evaluating modal frequencies considering 5% proportional damping. The modal frequencies corresponding to the mode shapes in the shorter direction of the model have been extracted and are furnished in Table 5.12. Modal frequencies in Table 5.12 indicate that modal frequencies corresponding to different diagonal strut analogies adopted for modeling GAP element are different from method to method. The modal frequencies of models corresponding to approach FEMA 306 and proposed correlation are close to each other.

Table 5.12 Modal frequencies of the numerical model of test Model W-I for different recommendations of diagonal strut

Diagonal Strut Analogies	**Modal Frequencies (rad/sec)**	
	First Mode	**Second Mode**
Paulay and Priestly (P&P)	46.69	248.40
Stafford-Smith (S-S)	47.12	282.36
Original Stafford-Smith & Carter (OSSC)	46.34	227.20
IITK-GSDMA	46.91	264.63
FEMA 306	45.54	193.81
Proposed	45.82	203.87

5.4 VALIDATION OF PROPOSED CORRELATIONS FOR WALL CONTRIBUTION

The study related to the contribution of infill wall to the lateral stiffness of scaled building models has been carried out in the previous section. Numerical modeling of diagonal strut in a full size building that corresponds to 1/5 scale laboratory test Model I has been carried out to examine whether the proposed expressions represented by Eq. 5.2 - 5.4 will be appropriate for full size building. Similar material properties as those for the laboratory test Model I have been considered to model full size building and infill walls on first storey in the shorter direction of the building. Different cases of wall openings have also been considered and natural frequencies have been evaluated through modal analysis

considering 5% proportional damping. Evaluated modal frequencies corresponding to the mode shape in the shorter direction of the building have been scaled as per similitude requirement. The scaled modal frequencies of the full size building with different sizes of opening have been compared with the corresponding modal frequencies of the model of the test Model I. These are furnished in Table 5.13.

Table 5.13 Modal analysis results of prototype building and corresponding scaled building model

Wall Opening	Frequency (rad/sec)					
	First Mode			Second Mode		
	Test Model W-I	Prototype Model	Prototype Model x $\sqrt{S}$	Test Model W-I	Prototype Model	Prototype Model x $\sqrt{S}$
Case-1	49.15	22.03	49.26	209.69	93.85	209.85
Case-2	48.55	21.73	48.60	191.97	85.89	192.05
Case-3	47.83	21.42	47.89	177.57	79.43	177.60
Case-4	46.64	20.92	46.78	158.94	71.12	159.03
Case-5	45.69	20.45	45.72	148.14	66.29	148.23
Case-6	45.00	20.14	45.03	142.08	63.56	142.13
Case-7	43.74	19.57	43.76	133.00	59.52	133.10
Case-8	39.14	17.52	39.17	117.85	52.73	117.90

A very good agreement may be observed between scaled natural frequencies of the full size building model with the corresponding modal frequencies of numerical model of the scaled test model. Thus, it may be inferred that though the correlations related to contribution of infill wall have been developed based on scaled laboratory models, these expressions are applicable to full size buildings without any further correction to address size effect related issues.

5.5 CONCLUDING REMARKS

Three different scaled laboratory building models with infill walls at first storey have been used for the identification of system parameters. As compared to the respective bare frame

identified system parameters, a substantial increase in the storey stiffness along the direction of infill wall have been observed, which can be easily attributed due to the presence of infill wall. Further, storey stiffness have been observed to reduce with increase in size of opening in the infill wall. All these changes in stiffness have been observed to be very consistent for all the three different test models and studied under four different known seismic excitations. The contribution of infill wall has been found to be insignificant when the size of wall opening becomes 45% of the full wall size. Considering the infill wall as an equivalent diagonal strut, a simple expression has been suggested to evaluate the stiffness of the strut. Further, a reduction factor in stiffness of diagonal strut has been suggested based on the correlation between reduction in storey stiffness due to opening in infill and opening ratios. The correlations related to the contribution of infill wall have also been verified on a numerically simulated model and the applicability of those expressions for full size models have also been established. Thus, the studies in this chapter may be concluded as:

- The system identification scheme, N4SID has been found to be efficient tool for determining the infill wall contribution of prototype buildings.
- Infill wall provides a substantial enhancement in lateral storey stiffness along the direction of infill. However, the contribution becomes insignificant, when the size of openings in walls become more than 45% of full wall size.
- The derived empirical relationships (based on data from laboratory test models) representing wall contribution as well as the influence of openings in infill walls have been observed to be independent of scale of the building and can be very easily applied to the modeling of full size existing building.

CHAPTER 6

IDENTIFICATION OF SYSTEM PARAMETERS OF AN EXISTING MULTI-STOREY SYMMETRIC-PLAN SHEAR BUILDING

6.1 INTRODUCTION

This chapter deals with the identification of system parameters of an existing multi-storey building using limited sensor data using subspace identification scheme. The parametric state space model makes use of recorded floor acceleration histories of the existing symmetric-plan shear building and ground acceleration time histories. Subsequently, least square solution of eigenvalue problem is used to determine structural parameters. An iterative approach is adopted to address the issue of identification of system parameters of building with limited sensors. The description of the building under study is presented and the detailed instrumentation scheme for recording earthquake induced structural responses has been explained. The recorded data are processed and used for the extraction of modal parameters using N4SID algorithm. A numerical model of the building has also been simulated to represent the dynamic characteristics of the existing building. Sensitivity of sensor allocation has been studied using structural responses of the simulated model to examine the appropriateness of use of limited sensors for system identification.

6.2 IDENTIFICATION OF SYSTEM PARAMETERS OF EXISTING MULTI-STOREY SYMMETRIC-PLAN SHEAR BUILDING

The study on identification of system parameters of existing building is found to be limited as observed using detailed survey on literatures. Nagarajaiah [1999] identified first few frequencies and corresponding damping ratios of base isolated USC hospital building through system identification based on frequency domain approach. Bani-Hani [2008] employed a parametric state space identification model for identification of modal

parameters of old minaret model simulated based on measured characteristics of old stone and mortar. This chapter is aimed at evaluation of modal as well as structural parameters of an existing symmetric-plan shear building. In the following subsections, the example building under study has been described along with the available instrumentation facilities.

6.2.1 Description of the Sample Building

The structure considered for this study is a nine storey building having ground plus nine floors. The building is situated on the south bank of mighty river Brahmaputra in Guwahati, Assam, India. The building is a residential apartment owned by Bharat Sanchar Nigam Limited (BSNL). This multi-storey building considered in the study is located in the seismic Zone-V (i.e. zone with highest seismicity) of seismic zone map of India. The ground storey height of the building is 2.75 m while heights of remaining storey are of 3.0 m. The building does not have any infill wall in the ground storey, but all the upper storey have similar infill walls. Thus, the distribution of stiffness and mass is not uniform along the height. A pictorial view of the building is shown in the Fig. 6.1. The plan of the building at the ground floor level along with column positions and its orientations is shown in Appendix – A [Fig. A – 3]. Floor masses as well as material and geometric properties of the building have been collected from the available drawings. All necessary data are furnished in Appendix – A [Table A – 2]. Material properties of the building relevant to this study are as furnished in Appendix – A [Table A – 3].

Fig. 6.1 Pictorial view of the BSNL building

6.2.2 Details of Instrumentations

The building has been instrumented with accelerometers and data recorder to acquire earthquake responses. Numbers of uni-axial and tri-axial accelerometers as described in the section 3.3.1 have been fixed for recording the floor responses due to earthquake, which generally occurs quite frequently at the site of the building. A tri-axial accelerometer has been mounted at the ground floor level to collect the ground accelerations in three principal orthogonal directions i.e. longer, shorter and vertical direction. Similarly, another tri-axial accelerometer has been fixed at the roof of the building. Uni-axial accelerometers have been fixed on selected floors in both X (longer) and Y (shorter) directions of the building. Three uni-axial accelerometers have been fixed

at first, third and seventh floor of the building along the Y direction while two uni-axial accelerometers have been fixed at first and fifth floor of the building along the X direction. The positions and directions of accelerometers at ground level are also indicated in Appendix – A [Fig. A – 3]. All the accelerometers at different floor levels have been fixed in the same vertical line. The episensor accelerometers have been set to a full scale level of 2g (±1g). The accelerometers have been connected to a data recorder (Model: Altus K2, Make: Kinemetrics Inc, USA). All the tri-axial accelerometers have been directly connected to the data recorder and the uni-axial accelerometers have been connected through conjunction boxes mentioned in section 3.2.2. The recorder has been set to record earthquake acceleration at every 0.005 sec discrete time interval. Out of 12 available channels in the recorder, 11 channels have been used for recording data from tri-axial and uni-axial accelerometer and details are shown in Table 6.1.

Table 6.1 Sensor allocation in different floors of the sample building

Floors	Shorter direction	Longer direction
Ground	Triaxial	
First	Uniaxial	Uniaxial
Third	Uniaxial	------
Fifth	------	Uniaxial
Seventh	Uniaxial	------
Roof	Triaxial	

6.2.3 Characteristics of Recorded Responses

The instrumented building experienced a number of earthquakes since installation of instrumentation. Recorded ground motions and structural responses in two lateral directions at different floor levels corresponding to earthquake on 11-02-2006 and 12-08-2006 have been considered for this study. The trigger and detrigger values have been kept at 0.05% of full scale value. Pre-event and post-event timings have been kept as 3 sec. Hence, the sensor senses any acceleration value with magnitude more than 0.001g. DAS

records data 3 sec before the onset of trigger value and recording continues till 3 sec beyond trigger value limit. The high amplitude part of each acceleration response as mentioned in section 3.5.2 have been processed separately and appropriate parts have been considered for formation of input and output matrices for use in system identification. High amplitude parts of ground level records for two selected events on two different dates are as shown in the Fig. 6.2 and 6.3.

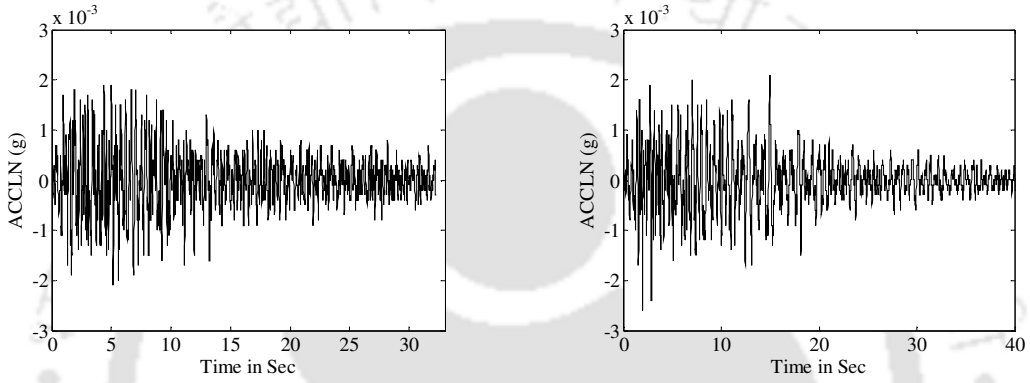

(a) Recorded on 11-02-2006 (b) Recorded on 12-08-2006

Fig. 6.2 Earthquake induced ground acceleration histories in longer direction

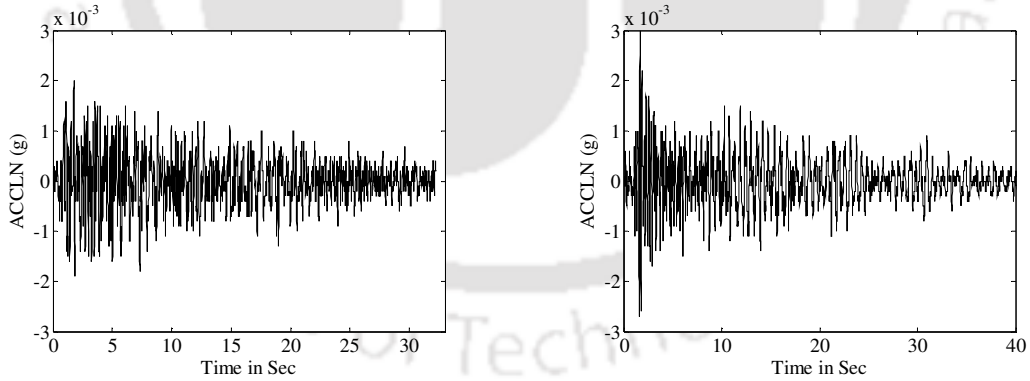

(a) Recorded on 11-02-2006 (b) Recorded on 12-08-2006

Fig. 6.3 Earthquake induced ground acceleration histories in shorter direction

It may be seen from the Fig. 6.2 and 6.3 that the peak ground accelerations (PGA) of earthquake on 12-08-2006 are higher than that of 11-02-2006. The high amplitude parts of

acceleration histories at different floor levels in longer and shorter directions are as shown in Fig. 6.4 and 6.5 respectively.

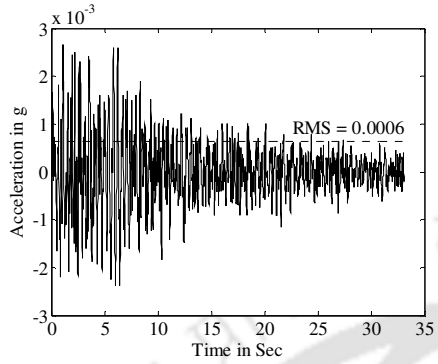

(a) Response at first floor on 11-02-2006

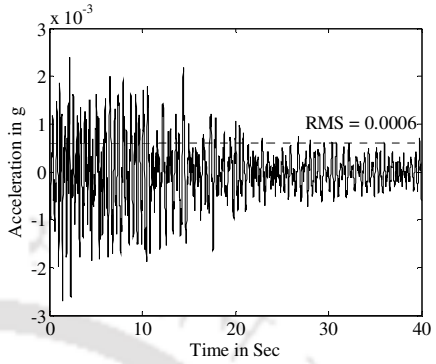

(b) Response at first floor on 12-08-2006

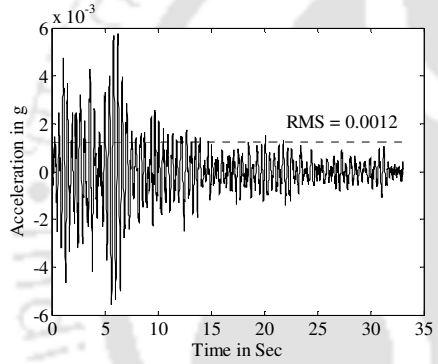

(c) Response at fifth floor on 11-02-2006

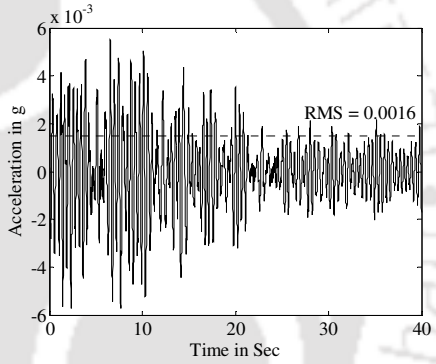

(d) Response at fifth floor on 12-08-2006

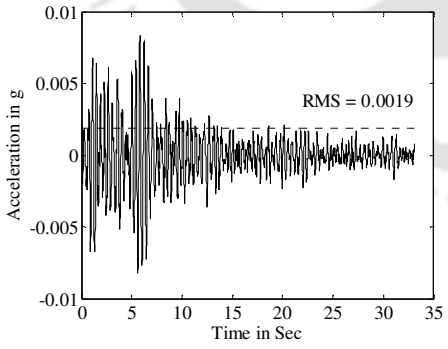

(e) Response at roof floor on 11-02-2006

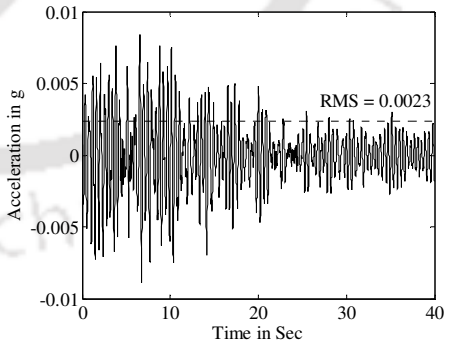

(f) Response at roof floor on 12-08-2006

Fig. 6.4 Earthquake induced acceleration responses at different floor levels in longer direction

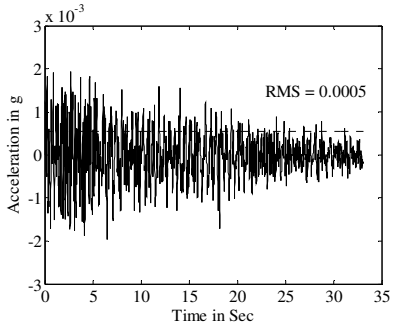

(a) Response at first floor on 11-02-2006

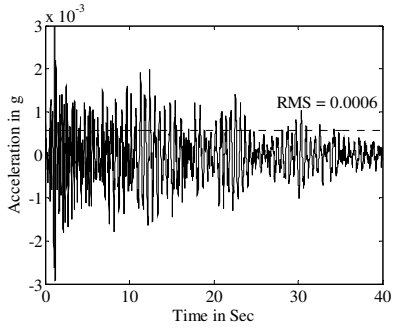

(b) Response at first floor on 12-08-2006

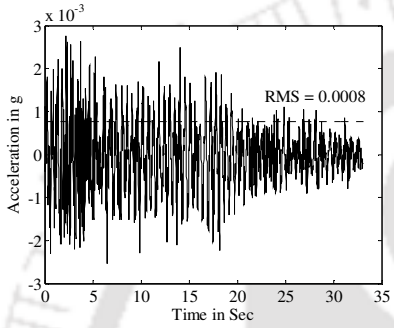

(c) Response at third floor on 11-02-2006

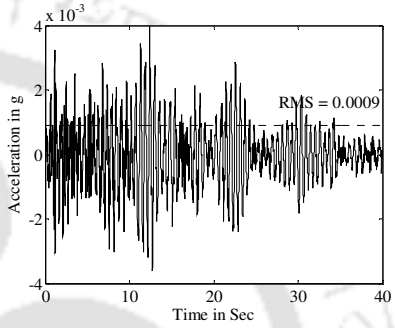

(d) Response at third floor on 12-08-2006

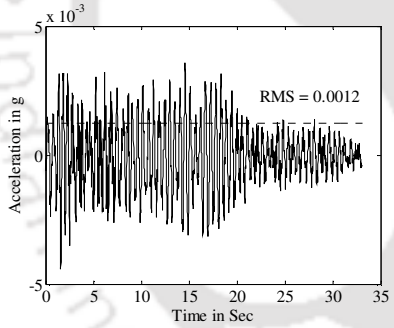

(e) Response at seventh floor on 11-02-2006

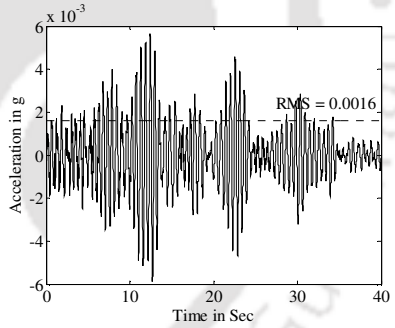

(f) Response at seventh floor on 12-08-2006

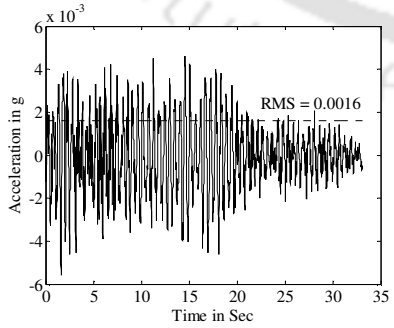

(g) Response at roof floor on 11-02-2006

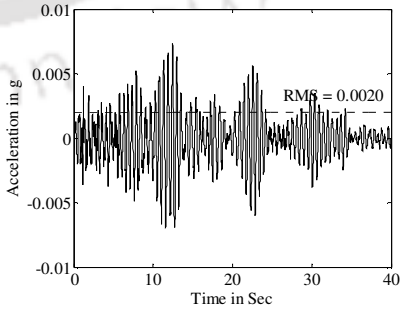

(h) Response at roof floor on 12-08-2006

Fig. 6.5 Earthquake induced acceleration responses at different floor levels in shorter direction

The peak acceleration values are found to be monotonically increasing with the height of the building in both the shorter and longer directions. The peak acceleration values of the recorded ground motions and structural responses at instrumented levels are presented in the Table 6.2.

Table 6.2 Peak acceleration values of recorded responses corresponding to two selected earthquakes

Floors	**Earthquake on 11-02-2006**		**Earthquake on 12-08-2006**	
	Peak acceleration (g)		**Peak acceleration (g)**	
	Longer	**Shorter**	**Longer**	**Shorter**
Ground	0.00209	0.00192	0.00258	0.00301
First	0.00249	0.00201	0.00266	0.00311
Third	------	0.00284	-----	0.00347
Fifth	0.00574	-----	0.00612	-----
Seventh	-----	0.00459	-----	0.00583
Roof	0.00815	0.00556	0.00862	0.00651

Frequency response spectrum of an acceleration response is considered to be a good indicator of frequency contents in the response. Hence, FFT plots of the recorded structural responses have been obtained to observe frequency contents. Some typical plots of FFT plots of recorded responses at few floor levels are shown in Fig. 6.6 and 6.7.

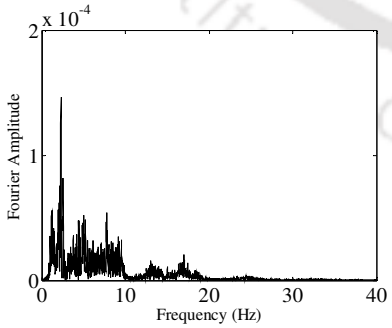

(a) At first floor

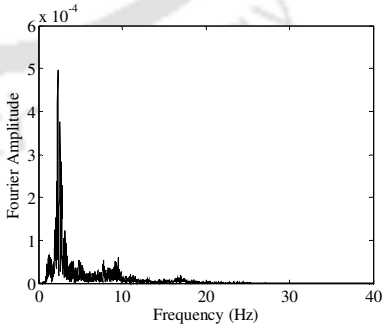

(c) At roof floor

Fig. 6.6 Fourier amplitude spectra of responses due to earthquake on 11-02-2006 in longer direction

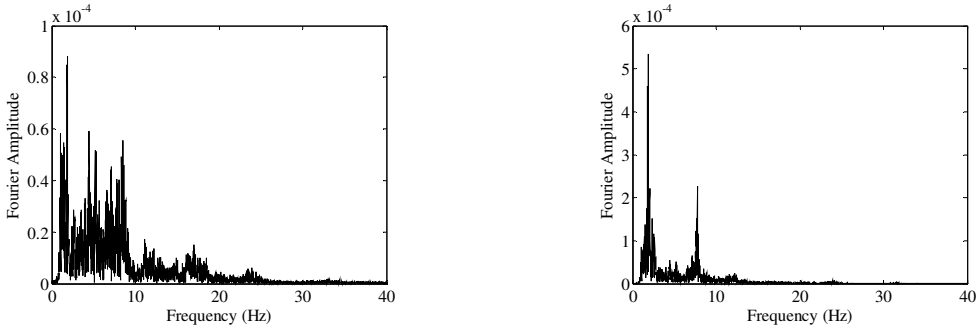

(a) At first floor (c) At roof floor

Fig. 6.7 Fourier amplitude spectra of responses due to earthquake on 11-02-2006 in shorter direction

It may be seen from the FFTs that the major frequency contents in all of the above cases are lower than 20 Hz. Hence, the cutoff frequency has been kept as 40 Hz, which approximately corresponds to twice the Nyquist frequency of the building. The time interval of data recording for the selected earthquakes has been kept as 200 Hz. Therefore, a 5^{th} order Butterworth digital filter has been adopted with a cut-off frequency of 40 Hz to remove noise in the acceleration signals. Further, 100 Hz has been considered as re-sampling frequency to reduce the data points.

6.2.4 Modal Parameters Identification

The recorded ground acceleration responses are considered as input, while the different floor acceleration responses are treated as outputs. Modal parameters such as frequencies, damping ratios and mode shapes have been identified through N4SID algorithm as described in Chapter 2 under section 2.2.1. The order of state space model is also very important to adequately describe the dynamic properties of the system. Since poles exist as pair of complex conjugate corresponding to each frequency, the order of the state space model has been considered as eighteen in order to extract nine predominant frequencies of nine storey shear building. In present study, acceleration histories available at limited number of floor levels have been utilized. The identified results based on acceleration

responses from the sample building due to 11-02-2006 and 12-08-2006 earthquake are presented in Table 6.3 and 6.4 respectively.

Table 6.3 Identified modal parameters for February 11, 2006 earthquake

Shorter Direction		Longer Direction	
Frequency (rad/sec)	**Damping (%)**	**Frequency (rad/sec)**	**Damping (%)**
10.44	2.20	12.46	2.20
31.56	4.40	32.29	4.40
48.49	7.50	52.25	7.50
58.89	1.72	70.36	1.72
75.98	9.33	82.72	9.33
85.84	1.54	93.10	1.54
97.96	4.21	110.42	4.21
105.04	2.30	129.76	2.30
120.51	3.39	149.45	3.39

Table 6.4 Identified modal parameters for August 12, 2006 earthquake

Shorter Direction		Longer Direction	
Frequency (rad/sec)	**Damping (%)**	**Frequency (rad/sec)**	**Damping (%)**
10.37	3.64	12.22	3.63
31.65	3.18	32.23	1.13
48.43	4.10	52.21	3.04
58.85	9.29	70.22	0.63
75.92	4.55	82.70	1.28
85.67	6.79	93.04	1.35
97.90	2.17	109.89	1.13
105.00	3.83	129.65	2.62
120.40	4.36	149.12	5.05

The identified frequencies in both the directions of the sample building based on accelerations responses corresponding to two recorded earthquakes are found to be agreeing well with each other. Thus, the identification of modal frequencies of an existing building with N4SID based on vibration response data due to two different earthquakes with different PGA has been observed to be quite reliable.

6.2.5 Stability of the Identified System

Stability of the system can be easily observed from poles obtained using Eq. 2.14. The identification algorithm has the capability to transform state space form to poles and zeros with the help of the transfer function as expressed by Eq. 2.13. The poles of the transfer functions have been plotted on the complex plane using the polar coordinates according to Eq. 2.14. Poles within the unit circle in the complex plane refer to the stable dynamic system, while poles outside the unit circle refer to the unstable dynamic system. Plots of poles based on acceleration responses subjected to two selected earthquakes are as shown in Fig. 6.8. It is observed from the Fig. 6.8 that nine numbers of complex conjugate poles marked as 'x' have been found to be lying within the unit circle indicating stable condition of the systems.

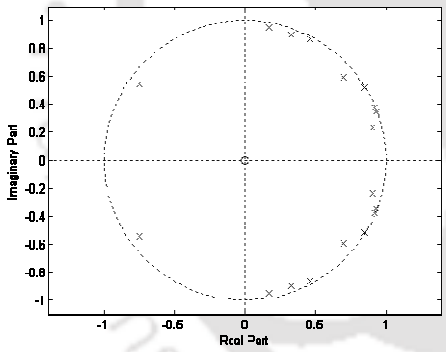

(a) In shorter direction on 11-02-2006

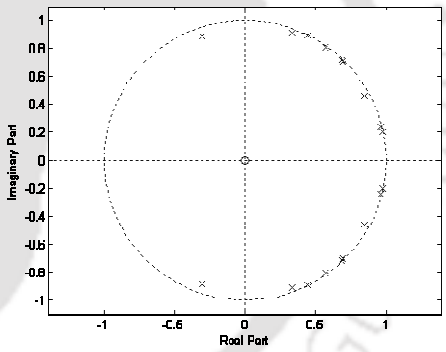

(b) In longer direction on 11-02-2006

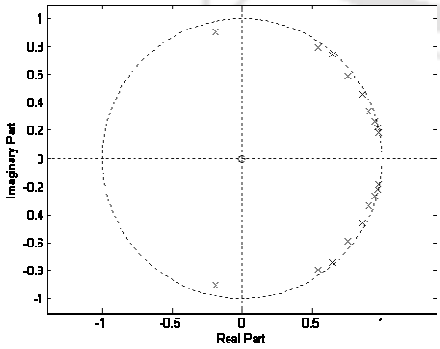

(c) In shorter direction on 12-08-2006

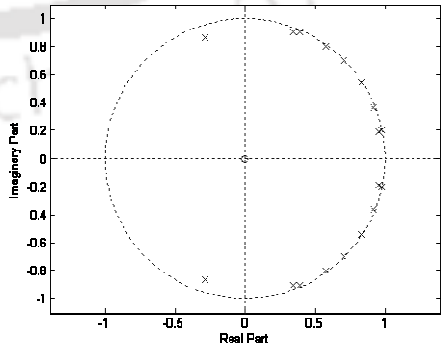

(d) In longer direction on 12-08-2006

Fig. 6.8 Poles for the system based on responses corresponding to two recorded earthquakes

6.2.6 Structural Parameter Identification

Stiffness of a structure can be evaluated using Eq. 2.42 described in Chapter 2 under section 2.4. Mass matrix of lumped floor masses in kg of the sample building is

$$\mathbf{M} = \begin{bmatrix} 511770 & 0 & 0 & 0 & 0 & 0 & 0 & 0 & 0 \\ 0 & 515930 & 0 & 0 & 0 & 0 & 0 & 0 & 0 \\ 0 & 0 & 515580 & 0 & 0 & 0 & 0 & 0 & 0 \\ 0 & 0 & 0 & 515580 & 0 & 0 & 0 & 0 & 0 \\ 0 & 0 & 0 & 0 & 515570 & 0 & 0 & 0 & 0 \\ 0 & 0 & 0 & 0 & 0 & 515570 & 0 & 0 & 0 \\ 0 & 0 & 0 & 0 & 0 & 0 & 515570 & 0 & 0 \\ 0 & 0 & 0 & 0 & 0 & 0 & 0 & 511080 & 0 \\ 0 & 0 & 0 & 0 & 0 & 0 & 0 & 0 & 362710 \end{bmatrix}.$$

The identified modal matrix is incomplete as values of modal displacement are not available at the floor levels where accelerometers have not been installed for recording acceleration histories. Hence, the approach in subsection 2.4.1 under Case-II has been utilized for the evaluation of complete modal matrix. The modal matrix from a numerically simulated model in SAP has been considered as initial values for the iterative analysis. Fig. 6.9 depicts iteratively converged frequency in shorter direction from the identification study based on February 11, 2006 earthquake responses. It can be observed that 50 iterations are sufficient for convergence. The iterative procedure depicted a similar convergence pattern for the study based on August 12, 2006 earthquake responses. The converged modal frequencies along with corresponding identified damping ratios in two directions for earthquake on 11-02-2006 are presented in Table 6.5. Similarly, converged modal frequencies along with corresponding identified damping ratios in two directions for earthquake on 12-08-2006 are presented in Table 6.6. It may be observed that the converged identified frequencies of the building as evaluated based on the measured

ground accelerations as well as floor accelerations on two different dates show very good agreement.

Table 6.5 Converged frequencies for February 11, 2006 earthquake

Shorter Direction		Longer Direction	
Frequency (rad/sec)	**Damping (%)**	**Frequency (rad/sec)**	**Damping (%)**
10.22	2.20	12.75	2.20
29.60	4.40	35.95	4.40
48.00	7.50	59.02	7.50
65.25	1.72	79.90	1.72
80.10	9.33	98.30	9.33
92.65	1.54	113.50	1.54
102.25	4.21	125.25	4.21
108.80	2.30	133.50	2.30
112.70	3.39	138.10	3.39

Table 6.6 Converged frequencies for August 12, 2006 earthquake

Shorter Direction		Longer Direction	
Frequency (rad/sec)	**Damping (%)**	**Frequency (rad/sec)**	**Damping (%)**
10.15	3.64	12.50	3.63
29.80	3.18	35.70	1.13
48.25	4.10	58.85	3.04
65.55	9.29	79.90	0.63
80.60	4.55	98.35	1.28
93.20	6.79	112.45	1.35
102.80	2.17	123.80	1.13
109.40	3.83	131.80	2.62
113.35	4.36	136.25	5.05

It may be observed from Fig. 6.9 that for the study with limited sensors, some of the converged identified frequencies are somewhat different than their respective initially identified frequencies. A similar trend has been noticed for the identified modal frequencies based on structural responses for both the considered earthquakes acceleration histories. Hence, it is worth noting that an iterative approach is mandatory for more accurate identification of eigen pairs for buildings with limited sensors.

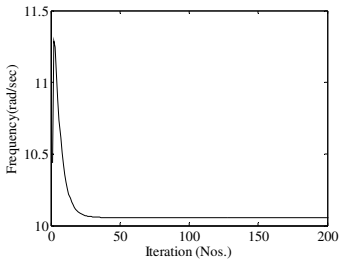

(a) First mode

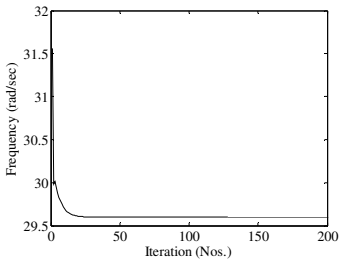

(b) Second mode

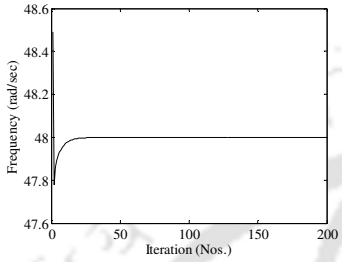

(c) Third mode

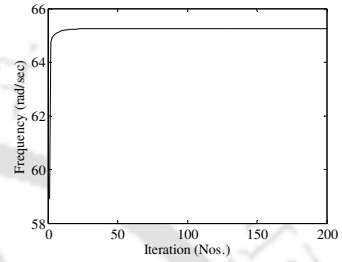

(d) Fourth mode

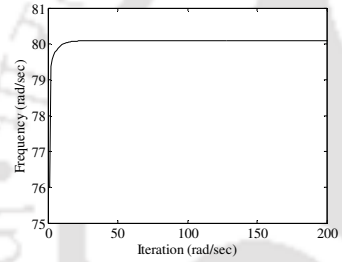

(e) Fifth mode

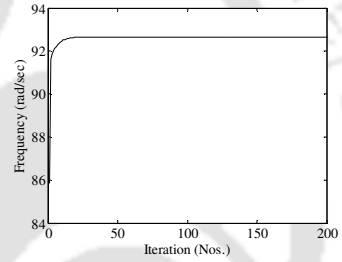

(f) Sixth mode

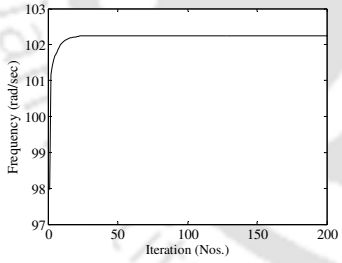

(g) Seventh mode

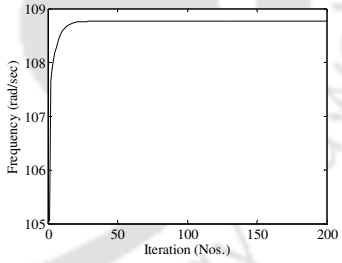

(h) Eighth mode

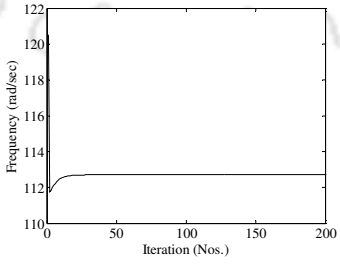

(i) Ninth mode

Fig. 6.9 Converged frequency in shorter direction corresponding to different mode shapes of the building for February 11, 2006 earthquake

An incomplete modal matrix is initially obtained from the identification study as the response data have been measured only at some selected floor levels. However, with the introduction of iterative procedure, a complete modal matrix is obtained at the end of convergence, which is considered as the modal matrix of the building under study. The converged normalized mode shapes along both the directions have been plotted for nine modes of the nine storey shear building and are as shown in Fig. 6.10 and 6.11.

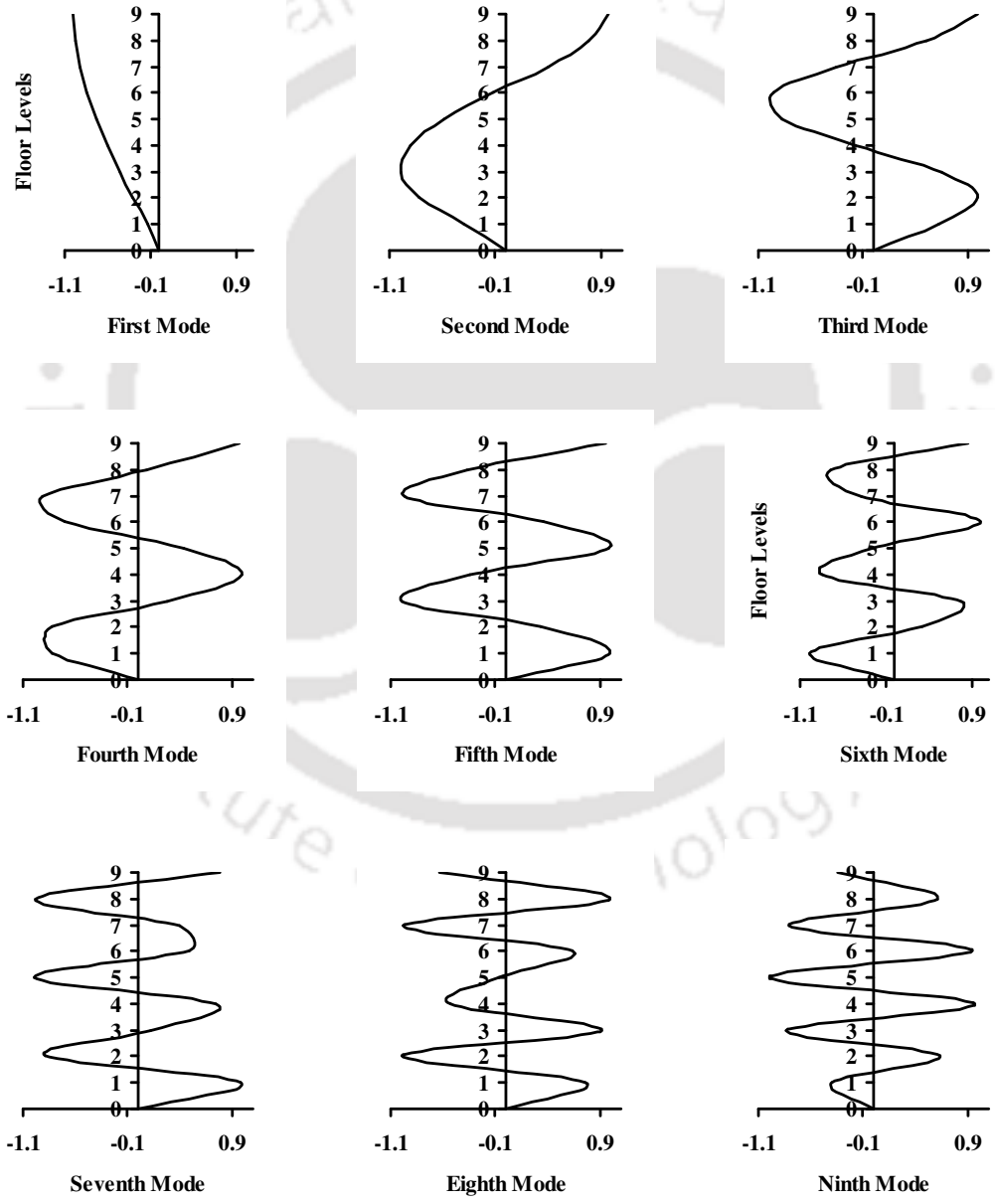

Fig. 6.10 Mode shapes along shorter direction of the building

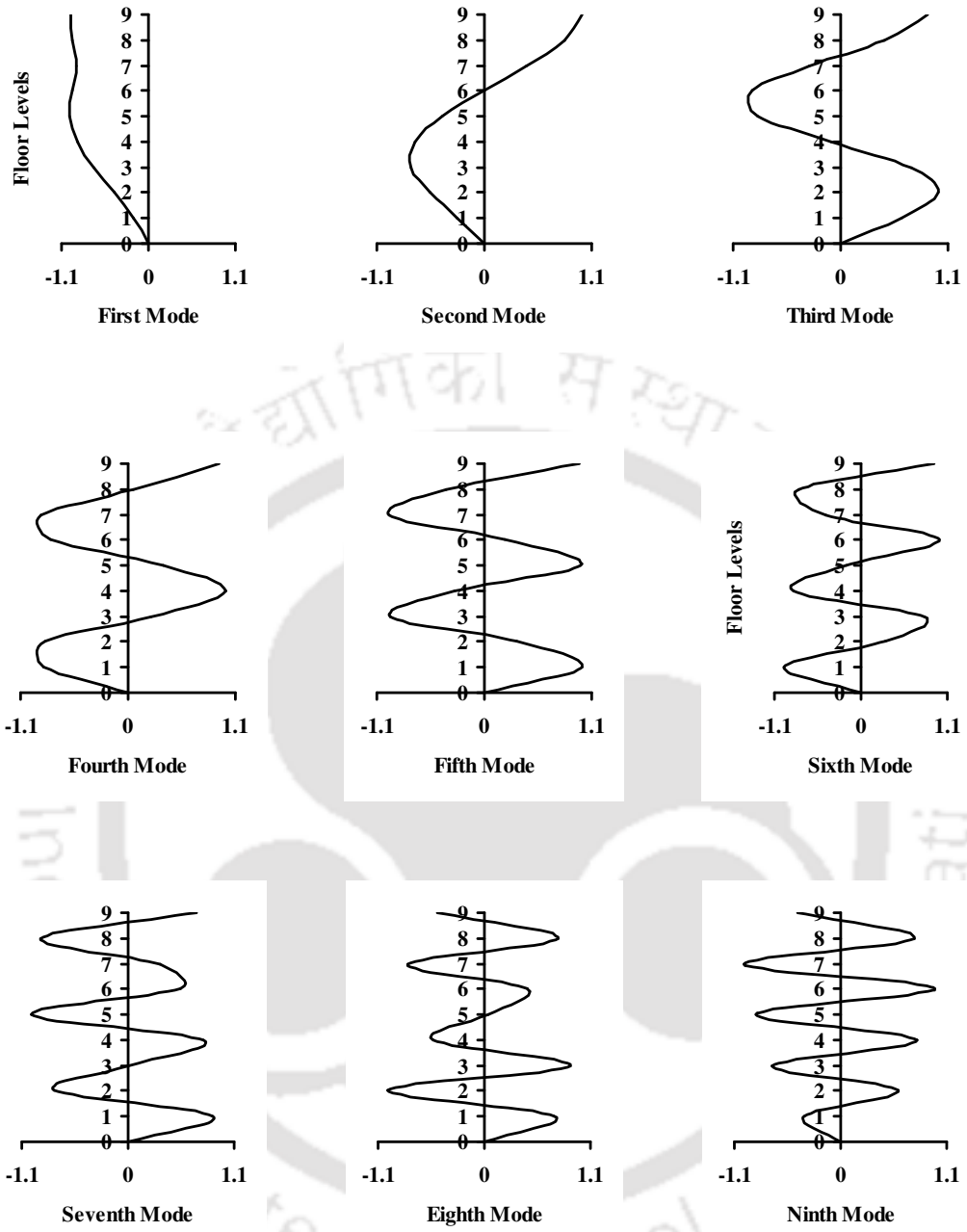

Fig. 6.11 Mode shapes along longer direction of the building

The identified storey stiffness as obtained after the convergence of the iterative procedure corresponding to both the earthquakes are presented in Table 6.7. The converged storey stiffness indicates that the stiffness of the building along the shorter direction is lesser than those along the longer direction of the building. Further, the stiffness of ground floor in

both the directions have been observed to be higher than the corresponding stiffnesses of the floors above, which indicates that though the building is vertically irregular, does not exhibit any soft storey effect in either of the directions. The reduced ground floor height has primarily compensated for the absence of infill wall in the ground floor. It has also been observed from Table 6.7 that the stiffness values of all the floors along each of the two directions are more or less similar and hence it can be inferred that the structure has not deteriorated after experiencing these two earthquakes.

Table 6.7 Identified storey wise stiffness of the sample building for earthquakes data on two different dates

Storey	Stiffness in 10^8 N/m			
	February 11, 2006		August 12, 2006	
	Shorter	Longer	Shorter	Longer
Ground	21.64	32.60	21.94	31.31
First	16.71	25.09	16.90	24.10
Second	16.70	25.12	16.89	24.13
Third	16.72	25.09	16.91	24.10
Fourth	16.71	25.10	16.91	24.11
Fifth	16.73	25.09	16.92	24.10
Sixth	16.70	25.10	16.90	24.10
Seventh	16.70	25.11	16.89	24.12
Eighth	16.71	25.10	16.90	24.11

6.3 NUMERICALLY SIMULATED MODEL OF THE SAMPLE MULTI-STOREY BUILDING

A numerical model of the building has been simulated using SAP 2000 Nonlinear (version 12). Few modal frequencies corresponding to mode shapes in two horizontal directions of the numerically simulated model have been compared with identified frequencies of the existing building. Parametric studies have been conducted using the numerical model to study the adequacy of the limited number of sensor data used for the identification of system parameters.

6.3.1 Description of the Model

3-D finite element model of the sample building as described in the section 6.2.1 developed using SAP 2000 Non-linear (version 12) is shown in Fig. 6.12.

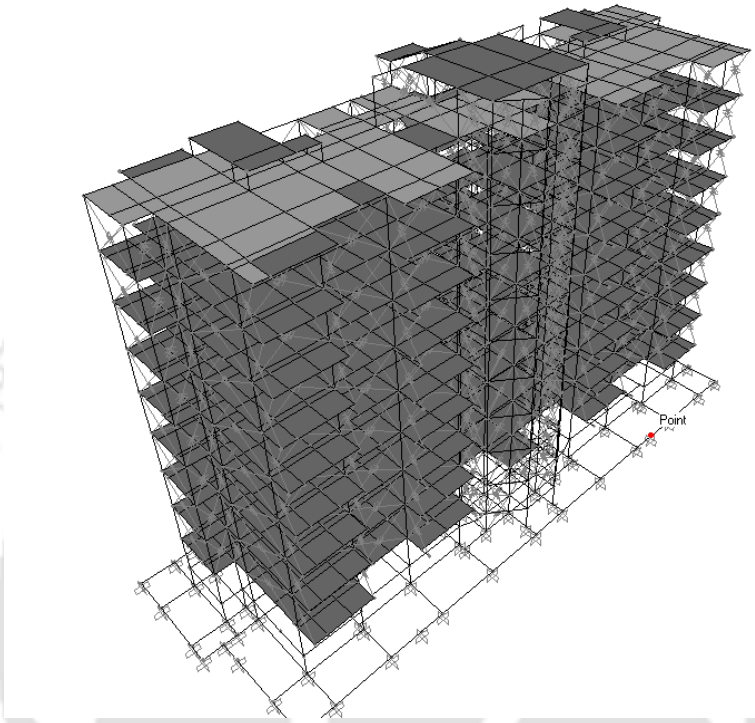

Fig. 6.12 3-D finite element model

The structural geometry of the model has been considered as shown in Fig. A - 3. The material properties have been considered as mentioned in Table A - 3. The building is a residential building and hence masonry infill walls are available on every floor of the building except ground floor. The walls have been modeled as compression strut using GAP element and the stiffness of the strut has been evaluated as per Eq. 5.2-5.4 by considering twenty percent wall opening. The model has been used for modal and time history analysis with the recorded ground accelerations as input.

6.3.2 Modal Analysis of the Numerical Model

Modal analysis of the simulated model has been carried out for evaluating modal frequencies. A proportional damping of 5% has been considered for modal analysis. Table 6.8 shows a few initial natural frequencies along both the horizontal directions as obtained from the modal analysis. The frequencies from modal analysis have been observed to be lower than the identified frequencies of the existing building as shown in Table 6.5. This may be attributed to the underestimation of material strength of the component members. However, as the variation is not large, modal updating has been carried out by increasing compressive strength of masonry alone. The modal analysis results obtained after modal updating are shown in the second column of Table 6.8. A very good agreement may be observed with the frequencies of the updated model with the identified frequencies and hence further studies have been carried out based on the updated model of the building.

Table 6.8 First few natural frequencies of the numerically simulated building

Initial SAP Model	**Updated SAP Model**
Frequencies in rad/sec for Shorter Direction	
8.27	10.16
25.78	31.69
48.13	57.66
66.62	67.44
Frequencies in rad/sec for Longer Direction	
9.79	12.84
29.89	39.59
52.36	65.84
70.26	72.68

6.3.3 Damage Identification Index

The converged identified mode shapes of the instrumented sample building have been compared with those of updated numerical model with the help of Modal Assurance

Criteria (MAC). The MAC number is defined as matrix of normalized inner product of mode shape vectors and expressed as,

$$MAC = \frac{\left|\sum_{l=1}^{p} \varphi_{l,i}^{a} \varphi_{l,i}^{b}\right|^2}{\left(\sum_{l=1}^{p} \varphi_{l,i}^{a} \varphi_{l,i}^{a}\right)\left(\sum_{l=1}^{p} \varphi_{l,i}^{b} \varphi_{l,i}^{b}\right)} \tag{6.1}$$

where, $\varphi_{l,i}^{a}$ is the modal amplitude at the location l of the i^{th} mode of model a (instrumented sample building), while $\varphi_{l,i}^{b}$ is the modal amplitude at the location l of the i^{th} mode model b (numerical model). The evaluated MAC numbers as shown in the Table 6.9 indicate very good agreement between the identified mode shapes of actual and numerically simulated model.

Table 6.9 Modal Assurance Criteria for nine modes of the BSNL building

Modes	Mode-1	Mode-2	Mode-3	Mode-4	Mode-5	Mode-6	Mode-7	Mode-8	Mode-9
Longer Dir	1.0	1.0	0.99	0.99	0.99	1.0	1.0	0.99	0.99
Shorter Dir	0.99	0.98	0.98	0.99	0.99	0.99	0.98	0.99	0.99

6.3.4 Time history analysis of the Numerical Model

Time history analysis has been carried out with the updated model in two orthogonal directions (longer and shorter) considering 5% proportional damping. High amplitude portions of the ground accelerations in two horizontal directions which were used as input in the subspace identification scheme have been utilized as inputs for the time history analysis. The acceleration responses at all the floor levels of the numerical model in longer and shorter directions have been compared with the corresponding acceleration responses from the existing building. A few sample acceleration responses from the simulated model are shown in Fig. 6.13 and 6.14.

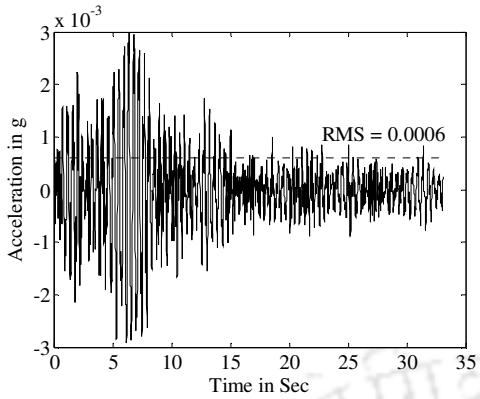

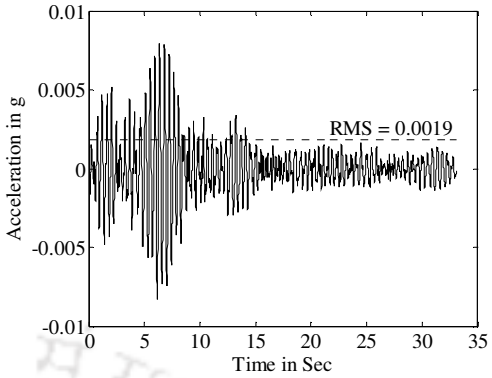

(a) Response at first floor on 11-02-2006 (b) Response at roof floor on 11-02-2006

Fig. 6.13 Acceleration responses at different floor levels along longer direction

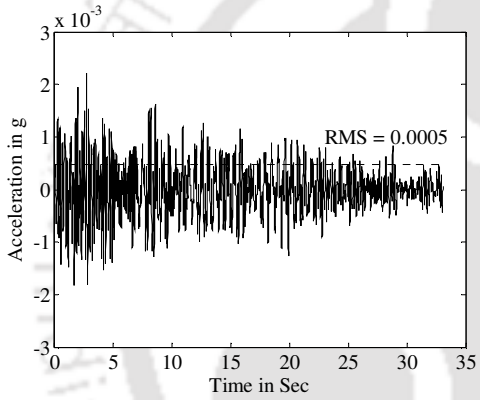

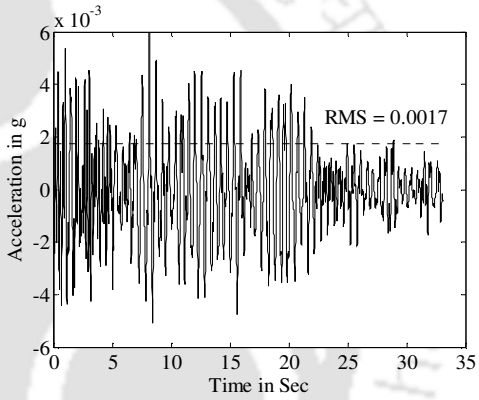

(a) Response at first floor on 11-02-2006 (b) Response at roof floor on 11-02-2006

Fig. 6.14 Acceleration responses at different floor levels in shorter direction

Acceleration histories shown in Fig. 6.13have been compared with the corresponding acceleration histories shown in Fig. 6.4. The comparison shows that the acceleration responses at different floor levels of the simulated building are very much identical with the corresponding acceleration responses of the existing building. Similar observations can be observed from the Fig. 6.14 and Fig. 6.5, which correspond to the acceleration histories at different floor levels for the simulated building and observed acceleration histories of the building for the earthquake input recorded on 11.02.2006. Further, the root-mean-square (RMS) values of amplitudes of acceleration responses at different floor levels of

both the numerical model and actual measured response from the sample buildings corresponding to 11-02-2006 and 12-08-2006 earthquakes in both the directions have been compared and found to be in close agreement. The peak values of floors acceleration responses from the simulated model are also presented in Table 6.10. Comparison of these peak acceleration values with the peaks of corresponding recorded acceleration responses of the existing building (Table 6.2), a very close agreement is observed.

Table 6.10 Peak acceleration values of acceleration responses from the simulated building corresponding to two selected earthquakes

Floors	**Earthquake on 11-02-2006**		**Earthquake on 12-08-2006**	
	Peak acceleration (g)		**Peak acceleration (g)**	
	Longer	**Shorter**	**Longer**	**Shorter**
Ground	0.00211	0.00198	0.00260	0.00303
First	0.00253	0.00209	0.00270	0.00313
Third	-----	0.00291	-----	0.00353
Fifth	0.00586	-----	0.00618	-----
Seventh	-----	0.00467	-----	0.00589
Roof	0.00823	0.00562	0.00871	0.00657

FFTs of some of the acceleration responses from the simulated building are also shown in Fig. 6.15 and 6.16 for comparison with those obtained from the recorded responses. It may be seen that the major frequency contents of all the extracted responses are lower than 20 Hz similar to those of the corresponding recorded responses of the existing building. Thus, in view of all the above-mentioned observations, the numerical model can be considered as appropriate representation of the existing building and further parametric studies have been conducted based on the numerical model.

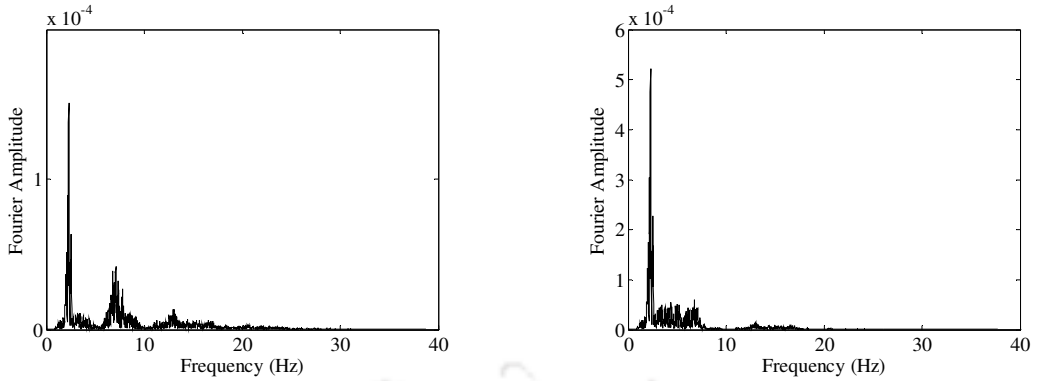

(a) At first floor (c) At roof floor

Fig. 6.15 Fourier amplitude spectra of extracted responses for earthquake on 11-02-2006 in longer direction

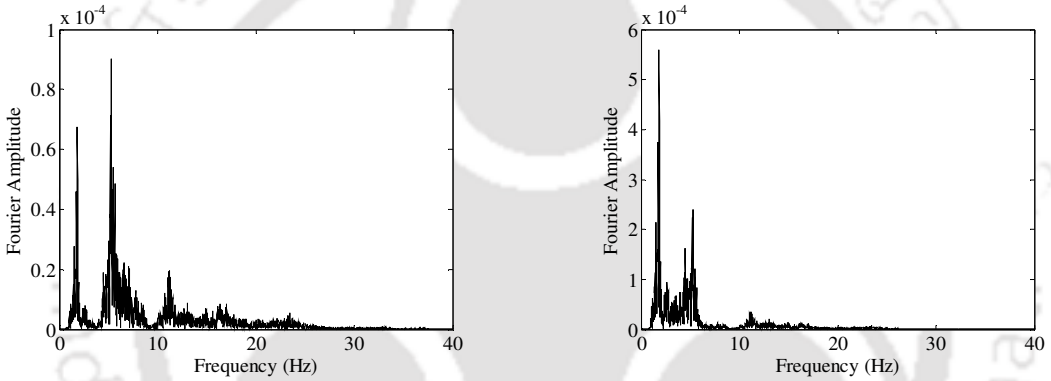

(a) At first floor (c) At roof floor

Fig. 6.16 Fourier amplitude spectra of extracted responses for earthquake on 11-02-2006 in shorter direction

6.3.5 Sensitivity of the Sensor Locations

The instrumentation of large civil structures can only be done with limited number of sensors due to prohibitive expenditure involved in such testing. However, the identification of optimum locations for placement of those sensors and number of sensors required for successful system identification is important. Lam et al. [2004] and Caicedo et al. [2004] carried out system identification of multi-storey buildings using limited number of sensors. Yang et al. [2004] demonstrated system identification with data from a single sensor in evaluating modal parameters of multi-storey building. In this section, the

numerically simulated BSNL building has been considered again for some parametric studies, where various cases of sensor locations and hence availability of extracted responses are considered for the system identification. The changes in identified natural frequencies due to various sensor locations has been utilized and a parameter has been introduced which is indicative of sensitivity of sensor location. Different cases of availability of sensors at different floor levels are shown in Table 6.11.

Table 6.11 Availability of sensors in various floors

Floors	**Case-1**	**Case-2**	**Case-3**	**Case-4**	**Case-5**	**Case-6**	**Case-7**
First	Yes	Yes	Yes	Yes	Yes	Yes	Single sensor in each floor one at a time
Second	Yes	No	No	No	Yes	No	
Third	Yes	Yes	No	No	No	No	
Fourth	Yes	No	Yes	No	No	No	
Fifth	Yes	Yes	Yes	Yes	No	No	
Sixth	Yes	No	No	No	No	No	
Seventh	Yes	Yes	No	No	No	No	
Eighth	Yes	No	No	No	No	No	
Top	Yes	Yes	Yes	Yes	Yes	Yes	

Yes: Accelerometer is installed; No: Accelerometer is not installed.

Thus, for Case-1, accelerometers are assumed to be available in all floors, while other cases refer to sensors at some selected floor levels. The available responses for all the individual cases have been used for identification of modal parameters and the identified results have been compared with those of Case-1. Performance index (*PI*) has been proposed to compare the identified frequencies based on different cases of sensor allocations with those corresponding to Case-1. Thus, the PI for a particular sensor allocation case may be expressed as

$$PI = I_b - I_s \tag{6.2}$$

where I_b is the index for the Case-1, which is taken as equal to 1. I_s is the index for the particular sensor allocation case other than Case-1. Thus, Eq. 6.2 may be written as

$$PI = 1 - I_s \tag{6.3}$$

Further, I_s is expressed as

$$I_s = \frac{\sum_{i=1}^{n} \left| (F_i^b - F_i^a) / F_i^b \right|}{n} \tag{6.4}$$

where F_i^a and F_i^b are the i^{th} identified frequency for a particular case of sensor allocation and the Case-1 respectively. Total number identified frequencies is denoted by n. For the sample building considered in this study, $n = 9$.

The performance indices (PI) for all other cases are presented in Table 6.12.

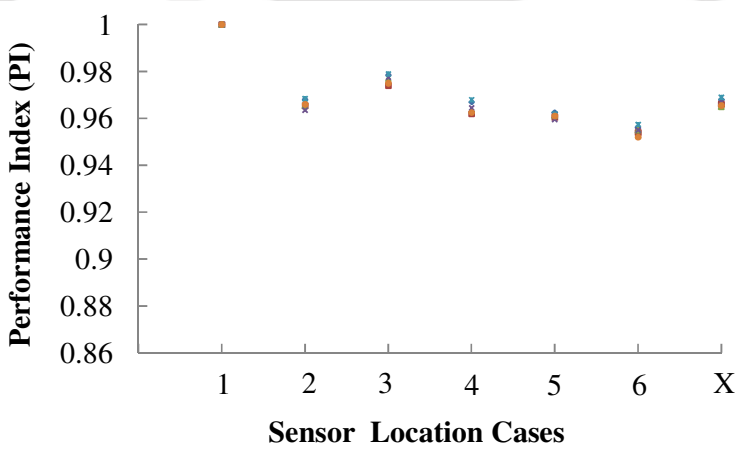

Fig. 6.17 Performance Index for different sensor allocation cases

Thus, PI may be used to visualize the closeness of the results in various sensor allocation cases to the corresponding results obtained form Case-I sensor allocation. Higher the value of the index better is the accuracy of identification. The PIs for various sensor allocation cases corresponding to three different earthquakes are evaluated.

Table 6.12 Performance Index (PI) for different sensor allocation cases

Case-1	Case-2	Case-3	Case-4	Case-5	Case-6
11 Feb, 2006 - shorter direction earthquake component					
1.0000	0.9689	0.9785	0.9670	0.9625	0.9560
11 Feb, 2006 - longer direction earthquake compon**ent**					
1.0000	0.9654	0.9740	0.9620	0.9605	0.9510
12 August, 2006 - shorter direction earthquake component					
1.0000	0.9654	0.9770	0.9635	0.9612	0.9520
12 August, 2006 - longer direction earthquake component					
1.0000	0.9615	0.9775	0.9605	0.9596	0.9505
El Centro (1940) Comp: 180 - in shorter direction					
1.0000	0.9695	0.9790	0.9680	0.9620	0.9575
El Centro (1940) Comp: 180 - in longer direction					
1.0000	0.9660	0.9750	0.9625	0.9610	0.9520

However, it may be noted that the system has been observed to be unstable for all the cases with single output data (Case-7). Hence, the results for Case- 7 have not been considered for further studies.

Fig. 6.17 shows the variation of PI for all the cases against different sensors allocation cases. The sensors allocation case that is actually adopted for the sample building has been designated as *X* and corresponding PIs are also shown in Fig. 6.17. Thus, it may be clearly observed that PIs for all the cases are quite comparable with little decreasing trend from Case-3 towards Case-6 as the number of sensors are reduced. Further, PI corresponding to minimum of two sensors has also been found to be quite acceptable. The PI corresponding to the number of sensors actually installed in the sample building (Case – X) indicates a very good performance.

6.4 CONCLUDING REMARKS

The Parametric State Space modeling has been utilized for the identification of modal parameters and system stiffness of an existing multi storey symmetric-plan shear building.

The studies have been carried out for two different earthquakes experienced by the sample building. A very consistent estimation of the modal parameters and structural stiffness have been made for an existing building, which has been instrumented with a limited number of sensors. The iterative approach adopted for the identification of complete modal matrix and stiffness of the system for the case with limited sensors has been observed to be very effective. A numerically simulated model of the multi-storey sample building has also been made, where the correlations proposed in Chapter 5 for representing wall stiffness and influence of wall openings have been adopted to model the infill walls using gap element. The converged identified eigen pairs have matched very well with those obtained from the numerically simulated model. However, it has been noted that the identified frequencies for the limited sensor case have changed significantly during the process of iteration and may be erroneous by a substantial margin, if the iterative approach is not adopted. The simulated model has been utilized for studying the adequacy of limited number of sensors placed in the building.

Thus, the following conclusions may be drawn based on the studies in this chapter:

- Parametric state space identification along with the iterative approach is directly useful for the health monitoring purpose of existing structures subjected to earthquake excitation and instrumented with limited number of sensors at a few pre-selected locations.
- Sensors at some selected floor levels of a multi storey symmetric-plan shear building are observed to be quite sufficient to accurately identify the system parameters.
- Proposed expressions representing stiffness of infill wall and influence of openings in infill wall are found to be suitable to model infill wall in numerically simulated models.

CHAPTER 7

IDENTIFICATION OF SYSTEM PARAMETERS OF TORSIONALLY COUPLED SHEAR BUILDING

7.1 INTRODUCTION

Most of the available literatures on identification of system parameters of multi-storey buildings are for planar frame systems, while a few works on system identification exist where modal parameters have been evaluated in two translational and one rotational direction separately. It is well understood that in the case of torsionally coupled building, disregard of torsional vibration may cause underestimation of structural response. Thus, it is important that the torsional parameters are also identified along with components in transverse directions. Literatures involving identification of system parameters of asymmetric building are really limited. The Ibrahim Time Domain (ITD) technique of system identification was first demonstrated by Ibrahim [1981] by identifying few modal parameters of an isotropic plate of uniform thickness. Ueng *et al*. [2000] identified frequencies and damping ratios of numerically developed model of a torsionally coupled multi-storey building through ITD identification procedure.

In this chapter, identification of system parameters of an existing torsionally coupled building has been attempted. However, verification of the identification procedure has initially been carried out on a scaled steel frame laboratory test model before applying the same for identification of modal parameters of the existing building. Further, the system parameters of the test model have also been evaluated through parametric subspace identification technique N4SID for verification purpose.

7.2 VERIFICATION OF IBRAHIM TIME DOMAIN TECHNIQUE THROUGH STUDY ON LABORATORY TEST MODEL

Review of available literatures revealed that ITD technique has so far been used for identification of modal parameters of numerically simulated asymmetric building models. Hence, experimental studies on a scaled laboratory test model of building have initially been carried out for assessing applicability of the method for identification of building system. The strategy has subsequently been applied for identification of modal parameters of an existing asymmetric building.

7.2.1 Description of Scaled Laboratory Test Model

A 1/5th scale steel frame building model as shown in Fig. 7.1 has been considered for the proposed study. The model is symmetric in plan and elevation. The plan of the test model is as shown in Appendix-A [Fig. A – 2]. The material and structural properties of building model are furnished in the Table 7.1.

Table 7.1 Material properties of the steel scaled building

Property	Columns/Floor beams
Section Type	ISMC 75
C/S Area (cm^2)	8.67
M.I (I_x) (cm^4)	76.0
M.I (I_y) (cm^4)	12.60
Young's Modulus E (x10^5 N/mm^2)	2.00
Mass per Unit Length (Kg/m)	6.80

The floor size of the test model is 2.0 m (2 bays of 1.0 m each) x 1.0 m with 0.66 m storey height. Additional mass for fulfilling requirement of gravity load similitude for the scaled test model has been evaluated on the basis of Table 4.1. The mass of the prototype building has been determined as 48000 kg. The detailed calculations of mass (floor wise) for the prototype building are as shown in Appendix-A [Table A -4]. The total mass of the

scaled test model is 384 kg. The mass required for fulfilling similitude requirement is 1920 kg. Hence, an additional mass of 1536 [= 1920 – 384] kg is required to be uniformly distributed over two floors.

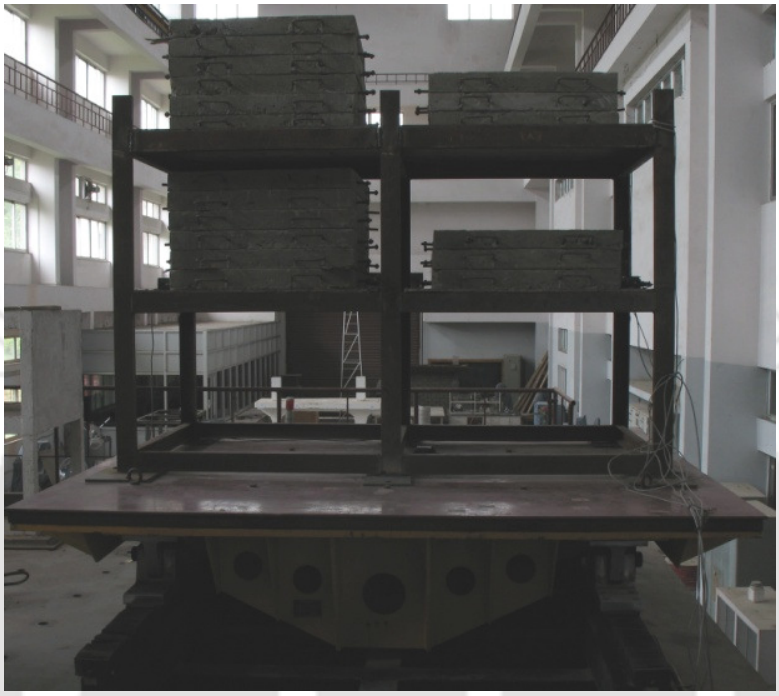

Fig. 7.1 Scaled steel laboratory test model with additional floor mass

Similar to the scaled RC laboratory test models described in the Chapter 4, the scaled steel building model has also been subjected to shake table excitation (Fig. 7.1) for obtaining floor responses to be used in the identification scheme.

7.2.2 Responses of Scaled Steel Frame Test Model

The test model has been excited using time scaled El Cento (1940): Comp – 180 earthquake motion and floor acceleration histories have been recorded. The acceleration responses recorded at first floor of the test model by the accelerometers CH2 and CH3 in the direction of excitation are as shown in Fig. 7.2(a) and 7.2(b) respectively. Similarly,

the acceleration responses recorded at roof floor by the accelerometers CH4 and CH5 at in the direction of excitation are as shown in Fig. 7.3(a) and 7.3(b). High amplitude portion of the recorded floor acceleration histories from both the floors have been processed for obtaining torsional component of the acceleration histories. Initially, the mass corresponding to gravity load similitude requirement have been placed uniformly over both the floors and hence the building model can be considered as symmetric from all respect. The rotational accelerations of the floors have been computed by dividing the difference in instantaneous acceleration values recorded by the two accelerometers along two parallel lines with the distance between the accelerometers. Fig. 7.2(c) and Fig. 7.3(c) show the torsional acceleration histories for first and roof floor respectively. The amplitudes of the torsional responses have been observed to be negligible as compared to those of the amplitudes of recorded accelerations in the direction of excitation. Further, it is well known that the asymmetricity in a building occurs due to irregularities in geometry, sizes of the structural components and non-uniform distribution of floors masses. Hence, in the present study the asymmetricity in the symmetric-plan model has been introduced through non-uniform distribution of floor masses. Test model with unequal floor masses during the shake table test is as shown in Fig. 7.1.

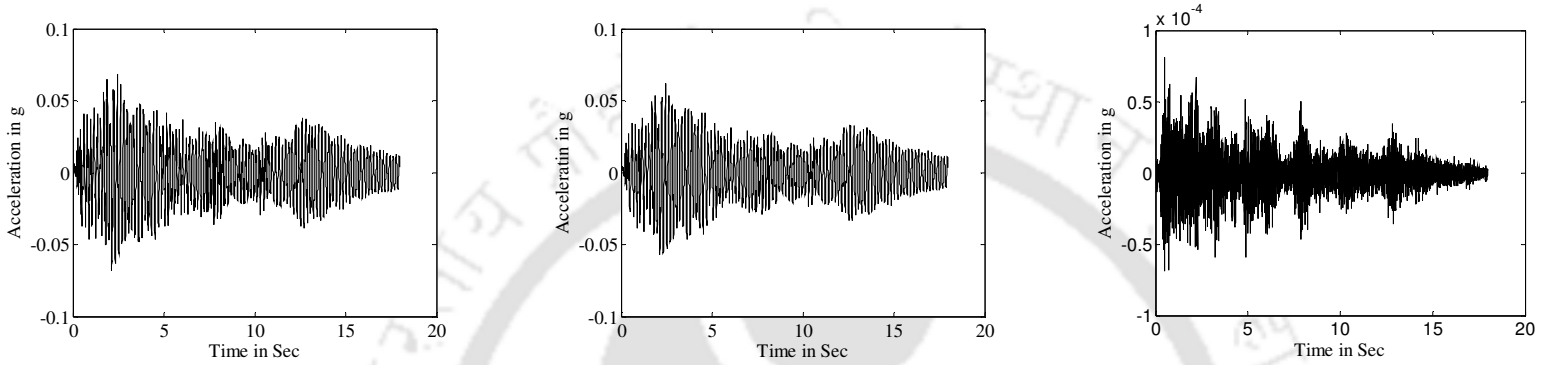

(a) Recorded responses: CH2 (b) Recorded responses: CH3 (c)Torsional response at first floor

Fig. 7.2 Responses at first floor of test model with equal floor masses in all the floor panels

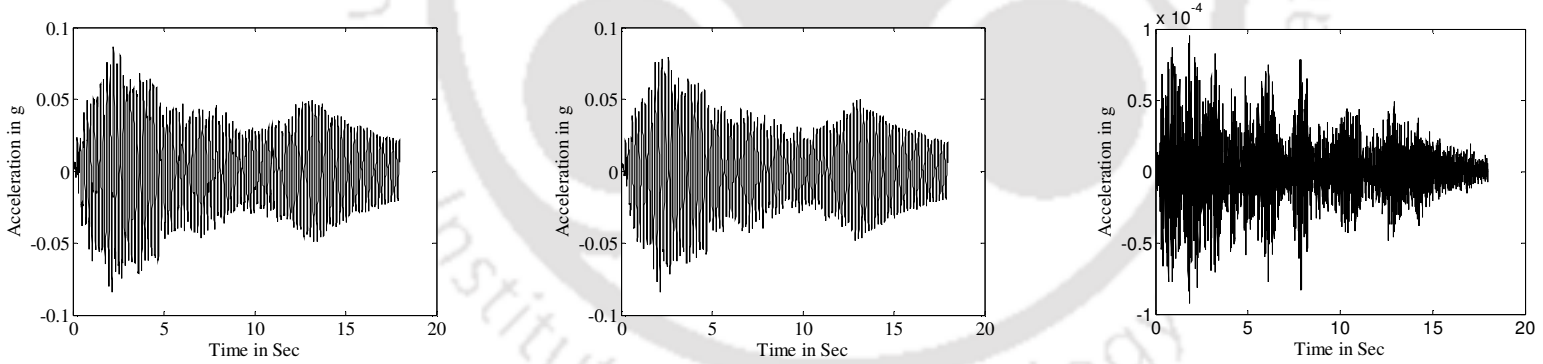

(a) Recorded responses: CH4 (b) Recorded responses: CH5 (c)Torsional response at roof floor

Fig. 7.3 Responses at roof floor of test model with equal floor masses in all the floor panels

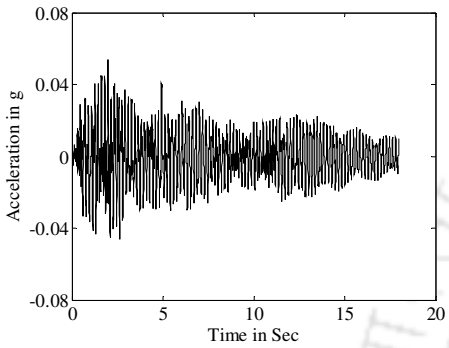

(a) Recorded responses: CH2

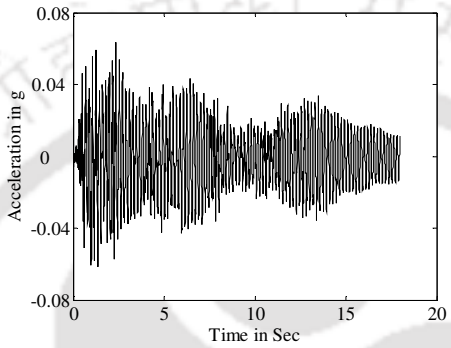

(b) Recorded responses: CH3

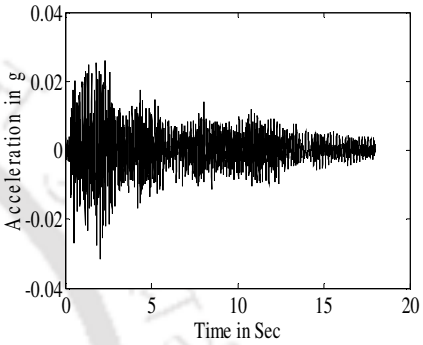

(c)Torsional response at first floor

Fig. 7.4 Responses at first floor of test model with unequal floor masses in all the floor panels

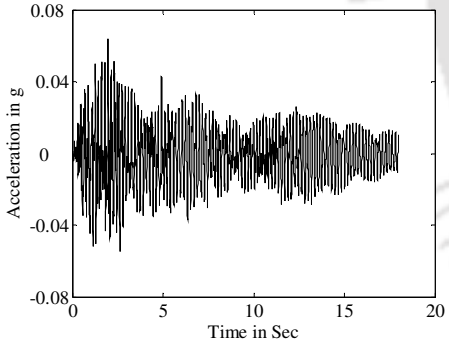

(a) Recorded responses: CH4

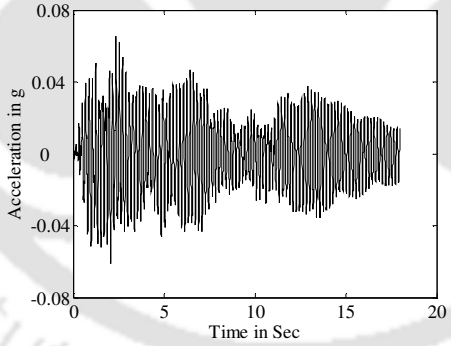

(b) Recorded responses: CH5

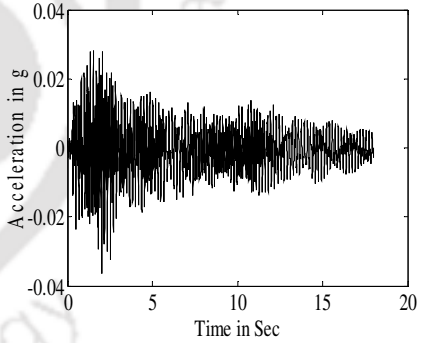

(c)Torsional response at roof floor

Fig. 7.5 Responses at roof floor of test model with unequal floor masses in all the floor panels

The acceleration responses recorded at first floor level [CH2 and CH3] of the building in the direction of excitation are as shown in Fig. 7.4(a) and 7.4(b) respectively. Similarly, the acceleration responses recorded at roof floor level [CH4 and CH5] of the building in the direction of excitation are as shown in Fig. 7.5(a) and 7.5(b) respectively. Computed torsional acceleration history components at first and roof floor levels are shown in Fig. 7.4 (c) and Fig. 7.5 (c) respectively. It is quite evident from Fig. 7.4(c) and 7.5(c) that the amplitudes of the torsional responses are quite comparable with those of the horizontal acceleration responses. Further, the torsional responses as seen from Fig. 7.4(c) and 7.5 (c) are much larger compared to the torsional responses from Fig. 7.2(c) and 7.3 (c). Thus, the existence of torsion due to asymmetricity caused by unequal distribution of floor masses has been ascertained.

7.2.3 Study of Fourier Amplitude Spectra

The FFT plots of the high amplitude portions of all the above mentioned acceleration histories of the test model with unequal floor masses have been plotted to see the frequency contents of the responses. These are as shown in Fig. 7.6 and the range of frequency contents have been estimated for finalizing the different time shifts required for formation of the response matrices of the identification scheme.

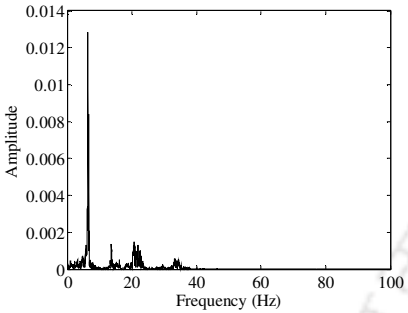

For Acceleration response: CH 2

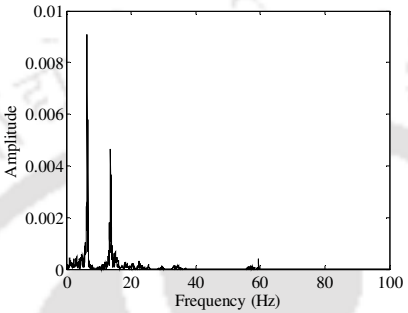

For Acceleration response: CH 3

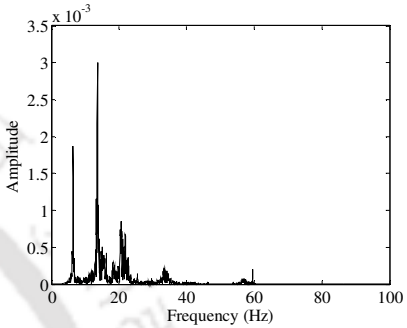

For torsional component

(a) At first floor

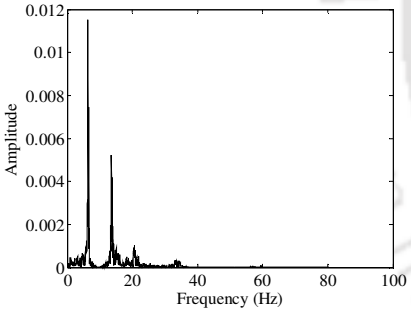

For Acceleration response: CH 4

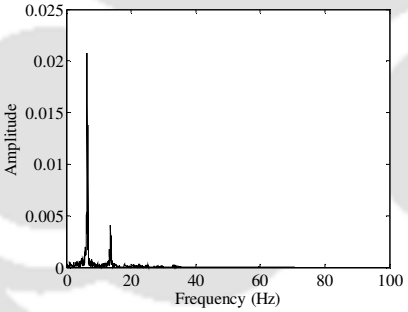

For Acceleration response: CH 5

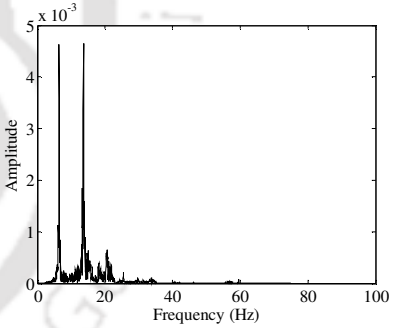

For torsional component

(b) At roof floor

Fig. 7.6 Fourier amplitude spectra of responses at various locations of steel test model with unequal floor masses in all the floor panels

The range of frequency content that dominates responses of the structure has been observed to be 0 to 35 Hz. Hence, the time shift $(\Delta t)_1$ for constructing delayed response matrix may be taken as 0.014 sec [i.e. 1/(2x35)] or less than 0.014 sec. In the present study, this has been considered as 0.010 sec, which is a multiple of sampling rate of 0.005 sec.

7.2.4 Evaluation of Free Decay Signatures of Recorded Responses and Torsional Responses

High amplitude portion of the recorded acceleration history at lowermost floor has been considered for the evaluation of crossing time as it contains greater weight for the higher modes as suggested by Ueng *et al* [2000]. The crossing time has been evaluated following the procedure mentioned in the section 2.3.1 and found to be 0.3268 sec corresponding to the RMS value of 0.0159 g. Thereafter, the free decay signature which is also termed as RANDOMDEC signature has been determined using the same crossing time through RANDOMDEC method. Acceleration histories recorded at first floor level [CH2] and roof floor level [CH4] and computed torsional acceleration responses at first and roof floors have been considered for extraction of free decay responses. Extended RANDOMDEC method has been adopted to obtain RANDOMDEC signatures of these acceleration time histories and are shown in Fig. 7.7.

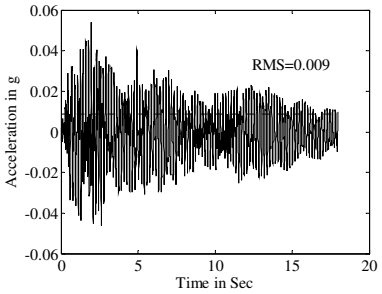

(a) Acceleration time histories: CH 2

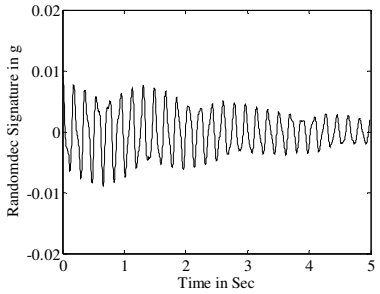

(b) Free decay response: CH 2

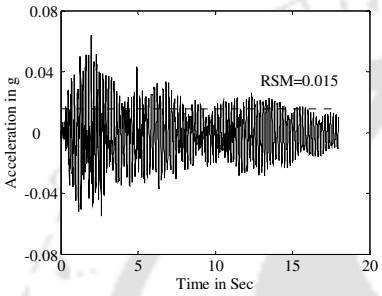

(c) Acceleration time histories: CH 4

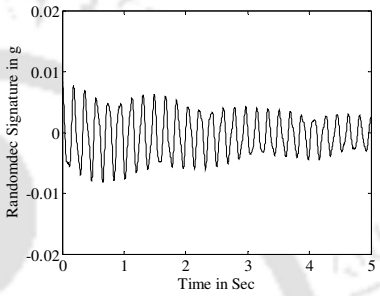

(d) Free decay response: CH 4

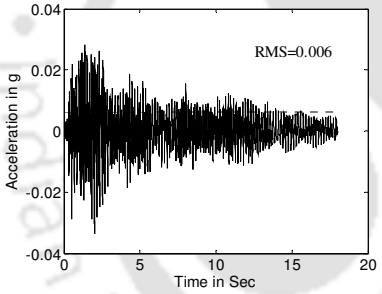

(e) First floor torsional response

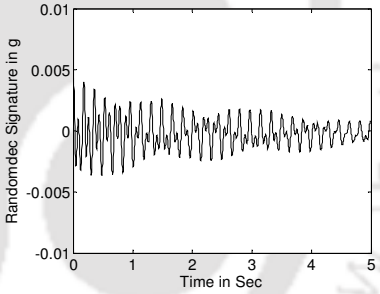

(f) Free decay response: torsion at first floor

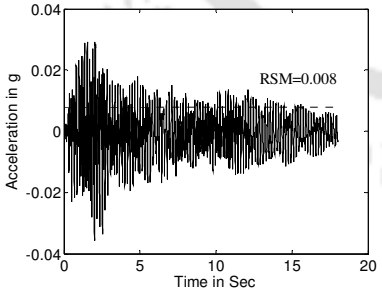

(g) Roof floor torsional response

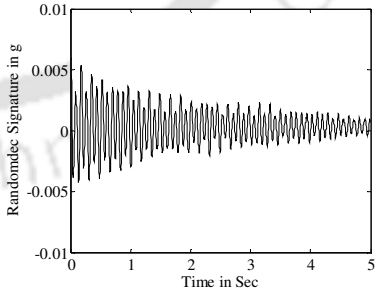

(h) Free decay response: torsion at first floor

Fig. 7.7 Acceleration histories and their free decay signatures at different locations of test model subjected to El Centro (1940): Comp – 180 earthquake excitation

7.2.5 Identification of Modal Parameters of Laboratory Test Model

Most of the FFT plots presented in Fig. 7.6 give preliminary idea of predominant frequency contents in the acceleration time histories. It has been proposed to identify four natural frequencies of the test model based on four extracted free decay responses. The first half of the original response matrix $[\Phi]$ has been filled with four unshifted free decay responses and the lower half of the matrix has been filled with transformed responses considering a time shift $(\Delta t)_3$ of 0.005 second (which is less than $(\Delta t)_1$ =0.010 second). The delayed response matrix $[\hat{\Phi}]$ has elements from transformed responses with time shift of 0.010 second $[(\Delta t)_1]$ having equal length as that of responses of $[\Phi]$. The system matrix, *A* for the test model has been evaluated through eigen solution using matlab command and modal parameters have been identified. The identified modal parameters are shown in Table 7.2.

Table 7.2 Identified modal parameters of scaled building model subjected El Centro (1940): Comp-180 earthquake

Modes	Frequencies (rad/sec)	Damping Ratios (%)
1 (Transverse)	39.54	1.00
2 (Torsion)	69.10	0.46
3 (Transverse)	103.28	0.16
4 (Torsion)	158.70	0.10

7.2.6 Mode Shapes

The eigenvectors are derived from the system matrix as evaluated in section 7.2.5. The normal modes corresponding to the identified complex modes have been evaluated by following Eq. 2.18 to Eq. 2.21. Negligible modal displacements have been observed in the longer direction (perpendicular to the direction of excitation). Typical mode shapes of the test model corresponding to identified frequencies are as shown in Fig. 7.8.

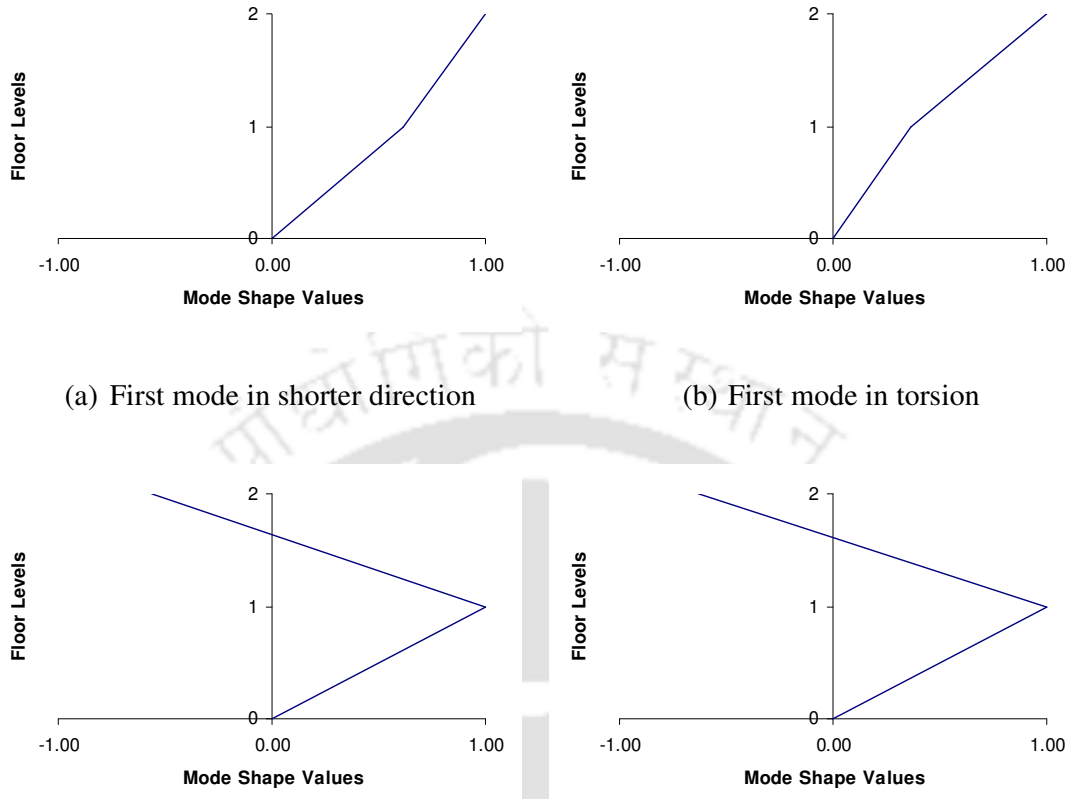

(a) First mode in shorter direction (b) First mode in torsion

(c) Second mode in shorter direction (d) Second mode in torsion

Fig. 7.8 Identified normalized mode shapes of test model

7.2.7 Identification of Structural Parameters of Laboratory Test Model

Characteristic equation [Eq. 2.47] has been solved by least squares technique for the evaluation of stiffness of a structure as mentioned in section 2.4 under Chapter 2. The evaluation of stiffness has been carried out corresponding to the mass matrix and identified modal displacement using Eq. 2.50. Submatrices of floor lumped masses (10^3 kg) of the test model have been estimated by considering all the components including additional mass for gravity load similitude. The mass matrix of the asymmetric building includes the mass moment of inertia (10^3 kg. m^2) about centre of masses. Thus, the floor wise mass submatrices of the two storey asymmetric shear building model are obtained as:

$$M_1 = \begin{bmatrix} 1170 & 0 & 0 \\ 0 & 1155 & 0 \\ 0 & 0 & 80.62 \end{bmatrix} \quad \text{and} \quad M_2 = \begin{bmatrix} 1170 & 0 & 0 \\ 0 & 1155 & 0 \\ 0 & 0 & 79.59 \end{bmatrix} \tag{7.1}$$

Identified storey stiffness for test model of torsionally coupled building are presented in Table 7.3.

Table 7.3 Identified storey stiffness of the test model with unequal floor masses

Storey	**In shorter direction** [(10^6) N/m]	**In torsion** [(10^6) N-m]
Ground	5.88	2.90
First	5.88	2.90

7.2.8 Modal Parameters Identification of Test Model using N4SID

The studies on the scaled steel test model have been further supplemented by considering the same model with symmetric mass on floor. The test model with equal masses on all the floor panels has been excited using El Centro (1940): Comp – 180 earthquake motion and floor responses have been recorded. The recorded acceleration time histories have been utilized for identification of modal parameters using N4SID algorithm. The identified modal parameters have subsequently utilized for creating a numerical model of the test model for further studies.

In this study, the structural responses from the sensors CH2 and CH4, which were installed in the same vertical line, have been used as outputs and response from the sensor CH1 have been used as input for identification of modal parameters. The acceleration time histories have been appropriately polished and filtered before applying for modal parameters identification. The order of the state space equation has been considered as four for identification of two modal parameters corresponding to two mode shapes of two storey shear building. The identified results using N4SID are shown in Table 7.4.

Table 7.4 Identified modal frequency of the test model using N4SID

Frequencies (rad/sec)	Damping Ratios (%)
38.35	1.05
114.82	0.92

7.2.9 Studies on Numerically Simulated Model of the Test Model

A 3-D finite element model of the test specimen with equal floor loads has been developed in SAP 2000Nonlinear. The material properties considered for creating the numerical model have been furnished in the Table 7.1. Modal analysis of the building model with equal floor masses has been carried out considering 2% proportional damping for all the modes and first two natural frequencies along the shorter direction are presented in Table 7.5.

Table 7.5 Frequencies in shorter direction of numerical model

Modes	Frequency (rad/sec)
First	38.25
Second	110.00

The extracted modal frequencies are compared with the identified frequencies of the test model (Table 7.4). The comparison shows very a good agreement between identified and computed results. Hence, the same numerically developed model has been considered for further studies.

The same numerical model with unequal floor masses in different floor panels has also been considered for modal and time history analyses with the same input as that of experimental studies. The evaluated modal frequencies are presented in Table 7.6.

Table 7.6 Frequencies of numerical model

Modes	Modal Frequency (rad/sec)
1 (Transverse)	40.10
2 (Torsion)	70.02
3 (Transverse)	104.21
4 (Torsion)	161.43

The acceleration responses of the numerical model from different floors have been compared with those from laboratory test model. Table 7.7 shows the values of peak floor acceleration for both the test models and the corresponding numerically simulated model. It may be observed that the peak accelerations at different floor levels are agreeing very well. Further, comparison of RMS values as observed from Fig. 7.7 with those from Fig. 7.9 also show a very good agreement between laboratory test models and their corresponding numerical models.

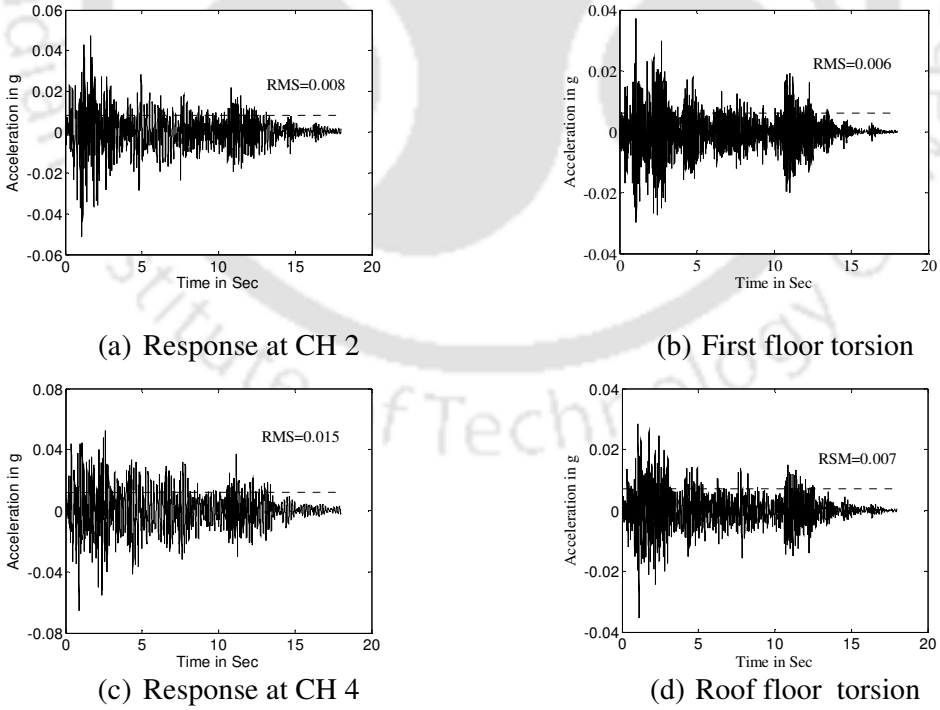

(a) Response at CH 2 (b) First floor torsion

(c) Response at CH 4 (d) Roof floor torsion

Fig. 7.9 Responses of numerically simulated model

Table 7.7 Peak floor accelerations of different models for El Centro (1940): Comp - 180 earthquake motion

Types of Reponses	Peak floor accelerations (g)					
	Sensors at first floor			Sensors at roof floor		
	CH 2	CH3	Torsion	CH 4	CH5	Torsion
Experimental	0.054	0.063	0.038	0.064	0.066	0.036
Numerical	0.051	0.061	0.039	0.063	0.065	0.035

Thus, the numerical model is considered as adequate representative of the test model as both modal and time history analyses have shown very well conformity in their analysed results with those from experimental studies.

7.3 STUDIES ON AN EXISTING TORSIONALLY COUPLED MULTI-STOREY SHEAR BUILDING

The understanding developed by using the scaled laboratory asymmetric test model for extracting modal parameters has been used for the study of an existing asymmetric multi-storey shear building. Uniaxial and Triaxial accelerometers have been fixed at different floor levels in two horizontal directions and connected to DAS. Acquired data during two earthquakes experienced by the building have been utilized for the identification of modal parameters. ITD technique described in subsection 2.3.2 has been used for identification of modal parameters from the free decay responses of the acquired acceleration histories. In the following subsections, descriptions of the sample building have been presented in detail.

7.3.1 Description of the Building

An asymmetric-plan building situated in IIT Guwahati campus, Assam, India has been considered for identification of system parameters through ITD technique. A photograph of the torsionally coupled building considered for the system identification study is shown in Fig. 7.10. The geometric plan of the building is shown in Appendix - A [Fig. A - 4 to A

- 7]. This building is founded on medium type of soil. Primary beams and columns are aligned at a spacing of 7.2 m in both orthogonal directions, while secondary grids are spaced at 3.6 m. It is having 9 major grid lines and 7 minor grid lines in each direction. Almost all structural elements are lying on grid lines. Plan dimensions of the building are 50.4 m x 50.4 m. The height of basement is 2.9 m, while all other floors are having a height of 4.0 m.

Fig. 7.10 Photograph of the torsionally coupled building

Floor masses as well as material and geometric properties of the building have been collected from the available drawings. All necessary data are furnished in Appendix – A [Table A – 5].

7.3.2 Details of Instrumentation

It has been proposed to acquire structural responses including torsional responses of the existing asymmetric-plan building for identification of system parameters. Hence, the four storey building has been instrumented with accelerometers and data recorder to acquire earthquake responses. Numbers of uniaxial and triaxial accelerometers as mentioned in the section 3.2.1 have been installed for acquiring the responses at different storey levels. Fig. A - 4 to A - 7 in Appendix - A present the positions of accelerometers in different floors of the building. A triaxial accelerometer has been mounted at the ground level to collect the

ground accelerations in three principal orthogonal directions i.e. N-S, E-W and vertical directions. The N-S and E-W axis of the building are termed as X and Y axis respectively. Two uniaxial accelerometers have been mounted in Y direction with a distance of 21.600 m between two sensors and one uniaxial accelerometer has been mounted in X direction of the building at the second floor of the building. At the third floor level, two uniaxial accelerometers have been mounted in X direction with a distance of 14.200 m between two sensors and one uniaxial accelerometer has been mounted in Y direction of the building. At the roof level two uniaxial accelerometers have been mounted in Y direction at distance of 21.600 m and one uni-axial accelerometer has been installed in X direction of the building. The accelerometers have been set to a full scale level of 2g (±1g). All the accelerometers are connected to a DAS (Model: Altus K2; Make: Kinemetrics Inc., USA) through conjunction boxes. The recorder has been set to record earthquake acceleration at every 0.005 sec discrete time interval. Out of 12 available channels in the recorder, 11 channels have been engaged for connection to triaxial and uniaxial accelerometer and details are presented in Table 7.8.

Table 7.8 Sensor placement at different floors of the sample building

Floor	Sensor Assignment		Sensor Type
	X (N-S) Direction	Y (E-W) Direction	
Ground	CH2	CH1	Triaxial
Second	CH10	CH11, CH12	Uniaxial
Third	CH7, CH8	CH9	Uniaxial
Roof	CH5	CH4, CH6	Uniaxial

7.3.3 Recorded Floor Acceleration Histories for Modal Parameters Identification

The building encountered number of earthquakes since installation of the accelerometers and DAS. Accelerations histories have been recorded in two directions of the building through accelerometers and DAS. Floor acceleration time histories recorded during two

earthquakes on 11-02-2006 and 12-08-2006 have been considered for identification of modal parameters. High amplitude portions of acceleration time histories recorded at ground floor level for two events on two different dates are shown in the Fig. 7.11 and Fig. 7.12.

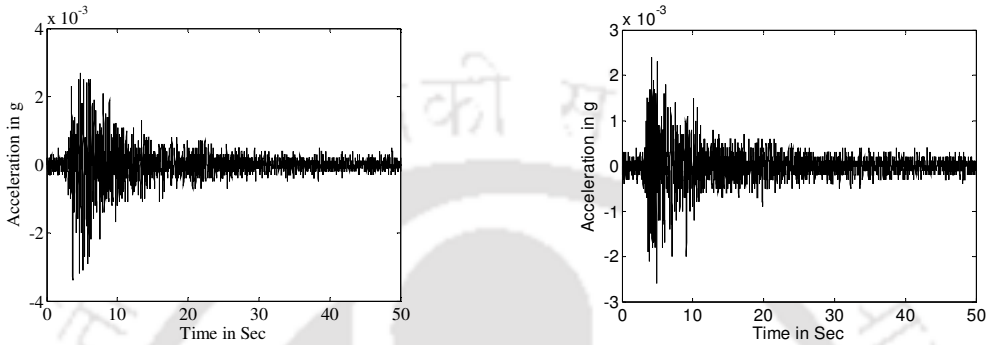

(a) E-W component (a) N-S component

Fig. 7.11 Recorded ground motion during earthquake on 11-02-2006

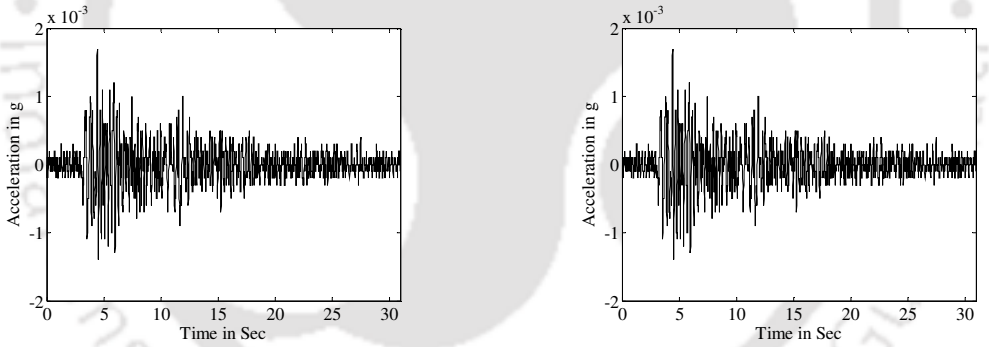

(a) E-W component (b) N-S component

Fig. 7.12 Recorded ground motion during earthquake on 12-08-2006

Acceleration histories during the earthquake on 12-08-2006 recorded by the accelerometers on the same floor level and in the same direction are shown in Fig. 7.13 (a) & (b), Fig. 7.14 (a) & (b) and Fig. 7.15 (a) & (b). The torsional responses of floors have been computed from two measured records in the same direction at a floor level. Computed second, third and roof floor level torsional responses are shown in Fig. 7.13(c), Fig. 7.14(c) and Fig. 7.15(c) respectively.

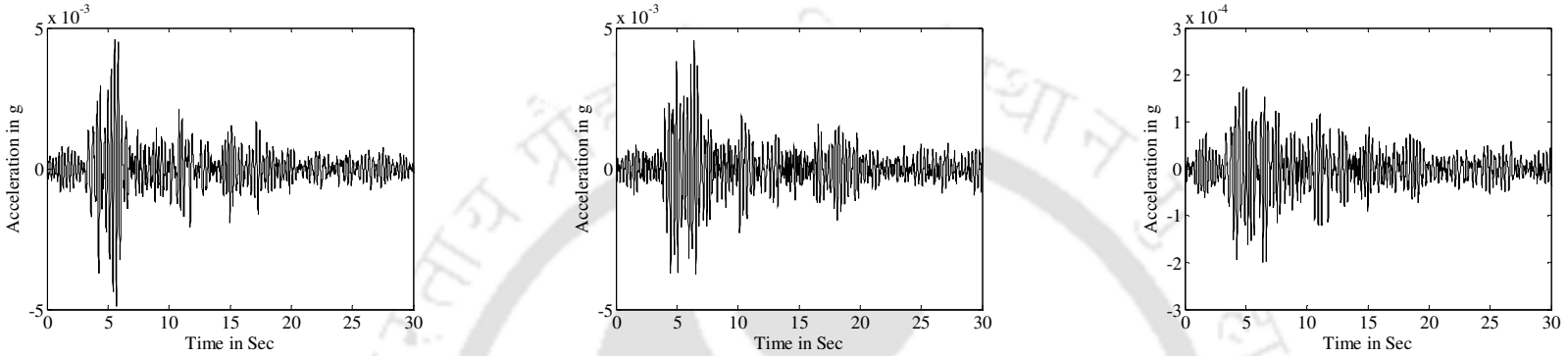

(a) For Acceleration response: CH 11 (b) For Acceleration response: CH 12 (c)For torsional component

Fig. 7.13 Recorded responses at 1st floor in Y direction during earthquake on 12-08-2006

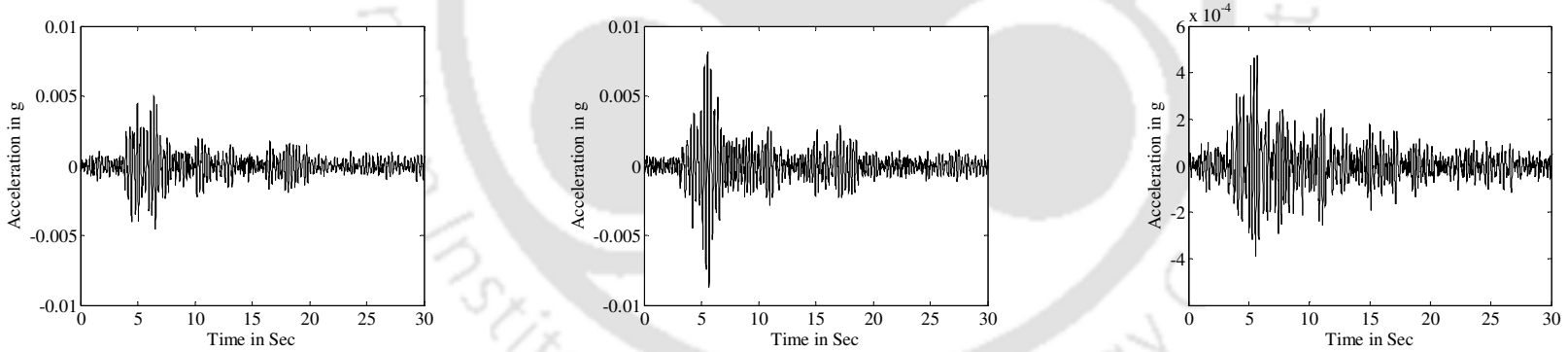

(a) For Acceleration response: CH 7 (b) For Acceleration response: CH 8 (c) For torsional component

Fig. 7.14 Recorded responses at 2nd floor in X direction during earthquake on 12-08-2006

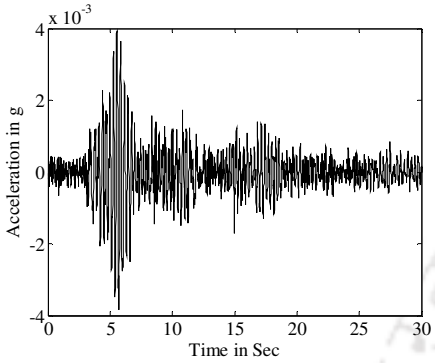

(a) For Acceleration response: Ch 4

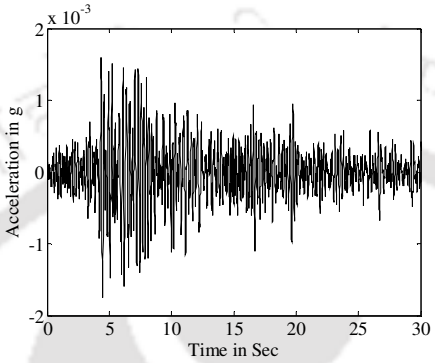

(b) For Acceleration response: CH 6

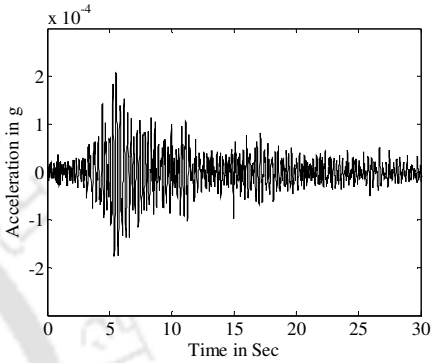

(c) For torsional component

Fig. 7.15 Recorded responses at roof in Y direction during earthquake on 12-08-2006

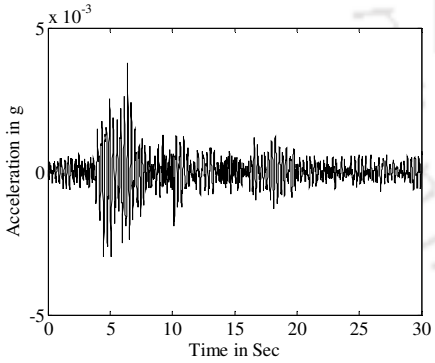

(a)For Acceleration response: CH 5

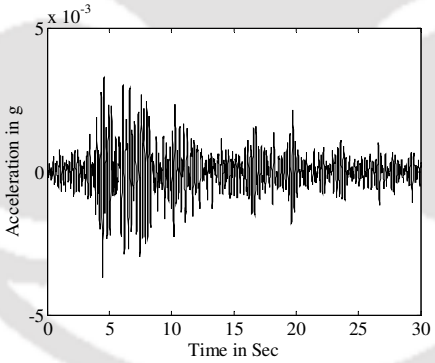

(b) For Acceleration response: CH 9

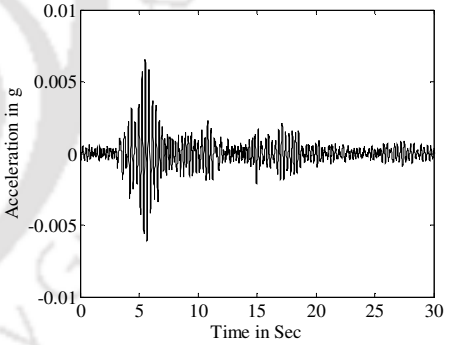

(c)For Acceleration response: CH10

Fig. 7.16 Recorded responses at various floors with single sensor during earthquake on 12-08-2006

7.3.4 Study of Fourier Amplitude Spectra

The FFT plots of high amplitude portions of structural responses have been obtained through FFT of acceleration responses recorded at the second floor and are shown in Fig. 7.17.

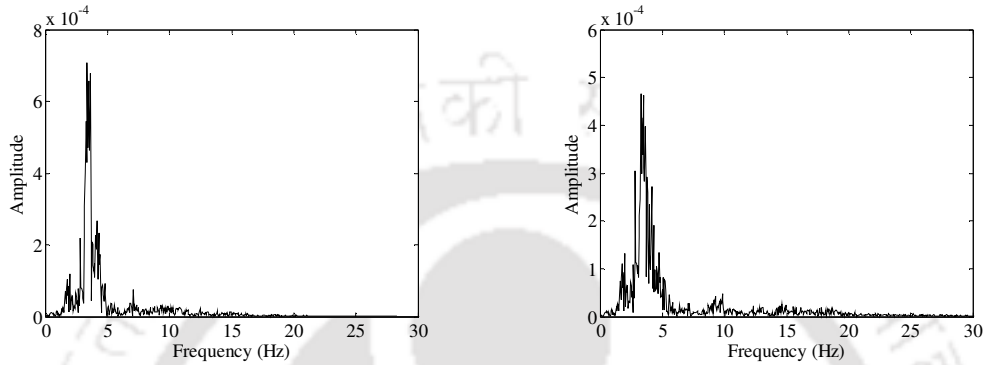

(a) In X-direction a) In Y-direction

Fig. 7.17 Fourier amplitude spectra of responses of second floor for 12.08.2006 earthquake

The range of predominant frequencies has been found to be 0 to 15 Hz. Hence, the time shift $(\Delta t)_1$ for constructing delayed response matrix may be taken as 0.033 sec [i.e. 1/(2x15)] or less than 0.033 sec. In the present study, this has been considered as 0.020 sec, which is a multiple of sampling rate of 0.005 sec.

7.3.5 Evaluation of Free Decay Signatures of Acceleration Responses

The high amplitude part of the recorded acceleration histories have been processed for extracting free decay responses to be used for system identification model. The structural response at second floor (CH11) has been considered as reference and free decay signature has been extracted. The crossing time has been evaluated following the procedure mentioned in the section 2.3.1 and found to be 1.240 sec corresponding to the RMS value of 0.00075 g. The extended RANDOMDEC method has been applied to obtain the free

decay signatures of the other structural responses including the computed rotational responses. These are shown in Fig. 7.18- 7.20.

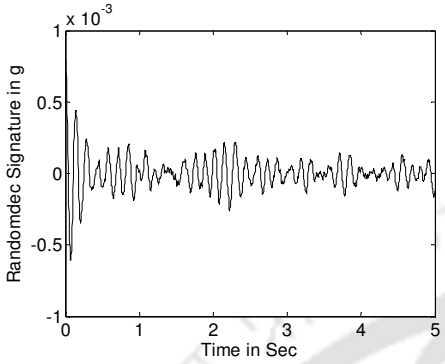

(a) For acceleration histories: CH 11

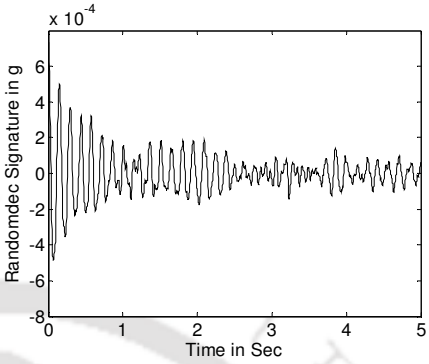

(b) For acceleration histories: CH 12

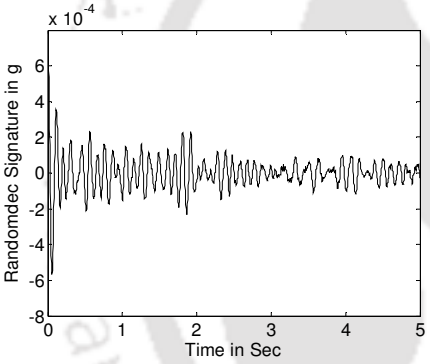

(c) For acceleration histories: CH 9

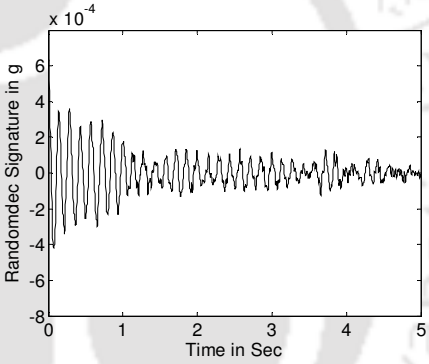

(d) For acceleration histories: CH 6

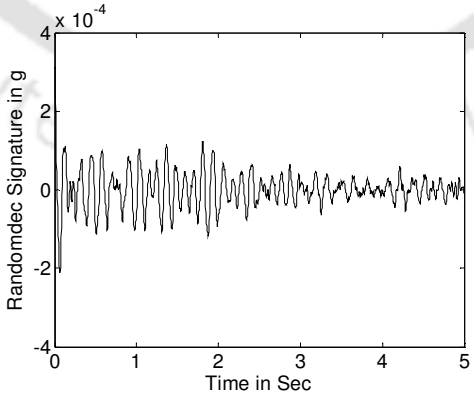

(e) For acceleration histories: CH 4

Fig. 7.18 Free Decay Response in Y Direction for earthquake on 12.08.2006

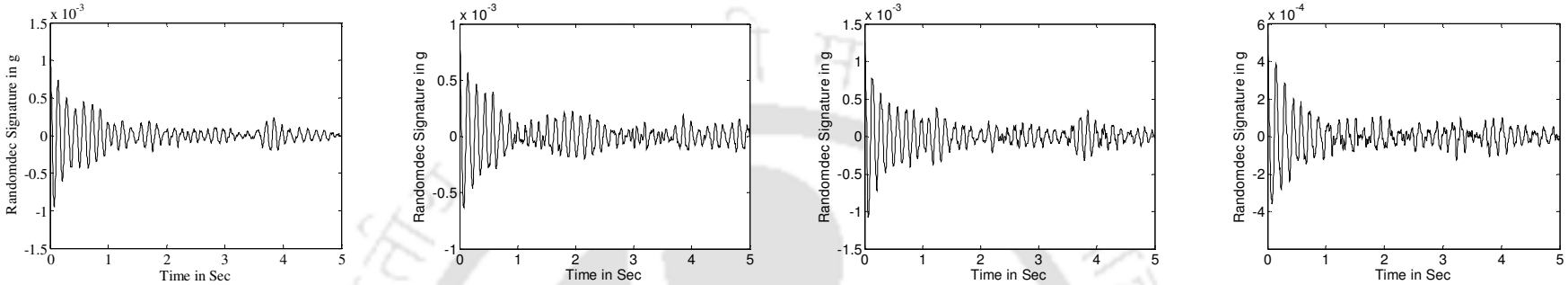

(a)For acceleration histories: CH 10 (b)For acceleration histories: CH 7 (c)For acceleration histories: CH 8 (d)For acceleration histories: CH 5

Fig. 7.19 Free decay responses in X direction for earthquake on 12.08.2006

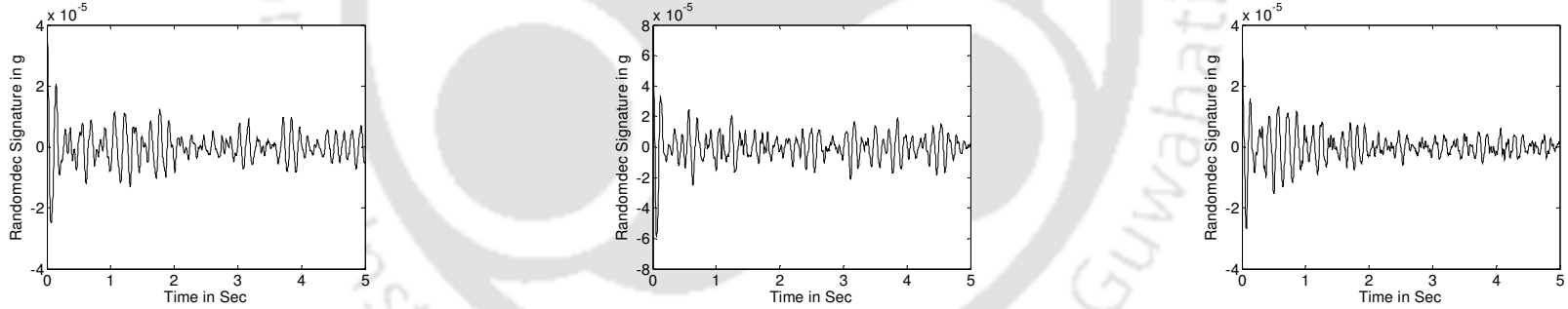

(a) For first floor torsion (b) For third floor torsion (c) For roof floor torsion

Fig. 7.20 Free decay of torsional response for earthquake on 12.08.2006

7.3.6 Identification of Modal Parameters of the Existing Building

It has been intended to identify twelve eigenpairs for this four storey torsionally coupled building. Three RANDOMDEC signatures (one in each of X, Y directions and one in rotation) from each floor levels have been considered for the formulation of original response matrix. The identified modal parameters are shown in the Table 7.9. Thus, nine rows of first half of the response matrix has been filled up by nine original RANDOMDEC signatures and the three rows have been filled up by time shift RANDOMDEC signatures for identification of twelve pairs of modal parameters of the building.

Table 7.9 Identified modal parameters of the torsionally coupled existing building corresponding to two earthquakes

Earthquake on 11.02.2006		**Earthquake on 12.08.2006**	
Frequency (rad/sec)	**Damping (%)**	**Frequency (rad/sec)**	**Damping (%)**
7.65	7.89	7.50	6.23
7.90	8.32	7.81	7.07
11.67	6.68	11.60	6.89
23.95	7.56	23.89	5.35
24.23	7.44	24.45	4.76
31.78	4.67	31.25	5.47
49.76	5.78	49.60	5.38
51.67	2.38	51.71	3.21
74.35	3.33	74.55	3.68
85.59	2.97	85.69	2.87
88.40	3.01	88.32	2.70
94.60	2.85	94.25	2.92

The time shift $(\Delta t)_3$, for obtaining transformed responses to fill up the lower half of the response matrix has been kept as 0.015 second (multiple of 0.005 second which is also less than $(\Delta t)_1$=0.020 second). The time shift $(\Delta t)_2$, which has been used to obtain transformed RANDOMDEC signatures for filling up last three rows of first half of the original response matrix, is 0.030 sec [i.e. 2 x $(\Delta t)_3$]. The delayed response matrix $[\hat{\Phi}]$ has

elements from transformed responses with time shift of 0.020 second [$(\Delta t)_1$] and has equal length as that of responses of $[\Phi]$. The system matrix $\boldsymbol{A}$ for the sample building has been evaluated through eigen solution using matlab command and frequencies and damping ratios have been identified.

7.3.7 Mode Shapes

The eigenvectors are evaluated from the identified system matrix $\boldsymbol{A}$. The eigenvectors identified using ITD method are complex modes. The normal modes corresponding to the identified complex modes have been evaluated by following Eq. 2.18 to 2.21. Typical mode shapes of the sample building corresponding to identified frequencies based on earthquake on 12.08.2006 are as shown in Fig. 7.21.

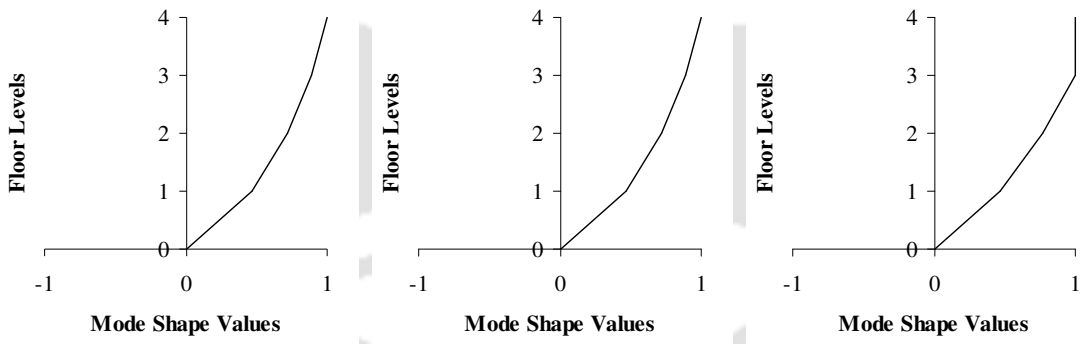

(a) First shorter (b) First longer (c) First torsion

Fig. 7.21 Identified normalized mode shapes of the sample building

7.3.8 Identification of Structural Parameters of the Existing Building

Characteristic equation has been solved by least square technique for the evaluation of stiffness of a structure as mentioned in section 2.5 under Chapter 2. The evaluation of stiffness has been carried out for the known mass matrix as represented by Eq. 2.47 and the identified modal displacement vector using Eq. 2.50. Matrix of floor lumped masses

(10^3 kg) of the sample building has been estimated by considering all the components including infill walls. The mass matrix of the asymmetric building includes the mass moment of inertia (10^3 kg. m^2) about centre of masses. Thus, the floor wise mass matrices of the four storey asymmetric-plan shear building are obtained as:

$$M_2 = \begin{bmatrix} 1057 & 0 & 0 \\ 0 & 1057 & 0 \\ 0 & 0 & 9682.12 \end{bmatrix} \qquad M_2 = \begin{bmatrix} 1010.42 & 0 & 0 \\ 0 & 1010.42 & 0 \\ 0 & 0 & 6729.40 \end{bmatrix}$$

$$M_3 = \begin{bmatrix} 1067 & 0 & 0 \\ 0 & 1067 & 0 \\ 0 & 0 & 5452.40 \end{bmatrix} \qquad M_4 = \begin{bmatrix} 908 & 0 & 0 \\ 0 & 908 & 0 \\ 0 & 0 & 5239.16 \end{bmatrix} \tag{7.2}$$

Identified storey stiffness of the torsionally coupled sample building model are presented in Table 7.10.

Table 7.10 Identified lateral stiffness in (10^8) N/m and torsional stiffness in (10^8) N-m of the sample building corresponding to two earthquakes

Storey	**Earthquake on 11.02.2006**			**Earthquake on 12.08.2006**		
	Shorter	**longer**	**Torsion**	**Shorter**	**longer**	**Torsion**
Ground	34.60	34.72	2420.23	34.67	34.77	2421.07
First	14.45	14.52	545.40	14.61	14.72	546.55
Second	14.46	14.59	340.60	14.63	14.73	340.40
Third	11.50	11.62	349.42	11.57	11.66	349.33

7.4 CONCLUDING REMARKS

The ITD technique, which uses multi-directional acceleration histories, has been observed to be very effective for the evaluation of modal parameters of torsionally coupled multi-storey building. The method uses response matrices of free decay signatures of acceleration time histories. The method has been observed to be simple and fast

converging. Oversize mathematical model can be formulated using few available recorded acceleration responses with time shifting technique.

The identified modal frequencies of the test model are quite close to the modal frequencies of the corresponding numerically simulated model of the test model. The identified system parameters of the existing building for both the earthquake excitations are close to each other.

CHAPTER 8

SUMMARY AND CONCLUSIONS

8.1 SUMMARY

Assessment of modal parameters using system identification has been gaining popularity among researchers as observed from detailed literature survey. The work presented in this dissertation uses two available system identification techniques. These techniques have been used by researchers mostly for identification of some numerically simulated models. However, in the present work, these two identification techniques have been applied for identification of modal parameters of two existing multi-storey buildings. One of the buildings considered is a symmetric-plan shear building, while the other building is an asymmetric-plan shear building. Laboratory based experimental studies have also been conducted on scaled models prior to the application of these techniques to existing buildings for better understanding of the applicability of these methods.

A parametric system identification technique, N4SID has been used for the symmetric-plan shear building, which uses ground motion and floor acceleration responses to form the input and output matrices respectively. The input and output data are processed appropriately before using them for the identification technique. Suitability of system identification algorithm N4SID has been initially studied with the help of three numbers of scaled laboratory RC models without any infill wall and with different column geometries in ground floor. Models have been excited by a shake table subjected to time scaled earthquake input after fulfilling all the similitude requirements and floor accelerations have been acquired. Identification of system parameters of all the three laboratory test models have been carried out based on the acquired accelerations under different earthquake excitations. Identified modal parameters of all the test models have been

observed to be consistent irrespective of earthquake excitations used in the shake table test. The same laboratory test models have again been tested with infill wall at first floor having different sizes of openings to visualize the influence of walls and wall openings on the lateral stiffness of the system. Adopting the identification technique N4SID, modal parameters and hence storey stiffness have been evaluated for all the three models with different sizes of wall opening and excited under a few prescribed earthquake input. The identified system parameters have been observed to be very consistent and following a trend which is very well conforming to the considered geometry of the structural system. The evaluated stiffness values of the structural system have been utilized to develop correlations signifying contribution of infill wall as an equivalent diagonal strut with different sizes of opening. These proposed expressions have been further verified through studies on numerically simulated 3-D models of the scaled laboratory specimens using SAP 2000 Nonlinear (version 12). The performances of the proposed correlations have been compared with some of the existing recommendations for modeling of infill wall. Thus, subspace identification scheme has been observed to be quite effective on the scaled laboratory building models and hence, the strategy has been applied for identification of an existing symmetric-plan shear building. However, due to the availability of limited number of sensors, the identification of modal parameters of the sample building has been carried out with acceleration data from a few selected floor levels only. Hence, an iterative approach has been adopted to evaluate missing modal displacement values at the floor locations where accelerometers have not been installed. Thus, starting with an assumed mode shape matrix, the iterative technique has been observed to converge in about 50 iterations and the complete modal as well as structural parameters are obtained at the end of convergence. A numerical model has also been simulated using in SAP 2000 Nonlinear where infill wall has been modeled as a diagonal strut and the stiffness of the strut is calculated using the proposed correlation to model the infill wall for an assumed 20%

opening in walls. The model has been validated with experimental findings by comparing modal parameters as well as dynamic responses. MAC has been used to verify the agreement between mode shapes from numerical model and identified mode shapes of the sample building. The validated model has been further used to examine the adequacy of number of sensors used for the identification study. The study has revealed that a minimum of two sensors are required for accurate identification of system parameters of the sample building.

The identification study has also been carried out for an asymmetric-plan shear building using ITD technique. The method has been initially verified through studies on a two storey scaled test model made of structural steel. The asymmetricity in the test model has been introduced with the use of non uniform floor masses in different floor panels in an otherwise geometrically symmetric model. The test model has been excited on a shake table with prescribed earthquake input and floor accelerations have been acquired from two sensors per floor kept at a distance apart. Thus, the two recorded translational acceleration data per floor also provides torsional component of the acceleration. High amplitude portions of recorded transverse and computed torsional acceleration histories have been considered for evaluation of crossing times and different time shifts. Crossing times have been utilized to obtain free decay responses of the acceleration histories. Free decay responses of certain durations have been extracted using Random Decrement (RANDOMDEC) method. Further, different time shifts have been utilized for assembling response matrices of RANDOMDEC signatures. The solution of Eigenvalue equations formulated correlating original and delayed response matrices gives the system matrix $\boldsymbol{A}$. The modal parameters such as natural frequencies, mode shapes and damping ratios have been evaluated from system matrix $\boldsymbol{A}$. Lumped floor masses, identified modal frequencies and identified modal displacement values have been utilized for evaluation of stiffness

using least squares solution of eigenvalue equations. A 3-D finite element model of the test specimen has been simulated using SAP 2000 Nonlinear. Corresponding modal frequencies of the simulated model have been observed to be quite close to those of identified frequencies of the test model. Time history analysis of the numerical model has been carried out using acquired table acceleration histories as input considering 2% proportional damping. The extracted acceleration histories have been compared with the corresponding acceleration histories of the test models and have been found to be agreeing well with each other. Thus, the ITD identification scheme has been observed to be quite effective on the scaled laboratory asymmetric building model and hence, the strategy has been applied for identification of an existing torsionally coupled shear building. Different earthquake induced floor acceleration histories of the existing asymmetric-plan R C shear building have been considered for system identification and very consistent modal parameters have been obtained.

8.2 MAJOR FINDINGS

Major findings ascribed to the present study may be summarized as follows:

- Parametric subspace identification, namely N4SID is found to be an efficient and robust system identification scheme for the evaluation of modal parameters of symmetric-plan shear buildings. The identified system parameters have been observed to be highly consistent irrespective of input excitations considered as long as the building exhibits similar stiffness characteristics.
- The proposed correlations for infill wall contribution to lateral stiffness of a building frame as derived from identification study have been observed to be quite adequate for numerical modeling of infill walls in a prototype building.

- The contribution of infill wall can be disregarded when the opening ratios in infill wall exceed 45%.
- Parametric subspace identification scheme is suitable for identification of modal parameters of existing buildings even with limited sensors. However, an iterative scheme needs to be used for accurate evaluation of system parameters for the cases with limited sensors.
- At least two numbers of sensors placed at appropriate locations have been found to be adequate for the sample building under study for reliable evaluation of system parameters.
- Ibrahim Time Domain (ITD) method is observed to be a suitable tool for identification of modal parameters of torsionally coupled shear buildings.

8.3. SCOPE FOR FUTURE WORK

Additional work is needed in the following areas:

- To study non-linear system identification based technique for the evaluation of system parameters of building beyond elastic range.
- To study optimal sensor requirements in terms of number of sensors and their placement at floor level for buildings taller than the sample building considered in the present study.

8.4. CONCLUDING REMARKS

Dynamic behavior of buildings before and after earthquakes can easily be assessed through system identification. Optimal locations of accelerometers will reduce cost and computational efforts associated with implementation of the methodology. Influence of infill walls in a system's behaviour can also be effectively evaluated using the

identification method. However, evaluation of system behavior with the additional influence of torsion needs to be addressed differently. The prospects of evaluation of system parameters through system identification techniques are very promising.

REFERENCES

Adams R. D., Cawley P., Pye C. J. and Stone B. J., " A Vibration Testing for Non-Destructively Assessing the integrity of Structures, *Journal of Mechanical Engineering Science,* Vol. 20, pp. 93-100, 1978.

Agarwal P and Shrikhande M, "Earthquake Resistant Design of Structures", *Prentice Hall India Private Limited*, 2006.

Angel R., Abrams D. P., Shapiro D., Uzarski J. and Webster M., "Behavior of reinforced concrete frames with masonry infills", *Structural research series report*, Department of Civil Engineering, University of Illinois, 589, 1994.

Armon Dror, Ben-Haim Yakov and Braun Simon, "Crack Detection in Beams by Rank Ordering of Eigenfrequency Shifts", *Mechanical Systems and Signal Processing*, Vol. 8(1), pp. 81-91, 1994.

Åström K. J. and Bohlin T., "Numerical Identification of Linear Dynamic Systems from Normal Operating Records, *Proceeding of the IFAC Symposium on Self-Adaptive Systems*, Teddington, UK, 1965.

Balageas Daniel, Fritzen Claus-Peter and Güemes Alfredo, "Chapter - 1, Structural Health Monitoring", *ISBN-13: 978-1-905209-01-9* - John Wiley & Son, January 2006.

Bani-Hani Khaldoon A., Zibdeh Hazem S. and Hamdaouli Karim, "Health Monitoring of a Historical Monument in Jordan Based on Ambient Vibration Test", *Smart Structures and Systems*, Vol. 4 (2), pp. 195-208, 2008.

Barroso L. R. and Rodriguez R., "Damage Detection Utilizing the Damage Index Method to a Benchmark Structure", *Journal of Engineering Mechanics, ASCE*, Vol. 130(2), pp. 142-51, 2004.

Basheer P. A. Muhammed, "Development in Health-Assessment of RC Structures", *The Indian Concrete Journal*, Vol. 79(2), pp. 15-22, February 2005.

Begg H., Mackenzie A. C., Dodds C. J., and Loland O., " Structural Integrity Monitoring Using Digital Processing of Vibration Signals", Proceeding of the 8th Annual Offshore Technology Conference, Houston, Texsas, pp. 305-311, 1976.

Bernal D. and Gunes B., "Flexibility Based Approach for Damage Characterization: Benchmark Application", *Journal of Engineering Mechanics, ASCE*, Vol. 130 (1), pp. 61-70, 2004.

Borsaikia A. C., Talukdar S., and Dutta A., "Study of Modal Parameters and Vibration Signatures of Notched Concrete Prisms", *Cement and Concrete Research*, Vol. 36, pp. 592-598, 2006.

Brandes K., Herter J. and Helmerich, "Non-destructive Testing Being Essential Part of the Safety assessment of Steel", *Laboratory for Structural Safety D-12205 Berlin*, Federal Institute of Materials Research and Testing, Germany, pp. 127-133, 2000.

Caicedo J. M., "Two Structural Health Monitoring Strategies Based on Global Acceleration Responses: Development, Implementation, and Verification", *M. S. Thesis*, Washington University Sever Institute of Technology Department of Civil Engineering, 2001.

Caicedo J. M., Dyke, S. J. and Burrell G., "Experimental Evaluation of Structural Health Monitoring Techniques for Flexible Structures", *Proceeding, Workshop on Advanced Sensors, Structural Health Monitoring and Smart Structures,* November 2003.

Caicedo J. M., "Structural Health Monitoring Flexible Civil Structures", *Doctor of Science Thesis*, Washington University Sever Institute of Technology, Department of Civil Engineering, 2003.

Caicedo J. M., Dyke S. J. and Johnson E.A., "Natural Excitation Technique and Eigensystem Realization Algorithm for Phase I of the IASC-ASCE Benchmark Problem: Simulated Data", *Journal of Engineering Mechanics, ASCE*, Vol. 130(1), pp. 49-60, 2004.

Chaker Amar A. and Cherifati A., "Influence of Masonry Infill Panels on The Vibration and Stiffness Characteristics of R/C Frame Buildings", *Earthquake Engineering And Structural Dynamics*, Vol. 28, pp.1061-1065, 1991.

Chakraverty S., "Identification of Structural Parameters of Multi-storey Shear Buildings from Modal Data", *Earthquake Engineering and Structural Dynamics,* Vol. 34, pp. 543-554, 2005.

Chaudhary Tariq Amin, Abe Masato, ujinoYozo F, and Yoshida Junji, "System Identification of Two Base-Isolated Bridges Using Seismic Records", *Journal of Structural Engineering, ASCE*,Vol.126(10), pp.1187-1195, 2000.

Chen Chi-Tsong, "Linear System Theory and Design", *Harcourt Brace College Publishers*, New York, 1984.

Chopra A. K.,"Dynamics of Structures-Theory and Application to Earthquake Engineering", *Prentice Hall of India Private Limited,* 2001.

Colangelo F., "Pseudo-Dynamic Seismic Response of Reinforced Concrete Frames Infilled with Non-structural Brick Masonry", *Earthquake Engineering and Structural Dynamics*, Vol. 34, pp. 1219–1241, 2005.

Cole Henry A., " Method and Apparatus for Measuring the Damping Characteristics of a Structure", *U S Patent No. 3-620-069*, 1971.

Design Manual No.2, "Guidelines for Structural Health Monitoring", *ISBN-0-9689006-0-7*, ISIS Canada, September 2001.

Dionisio Bernal, "Load Vectors for Damage Localization", *Journal of Engineering Mechanics*, Vol. 128(1), January 2002.

Doebling S. W., Farrar C. R., Prime M. B., and Shevitz D. W., "Damage Identification and Health Monitoring of Structural and Mechanical Systems from Changes in Their Vibration Characteristics: A Literature Review", *Los Alamos National Laboratory,* Report No. LA-13070- MS, Los Alamos N.M, 1996.

Dutta A. and Talukdar S., "Damage Detection in Bridge using Accurate Modal Parameters", *Journal of Finite Element Analysis and Design*, Vol. 40(3), pp. 287-304 2004.

Dyke S.J., Caicedo J.M., Turan G., Gergman L.A. and Hague S., "Phase I Benchmark Control Problem for Seismic Response of Cable-Stayed Bridges", *Journal of Structural Engineering, ASCE*, Vol. 129(7), pp. 857-872, 2003.

Farrar Charles R. and Sohn Hoon, "Pattern Recognition for Structural Health Monitoring", *Workshop on Mitigation of Earthquake Disaster by Advanced Technologies,* Las Vegas, NV, USA, Nov. 30- Dec. 1, 2000.

Fasel T. R., Sohn H., Park G. and Farrar C.R., "Active Sensing using Impedance-based ARX Models and Extreme Value Statistics for Damage Detection", *Earthquake Engineering and Structural Dynamics*, Vol. 34(7), pp. 763-785, 2005.

FEMA (Federal Emergency Management Agency U.S. Department of Homeland Security) 306, **"**Evaluation of Earthquake Damaged Concrete and Masonry Wall Buildings", *Basic Procedures Manual*, Washington D. C., 1998.

Ferhi A. and Turman K. Z., "Behaviour of Asymmetric Building Systems under Monotonic Load-I &II." Engineering Structures, Vol. 18(2), pp. 133-141 & 142-153, 1996.

Furukawa T., Ito M., Izawa K., and Noori M. N., "System Identification of Base-Isolated Building using Seismic Response Data", *Journal of Engineering Mechanics, ASCE*, Vol. 131 (3), pp. 268-275, 2005.

Ghanem R. and Shinozuka M., "Structural-System Identification. I: Theory & II: Experimental Verification", *Journal of Engineering Mechanics, ASCE*, Vol. 121(2), pp. 255-273, 1995.

Ghassan Al-Chaar, "Evaluating Strength and Stiffness of Unreinforced Masonry Structures", *Construction Engineering Research Laboratory, US Army Corps of Engineers*, TR-02-1*,* January 2002.

Ghassan Al-Chaar, M.ASCE1; Mohsen Issa, M.ASCE2; and Steve Sweeney, "Behavior of Masonry-Infilled Nonductile Reinforced Concrete Frames", *Journal of Structural Engineering*, pp.1055-1063, August 2002.

Gudmundson P., "Eigenfrequency Changes of Structures due to Cracks, Notches, or other Geometrical Changes", *Journal of Mechanics and Physics of Solids*, Vol. 30(5), pp. 339-353, 1982.

Hejal R. and Chopra A. K., "Earthquake Analysis of a Class of Torsionally - coupled Buildings", *Earthquake Engineering and Structural Dynamics*, Vol. 18, pp. 305-23, 1989.

Hemalatha G. and Mary S. A., "Inclined Crack Study using NDT Techniques", *The Indian Concrete Journal,* pp. 90-92, February 2000.

Hemant B. Kaushik, Durgesh C Rai and S. K. Jain, "Stress-Strain Characteristic of Clay Brick Masonry under Uniaxial Compression", *Journal of Materials in Civil Engineering, ASCE*, pp. 728-739, 2007.

Hera Adriana and Hou Zhikun, "Application of Wavelet Approach for ASCE Structural Health Monitoring Benchmark Studies", *Journal of Engineering Mechanics, ASCE*, Vol. 130 (1), pp. 96-104, 2004.

Hilmi Lus, Raimondo Betti, Jun Yu and Mauizio De Angelis, "Investigation of System Identification Methodology in the Context of ASCE Benchmark Problem", *Journal of Engineering Mechanics, ASCE*, Vol. 130(1), pp. 71-84, 2004.

Ho B. L. and Kalman R. E.,"Effective construction of Linear State Variable Models from Input-Output Functions", *Regelungstechnik*, Vol. 12, pp. 545-548, 1965.

Ibrahim S. R. and Pappa R. S., "Large Modal Survey Testing Using the Ibrahim Time Domain Identification Technique", *Journal of Spacecraft and Rockets*, Vol. 19(5), pp. 459-465, Sept-Oct 1982.

Ibrahim S. R., "Computation of Normal Modes from Identified Complex Modes", *American Institute of Aeronautics and Astronautics*, Vol. 21(3), pp. 446-451, March 1983.

IITK-GSDMA (Indian Institute of Technology Kanpur-Gujarat State Disaster Management Authority), "A Project Report on Review of Building Codes on Earthquakes", 2005.

Jain S. K., Lettis W. R., Murty C. V. R., and Bardet J. P., "Postearthquake Handling of Buildings," In 2001 Bhuj, India Earthquake Reconnaissance Report, *Earthquake Spectra*, supplement A to volume 18. Oakland, CA: Earthquake Engineering Research Institute, pp. 297 – 317, July 2002.

Johnson E. A., Lam H. F., Katafygiotis L. S., and Beck J. L., "Phase I IASC-ASCE Structural Health Monitoring Benchmark Problem Using Simulated Data", *Journal of Engineering Mechanics, ASCE*, Vol. 130(1), pp. 3-15, 2004.

Juang Jer-Nan, "Applied System Identification", *PTR Prentice Hall Englewood Cliffs, New Jersey*, 1994.

Kenley R. M. and Dodds C. J., "West Sole WE Platform: Detection of Damage by Structural Response Measurements", *Proceeding of the 12th Annual Offshore Technology Conference*, pp. 111-118, 1980.

Khiem N. T., "A Simplified Method for Natural Frequency Analysis of a Multiple Cracked Beam", *Journal of Sound and Vibration*, Vol. 245(4), pp. 737-751, 2001.

Klingner R. E., and Bertero V. V., "Earthquake Resistance of Infilled frames", *Journal of Structural Division*, Vol. 104(6), pp. 973–989, 1978.

Lam H. F., Katafygiotis L. S. and Mickleborough N. C., "Application of a Statistical Model Updating Approach on Phase I of the IASC-ASCE Structural Health Monitoring Benchmark Study", *Journal of Engineering Mechanics, ASCE*, Vol. 130(1), pp. 34-48, 2004.

Lei Y., Kiremidjian A. S., Nair K. K., Lynch J. P., Law K. H., Kenny T. W. Ed Carryer, and Kottapalli A., "Statistical Damage Detection Using Time Series Analysis on a Structural Health Monitoring Benchmark Problem", *Proceedings of the 9th International Conference on Applications of Statistics and Probability in Civil Engineering*, San Francisco, CA, USA, July 6-9, 2003.

Lieu K. M. and Wang Q., "Application of Wavelet Theory for Crack Identification in Structures", *Journal of Engineering Mechanics*, February 1998.

Lifshitz J.M. and Rotem A., "Determination of Reinforcement Unbonding of Composites by a Vibration Technique", *Journal of Composite Materials*, Vol. 3, pp. 412-423, 1969.
Ljung Lennart, "System Identification: Theory for the User", *Prentice Hall Englewood Cliffs*, New Jersey, 1987.

Lynch J. P., "Linear Classification of System Poles for Structural Damage Detection using Piezoelectric Active Sensors", *SPIE 11th Annual International Symposium on Smart Structures and Materials*, San Diego, CA, USA, March 2004.

Maeck J. and Roeck G De., "Dynamic Bending and Torsion Stiffness Derivation from Modal Curvatures and Torsion Rates", *Journal of Sound and Vibration*, Vol. 225(1), pp. 153-170, 1991.

Mainstone R. J., "On the Stiffness and Strength of Infilled Frames", *Proc. Instn. Civ. Engrs.*, Supplement IV, pp. 57–90, 1971.

Malhotra V. M. and Carino N. J., "Nondestructive Testing of Concrete", *CRC Press, Second Edition*, 2004.

Marwala T.,"Using Computers to Monitor the Health of Structures", *Science in Africa*, June 2003.

Maruki T.," Structural Health Monitoring using Parametric Models in System Identification", *University of California*, REUJAT 2004.

Medhi, M., Dutta, A., and Deb, S.K., Health monitoring of multi-storeyed shear building using parametric state space modeling , *Smart structures and systems,* 4 (1), pp-47-66, 2008.

Mehrabi A. B., Shing P. B., Schuller M., Noland J., "Experimental Evaluation of Masonry-infilled RC Frames", *Journal of Structural Engineering*, ASCE, Vol. 122 (3), pp. 228-237, 1996.

Nagarajaiah Satish, "System Identification of Base-Isolated USC Hospital Building from Recorded Response", *Proceeding of 17th International Modal Analysis Conference,* Structural Engineering , pp.159-165, 1999.

Nagarajaiah Satish and Xiaohong Sun, "Response of Base-Isolated Building in Northridge Earthquake", *Journal of Structural Engineering, ASCE*, Vol. 126(10), pp. 1177-1186, 2000.

Nandwana B. P. and Maiti S. K. "Detection of the Location and Size of a Crack in Stepped Cantilever Beams based on Measurements of Natural Frequencies", *Journal of Sound and Vibration*, Vol.203(3), pp.435-446, 1997.

Narkis Y., "Identification of Crack Location in Vibrating Simply Supported Beams", *Journal of sound and vibration*, Vol. 172(4), pp. 549-558, 1994.

Nataraja R., "Structural Integrity Monitoring in Real Seas", *Proceeding of 15th Annual Offshore Technology Conference*, pp. 221-228, 1983.

OVERSCHEE Peter VAN and MOOR Bart DE, "Subspace Identification for Linear Systems, Theory-Implementations-Applications", *Kluwer Academic Publishers,* Massachusetts 02061, 1996.

Pandey A. K., Biswas M. and Samman M. M., "Damage Detection from Changes in Curvature Mode Shapes", *Journal of Sound and Vibration*, Journal of Sound and Vibration, Vol. 145(2), pp. 321-332, 1991.

Pappa R. S. and Ibrahim S. R., "A Parametric Study o f the Ibrahim Time Domain Modal Identification Algorithm," *The Shock and Vibration Bulletin*, pp. 43-72, May 1981.

Paulay T. and Priestly M. J. N., "Seismic Design of Reinforced Concrete and Masonry Buildings", *Wiley*, 1992.

Polyakov, S. V., "On the Interaction between Masonry Filler Walls and Enclosing Frame when Loaded in the Plane of the Wall", *Translations in Earthquake Engineering*. EERI, San Francisco, pp. 36–42, 1960.

Qian G. L., S Gu. N. and Jiang J. S., "The Dynamic Behaviour and Damage Detection of a Beam with Crack", *Journal of Sound and Vibration*, Vol. 138(2), pp. 233-243, 1990.

Ratcliffe C. P., "Damage Detection using a Modified Laplacian Operator on Mode Shape Data", *Journal of Sound and Vibration*, Vol. 204(3), pp. 505-517, 1997.

Richardson M. H. and Mannan M. A., "Remote Detection and Location of Structural Faults Using Modal Parameters", *Proceeding of the 10th International Modal Analysis Conference,* pp. 502-507, 1992.

Rizos P. F., Aspragathos N. and Dimarogonas A.D., "Identification of Crack Location and Magnitude in a Cantilever Beam from the Vibration Modes", *Journal of Sound and Vibration*, Vol. 138(3), pp. 381-388, 1990.

Rytter A., "Vibration Based Inspection of Civil Engineering Structures", *Ph. D. Dissertation*, Department of Building Technology and Structural Engineering, Aalborg University, Denmark, 1993.

Saavedra P. N. and Cuitino L.A., "Crack Detection and Vibration Behaviour of Cracked Beam", *Computers and Structures*, Vol. 79, pp. 1451-1459, 2001.

Salawu O S. and Williams C., "Bridge Damage Location Using Vibration Mode Shapes", *Proceeding of 12th International Modal Analysis Conference*, pp. 933-939, 1994.

Salawu O S. and Williams C., "Bridge Assessment Using Forced-Vibration Testing", *Journal of Structural Engineering*, Vol. 121(2), pp. 161-173, 1995.

Salawu O S., "Nondestructive Assessment of Structures Using the Integrity Index Method Applied to a Concrete Highway Bridge", Insight, Vol. 37 (11), pp. 875-878, 1995.

Shah Surendra P., Popovics John S., Subramaniam Kolluru V., Aldeea Corina-Maria, "New Direction in Concrete Health Monitoring Technology", *Journal of Engineering Mechanics,* pp. 754-760, July 2000.

Silva Samuel da, Junior Milton Dias and Junior Vicente Lopes, "Damage Detection in a Benchmark Structure Using AR-ARX Models and Statistical Pattern Recognition", *Journal of the Brazilian Society of Mechanical Science & Engineering*, Vol. XXIX(2/175), pp. 174-184, April-June 2007.

Sinha J. K., Friswell M. I. and Edwards S., "Simplified Models for the Location of Cracks in Beam Structures using Measured Vibration Data", *Journal of Sound and Vibration*, Elsevier Science Ltd., Vol. 251(1), pp. 13-38, 2002.

Sohn Hoon and Farrar Charles R, "Damage Diagnosis Using Time Series Analysis of Vibration Signals", *Smart Materials and Structures*, I O P Publishing Ltd., pp. 446-451, 2001.

Stafford-Smith, B, "Lateral stiffness of infilled frames", *Journal of Structural Division.*, Vol. 88 (6), pp. 183–199, 1962.

Stafford-Smith B., and Carter C, "A Method for the Analysis of Infilled Frames", *Proceeding of Institution of Civil Engineers*, Vol. 44, pp. 31–48, 1969.

Swartz R. Andrew, "Active Sensing for Structural Health Monitoring", December 2004.

Talukdar S. and Borsaikia A. "An Assessment of the Progressive Failure of Concrete using Pulse Velocity Measurements", *The Indian Concrete Journal*, Vol. 79(2), pp. 61-64, February 2005.

Ueng J. M., Lin C. C. and Lin P. L., "System Identification of Torsionally Coupled Buildings" *Computers and Structures*, Vol. 74, pp. 667-686, 2000.
Vandiver J. K., "Detection of Structural Failure on Fixed Platforms by Measurement of Dynamic Response", *Journal of Petroleum Technology Conference*, pp. 305-310, March 1977.

Vestroni Fabrizio and Capecchi Danilo, "Damaged Detection in Beam Structures Based on Frequency Measurements", *Journal of Engineering Mechanics*, Vol. 126(7), July, 2000.

Wahab M. M. Abdel and Roeck G. De, "Damaged detection in bridge using modal curvatures: Application to a real damage scenario", *Journal of Sound and Vibration*, Vol. 226(2), pp. 217-235, 1991.

Xu Y. L. and Chen J., "Structural Damage Detection Using Empirical Mode Decomposition", *Journal of Engineering Mechanics-ASCE,* Vol. 130(11), pp. 1279-1288, November 2004.

Yang and Everstine, "Measurement of Structural Damping Using the Random Decrement Technique", *The Shock and Vibration Bulletin, Bulletin*, Vol. 53(4), pp. 63-71, May 1983.

Yang X.F., Swamidas A. S. J. and Seshdri R., "Crack Identification in Vibrating Beams using the Energy Method", *Journal of Sound and Vibration*, Vol. 244(2), pp. 339-357, 2001.

Yang J. N., Lei Y., Lin S. and Huang N., "Hilbert-Huang Based Approach for Structural Damage Detection", *Journal of Engineering Mechanics, ASCE*, Vol. 130(1), pp. 85-95, 2004.

Yang J. N., Lei Y., Lin S. and Huang N., "Identification of Natural Frequencies and Dampings of Insitu Tall Buildings Using Ambient Wind Vibration Data", *Journal of Engineering Mechanics, ASCE*, Vol. 130(5), pp. 570-5775, 2004.

Yuen K., Au S. K. and Beck J. L., **"**Two-Stage Structural Health Monitoring Approach for Phase I Benchmark Studies", *Journal of Engineering Mechanics, ASCE*, Vol. 130(1), pp. 16-33, 2004.

APPENDIX-A

Table A - 1 Component wise mass distribution for the RC prototype building

Components	Size in mm	Storey Masses (Kg)		Total Mass (Kg)
		Ground	First	
Slab	10300 x 5300 x 200	26749.10	26749.10	53498.20
Beam in				
Longer Direction	2 x 10300 x 250 x 300	3785.25	3785.25	7570.50
Shorter Direction	3 x 4700 x 250 x 300	2590.875	2590.875	5181.75
Column	6 x375 x 375 x 2850	5891.50	2945.75	8837.25
	Grand Total	**M1= 39017**	**M2 = 36071**	**75088.00**

Table A - 2 Structural properties and floor masses of the BSNL building

Floors	Size of Column (mm)	Slab Thickness (mm)	Floor Mass (Kg)
First	As described in Fig. A-1.1	100 for all the down slab and 150 mm for all the other parts	511770
Second			515930
Third			515580
Fourth			515580
Fifth			515570
Sixth			515570
Seventh			515570
Eighth			511080
Roof			362710

Table A - 3 Material properties of the BSNL building

Material Type	Young's Modulus (N/mm^2)	Poisson's Ratio	Material Density (kg/m^3)
Concrete	22360	0.2	2450
Steel	$2x10^5$	0.3	7850

Table A – 4 Component wise mass distribution for the steel prototype building

Components	Size (mm)	Storey Masses (Kg)		Total Mass (Kg)
		First	Second	
Slab	10500 x 5250 x 50	21636.56	21636.56	43273.13
Beam in				
Longer Direction	2 x 10500 x ISMC-375	884.10	884.10	1768.20
Shorter Direction	3 x 5250 x ISMC-375	663.10	663.10	1326.20
Column	6 x ISMC-375 x 3300	833.58	833.58	1667.16
	Grand Total	**M1= 24017.35**	**M2 = 24017.35**	**48034.70**

Table A – 5 Structural properties and floor masses of the torsionally coupled building

Floors	Floor Mass (Kg)	Centre of Resistance (m)	Center of Mass (m)
First	1057000	25.40, 26.58	16.64, 23.90
Second	1010420	25.00, 28.00	18.52, 26.45
Third	1067000	25.00, 28.00	19.95, 27.23
Roof	908000	23.00, 28.90	17.32, 27.78

Table A – 6 Size of column sections of torsionally coupled sample building

Column Marking	Size (mm)	Column Marking	Size (mm)
C1, C2, C3, C4, C5, C6, C7, C9, C10, C12	500 x 500	C8	900 x 900
C6′	300 x 300	C11	600Ø

Table A– 7 MAC values for scaled RC test models

Models	Experimental Vs Raw Numerical Model		Experimental Vs Updated Numerical Model	
	Mode 1	Mode 2	Mode 1	Mode 2
Model I	0.98	0.93	0.99	0.99
Model II	0.95	0.94	0.99	0.99
Model III	0.97	0.97	0.99	0.99

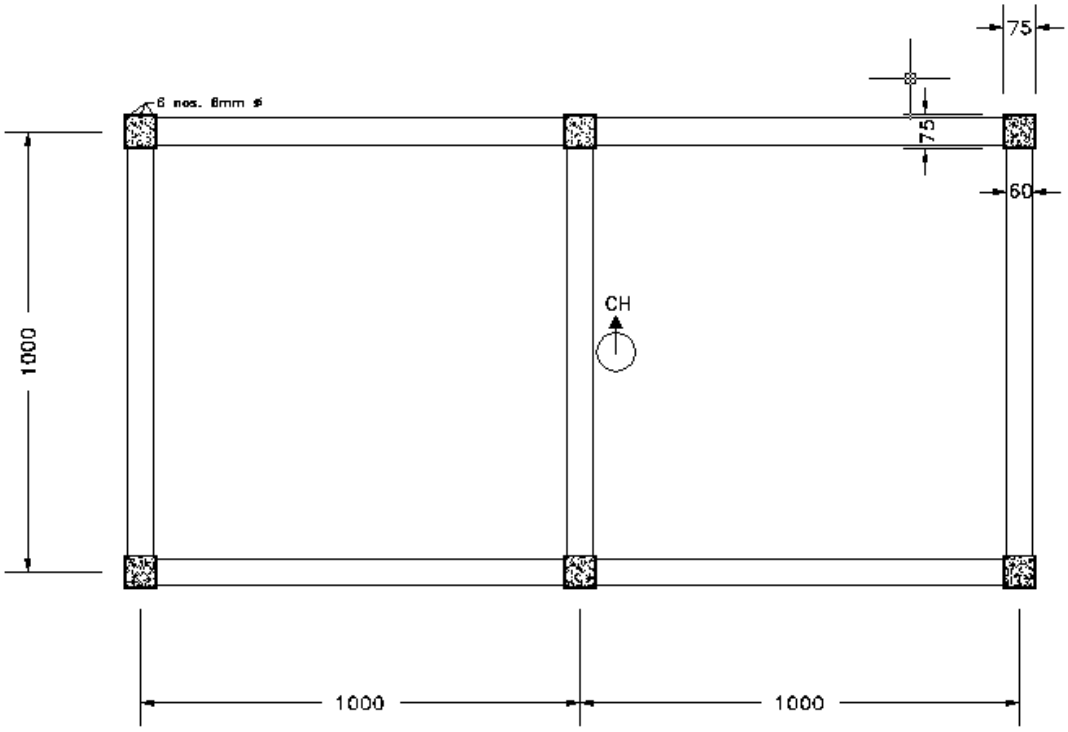

(a) Column positions of Model I and II

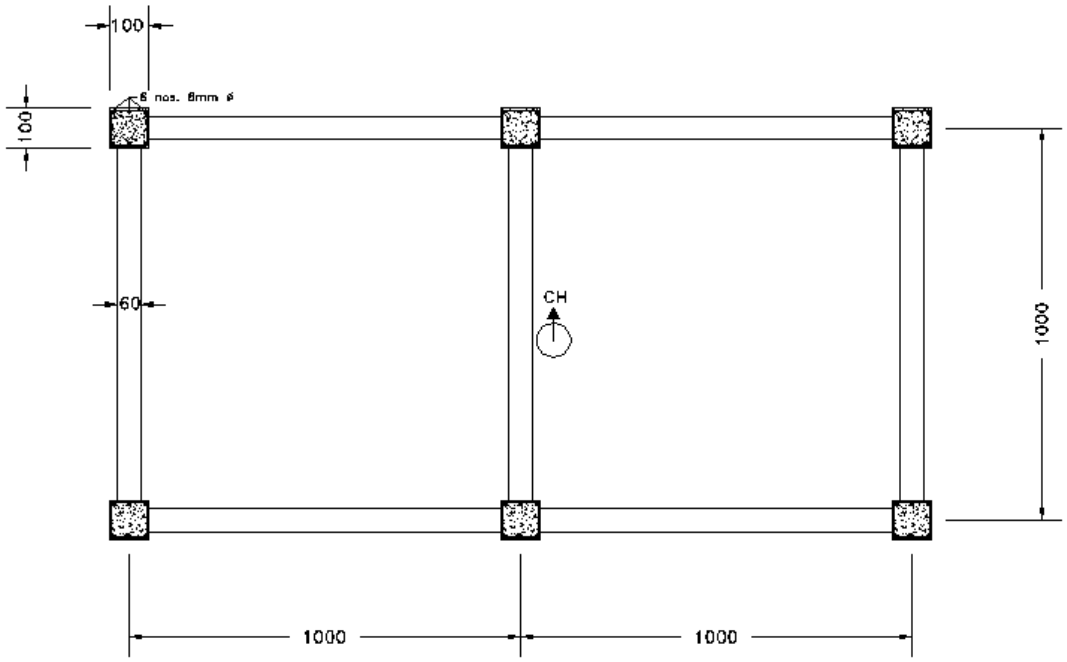

(b) Column positions of Model III

Fig. A – 1 Plans showing column positions of scaled RC laboratory test models

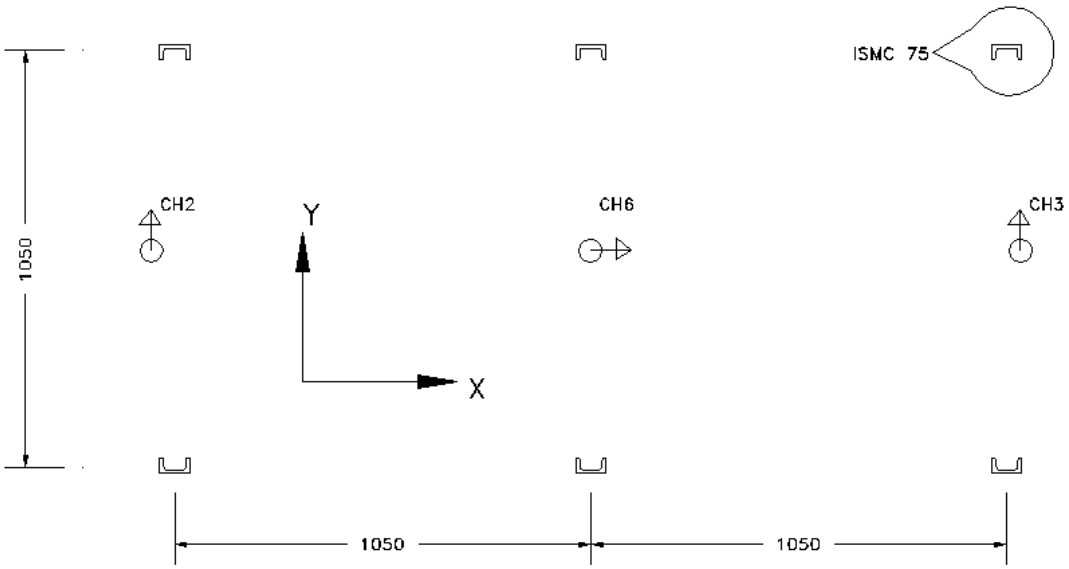

(a)Column and sensor positions at first floor

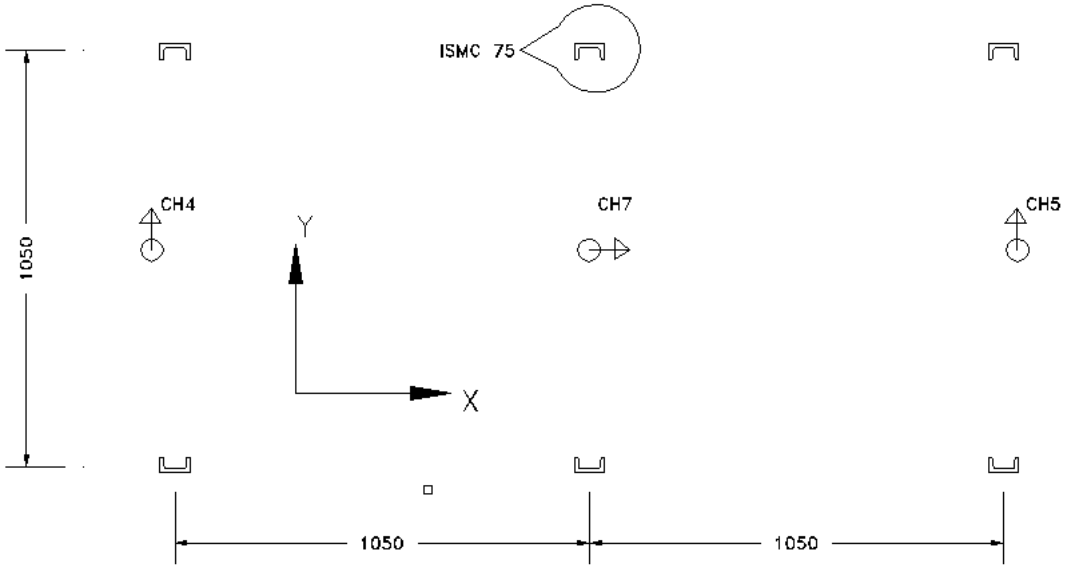

(b) Column and sensor positions at roof floor

Fig. A – 2 Plans showing columns and sensor locations of scaled steel laboratory test model

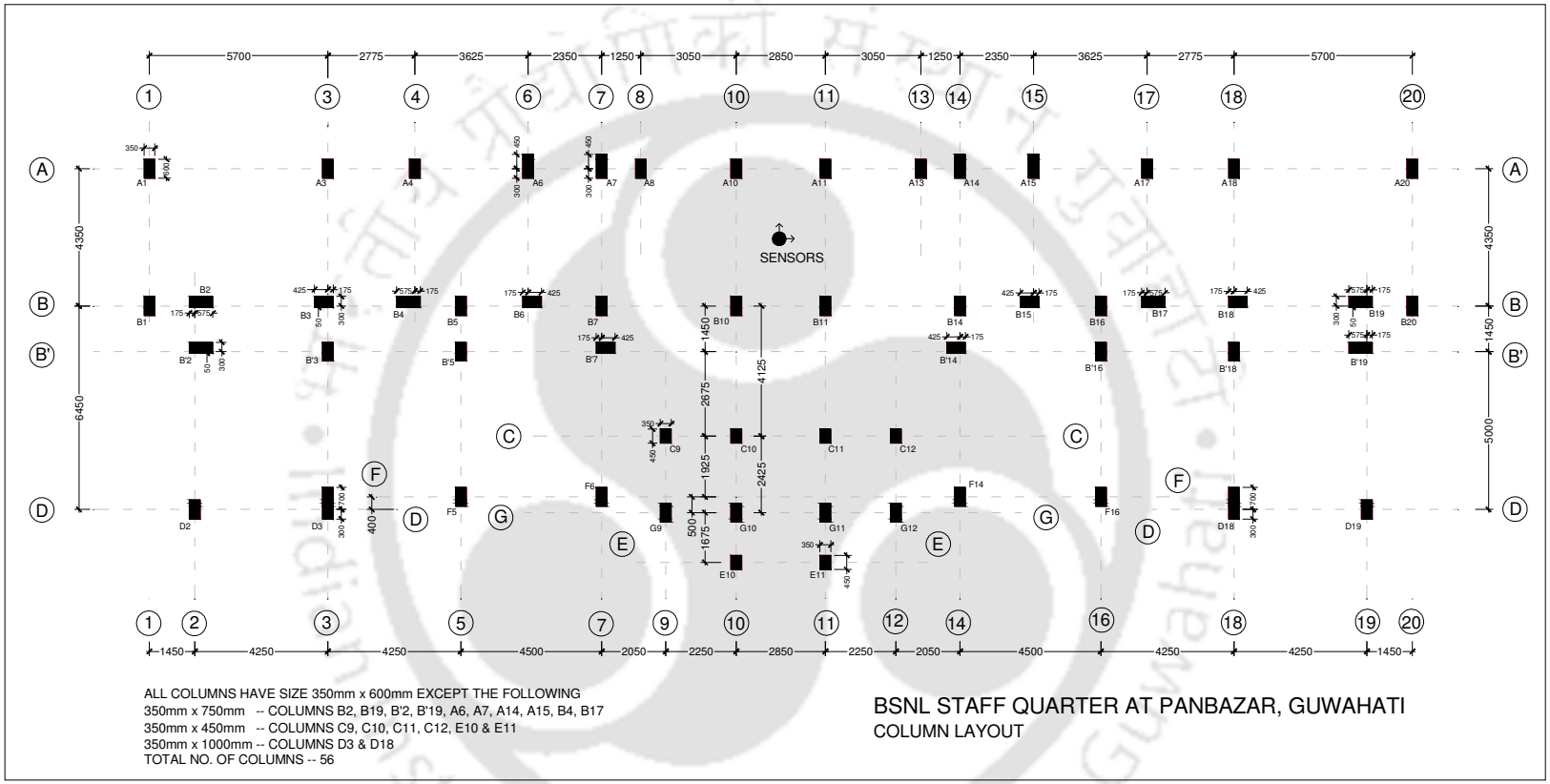

Fig. A - 3 Plan showing column position and sensor location in the ground storey

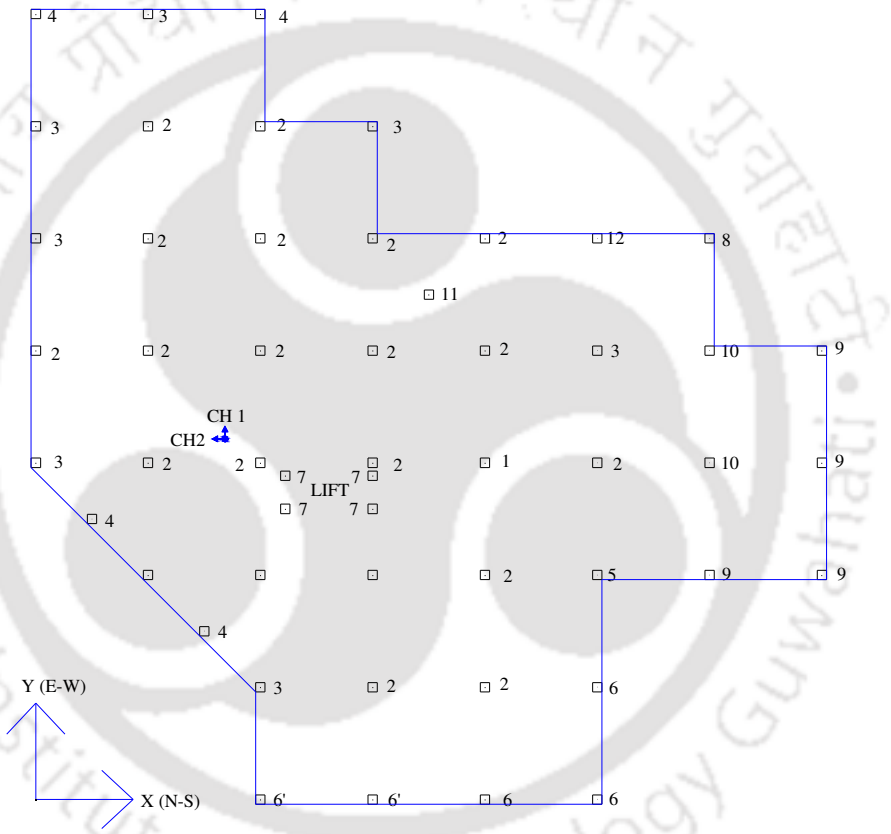

Fig. A - 4 Plan showing column position and sensor location in the ground floor of torsionally coupled sample building

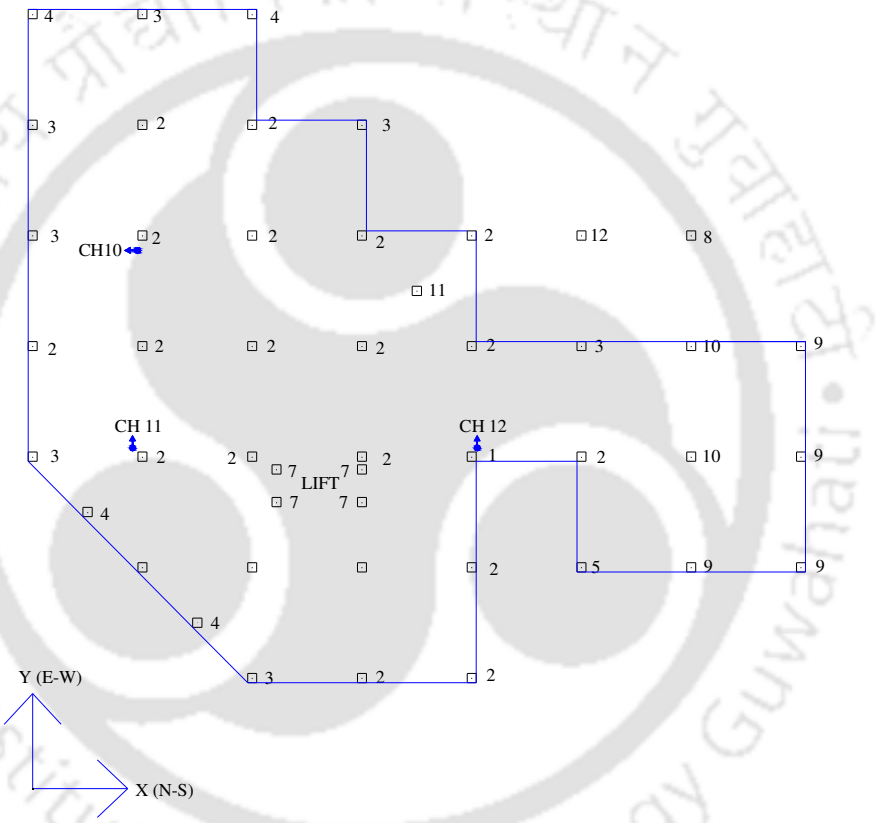

Fig. A - 5 Plan showing column position and sensor location in the second floor of torsionally coupled sample building

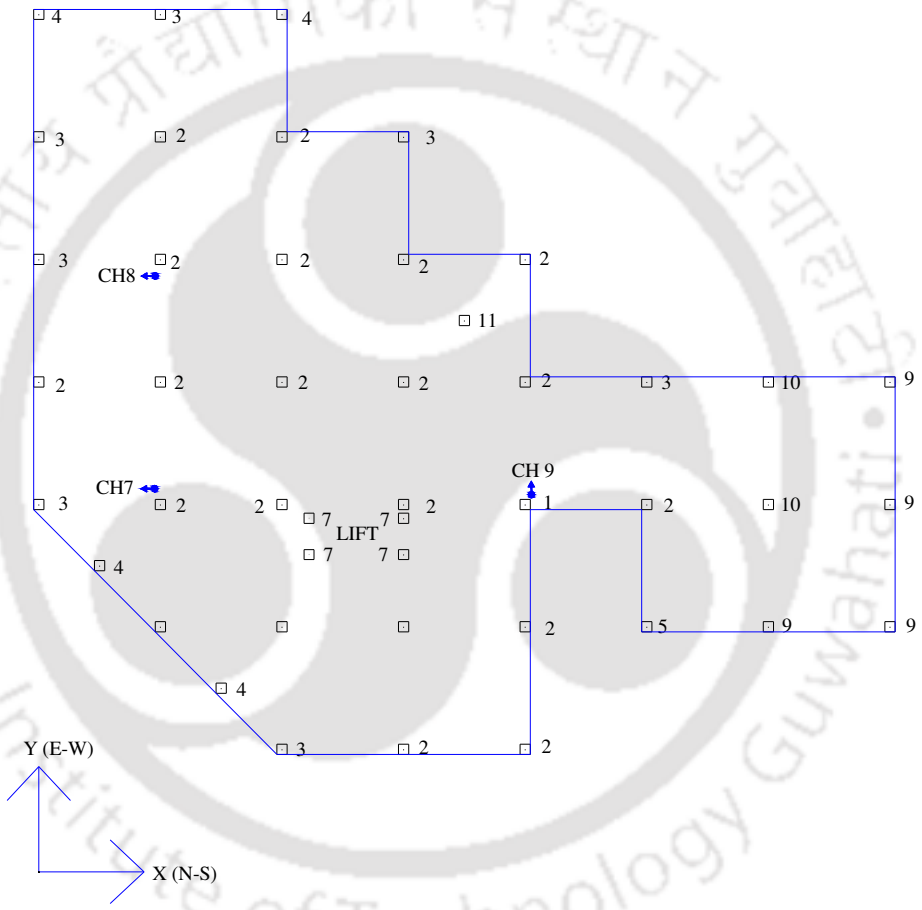

Fig. A - 6 Plan showing column position and sensor location in the third floor of torsionally coupled sample building

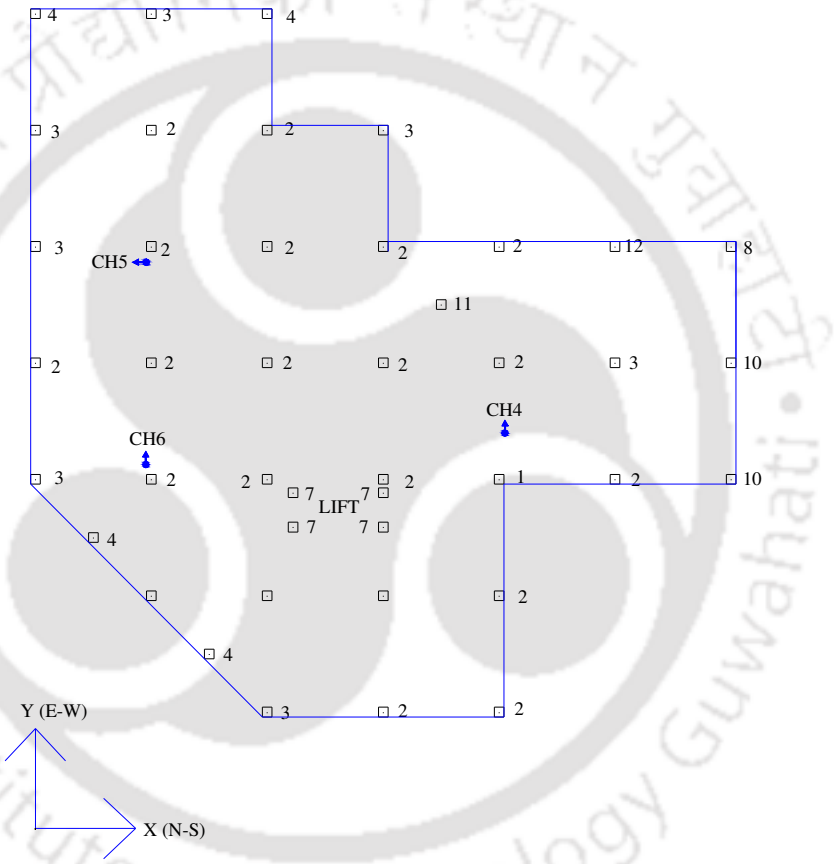

Fig. A - 7 Plan showing column position and sensor location in the roof floor of torsionally coupled sample building

PUBLICATIONS BASED ON PRESENT INVESTIGATION

Journals: Published

1. Borsaikia A C, Dutta A and Deb S K, "System Identification of Multistoreyed Non Standard Shear Building Using Parametric State Space Modeling", *Structural Control and Health Monitoring,* DOI:10.1002/stc.385.

Conference Proceedings:

1. Borsaikia A C, Dutta A and Deb S K, "Identification of Influence of Infill Walls on Lateral Stiffness of R C Framed Structure", *Proceedings of 5th International Civil Engineering Conference (CECAR5) together with the Australasian Structural Engineering Conference (ASEC 2010)*, Sydney, August 8-12, 2010.

Recent Communication in Conference Proceedings:

1. Borsaikia A C, Dutta A and Deb S K, "Identification of System Parameters of Test Models with Infill Walls", *21st International Conference on Structural Mechanics in Reactor Technology*, New Delhi to be held on 6-11 November, 2011.